Monitoring of systemic and local immune signatures in response to HCMV reactivation during lactation

Dissertation

der Mathematisch-Naturwissenschaftlichen Fakultät

der Eberhard Karls Universität Tübingen

zur Erlangung des Grades eines

Doktors der Naturwissenschaften

(Dr. rer. nat.)

vorgelegt von

M.Sc. Katrin Lazar

aus Ellwangen

Tübingen

2021

Gedruckt mit Genehmigung der Mathematisch-Naturwissenschaftlichen Fakultät der Eberhard Karls Universität Tübingen.

Tag der mündlichen Qualifikation:	11.05.2021
Dekan:	Prof. Dr. rer. nat. Thilo Stehle
1. Berichterstatter:	Apl. Prof. Dr. med. Dr. rer. nat. Klaus Hamprecht
2. Berichterstatter:	Prof. Dr. rer. nat. Hans-Georg Rammensee

List of publications

Maschmann J, Müller D, **Lazar K**, Goelz R, Hamprecht K. (2019). New short-term heat inactivation method of cytomegalovirus (CMV) in breast milk: impact on CMV inactivation, CMV antibodies and enzyme activities. Arch Dis Child:fetalneonatal-2018-316117.

Lazar K, Rabe T, Goelz R, Hamprecht K. (2020). Human Cytomegalovirus Reactivation During Lactation: Impact of Antibody Kinetics and Neutralization in Blood and Breast Milk. Nutrients 12:338.

Rabe T, **Lazar K**, Cambronero C, Goelz R, Hamprecht K. (2020). Human Cytomegalovirus (HCMV) Reactivation in the Mammary Gland Induces a Proinflammatory Cytokine Shift in Breast Milk. Microorganisms 8:289.

Götting J, **Lazar K**, Suárez NM, Steinbrück L, Rabe T, Goelz R, Schulz TF, Davison AJ, Hamprecht K and Ganzenmueller T (2021) Human Cytomegalovirus Geno me Diversity in Longitudinally Collected Breast Milk Samples. Front. Cell. Infect. Microbiol. 11:664247

In preparation: Lazar K & Kussman T, Pawelec G, Goelz R, Hamprecht K, Wistuba-Hamprecht K. Imaging flow cytometry of breast milk cells and lymphocyte populations during HCMV reactivation

In preparation: Lazar K, Pawelec G, Rabe T, Goelz R, Hamprecht K, Wistuba-Hamprecht K. Longitudinal breast milk and blood leukocyte populations during HCMV reactivation.

Table of content

1 Summary

The human herpesvirus cytomegalovirus (HCMV) persists in the host in latent form for a lifetime and may periodically reactivate. During lactation, reactivation of HCMV occurs locally in the mammary gland without detectable systemic DNAemia. Preterm infants are at risk of infection through ingesting breast milk and may develop life-threatening disease with sepsis-like symptoms. In this thesis, the modulation of the immune signature in response to HCMV reactivation in the mammary gland, investigated non-invasively by analyzing breast milk, was compared to corresponding simultaneously drawn blood samples of HCMV-seropositive, as well as HCMV-seronegative mothers. This “BlooMil” study was performed on longitudinal samples taken from birth through 60 days postpartum over four time ranges.
The viral load in breast milk whey of HCMV-seropositive mothers showed a unimodal course and revealed high differences in peak viral loads between individuals (10^4 – 10^6 copies/ml). Breast milk whey of only one of 18 HCMV-seropositive mothers did not contain reactivated virus during the observation period.
The humoral immune response against HCMV assessed as IgG in breast milk was very low. However, six of 18 mothers showed an increase of HCMV-specific IgGs after peak viral load. Five of 18 mothers had no measurable HCMV-IgG concentrations in breast milk using an electro-chemiluminescence immunoassay. Nevertheless, recomLine blots for six prominent HCMV antigens (IE1; CM2, fusion protein of pUL44 and UL57; p150; p65 and gB glycoprotein 1 and 2) detected anti-p150-IgG reactivity with intensities at least around the cut-off level in all breast milk samples. Anti-gB1 IgG was detected in all plasma samples, but only in 5 of 18 milk samples. Plasma HCMV-IgG titers increased over the analyzed time range.
Immunomonitoring of mothers revealed a significant increase of $CD3^+$ T cells in breast milk of HCMV-seropositive but not seronegative mothers over time. The $CD4^+/CD8^+$ T cell ratio was significantly lower in breast milk of HCMV-seropositive than seronegative mothers. Additionally, most T cells were activated ($HLA\text{-}DR^+$) memory T cells, which increased over time. Naïve T cells were present only in very limited numbers in breast milk. HCMV-specific T cells were measured by quantifying $CD8^+$ T cells binding to pp65 and IE1 peptides using MHC class I tetramers. Most breast milk samples displayed slightly higher frequencies of HCMV-specific T cells than the corresponding blood samples.
The analysis of 92 inflammatory cytokines revealed elevated levels of CC- and CXC-chemokines in HCMV-seropositive compared to -seronegative mothers’ breast milk.
The humoral IgG immune response in breast milk of most HCMV-seropositive mothers resulted in no evidence of interrelation to the observed decreasing viral load in the milk during the unimodal course of reactivation. However, a compartmentalization in the mammary gland regarding immune cells, such as $CD3^+$ T cells and activated ($HLA\text{-}DR^+$) $CD8^+$ T cells, was

observed. These immune cells showed increasing frequencies in breast milk over time compared to corresponding blood samples or seronegative mothers' breast milk and might therefore contribute to the decrease of HCMV loads in breast milk after the peak.

2 Zusammenfassung

Das humane Zytomegalievirus (HCMV) gehört zur Familie der Herpesviren und ruft lebenslange latente Infektionen mit wiederkehrenden Reaktivierungen hervor. Die Reaktivierung des Virus während der Laktation ist ein lokaler Prozess in der Brustdrüse ohne Detektion von DNAämie. Frühgeborene Kinder laufen Gefahr sich durch Muttermilch zu infizieren und können schwere Erkrankungen, wie z.B. Sepsis-ähnliche Symptome entwickeln. In dieser Dissertationsschrift wurden die Veränderungen der Immunsignatur in Hinblick auf die HCMV-Reaktivierung in der Brustdrüse untersucht. Milchproben sowie entsprechende Blutproben von HCMV-seropositiven und seronegativen Müttern wurden longitudinal analysiert. Dafür wurde die BlooMil Studie etabliert und Proben in vier Beobachtungszeiträumen bis zu 60 Tage nach der Geburt genommen. Die Viruslast in der Muttermilch von HCMV-seropositiven Müttern zeigte einen unimodalen Verlauf und große Unterschiede der maximalen Viruslast (10^4 – 10^6 Kopien/ml). Nur eine der 18 Mütter (5,6%) reaktivierte das Virus zu den unterschiedlichen Zeitpunkten nicht in der Muttermilch.

Die humorale Immunantwort gegen HCMV in Bezug auf das Immunglobulin G in der Muttermilch war nicht stark ausgeprägt. Sechs der 18 Mütter zeigten einen Anstieg der HCMV-spezifischen IgGs nach der maximalen Viruslast. Fünf Mütter hatten keine messbaren ECLIA HCMV-IgG Werte in der Muttermilch. RecomLine blots zur Analyse von sechs wichtigen Antigenen (IE1; CM2, ein Fusionsprotein aus pUL44 und UL57; p150; p65 und gB Glykoprotein 1 und 2) zeigten trotzdem in allen Muttermilchproben Ergebnisse für anti-p150-IgG, auch wenn diese nur um den Cut-off Level zu finden waren. Anti-gB1 IgGs wurden in allen Plasmaproben detektiert, aber nur in fünf Müttern war es auch in der Muttermilch nachweisbar. Interessanterweise stiegen die HCMV-IgGs in Plasma über den zeitlichen Verlauf signifikant an.

Die zelluläre Analyse zeigte einen signifikanten Anstieg der $CD3^+$ T Zellen in der Muttermilch von HCMV-seropositiven, aber nicht von seronegativen Müttern. Das Verhältnis von $CD4^+$ zu $CD8^+$ T Zellen war in HCMV-seropositiven Müttern niedriger. Zusätzlich konnte gezeigt werden, dass die meisten der T Zellen in der Muttermilch aktivierte ($HLA\text{-}DR^+$) Gedächtnis T Zellen waren. Naive T Zellen waren jedoch selten in Muttermilch zu finden.

HCMV-spezifische T Zellen wurden durch $CD8^+$ T-Zellen gemessen, die an pp65- und IE1-Peptiden auf MHC-Klasse-I-Tetrameren binden. In diesem Ansatz zeigten Muttermilchproben etwas höhere Frequenzen als die entsprechenden Blutproben.

Die Analyse von 92 inflammatorischen Zytokinen ergab einen erhöhten Gehalt an CC- und CXC-Chemokinen in HCMV-seropositiver Muttermilch im Vergleich zu HCMV-seronegativer Muttermilch.

Die humorale IgG-Immunantwort in der Muttermilch der meisten HCMV-seropositiven Mütter führte während des unimodalen Verlaufs der Reaktivierung zu keinem Hinweis auf eine Wechselbeziehung mit der beobachteten abnehmenden Viruslast in reifer Milch. Stattdessen könnten die Immunzellen, mittels einer distinkten Kompartimentierung und dem Anstieg der T Zell-(Sub)Populationen ($HLA\text{-}DR^{+,}$ $CD8^{+}$ T Zellen) im Vergleich zu korrespondierenden Blutzellpopulationen oder Muttermilch von seronegativen Müttern, zur Abnahme der HCMV-Viruslast in der Muttermilch nach dem Maximum der Virusausscheidung im abfallednden Ast der Reaktivierung beitragen.

3 Introduction

3.1 Human Cytomegalovirus

3.1.1 History and Taxonomy

Human cytomegalovirus (HCMV), or also called human herpesvirus 5 (HHV-5), belongs to the herpesvirus family, more specifically to the subfamily betaherpesvirinae. Other prominent herpesvirus family members are herpes simplex virus I (HHV-1) and II (HHV-2), as well as varicella zoster (HHV-3) and Epstein-Barr virus (HHV-4) [1].

HCMV itself was noticed first by Ribbert in 1881, when he microscopically investigated kidney and parotid gland tissue of a stillborn infant and described enlarged cells and intranuclear inclusions (owl's eye appearance) as protozoan like cells [2, 3]. By 1950, several cases of congenital infections with lethal outcomes and the same cell characteristics had been found and Wyatt et al. [4] called it cytomegalic inclusion disease (CID). The virus was then isolated for the first time in the years 1955/56 and 1957 independently by Smith [5], Rowe [6] and Weller et al. [7]. Weller et al. [8] named the virus cytomegalovirus in 1960.

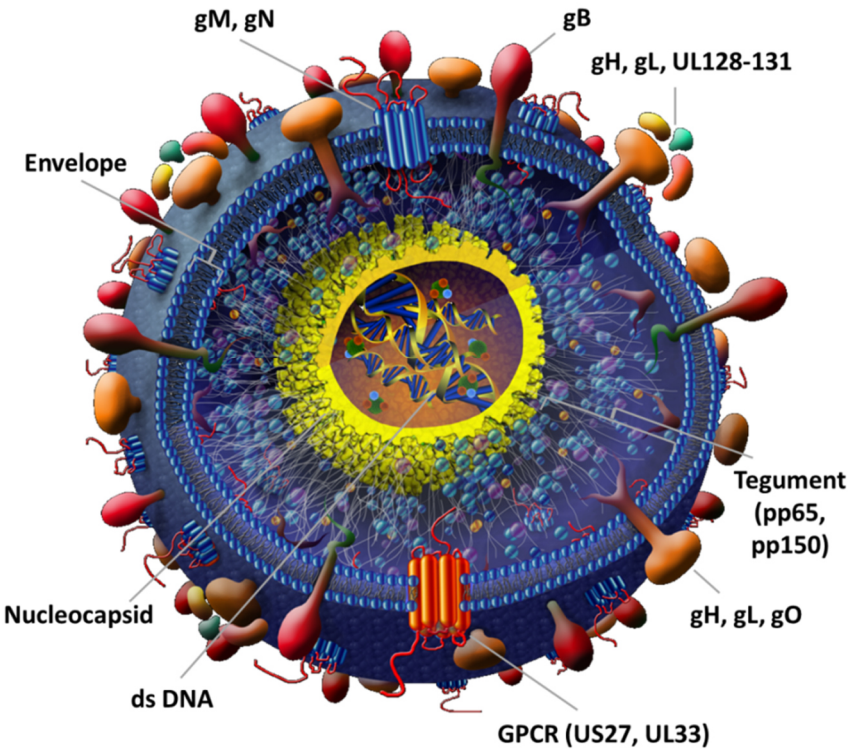

Figure 1: Human Cytomegalovirus.
The human cytomegalovirus has a double-stranded (ds) DNA enclosed by a nucleocapsid, which is surrounded by the tegument harboring many proteins (for example, pp65 and pp150). It is enveloped by a lipid bilayer with glycoproteins (g). Modified after and reprinted with permission from Daniel Streblow, co-author of the article cytomegalovirus proteomics [9] and the Caister Academic Press.

Nowadays, it is well known that HCMV is an enveloped, double stranded DNA virus and has the largest genome of all human herpesviruses. The mature virion is composed in the center of a ~ 235 kilo base pair (kbp) double-stranded linear DNA, which translates into 165 genes [10]. It is surrounded by a 100 nm icosahedral capsid, which is enclosed by an abundant protein layer termed tegument or matrix (Figure 1) [11]. The immunogenic phosphoproteins pp65 and pp150 are the most abundant proteins of the tegument [12, 13]. The tegument is enveloped by a lipid bilayer with different glycoproteins (g) for cell attachment (Figure 1).

3.1.2 Replication cycle

The viral entry into cells is strongly host-specific and mediated by several different proteins and can therefore occupy a wide spectrum of cell tropism [14]. gB functions as fusion protein, possibly without receptor binding [15]. The trimeric gH/gL/gO complex binds to PDGFRα and mediates a pH-independent fusion mainly into fibroblasts. The pentamer complex gH/gL/UL128/UL130/UL131 was shown to bind to Nrp2 and mediates entry into epithelial/endothelial cells [16] (Figure 2 A). Additionally, CD90, which is interacting with gH and gB, as well as CD147, which is important in pentamer dependent entry, were shown to be host cell surface proteins important for viral entry [14]. After viral entry, where the tegument is released into the cytoplasm and the capsid stays intact, the capsid is transported with the help of tegument proteins to the nucleus by microtubules [17] (Figure 2 B). The capsid delivers the genome into the nucleus and a transcription cascade starts [18]. Immediate early (IE) proteins are transcribed first and are necessary for the initiation of further steps, like the transcription of delayed early proteins, including the DNA-polymerase (pUL54), followed by genome replication and transcription of late proteins [19]. The capsid is formed in the nucleus and exits via a nuclear egress complex through the double membrane of the nucleus [20].

A viral assembly complex (Figure 2 AC) in the cytoplasm is established by hijacking the host cell's secretory pathways via endoplasmic reticulum, Golgi apparatus and endosomal pathways [20]. The fully infectious virion is then transported out of the cell (Figure 2 D).

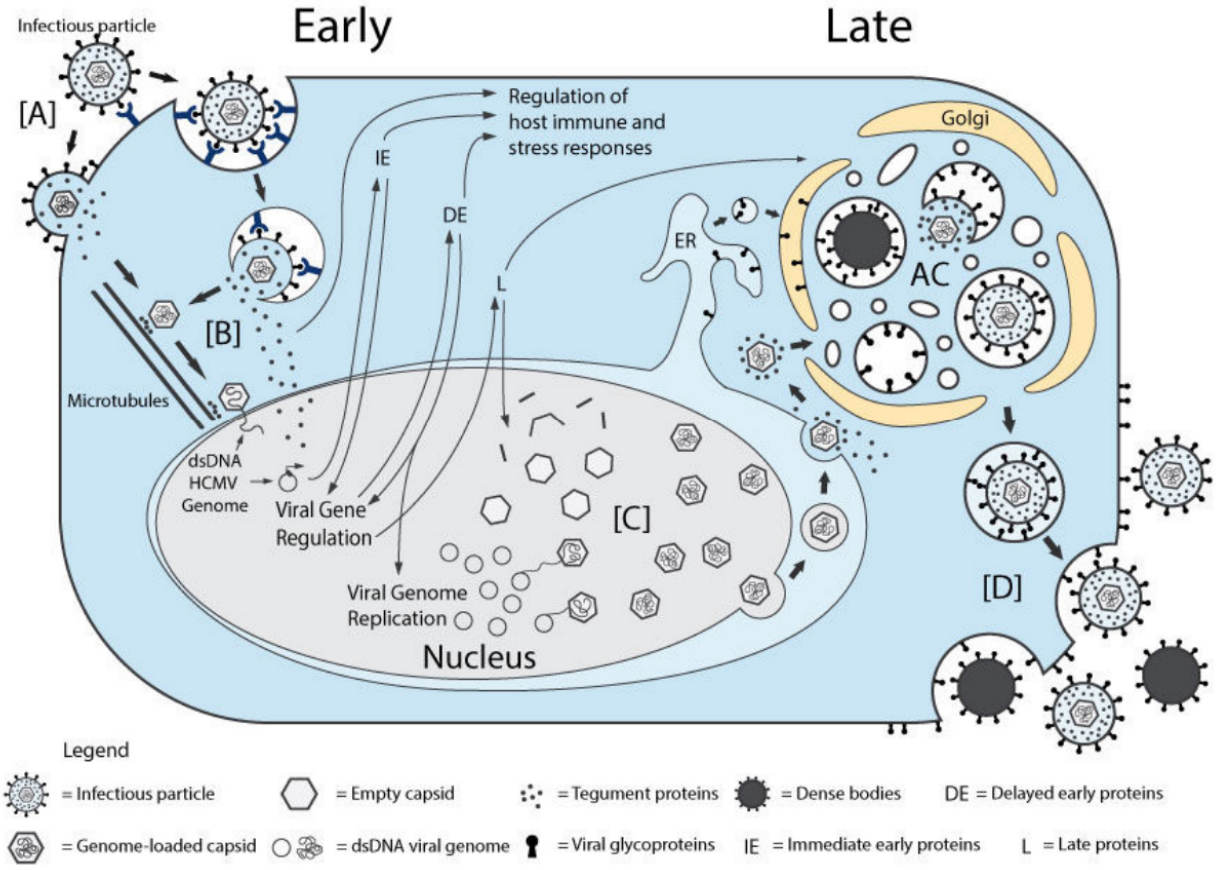

Figure 2: HCMV replication cycle.
After viral entry [A], the DNA is released into the nucleus [B] and transcribed. In a next step, the viral genome is replicated and the nucleocapsid is formed. After nuclear egress [C], the capsid is enveloped by a lipid bilayer with viral glycoproteins in the Golgi apparatus [AC] and the whole infectious particle or dense bodies are transported out of the cell [D]. Adapted from Jean Beltran and Cristea [20].

3.1.3 HCMV latency and reactivation

The replication cycle is not always taking place. HCMV can, upon entry into a cell, either go into the lytic cycle or enter a latent state [21]. Whether the DNA is transcribed or not seems to be based on a complex system, which is not fully understood, but seems to depend on the cell type. $CD34^+$ progenitor cells and $CD14^+$ monocytes, as well as granulocyte-macrophage progenitors are cell types in which latency may occur [22-25]. In contrast, endothelial-, epithelial cells and fibroblasts usually enter the lytic cycle [26]. Some cell types are replicating the virus fast and in high amounts, while others only show low or chronic HCMV replication [27, 28] (Figure 3).

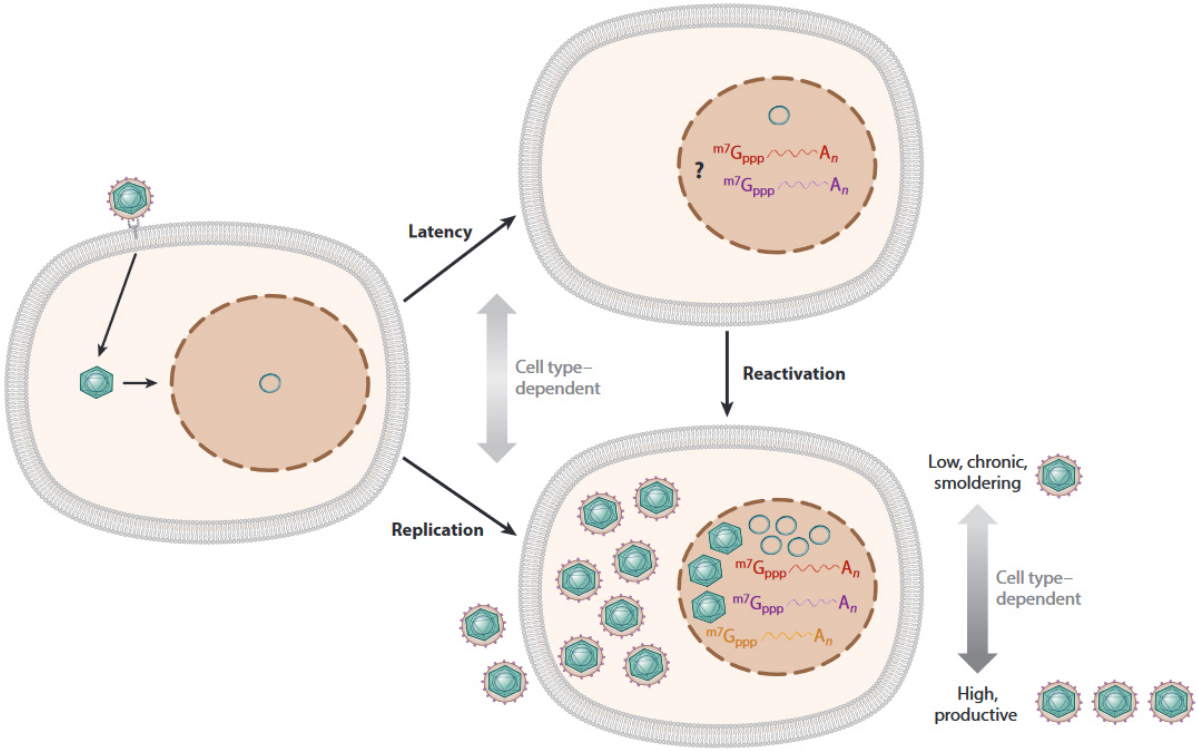

Figure 3: HCMV latency versus replication.
HCMV infection of cells leads to transport of the viral DNA into the nucleus. Depending on the cell type, the viral genome is either silenced (latency) or replicated and infectious particles are formed. Adapted from Goodrum [27].

Latently infected $CD34^+$ or $CD14^+$ cells are persistent sites of HCMV. The whole mechanism of latency is not fully understood, but some key players are reviewed by Goodrum et al. [28] and displayed in Figure 4. Transcription of the IE-genes is a vital factor: if there is a lack of very early transcription the replication cascade does not follow. The major immediate early promotor (MIEP) plays here an important role. During latency, the MIEP is found in a repressive chromatin structure [29, 30]. The protein pp71 usually travels into the nucleus, binds a host repressor called Daxx for degradation and therefore prevents silencing [31]. When it is retained in the cytoplasm, latency can occur. Other domains and factors like nuclear domain 10 (ND10), heterochromatin protein 1 (HP1) or histone deacetylase (HDAC) are also involved in the chromatin remodeling [30, 32] (Figure 4).

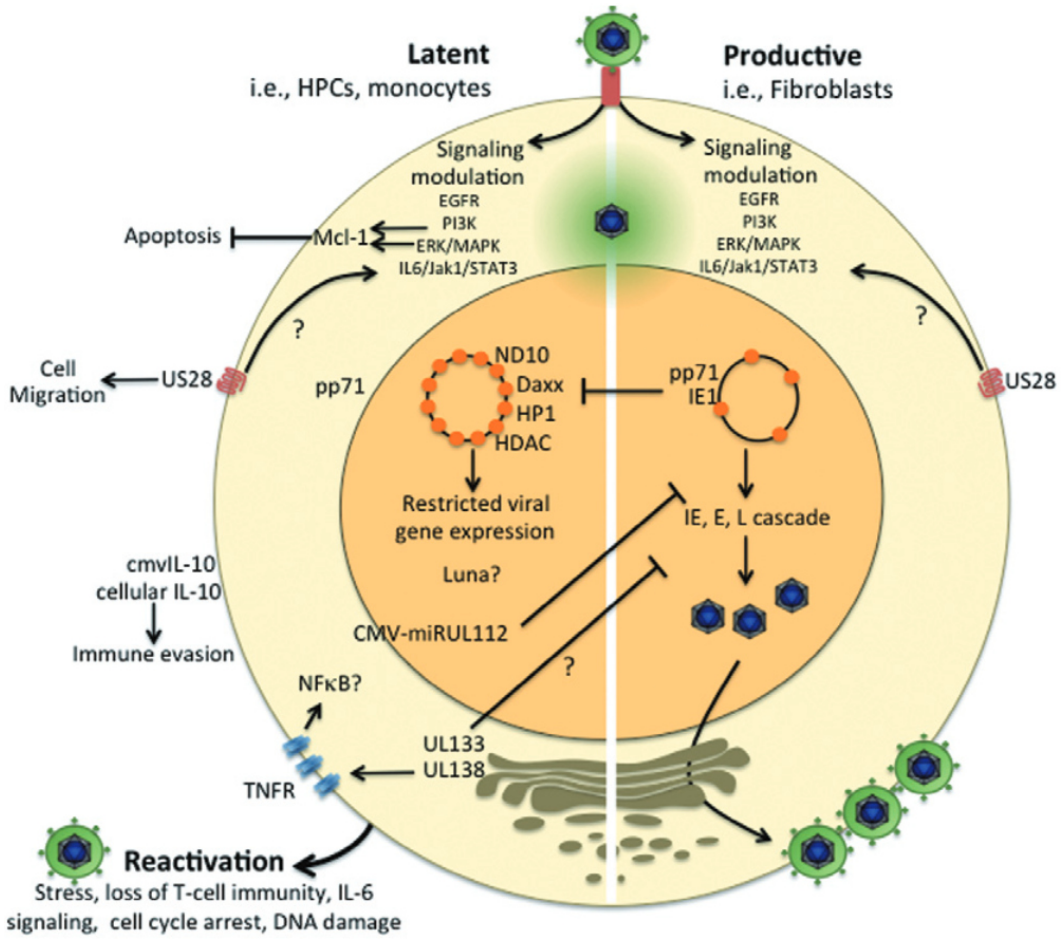

Figure 4: Latent versus productive HCMV life cycle.
After infection with HCMV two cycles the latent or the productive cycle can happen. In for example monocytes or Hematopoietic progenitor cells (HPCs) latent infections can occur, where the HCMV-DNA is silenced upon entry into the nucleus by several different factors (nuclear domain 10 (ND10), Heterochromatin protein 1 (HP1), Histone deacetylase (HDAC). Reactivation can occur under stress or loss of T cell immunity. In the productive phase (on the right), the DNA can be transcribed directly upon entry into the nucleus and viral particles can be produced. Adapted with permission from Goodrum et al. [28].

The reactivation of HCMV is not fully understood, but several influences were found. HCMV can reactivate upon differentiation of monocytes to macrophages or dendritic cells [33, 34]. Stress and an inflammatory milieu with increased IL-6 levels [35, 36] and the loss of T cell immunity can also lead to reactivation [37].

3.1.4 Epidemiology and Pathology

The worldwide HCMV seroprevalence is estimated to be around 83% [38]. Developed countries hold often lower rates (Ireland with 39%) than developing countries (African region 88%) [38]. Women in Germany show seroprevalences around 62.3%, while men have lower percentages with 51.0% [39]. An increase of seroprevalence is seen by age; the older the population, the higher the HCMV seroprevalence. In women an increase from 44.1% to 77.6% was found in Germany in the age groups 18-29 and 70-79, respectively [39].

HCMV infection is usually asymptomatic. Transmission occurs horizontally and vertically. Many body fluids can contain virus, such as tears, saliva, cervical mucus, liquor, blood, urine, semen and breast milk [40]. Major transmission routes are sexual contact, solid organ transplantations (SOT) or stem cell transplantations (SCT), blood transfusions, congenital infections, as well as breast-feeding [11]. In the SOT and SCT settings, HCMV seropositive donors can infect the recipient, or the immunosuppressed status can lead to reactivation in already positive recipients.

Initial asymptomatic HCMV infections can develop to severe HCMV disease, such as gastrointestinal diseases, myocarditis, cystitis, retinitis, nephritis, encephalitis/ ventriculitis, pneumonia, hepatitis and pancreatitis in immunosuppressed individuals [41].

In contrast, pregnant women, who have a primary HCMV infection, do not necessarily show symptoms, but transmission to the fetus may occur in about 30-70% of the time [42, 43]. HCMV is the most common cause of congenital infections [44] and can lead to disabilities and hearing disorders in the children [45].

The treatment of HCMV disease is mostly based on antiviral substances like ganciclovir and valganciclovir [46].

3.2 The immune system - an overview

3.2.1 Innate immune system

Humans are constantly exposed to bacteria, viruses, fungi and toxins, which could harm the organism. Two different subgroups of the immune system, the innate and the adaptive immune system, can differentiate between self and non-self-antigens and are interacting with each other to protect the body from infections and disease. The skin is the first barrier, preventing pathogens from an easy entry. The complement system, the recognition of pathogen-associated molecular patterns (PAMP, by for example toll-like receptors (TLRs)) and damage-associated molecular patterns (DAMP), as well as inflammation processes are important steps of the innate immune system. Cells belonging to the innate immune system are, for instance, macrophages, dendritic cells, granulocytes, like neutrophils, basophils and eosinophils, and natural killer (NK) cells. All these components generate a first line defense to pathogens or diseases, since they are present in the tissue and can directly react.

3.2.1.1 Inflammation/Cytokines

Inflammation of tissue is achieved by secretion of cytokines by, for example, infected or damaged cells, as well as tissue residing immune cells and later on by invading immune cells. Cytokines are small proteins which are indispensable for communication between cells and can attract, activate or help differentiating immune cells [47]. They are produced by various

cell types particularly by immune cells (for instance macrophages and helper T cells) but also by fibroblasts, endothelial or epithelial cells. Many subgroups, such as interleukins (IL), interferons (IFN), chemokines and tumor necrosis factors (TNF) exert distinct functions. Important proinflammatory interleukins are for example IL-1, IL-6 or IL-12 , while anti-inflammatory interleukins are for instance IL-4, IL-10, IL-11 and IL-13 [48]. Chemotactic cytokines are small proteins with the ability to attract immune cells and are, therefore, called chemokines. Cysteine residues are used to differentiate between the most frequent C-X-C (for example IL-8, CXCL10) and C-C and seldom C- and C-X-X-X-C chemokines [49]. Interferons can show antiviral activity. A prominent member is IFNγ, which is mainly excreted by NK cells and activated T cells. Amongst many other functions, IFNγ facilitates major histocompatibility complex (MHC, also called human leukocyte antigen (HLA)) class I and II upregulation on somatic cells and professional antigen presenting cells, respectively. The tumor necrosis factor super family (TNFSF) consists of type II transmembrane proteins, which after extracellular cleavage function as cytokines leading to activation, differentiation, proliferation and many other regulatory functions.

3.2.1.2 Professional antigen presenting cells/monocytes

Professional antigen presenting cells (APCs) can digest and process pathogens or apoptotic cells in their surroundings to finally present (foreign) antigens on MHC class II molecules (pMHC), which is a prerequisite for initiation of an adaptive immune response.
Monocytes are, for example, professional APCs and originate from myeloid precursors, namely monoblasts in the bone marrow. Three types of monocytes exist: Classical monocytes express high expression levels of CD14 on their cell surface, while non-classical monocytes have low CD14 expression and co-express CD16, a Fcγ receptor type III. Intermediate monocytes are defined by high CD14 and low CD16. Monocytes are mainly found in the blood stream and differentiate into macrophages (through M-CSF and other cytokines into various subtypes like M1 and M2 macrophages) or dendritic cells (through cytokines like GM-CSF, IL-4) when migrating into tissue. Macrophages and dendritic cells are phagocytes representing the majority of professional APCs.
Another important role of macrophages is in the initiation of inflammation by secreting cytokines that can activate or attract other cells to the location of infection.

3.2.1.3 Myeloid-derived suppressor cells

Myeloid precursors also can differentiate into myeloid-derived suppressor cells (MDSCs) when chronic/persistent infections or cancer lead to weaker and longer activating stimulation [50]. Therefore, MDSCs are immature myeloid cells, bearing anti-inflammatory cytokines and

showing only weak phagocytic performances [50]. A key feature of these cells is that they inhibit adaptive immune responses, especially T cell responses [51, 52]. They can be of granulocytic or monocytic origin. In this thesis, monocytic MDSCs (M-MDSCs) were identified by their characteristic CD14 and low to dim HLA-DR expression.

3.2.1.4 NK cells

NK cells are cytotoxic lymphocytes expressing amongst other receptors the neural cell adhesion molecule (NCAM, CD56) that is usually used to identify these cells in flow cytometry based assays. They can lyse cells without prior priming and are independent of the MHC-peptide presentation and recognition axis. The verdict to kill cells is influenced by a balance of inhibitory (for example killer-cell immunoglobulin-like receptors (KIRs), NKG2A, NKG2B) or activating receptors (CD16, NKG2C, NKG2D) on the NK cell surface. For instance, a strong inhibiting signal is given by KIRs, which can bind to the MHC class I [53]. MHC class I is a protein complex presenting peptides from within the cell. Virus infected cells or tumor cells can downregulate these complexes and NK cells receive, therefore, no inhibitory signal from MHC I and kill the cell with help of other activating receptors by releasing cytotoxic granules filled with granzymes and perforins. However, NK cells can also show features of adaptive immunity and were shown to have antigen-specific memory [54] (also see 3.3.1.1).

3.2.1.5 NKT-like cells

Another link to adaptive immunity form NKT-like cells, which are expressing markers for both NK cell and T cell features. They can rapidly react upon antigen-stimulation with expression of a wide range of cytokines [55]. Their T cell receptors (TCRs) bind often to CD1d, a MHC-like molecule presenting lipids. Two types of NKT-like cells exist [56]. Type I cells are called invariant NKT-like cells, expressing a semi-invariant T cell receptor (TCR) [57]. Type II NKT-like cells are less well studied and are assumed to recognize glycolipids [58]. In this thesis, co-expression of CD56 and CD3 of lymphocytes were used to define this population. Therefore, they were termed $CD56^+$ T cells in the following.

3.2.2 Adaptive immune system

The reactions of the adaptive immune system need several days to develop [59]. The main purposes are a more specific and to the situation adapted immune response, as well as to generate immunological memory. The humoral immunity (B cells) mainly protects from extracellular pathogens, while the cellular immunity (for instance $CD8^+$ T cells) targets for example intracellular pathogens. Additionally, both can participate in tumor surveillance.

3.2.2.1 B cells and antibodies

The humoral immune response is generated by B cells that can be identified, for instance, by their CD19 expression. B cells encounter antigens in lymph nodes with their B cell receptor; a membrane bound immunoglobulin (mIg). This can result in B cell activation. With additional help of $CD4^+$ T cells and/ or others, B cells can differentiate into plasma cells and are able to express high-affinity immunoglobulins (Ig) or transform into memory B cells [60].
Immunoglobulins consist of two heavy and two light chains linked through disulfide bonds. The secreted immunoglobulins can be divided into five subclasses: IgA, IgG, IgM, IgE and IgD [61]. mIgD and mIgM are co-expressed on mature B cells. Upon antigen stimulation and activation in the lymph node, IgM is secreted as a pentamer. After somatic hypermutation, the produced antibodies have either higher or lower affinity to antigens. However, only the B cell clones expressing antibodies of higher affinity undergo further proliferation. The binding strength of the whole molecule (IgM has ten binding sites) is called avidity. With additional help of $CD4^+$ T cells, irreversible DNA recombination eliminating heavy chain exons in the C-region (μ, δ, γ, α, ε) can occur and leads to a class-switch to IgA, IgG or IgE. IgG is the main isotype in serum with the longest half-life [61]. Neutralizing IgG antibodies are very important, since they are, amongst other antigens, directed against viral surface proteins and can for example prevent the cell entry of pathogens. IgA is mostly expressed at mucosal surfaces as a dimer, termed secretory (s) IgA and, for instance, is the most abundant antibody in breast milk [61] (see 3.4.4).

3.2.2.2 T cells

Progenitor cells originate in the bone marrow and can migrate to the thymus, where their development to T cells by somatic gene rearrangements takes place. At the early stage of double negative (DN, double negative for CD4 and CD8), thymocytes undergo TCR β, γ and δ gene rearrangements and the lineage of either γδ or αβ T cells is determined by which of the genes is rearranged faster and amongst several other factors, presumably also the TCR signaling strength [62]. Strong TCR signaling may lead to γδ, weak signaling to αβ T cells. αβ T cells undergo then positive and negative selection processes and finally develop into CD4 or CD8 positive, not self-antigen recognizing but functional naïve T cells. Their TCR binds to specific pMHCs [59, 63].

3.2.2.2.1 γδ T cells

The γδ T cells exiting the thymus can either show innate like features or need activation in the periphery [62]. Therefore, γδ T cells bridge both parts of the immune system through the combined use of innate and adaptive functions [64, 65]. They can show a rapid response to

antigens and can mostly be activated in a pMHC independent-manner. Some of the γδ T cells might also undergo extrathymic selection processes [66]. Less than 6% of the peripheral blood T cell compartment consists of γδ T cells mainly expressing Vγ9 and Vδ2 chains in their TCR [67, 68]. Most of their antigens are still unknown. However, Vγ9Vδ2 T cells were shown to be activated by phosphoantigens, defined as phosphorylated small non-peptide antigens produced for example by either microbes or transformed cells [69]. Despite the main occurrence of Vδ2 chains (around 70%, show more innate like-features), Vδ1 (presumably more adaptive features) and Vδ3 form minor subsets, whereas other δ chains are very rare [70, 71]. Non-Vγ9Vδ2 T cells, such as Vδ1 γδ T cells, were reported to undergo clonal expansion upon exposure to different pathogens or in diseases [72, 73].

3.2.2.2.2 $CD4^+$ αβ T cells

$CD4^+$ T cells, also called simplified helper T cells, bind to pMHC class II, which are displayed by professional APCs (see 3.2.1.2). For antigen-specific activation in the lymph node, costimulatory signals like CD28 binding to B7 (mainly expressed by dendritic cells) are important. After activation, stimulation with different cytokines helps them to differentiate into several subpopulations, for example Th1, Th2, Th9, Tfh, Th17, Th22 and regulatory T cells (Tregs). Activated $CD4^+$ T cells mainly secrete cytokines to help initiate other immune responses. For example, Th1 cells mainly help by infections with intracellular microorganisms, like bacteria or viruses (and therefore cytotoxic $CD8^+$ T cells) and mainly secrete IFNγ. Th2 cells help with extracellular parasites (and therefore antibody-producing B cells) and mainly secrete cytokines like IL-4, IL-5 or IL-13. Tregs display immune regulatory functions, inhibit dendritic cells and, consequently, T cell activation [74].

3.2.2.2.3 $CD8^+$ αβ T cells

$CD8^+$ T cells, also called simplified cytotoxic T lymphocytes (CTLs), bind with their TCR and the CD8 molecule to pMHC class I, which are almost expressed on all cells of the body [59]. The naïve $CD8^+$ T cell is activated, when its TCR binds to pMHC class I on APCs. Additional help of costimulatory signals like CD28 binding to B7- in presence of a defined cytokine milieu is needed. They leave the lymph node and can upon antigen recognition, directly kill the target cell. One way are cytotoxic granules filled with granzymes and perforins, which can specifically be released in the direction of the target cell. While perforins form pores into the membrane of the target cell, the granzymes can enter the cell and cleave proteins (activation of caspase 3) and the cell undergoes apoptosis. Another way is the Fas/Fas ligand axis, which also directly leads to the caspase cascade setting the target cell into apoptosis [75].

3.2.2.2.4 Activation marker CD38 and HLA-DR

T cells are activated by for example contact with their specific antigen and other costimulatory factors and can then proliferate and fulfill their cytotoxic or helper functions. During this activation, several activation markers are expressed like for instance CD69, CD25, CD38 or HLA-DR [76, 77]. In this thesis, CD38 and HLA-DR were used as activation markers on T cells. CD38 is a glycoprotein, which is also called cyclic ADP ribose hydrolase. Among several other functions, it is a general marker for activation and an adhesion molecule, helping leukocytes pass through endothelium [78].
HLA-DR belongs to the MHC class II receptors and is expressed by professional APCs. It is upregulated upon activation of T cells, but slowly and counts as a 'late' marker [76].

3.2.2.2.5 T cell memory

Two models of T cell differentiation are discussed in the field. The on-off-on hypothesis leans to the theory that antigen-activated naïve T cells differentiate into effector cells, which then undergo clonal expansion. After the pathogen is cleared, most effector cells undergo apoptosis. However, some effector cells transform to memory cells and can easily be reactivated and proliferate upon another recognition of the antigen [79, 80].
Another theory, called developmental or linear differentiation model, is suggesting that memory T cells directly differentiate from naïve T cells after activation and antigen recognition [81]. This hypothesis is supported by reports of longer telomere lengths of memory cells compared to effector cells, which underwent several cell divisions [82].
Markers identifying naïve T cells are CD27, CD28, CD62L, CCR7 and CD45RA. Upon antigen stimulation they differentiate into central memory T cells (T_{CM}). T_{CM} (CD45RA-, $CD27^+$, $CD28^+$, $CD62L^+$, $CCR7^+$), have no immediate effector function, but are more sensitive to antigen stimulation than naïve T cells and need less co-stimulation [83]. They still express homing receptors for secondary lymphoid tissues and have a high proliferation capability [84]. After another stimulation, they can differentiate further into effector memory T cells (T_{EM}), characterized by CD45RA-, $CD27^+$/-, $CD28^+$/-, CCR7- [85]. T_{EM} are mostly found in blood or non-lymphoid tissues and have a rapid effector function [83]. Terminally differentiated memory T cells re-expressing CD45RA are termed TEMRA cells ($CD45RA^+$, CD27-, CCR7-). They have low proliferative capability and a high capacity to produce IFNγ [86].
The expression patterns of CCR7 and CD45RA were used to detect naïve, T_{CM}, T_{EM} and TEMRA cells in this thesis. CCR7 (C-C chemokine receptor type 7) is an important chemokine receptor, which can result in homing of the T cell to secondary lymphoid tissues [87]. CD45RA is a splice variant (exon 4) of the tyrosine phosphatase CD45. CD45 is found on all (nucleated) hematopoietic cells and has a very high abundance on the cell surface [88]. CD45 and its

different splice variants can show the developmental or activation stages of the cell. CD45RA is expressed on naïve T cells and is finally reexpressed in TEMRA cells (see above).

3.3 Immune response to HCMV

3.3.1 Innate immune response to HCMV

At first, an innate immune response to HCMV is triggered, which is vital for the development of an adaptive immune response [89]. One of many innate immune response mechanisms is already triggered upon HCMV binding or entry into the cell by recognition of gB/gH on the surface of HCMV particles via TLR 2 [90, 91]. This results in inflammatory cytokine secretion of the host cell and leads to attraction of immune cells to the site where an infection was induced [92].

3.3.1.1 NK cells and NKT-like cells in context of HCMV

Another essential component of the innate immune response to HCMV is NK cells [93-95]. HCMV belongs to a group of pathogens, which can induce downregulation of MHC class I molecules on infected host cells as part of their immune evasion strategies. However, MHC downregulation makes the cell more susceptible to NK cell recognition and lysis [96, 97].
NK cells were found to be important during HCMV infections in 1989, when an adolescent individual without NK cells was shown to develop HCMV disease [98].
However, HCMV developed several immune evasion strategies against NK cells. For example, the genes UL18 and UL142 are encoding MHC class I-like molecules to counteract the recognition by NK cells [93, 99].
Additionally, as already mentioned above, NK cells form a bridge to the adaptive immune response [54]. In particular, a subpopulation, expressing the activating receptor CD94/NKG2C (binds to the non-classical MHC class I molecule HLA-E), can show clonal expansion in HCMV-seropositive individuals or *in vitro* using HCMV infected fibroblasts [100-102]. These NK cells were documented to increase and produce high amounts of IFNγ in SCT patients during HCMV reactivation [103].

NKT-like cells might also have a function in the defense against HCMV. Their frequency and activity in peripheral blood was found to be elevated in healthy HCMV-seropositive individuals [104], as well as in patients with HCMV infection after kidney transplantation [105].

3.3.2 Adaptive immune response to HCMV

3.3.2.1 B cells and antibodies in context of HCMV

Individuals with primary HCMV infections present in the first ten days after HCMV exposure only IgM antibodies and no IgG in serum [106] (Figure 5). IgM can either rapidly decrease after a strong increase post primary infection or show persistence for several months [106]. HCMV-specific IgGs increase with a delay to a constant level about three months post infection (Figure 5). The HCMV-IgG avidity is slowly increasing until five to six months after infection [106, 107]. The definition of a latently infected individual is, therefore, defined as IgM negative, IgG positive and expressing high IgG avidity.

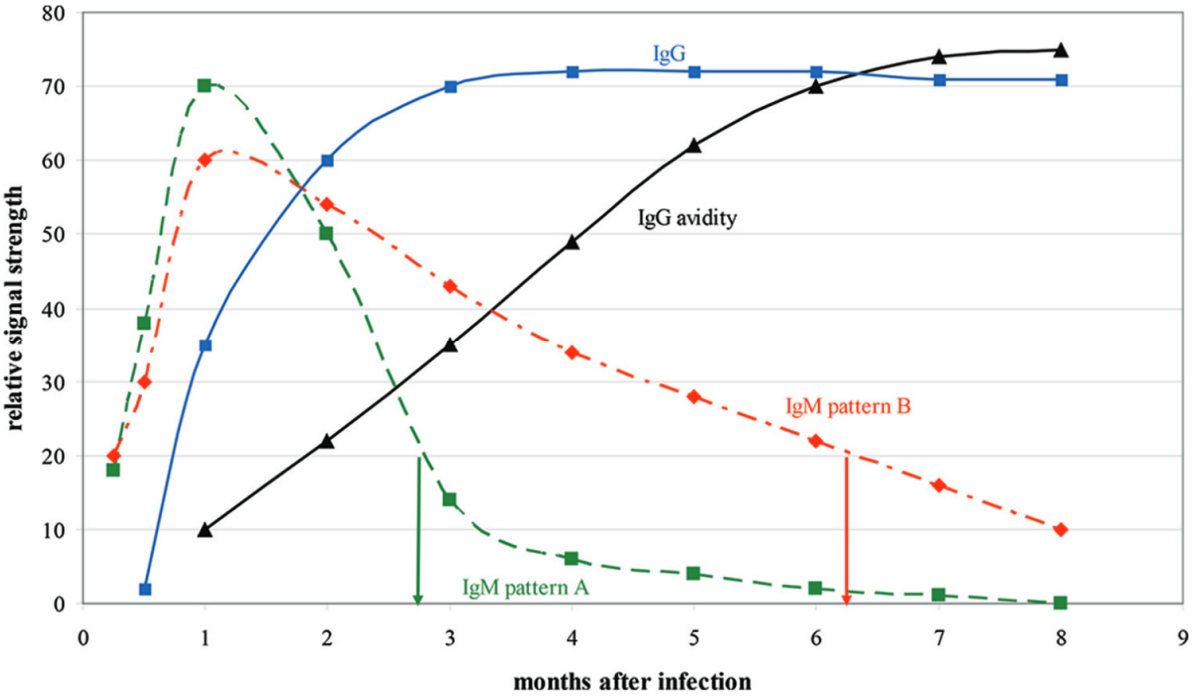

Figure 5: Humoral immune response after primary HCMV infection.
IgM pattern A shows the normal course of IgM, while IgM pattern B shows the course of persisting IgM. With permission after Prince and Lapé-Nixon [106].

The humoral immune response to HCMV is important for restriction of viral dissemination [108, 109]. The IgM and the IgG-antibody response is mainly directed against pp150, a large matrix phosphoprotein [110, 111]. High proportions of IgG-antibodies are also directed against IE1, pp65 (lower matrix phosphoprotein) and gB (antigenic domain 1 and 2), as well as against the processivity factor pUL44 (p52) and single-stranded binding protein pUL57 [110, 112]. Neutralizing IgG antibodies were found against gB [113-115], gH [116] and the pentamer complex [117], whereas IgG antibodies against the latter seem to have potent neutralizing capabilities [118].

3.3.2.2 T cells in context of HCMV

Nevertheless, the main adaptive immune response against HCMV, as well as a strong immunological memory, is managed by T cells [108, 119].

3.3.2.2.1 $CD4^+$ T cells in context of HCMV

$CD4^+$ T cells were thought to have lesser impact during infection and probably more during latency maintenance [120]. However, a functional effector-memory $CD4^+$ T cell compartment was shown to be important for recovery from HCMV primary infection [121, 122]. Additionally, $CD4^+$ T cells were required for the persistence of $CD8^+$ T cells after adoptive transfer [123]. $CD4^+$ T cells were also necessary for $CD8^+$ T cell expansion in SCT patients [124]. Furthermore, extended viral shedding in children with deficiency in $CD4^+$ T cell immunity could also be observed [125].

3.3.2.2.2 $CD8^+$ T cells in context of HCMV

In peripheral blood of HCMV-seropositive individuals, relatively high frequencies of $CD8^+$ T cells target HCMV in comparison to other pathogens [37]. Regarding 213 open reading frames (ORFs) of HCMV, a median of more than 10% of HCMV-specific memory $CD8^+$ T cells were found in blood of healthy virus carriers [126]. Most of the T cell responses seem to be directed against pp65 and IE1 peptides [127-131], but responses were also found against pp28, pp50, gH, gB, US2, US3, US6, and UL18 [132]. The importance of $CD8^+$ T cells was observed in bone marrow transplant patients, where the establishment of cytotoxic T cell responses showed recovery from HCMV infection [133]. Accordingly, patients lacking HCMV T cell responses against these prominent antigens more often developed HCMV disease (six out of ten individuals) [134]. Similar results were also found in the SOT setting [135-137]. Already in 1992 [138] and 1995 [123], it was demonstrated that adoptive $CD8^+$ T cell transfer to SCT patients could reconstitute their immune response to HCMV.
An overview of some major immune cell subsets involved in the immune responses to HCMV is shown in Figure 6.

3.3.2.2.3 γδ T cells in context of HCMV

In 1999, Déchanet et al. [139] showed that γδ T cells highly increased in renal allograft recipients, who had an HCMV infection. Expansion mainly occurred of the $Vδ1^+$ γδ T cell subset [140]. γδ T cell expansion was associated with antiviral activity as well as control of HCMV disease or infection in several studies in the transplant setting [141-146].

Furthermore, healthy HCMV-seropositive individuals also showed elevated levels of γδ T cells [147].

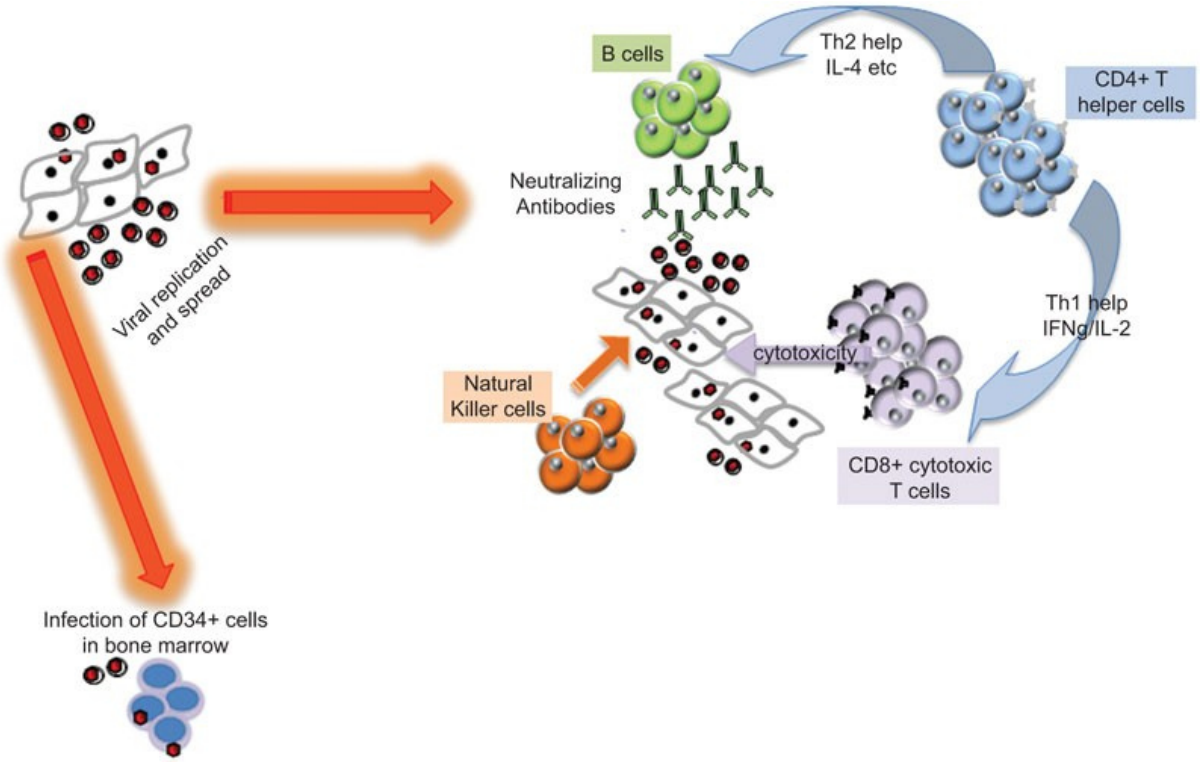

Figure 6: Immune response to HCMV.
Viral replication and spread is fought by B cells expressing neutralizing antibodies, and CD8⁺ cytotoxic T cells. Both are supported and activated by CD4 T helper cells. Additionally, natural killer cells can directly act on infected cells. Nevertheless, HCMV is infecting CD34⁺ cells in the bone marrow and develops a latent state. Adapted with permissions from Wills et al. [148].

3.3.2.2.4 T cell memory in context of HCMV

HCMV infections have great impact on the immune system. $CD8^+$ T cells show similar responses in young infants and children to congenital or postnatal HCMV infections as adults to primary HCMV infections [149, 150]. However, at the latent stage of HCMV, with possibly reoccurring reactivations throughout life, a memory inflation over time seems to take place [151]. A clear imprint on late differentiated T cells in the periphery was found in the HCMV-seropositive elderly population in several studies indicating some sort of senescence [152-158]. For both, $CD4^+$ and $CD8^+$ T cells, naïve T cells were diminished and T_{EM} as well as TEMRA cells, especially in the $CD8^+$ compartment, were elevated in HCMV-seropositive compared to seronegative individuals [159, 160].

As soon as this cellular immune response is impaired in any way, for example in SOT recipients or HIV-positive individuals, or even in preterm newborns, where the immune system is not yet fully developed, HCMV reactivation or infection can lead to severe complications.

3.4 Human breast milk

3.4.1 Anatomy of the lactating breast

The first one to describe the human anatomy of the lactating breast was Sir Astley Cooper in 1840 [161]. He dissected breasts of women, who died during lactation, and made a detailed report. The main milk production takes place in the alveoli by secretory epithelial cells, also called lactocytes. In addition to contractile myoepithelial cells and adipocytes also blood circulation surrounds the alveoli [162] (Figure 7 C). About 10 to 100 of these alveoli form a lobule of which 15-20 are present in the lactating breast [163] (Figure 7 A, B). Cooper found up to 22 ducts, but considered that only 12 were functioning ducts [161]. The ducts transport milk from the alveoli to larger ducts which end in the lactiferous sinus. From there the milk passes the nipples and reaches the suckling infant.

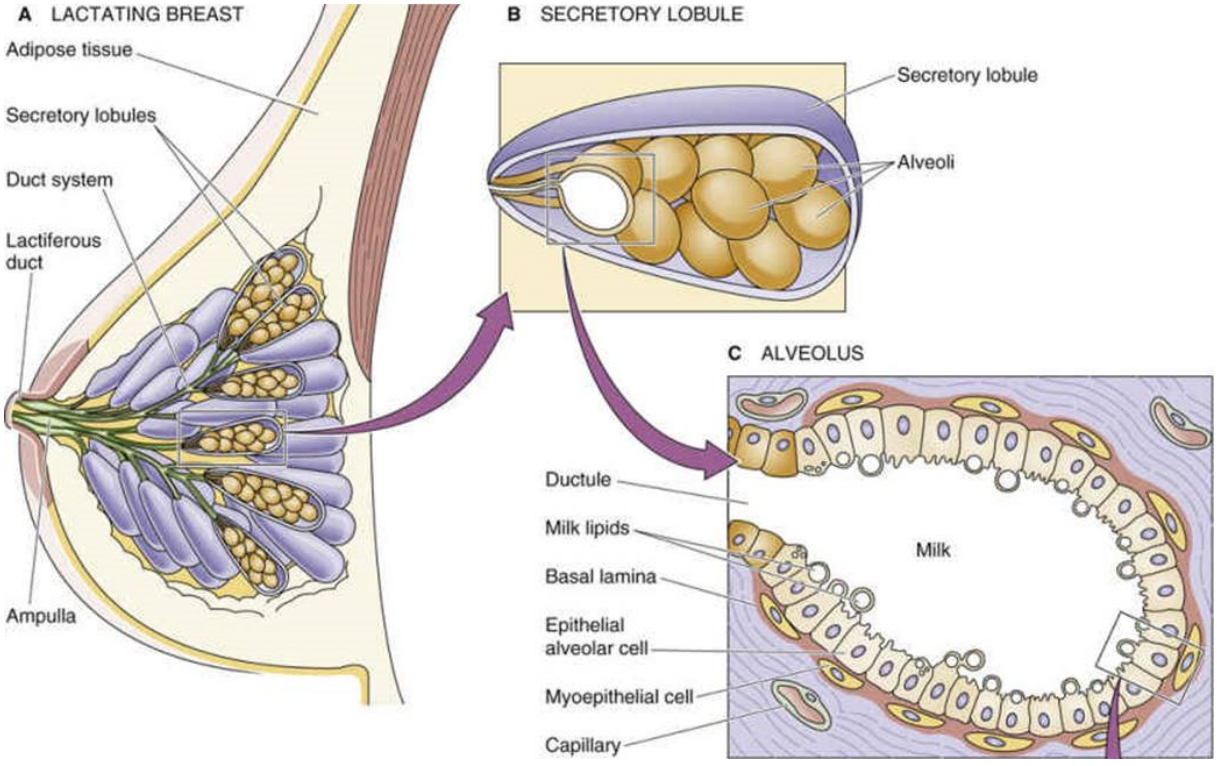

Figure 7: The lactating breast.
A) The lactating breast, B) a secretory lobule and C) an alveolus are shown. Modified from Medical Physiology, 3rd Edition, chapter 56 [164].

Lactocytes produce the major proteinaceous amounts of milk. Lactalbumin, casein and other proteins, which are synthesized in the endoplasmic reticulum and the Golgi apparatus, are transported to the lumen of the alveoli through exocytosis (Figure 8 -1). Additionally, proteins are transcellularly transported via endo- and exocytosis into the lumen of the alveoli (Figure 8 -2). Many macromolecules, like immunoglobulins [165], albumin and transferrin from serum [166, 167], as well as endocrine hormones and cytokines [168] get transported to the lumen by transcytosis. The milk lipids mainly come from the mothers diet or fat stores and move in

form of lipid droplets to the apical membrane, where they are secreted into the lumen [169] (Figure 8 -3). Electrolytes and water from the interstitial fluid reach through an osmotic gradient (mainly due to the lactose) and by passing the tight junctions into the lumen (Figure 8 -5). Cells, mainly leukocytes, also reach the alveolar lumen through a paracellular pathway [170]. For instance, breast milk-derived B cells were found to originate presumably from the gut-associated lymphoid tissue forming an entero-mammaric link [171, 172].

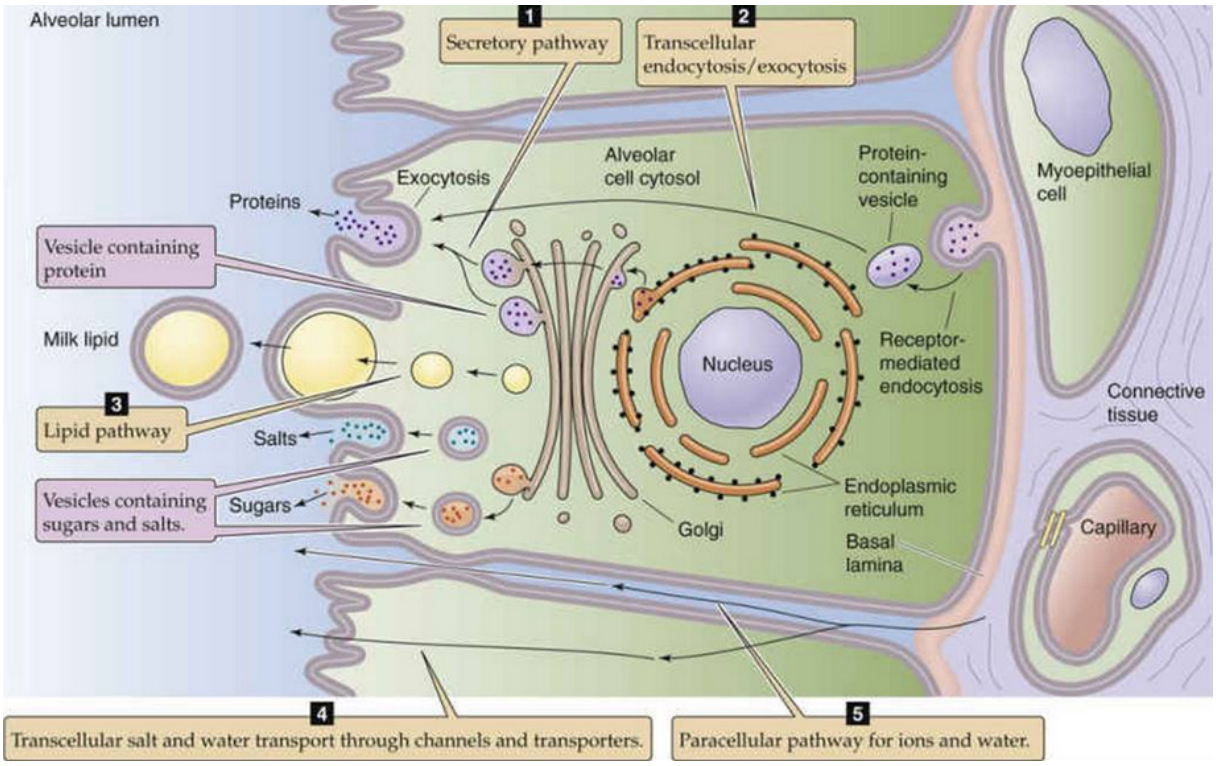

Figure 8: Secretion pathways of secretory epithelial cells.
Breast milk components can be transported into the alveoli lumen by the secretory (1) or lipid (3) pathway of the secretory epithelial cell, by transcellular endocytosis/exocytosis (2) or through transcellular salt and water transport through channels and transporter (4), as well as paracellular pathways for ions or water (5). Adapted from Medical Physiology, 3rd Edition [164] with permissions from Elsevier.

The infant's suckling is very important to stimulate milk ejection [173]. Without the nerve impulses from the nipple to the hypothalamus, which then stimulates the posterior pituitary to excrete oxytocin, only 1-10 ml of milk can be expressed or removed by the infant [174, 175]. Oxytocin stimulates the myoepithelial cells to contract and press the milk through the ducts towards the infant. Duct diameter and milk flow rate increase during this process [173, 176, 177].

3.4.2 Breast milk components and benefits

Breast milk contains important macronutrients to fit the infant's needs. Throughout a feeding, watery foremilk is expressed first, which should satisfy the infant's thirst. It is followed by hind milk, which is richer in fat and energy, as well as total protein content [178, 179]. Breast milk composition also changes over the lactation period. During the first week colostrum is

expressed, then transient milk to about 30 days postpartum (p.p.), followed by mature milk after 30 days p.p. Mature milk consists of about 87% water and the average overall content of protein, fat and lactose is 0.9-1.2 g/dl, 3.2-3.6 g/dl and 6.7-7.8 g/dl, respectively [180]. The energy contained in breast milk is estimated around 65-70 kcal/dl [180]. Breast milk also contains all of the necessary vitamins, trace elements and essential minerals for newborns to grow and develop [181].

Breast milk does not only have nutritive aspects but also many bioactive components and is therefore very important to help the newborns still developing immune system [182]. Antibodies, exosomes, micro RNAs, immune cells and many more components are present in breast milk (most essential ones shown in Table 1). Many of these immunologically important compounds even survive the newborn's stomach, since the pH (3-6) is much higher as in adults (1-3) [183, 184].

Table 1: Important breast milk components

Breast milk components	**Reference**
Major milk proteins:	
β-casein	[185]
κ-casein	[186]
α-lactalbumin	[187]
Lactoferrin	[188-191]
Lysozyme	
Immunoglobulins:	
Secretory IgA (sIgA)	[192]
IgG	[193]
IgM	
IgE	
Micronutrients, minerals and vitamins	[194, 195]
Milk fat lipid globules and their membrane proteins	[196-198]
Microbiota	[199]
Growth factors, hormones, peptide hormones and glucocorticoids	
Proteases and other enzymes	[200-202]
Other proteins: Serum albumin, haptocorrin, α-antitrypsin, osteopontin, folate binding protein, complement system proteins	[187, 203-207]
Oligosaccharides	[208]
Cytokines, chemokines, adipokines	[209]
Metabolic compounds: Urea, glutathione, creatinine, carotene	
Exosomes	[210]
Amino acids	[211]
Nucleotides, micro RNAs	[212]
Breast milk cells (BMC)	[213]

Breast milk is therefore considered very important for the infant. For the first six months after birth, it is recommended by the World Health Organization (WHO) to exclusively feed breast milk [214]. It was also shown that infections to the upper and lower respiratory tract, as well as to the gastrointestinal tract, were significantly reduced in infants breast fed exclusively for at least four to six months [215-218]. Breastfeeding was even associated with higher intelligence test scores in children and adolescents [219, 220].

3.4.3 Immunological active components in breast milk

Many of the described components of breast milk in Table 1 carry out immunological functions to help protecting the infant from infections. For example, lactoferrin was shown to be microbicidal, regulating immune cell activation, migration and growth, as well as showing anti-inflammatory functions [191, 221]. Oligosaccharides protect the infant's gut from pathogenic bacteria and are prebiotic for beneficial microbes [222, 223]. Lipids, nucleotides, casein, cytokines, lactalbumin, lysozyme and many other components show immunological effects on the infant's health or immune system [182, 224-228] (Figure 9).

3.4.4 Antibodies in breast milk

B cells home to the mammary gland and effectively produce high amounts of antibodies (mostly sIgA), while the secretory epithelial cells are transporting the antibodies via the polymeric Ig receptor (pIgR) into the lumen of the alveoli [229]. Some B cells are also found in breast milk, mostly consisting of highly activated plasma cells [171]. Immunoglobulins in breast milk in general are very important for the infant. The newborn infant's immature immune system has some humoral protection by IgG transferred through the placenta, but is IgA deficient [230-232]. Accordingly, sIgA is the most abundant antibody in colostrum and transient milk followed by much lesser amounts of IgM and IgG [233]. sIgA is not reaching the infants circulation [234], but it can protect the infant gut's mucosal surfaces by binding bacteria, other pathogens or toxins [235] (Figure 9). Immunoglobulins in breast milk were shown to be mostly directed against intestinal or respiratory pathogens of the mother [182, 232, 236]. It was reported that total sIgA declines into mature milk whereas IgG frequencies of total immunoglobulins increase, whereas IgM constantly stays at a low level [207].

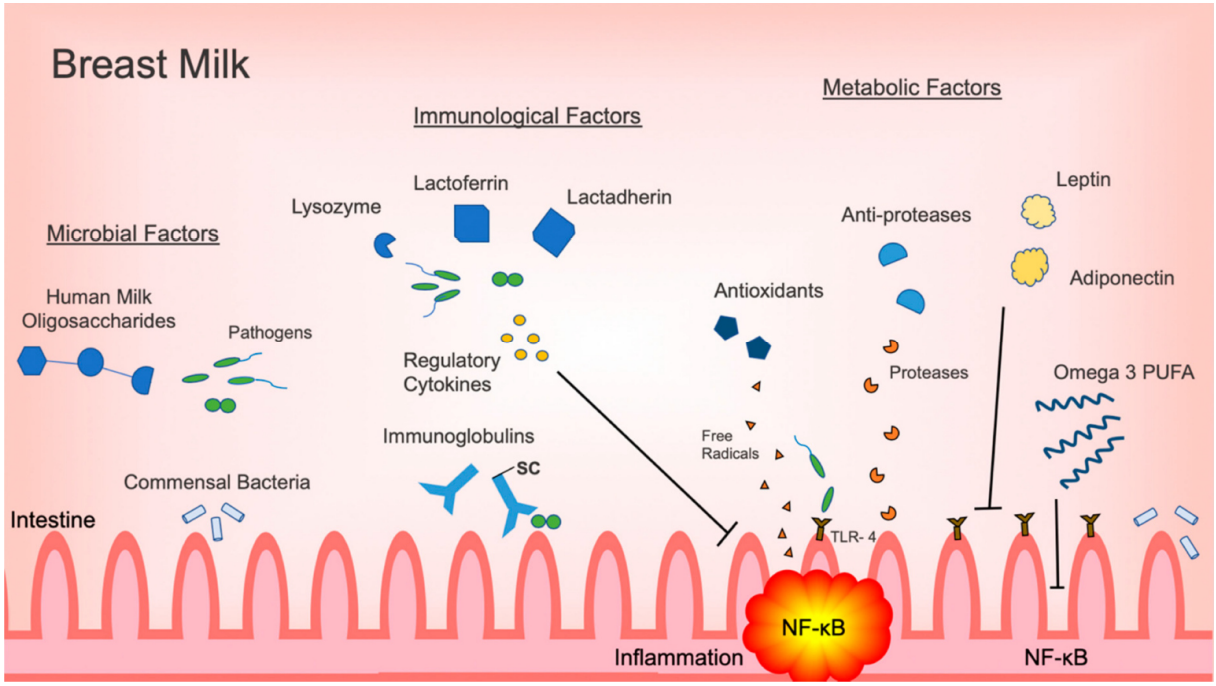

Figure 9: Immune supporting components of breast milk for preventing inflammation of the infant's gut. *Breast milk has microbial, immunological and metabolic factors, which can all contribute to the protection of the infant's intestine. Abbreviations stand for secretory component (SC), polyunsaturated fatty acid (PUFA) Toll-like receptor 4 (TLR4), nuclear factor kappa-light-chain-enhancer of activated B cells (NF-κB). Adapted from Thai and Gregory [228].*

3.4.5 Breast milk cells

Breast milk cells (BMCs) mainly consist of epithelial cells with up to 98%, comprising lactocytes, myoepithelial cells and ductal epithelial cells [213, 237] (Figure 10). However, other cells, like stem cells and leukocytes, are also present [238]. Leukocyte frequencies decrease during the lactation period. In colostrum 13 to 70% of cells consist of leukocytes, while in mature milk of healthy mothers only 0-2% of total BMCs are leukocytes [239]. The frequency of leukocytes can show an increase from 2 to as much as 94%, when the mother is infected with a pathogen [240]. The main leukocyte populations were reported to be monocytes/macrophages (55-60%), followed by neutrophils (30-40%), and lymphocytes (5-10%) [236]. The lymphocytes mainly consist of T cells (~83%), followed by B cells (4-6%) [241]. Most leukocytes in breast milk seem to be activated. T cells mainly consist of HLA-DR and CD25 expressing, activated effector memory T cell phenotypes in breast milk [242-244]. Breast milk of mothers with term infants shows very little differences to breast milk leukocyte populations of mothers with preterm infants [245].

In humans, the role of immune cells in breast milk is not well understood and needs further investigation. If the cells are there to protect the mammary gland or the breastfed infant from pathogens is unclear. However, studies in animals and a few in humans showed an immune modulating effect of milk leukocytes on infant's pediatric disease developments [246].

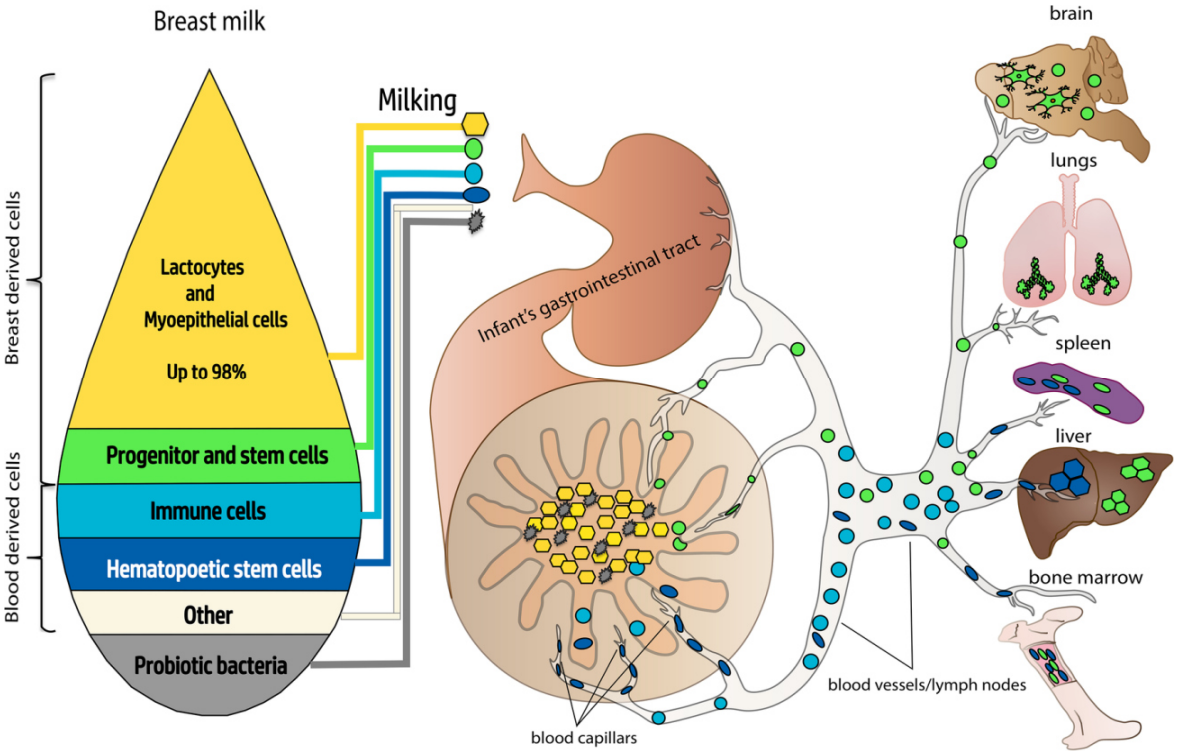

Figure 10: Breast milk cells.
Breast milk mainly consists of epithelial cells, like lactocytes and myoepithelial cells with up to 98%. Other breast derived cells are progenitor and stem cells. Blood derived cells consist of immune cells, like T cells, B cells, monocytes and macrophages, hematopoietic stem cells and others. Probiotic bacteria are also present and help colonize the infant's gut. Stem cells and immune cells might even reach the infants circulation or different organs. Adapted from Ninkina et al. [238]. With permission: http://creativecommons.org/licenses/by/4.0/, no changes made.

Another component of breast milk is bacteria. The breast milk microbiome helps colonizing the infant's gut [247]. Many different bacteria were found [248].

3.5 HCMV in breast milk

In addition to those milk components supporting the infant's healthy development, breast milk is also harboring HCMV as published first by Diosi et al. [249] in 1967. Methods used for detection of HCMV in breast milk include PCR (mostly IE1 nested PCRs and real-time PCR, DNAlactia), as well as microculture assays to isolate the virus (virolactia).

Around 95% of all HCMV IgG-seropositive, immunocompetent and healthy mothers locally reactivate the virus in the mammary gland shedding it into breast milk without establishing a systemic infection [250-253]. Without viral DNAemia during the perinatal [254] or postnatal phase [255, 256], additional other sites of HCMV shedding with much lesser frequencies were found in urine, saliva or cervical swabs. HCMV in breast milk can reactivate as early as in the

first week (colostrum) and is usually shed until around three months p.p. [257, 258]. During this period, most reactivations display a self-limited, unimodal course with peak viral loads highly differing from 10^3 to 10^6 copies/ml [258]. The reactivation event in the mammary gland is not fully understood [251]. Transmission to the child seems to appear in about 37 – 42% of cases. Cell-free virus in milk whey is the most frequent mother-infant transmission route. Accordingly, HCMV transmission can occur without any cell-associated virus [250, 251]. BMCs were found less often positive for HCMV DNA than milk whey [252, 259]. Term infants usually show no symptomatic infection, but HCMV infection by maternal breast milk can lead to severe symptoms in preterm infants with gestational age (GA) under 32 weeks or a birthweight under 1500 g [260-262]. Maschmann et al. [260] described symptoms like hepatopathy, neutropenia, thrombocytopenia and sepsis-like deteriorations. Meier et al. [250] found similar symptoms including hepatitis with cholestasis/icterus, sepsis-like symptoms and severe neutropenia with second-stage bronchopulmonary dysplasia due to postnatally acquired HCMV. Postnatally acquired HCMV colitis and volvulus were recently described [263, 264]. However, the clinical presentation of HCMV infections of preterm infants via breast milk is not as well defined as the clinical presentation of infections of immunosuppressed transplant recipients [41].

Breast milk can be pasteurized to avoid transmission and infection of preterm infants. Different methods like Holder pasteurization (30 min, 62.5°C) or short-term pasteurization (5 sec, 62°C) are applied to eliminate viral infectivity [265, 266], but can also decrease the functionality of immunologically important components. More gentle methods like freeze thawing are less common, since freeze thawing does not reliably eliminate viral infectivity. Nevertheless, it can decrease viral loads [266-268].

Monitoring the immune response to HCMV reactivations in breast milk offers the possibility to observe virus induced changes of the immunological profile in a healthy, not immunosuppressed, individual. However, few data are available. This thesis is an approach to obtain data on the different immune profile modulations by HCMV.

3.6 Aims

Breast feeding is one of the most efficient vertical transmission routes of HCMV. In extremely preterm born infants, this may result in severe disease. The mechanism and the immune response to local HCMV reactivation in the mammary gland in otherwise healthy individuals are far from being understood. Breast milk harbors many immunologically active components. For instance, it is still widely unknown how or if at all HCMV influences the leukocyte subsets or immunoglobulins in breast milk during its local reactivation process. Most studies use snapshots for analysis, but since breast milk is a highly dynamic fluid, it is important to perform longitudinal studies to monitor time depended variations during the reactivation kinetics of HCMV. Therefore, the major aim of this thesis was to longitudinally investigate the impact of a local HCMV reactivation on breast milk components like antibodies, cytokines, and leukocyte subpopulations compared to their counterparts in corresponding blood samples. Several immunological and virological aspects were investigated under the following questions:

1. Are there fluctuations in the proportions of immune cell subsets over time under local HCMV reactivation in breast milk of HCMV-seropositive compared to –seronegative mothers? Is there any evidence of a compartmentalization of immune cell phenotypes in breast milk versus blood?
2. Is it possible to identify HCMV-specific T cells in breast milk and are they accumulating in breast milk or blood?
3. Regarding the humoral immunity: Do HCMV-specific IgG concentrations in milk whey increase compared to plasma due to the local HCMV reactivation? Additionally, are milk whey IgGs directed against the same main HCMV-antigens than plasma IgGs or does a compartmentalized antibody pool exist in milk?
4. By looking at the expression level of 92 proinflammatory cytokines in breast milk whey: exist defined expression patterns in HCMV-seropositive mothers compared to -seronegative?

4 Materials and Methods

4.1 Material

4.1.1 Study cohorts

The investigated cohort consisted of mothers who mostly delivered preterm infants at the Neonatology Department of the Children's Hospital Tuebingen. For analysis, breast milk samples or breast milk with corresponding blood samples were collected at defined time ranges. The total numbers of participating mothers are shown in Figure 11. A clinical-virological study termed BlooMil and individual courses of mothers termed A to D were highlighted, since the main results are based on them. Anti-HCMV-IgG-seropositive individuals were called HCMV^{+}, pos or HCMV-seropositive in the following (same was done for HCMV-seronegative individuals). In the beginning of this work, breast milk samples were collected in the Neonatology Department without knowledge of the HCMV-serostatus, to generate general information in cytospin preparations.

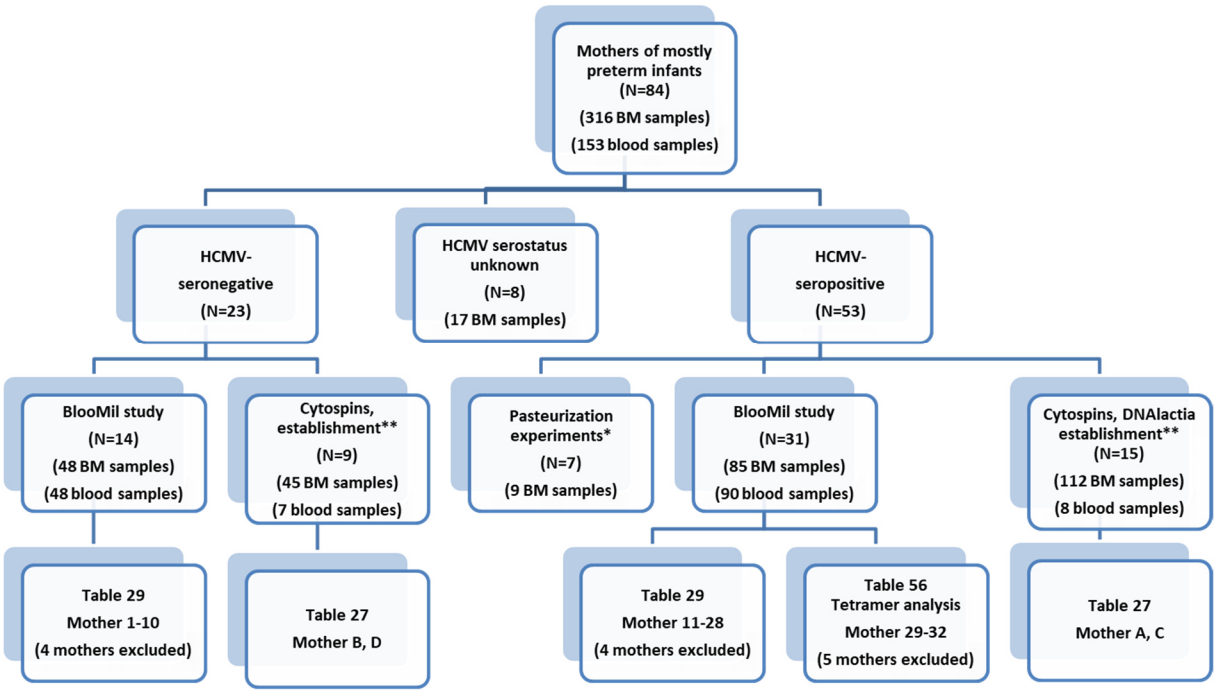

Figure 11: Organigram of participating mothers and samples acquired.
**for the pasteurization experiments short-term, Holder pasteurized as well as raw milk was used for neutralization assays. **Despite the BlooMil study, breast milk and few blood samples were collected between 12/2016 and 3/2018 for Cytospin preparations, nPCRs, qPCRs, establishment of methods, like HCMV-IgG measurements from whey, cell counts, total protein amounts (mother A and B), flow cytometry tests including γδ T cells (mothers C and D).*

4.1.2 Cells

Human Foreskin Fibroblasts (HFF, SCRC-1041™, ATCC®, Manassas, VA, USA) were purchased and used up to cell passage 40.
Human retinal pigment epithelial cells (ARPE-19, CRL-2302™, ATCC®) were purchased and used up to cell passage 25.

4.1.3 Virus

The clinical isolate H2497-11 was used for neutralization assays. The virus was isolated from amniotic fluid of a terminated pregnancy in Tuebingen in 2011. The amnion fluid was directly inoculated following a high-speed centrifugation step of 50,000g on epithelial cells (ARPE-19) This primary cell associated clinical isolate was cultured for 22 passages on ARPE-19 epithelial cells to generate cell-free virus.
AD169, a high passage HCMV laboratory strain, was used as positive control for nested PCRs.

4.1.4 Equipment

Table 2: Equipment

Equipment	Company
Microscopes	
Diavert	Leitz
Labovert FS	Leitz
Axiolab 66238C	Zeiss
Olympus BX51 TF	Olympus
Microscope cameras	
TK-C1380	JVC
Olympus DP71	Olympus
Centrifuges	
Eppendorf centrifuge 5415D (max. 16,100 g)	Eppendorf
Eppendorf centrifuge 5804R (max. 20,913 g)	Eppendorf
Eppendorf centrifuge 5810R (max. 20,913 g)	Eppendorf
Universal 32R (max. 4,193 g)	Hettich Zentrifugen
Centra GP8R Unity lab (max. 4,550 g)	International Equipment Company (IEC)
Heraeus Multifuge X3 FR (max. 25,314 g)	Thermo Scientific
Shandon Cytospin3 (max. 451 g)	Thermo Scientific
Biofuge Stratos (max. 50,377 g)	Thermo Scientific
Cell culture	
96-well cell culture plate (Advanced TC™)	Greiner Bio-One (#655980)
CELLSTAR® cell culture flask 50 ml 25 cm²	Greiner Bio-One (#690175)
CELLSTAR® cell culture flask 250 ml 75 cm²	Greiner Bio-One (#658175)
BD™LSR II	BD Biosciences
Cobas 6000 Analyzer (module e601)	Roche
Eppendorf Bio Photometer	Eppendorf
Fine scale	Kern

Incubator 37°C; 5% CO_2; 97% rAh BBD 6220	Heraeus
Incubator 37°C; 5% CO_2; 97% rAh C200	Labotect
pH-meter MultiCal®	WTW
QIAcube	Qiagen
Thermal Cycler MJ Research PTC-200	MJ Research Inc.

4.1.5 Reagents

Table 3: Reagents

Reagents	Catalog number	Company
2N HCl	# 1.09063.1000	Merck
3-amino-9-Ethyl-carbazole (AEC)	# A-5754	Sigma
Acetone pro analysi (p.a.)	#LC-4916.2	BioFroxx
Anti-Mouse Ig, κ/Negative Control Compensation Particles Set	#552843	BD Biosciences
Bromphenol blue Xylene Cyanole dye solution (0.5% bromphenol blue, 0.5% xylen cyanole)	# B3269-5ML	Sigma-Aldrich
Clean	# 340345	BD
Dimethyl sulfoxide (DMSO)	# 20385.01	Serva
dATP [100 mM]	# U120A	Promega
dCTP [100 mM]	# U122A	Promega
dGTP [100 mM]	# U121A	Promega
dTTP [100 mM]	# U123A	Promega
Ethylenediamine tetraacetic acid (EDTA, analytical grade)	# 11278.02	Serva
Ethanol absolute EMSURE®	# 1.00983.1011	Merck
Ethidium monoazide bromide (EMA)	# 40015	Biotium
Fetal calf serum (FCS)	# 10500	Gibco
FicoLite-H	# GTF1511KYK	Linaris-blue
Flow	# 342003	BD
Formamide	# A2156,0100	AppliChem
Giemsa's azur eosin methylene blue solution	# 1.09204.1000	Merck
Glacial acetic acid	# 1.00063.2511	Merck
H_2O_2, 30%	# 1.07209.0250	Merck
Mayers hamalaun	# 1.09249.0500	Merck
May-Gruenwald's eosin methylene blue	# 1.01352.0025	Merck
Methanol p.a.	# 20847.307	Prolabo
Midori green Advance	# MG04	Nippon Genetics Europe GmbH
Mineral oil	# M5904	Sigma
Mouse serum	# S25-10ML	Merck Millipore
N,N-Dimethylformamide (DMF)	# D-4551	Sigma

Penicillin/streptomycin (pen/strep)	# 15140-122	Gibco
Rinse	# 340346	BD
Sodium chloride (NaCl)	# 1.06404.1000	Merck
Sodium azide (NaN_3, 10%)	# 13553.001	Morphisto
Sodium acetate	# 1.06268.0250	Merck
SeaKemLE agarose	# 50004	Lonza Group AG
Trizma® base	# T-6066	Sigma
Trypan blue	# T-8154 20ML	Sigma
TrypLE™ Express (trypsin)	# 12604-013	Gibco
Tween®20	# 8.22184.0500	Merck

Table 4: Enzymes

Enzymes	**Catalogue number**	**Company**
ScaI (5´…AGT'ACT…3´, 3´…TCA'TGA…5´)	# R0122	New England Biolabs (NEB)
Hin6I (5´…G'CGC…3´, 3´…CGC'G…5´)	# R0124S	NEB
RsaI (5´…GT'AC…3´, 3´…CA'TG…5´)	# R0167S	NEB

4.1.6 Buffers and Solutions

Table 5: Buffers and solutions

Buffers/solutions	**Composition / Company**
AEC stock solution	0.4% AEC In DMF
AEC working solution	5% AEC stock solution Diluted in sodium acetate buffer 0.1% H_2O_2
Brilliant Stain Buffer	BD Horizon™ (# 563794)
CutSmart® buffer (pH 7.9)	NEB (# B7204S)
Dulbecco's Phosphate buffered Saline (PBS) pH 7	SIGMA (# D8537) /GIBCO (# 14190-169)
Flow cytometer staining buffer (PFEA)	PBS with: 2% FCS 2 mM EDTA 0.01% sodium azide
Hank's Balanced salt Solution with sodium bicarbonate (HBSS)	Sigma Aldrich (# H6648)
Loading dye	20% Bromphenol blue Xylen Cyanole dye solution Diluted in formamide
Red blood cell (RBC) lysis buffer 10x	Biolegend (#420301)
Sodium acetate buffer	Stock solution 10x: 1 M sodium acetate

	2.9% glacial acetic acid Diluted in ddH_20 pH 4.9 (adjusted with HCl)
Tris/borat/EDTA buffer 10x (TBE, pH 8.3)	Roth (# 3061.1)
Tris-buffered saline 10x (TBS)	Stock solution 10x: 0.5 M Trizma® base 1.5 M NaCl Diluted in ddH_2O pH 7.6 (adjusted with HCl)
TBS wash buffer	1x TBS + 0.2% Tween®20

Table 6: Cell culture media

Cell culture media	**Company / Composition**
Dulbecco's Modified Eagle's Medium (DMEM), high Glucose w/o PYR, w/ HEPES	Gibco (# 42430-085) + 5/10% FCS + 100 U/ml Penicillin/streptomycin
DMEM:F-12	ATCC® (# 30-2006™) + 5/10% FCS +100 U/ml Penicillin/streptomycin
Roswell Park Memorial Institute (RPMI-1640)	Sigma Aldrich (# R8758)
Luria Broth (LB) broth	Carl Roth (# X968.2) 5 g LB-broth + 250 ml VE H_2O autoclaved

4.1.7 Reagent kits

Table 7: Kits

Kits	**Catalogue number**	**Company**
α-Naphthyl acetate esterase	# 91A-1KT	Sigma-Aldrich
CMV R-gene®	# 69-003B	Argene (Biomerieux)
LightCycler FastStart DNA Master HybProbe	# 03003248001	Roche
Nucleo Spin Gel and PCR clean-up	# 740609.50	Macherey-Nagel
Plasmid DNA purification NucleoBond® Xtra Midi	# 740410.50	Macherey-Nagel
PWO Master	# 03 789 403 001	Roche
Qiaamp blood mini	# 51106	Qiagen
RecomLine CMV IgG [avidity] / IgM	# 5572 / 5573	Mikrogen Diagnostik
Taq DNA polymerase	# 11 418 432 001	Roche

4.1.8 Immunoglobulin preparations, antibodies and tetramers

Table 8: Antibodies

Antibodies	Conjugate	Catalogue number	Clone	Company
Cytotect® CP (100 E/ml infusion solution IgG subclasses: 65% IgG1, 30% IgG2, 3% IgG3, 2% IgG4, IgA<2mg/ml)	-	# 626010	-	Biotest
GAMUNEX-C 10% (immunoglobulin: IgG subclasses: 62.8% IgG1, 29.7% IgG2, 4.8% IgG3, 2.7% IgG4, IgA<84mg/ml)	-	# 10920606	-	Grifols
Anti-HCMV-IEA	-	# 11-003	E13	Biomerieux
Polyclonal rabbit anti-mouse-immunoglobulins	Horseradish Peroxidase (HRP)	# P026002	-	DakoCytomation
Anti-IgA pure, human	-	# 130-093-073	IS11-8E10	MACS Miltenyi Biotec

Table 9: BlooMil antibodies and fluorophore conjugates

BlooMil antibodies	Conjugate	Catalogue number	Clone	Company
Mouse Anti-Human cluster of differentiation (CD) 3	Alexa Fluor® (A) 700	# 557943	UCHT1	BD Pharmingen™
Anti-human CD4 antibody	Brilliant Violet (BV) 605™	# 317438	Okt 04	Biolegend
Mouse anti-Human CD8	Allophycocyanine (APC)-H7	# 560179	SK1	BD Pharmingen™
Anti-human CD14 antibody	Phycoerythrin (PE)-Cy7	# 301814	M5E2	Biolegend
Anti-human CD38 antibody	PE	# 356604	HB-7	Biolegend
Anti-human CD45 antibody	BV 421™	# 304032	HI30	Biolegend
Anti-human CD45RA antibody	APC	# 304112	HI100	Biolegend
Anti-human CD56 (Neural cell adhesion molecule (NCAM)) antibody	Fluorescein isothiocyanate (FITC)	# 318304	HCD56	Biolegend

Anti-human CD197 (C-C chemokine receptor type 7 (CCR7)) antibody	Biotin	# 353240	G043H7	Biolegend
Streptavidin Brilliant Violet 510™	BV 510™	# 405234	-	Biolegend
Mouse Anti-Human HLA-DR	Peridinin-Chlorophyll-Protein (PerCP)-Cy™5.5	# 552764	G46-6	BD Pharmingen™

Table 10: Additional antibodies for individual courses C and D

Individual courses mother C and D antibodies	**Conjugate**	**Catalogue number**	**Clone**	**Company**
Anti-human CD4 antibody	BV 711™	# 317440	OKT-4	Biolegend
Mouse anti-human CD197 (CCR7)	PE	# 560765	150503	BD Pharmingen™
Purified Mouse Anti-Human TCRγ/δ	-	# 347900	11F2	BD Pharmingen™
F(ab')2-Goat anti-Mouse IgG (H+L) Cross-Adsorbed Secondary Antibody	Pacific Orange™ (PO)	# P31585	-	Invitrogen
TCR V delta 1 Monoclonal Antibody	FITC	# TCR2730	TS8.2	Thermo Fisher Scientific
Anti-human TCR Vδ2 Antibody	PerCP	# 331410	B6	Biolegend

Table 11: HLA-A2 typing

HLA-A2 antibody	**Conjugate**	**Catalogue number**	**Clone**	**Company**
Anti-human HLA-A2 antibody	PE	# 343305	BB7.2	Biolegend

Table 12: Tetramers

Tetramer allele	**Conjugate**	**Peptide**	**Catalogue number**	**Company**
HLA-A*02:01	APC	pp65 (495-504) NLVPMVATV	# HA02-010 (APC)	Tetramer Shop
HLA-A*02:01	PE	pp65 (495-504) NLVPMVATV	# HA02-010 (PE)	
HLA-A*02:01	APC	IE1 (316-324) VLEETSVML	# HA02-028 (APC)	
HLA-A*02:01	BV510	IE1 (316-324) VLEETSVML	# HA02-028 (BV510)	

4.1.9 Primer

Table 13: nested IE1-Exon 4 PCR primer

Primer	Nucleotide position	Sequence 5'-3'
IEP4 C (outer)	1729 - 1748	TGA GGA TAA GCG GGA GAT GT
IEP4 D (outer)	1951 - 1970	ACT GAG GCA AGT TCT GCA GT
IEP4 D* (outer)	1951 - 1970	A**T**T GAG GCA AGT TCT G**T**A **AC**
IEP4 A (inner)	1767 - 1786	AGC TGC ATG ATG TGA GCA AG
IEP4 A* (inner)	1767 - 1786	A**A**C T**CT** AT**A** ATG TGA **C**CA AG
IEP4 B (inner)	1970 - 1951	GAA GGC TGA GTT CTT GGT AA

Table 14: gB PCR primer and probes

Primer	Nucleotide position	Sequence 5'-3'
gB-F	83228 - 83209	TAC CCC TAT CGC GTG TGT TC
gB-R	82975 - 82994	ATA GGA GGC GCC ACG TAT TC
Fluorescein probe	83050 - 83026	CGT TTC GTC GTA GCT ACG CTT ACA T-Fluorescein
LightCycler (LC) Red-640	83023 - 83001	LCRed640 - ACA CCA CTT ATC TGC TGG GCA GC - PH

Table 15: UL10-13 primer for half-nested PCR (RFLP)

Primer	Nucleotide position	Sequence 5'-3'
pg1up (forward primer)	17973 - 17992	ACG GGT CTG CCG AAA GGC TT
pg3do (outer reverse primer)	20110 - 20091	ACC GTC AGT TGT TGG CGT AG
pg2do (inner reverse primer)	19945 - 19926	ACG GGT CTG CCG AAA GGC TT

4.1.10 Software

Software	Company
BD FACSDiva™ (version 6.1.3)	BD Biosciences
Chromas (version 2.6.5)	Technelysium Pty Ltd
EndNote X9 (Bld 12062)	Clarivate Analytics
FlowJo (version 10.6.1)	BD Biosciences
GraphPad Prism (version 8.1.0)	GraphPad Software Inc.
LightCycler® Software 4.1	Roche
Microsoft Office 2016	Microsoft
SPSS (version 25.0.0.1)	IBM
SwissLab (version 2.21.10)	Nexus / SWISSLAB GmbH

4.2 Methods

4.2.1 Cell culture

HFF or ARPE-19 cells were cultivated in T75 flasks. At a confluency of approximately 80 to 90% cells were splitted three-fold (ARPE-19) or two-fold (HFF). Therefore, medium was aspirated, and the cell layer was washed once with PBS with 1% penicillin-streptomycin (pen/strep, Thermo Fisher Scientific, Waltham, Massachusetts, USA). Afterwards, 3 ml Trypsin were added and incubated for 6-8 min or until cells detached at 37°C and 5% CO_2. Finally, 9 ml of medium (DMEM with 10% FCS and 1% pen/strep for HFF and DMEM:F12 medium with 10% FCS and 1% pen/strep for ARPE-19 cells) were added and the cell suspension was equally distributed into the new flasks and medium was added until 12 ml were reached. The cells were maintained at 37°C and 5% CO_2 with medium exchanges every 2-3 days (HFF) or every week (ARPE-19).

4.2.2 Breast milk fractionation

Freshly pumped or up to four hours old (stored at 4°C) breast milk (up to 80 ml) was collected in the Department of Neonatology of the Children's Hospital Tuebingen. The mothers used the breast milk pump Symphony from Medela Medizintechnik (Echingen, Germany). The breast milk fractionation protocol was based on Hamprecht et al. [269]. Shortly, breast milk was centrifuged at 500 g for 10 min at 4°C. The creamy fat top layer was discarded and the middle layer, consisting of whey, was centrifuged again at 1780 g for 10 min and sterile filtrated using a 0.45 µm pore size. The cell pellet from the first centrifugation step was washed twice with 2.5 ml PBS at 400 g for 5 min. Afterwards, the cells were resuspended in 1 ml PBS and a 40 µm EASYstrainer (Greiner Bio-One, Kremsmuenster, Austria) was used to separate cell aggregates. Cells were then counted under a two-fold trypan blue dilution in a Neubauer chamber and diluted to the working concentrations, needed for each experiment.
If the cell pellet showed a slightly red coloration during the breast milk fractionation, the samples were indicated with a different data point in the graphs. The red coloration presumably is from erythrocytes and might therefore indicate mastitis.

4.2.3 Blood sample preparation

Mothers were asked to additionally donate up to 9 ml EDTA-blood. The pumping of breast milk and the blood donation was not further apart than one and a half hours. Equal volumes of EDTA-Blood and HBSS (Sigma-Aldrich, St. Louis, MO, USA) were mixed in a 50 ml falcon tube. 15 ml of Fico-H Lite (Linaris Blue, Dossenheim, Germany) warmed up to RT were added to another 50 ml falcon tube and carefully overlayed by the diluted EDTA-blood. The Ficoll-gradient was centrifuged at 810 g for 25 min at 20°C. After centrifugation, 5 ml of the top layer

plasma were frozen at -80°C as 1 ml aliquots. The interphase, containing peripheral blood mononuclear cells (PBMCs) was extracted from the gradient and washed 3 times with 50 ml of HBSS at 200 g for 10 min. At the last washing step 10 µl were taken for cell counting and mixed with 10 µl of trypan blue. After the washing steps the cell pellet was resuspended in RPMI medium (Sigma-Aldrich) and diluted to an end concentration of $1x10^6$ cells/ml and used for the FACS staining procedures.

4.2.4 Experiments with whey and plasma

Different experiments were performed with either breast milk whey and plasma or with PBMCs and BMCs (see 4.2.5). A short overview of the main experiments is given in Figure 12.

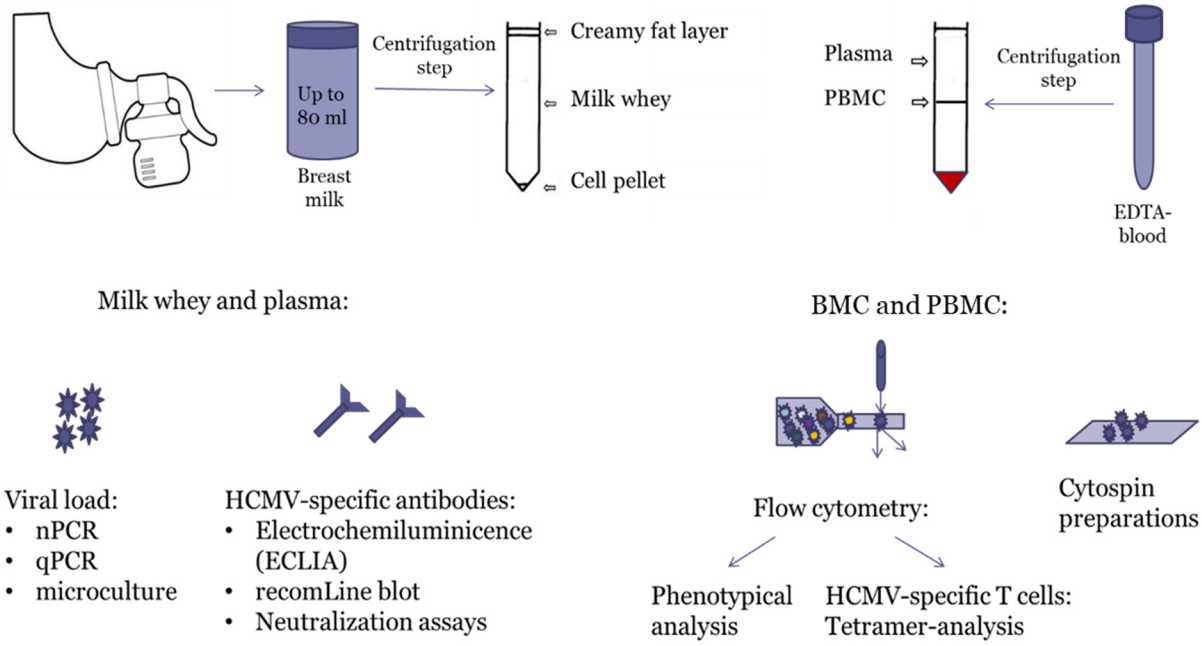

Figure 12: Schematic figure of methods used for the BlooMil study.
Breast milk and blood were obtained from mothers of mostly preterm infants in the Department of Neonatology at the University Hospital Tuebingen. Milk whey and plasma as well as breast milk cells (BMCs) and peripheral blood mononuclear cells (PBMCs) were gained by several centrifugation steps and used for the shown experiments in the graph.

4.2.4.1 Virus isolation procedures

Sterile filtrated milk whey was used to detect infectious virions. This was mainly done by the routine diagnostic lab and performed as described before [269]. In total, 2 ml of milk whey for short- and long-term microculture were equally aliquoted into two ultra-centrifugation tubes (á 1 ml) and centrifuged at 50,000 g for 1h at 4°C (Biofuge Stratos, Thermo Scientific, Waltham, MA, USA). The supernatant was discarded, and both pellets were resuspended in 400 µl DMEM + 5% FCS each. On the previous day, two 96 well microtiter plates were seeded with $2x10^4$ human foreskin fibroblasts (HFF) per well in a volume of 100 µl. The next day, the medium overlay of the fibroblasts was aspirated, and four wells of each plate were filled with

100 µl of the concentrated virus resuspension. Microplates were centrifuged for 30 min at 200 g and afterwards incubated for 30 min at 37°C in 5% CO_2. Then 100 µl DMEM with 5% FCS were added to each well. The first plate was incubated for 36 h and the second plate for 14 days. After the 36 h short-term incubation a staining procedure followed (see below). The plate with the 14 days long-term incubation period was controlled every two days for the manifestation of HCMV-specific cytopathic effects (CPE) and medium was exchanged once. If an HCMV-specific CPE was detected, virus infected cells were trypsin-treated and transferred to a small cell culture flask previously seeded with HFF (approximately 70% confluency). When the CPE reached 90% confluency, the cells were resolved and frozen at -80°C in DMEM with 10% DMSO and 20% FCS.
A similar microculture procedure was performed for BMCs diluted to a concentration of $1.5x10^6$ cells/ml and 100 µl of the cell suspension were added to the microtiter plate per wells. The same procedures for short and long-term microculture as described above were applied after inoculation with BMCs.

4.2.4.2 Immediate early staining procedure

The following immuno-staining protocol was used to detect immediate early antigens (IEA) in fibroblast (HFF) nuclei of the microculture assays and neutralization assays. The cells were fixed with 100 µl/well of equal volumes of ethanol and acetone for 5 min at RT. The ethanol/acetone mix was aspirated and 200 µl TBS wash buffer (TBS with 0.2% Tween20) per well were added. The microtiter plates were incubated for 20 min at 37°C + 5% CO_2. HCMV IE1 antibody (bioMérieux, Marcy-l'Étoile, France) was diluted 500-fold in PBS with 0.5% FCS. After the incubation, the TBS wash buffer was aspirated from the wells and 100 µl/well HCMV IE1 antibody solution was added and incubated for 1 h at 37°C and 5% CO_2. The wells were washed three times with 200 µl TBS wash buffer and 100 µl/well secondary rabbit anti-mouse antibody coupled with HRP were added per well in a 500-fold dilution in PBS with 0.5% FCS. After a one hour incubation at 37°C + 5% CO_2, another washing procedure was performed. The 0.4% (w/v) AEC stock solution in DMF was used to prepare the working solution with a 20-fold dilution in sodium-acetate buffer and 0.1% H_2O_2. 100 µl of the working AEC-solution was added to each well and incubated for 20 min at 37°C and 5% CO_2. The wells were washed with 200 µl TBS wash buffer followed by a wash step with 200 µl PBS. Microtiter plates were directly analyzed or stored in 200 µl/well PBS at 4°C. For analysis, red to brownish colored fibroblast nuclei were then counted as IE1 positive cells, either each one or as plaque (≤7 infected nuclei).

4.2.4.3 DNA extraction

DNA extraction of 200 µl of different material (plasma, breast milk whey, BMCs ($1.5x10^5$)) was performed with the QIAamp Blood Mini Kit using the Qiacube DNA Extractor (Qiagen, Hilden, Germany). Elution volume was 100 µl.

4.2.4.4 IE1-Exon 4 nested PCR

A nested PCR (nPCR) was performed as described earlier [270], except for the following modifications. Mastermix' were prepared as described in Table 16 and Table 17. Mastermix 1 was once prepared with primer IEP4 D and once with the mutation primer IEP4 D*, the same counts for mastermix 2 and IEP4 A/A*. Mastermix' were prepared for 100 samples and stored at -20°C until usage.

Table 16: nested PCR mastermix 1 for the first round (per sample)

	Final concentration	**Amount [µl] per sample**
IEP4 C [100 pmol/µl]	0.1 µM	0.05
IEP4 D / D* [100 pmol/µl]	0.1 µM	0.05
Tween20	1%	0.5
PCR buffer [10x, 100 mM Tris-CL pH 9.6, 500 mM KCL]	1x	5
$MgCl_2$ [25 mM]	2.5 mM	5
dNTP [25 mM each]	100 µM (each)	0.2
H_2O		29.2

Table 17: nested PCR mastermix 2 for the second round (per sample)

	Final concentration	**Amount [µl] per sample**
IEP4 A / A* [100 pmol/µl]	0.4 µM	0.2
IEP4 B [100 pmol/µl]	0.4 µM	0.2
10x PCR buffer [100 mM Tris-CL pH 9.6, 500 mM KCL]	1x	5
$MgCl_2$ [25 mM]	2.5 mM	5
dNTP [25 mM, each]	200 µM (each)	0.4
H_2O		28.2

For the first round, 45 µl mastermix 1 or 1* (Table 17), 1.3 µl Taq-polymerase and 5 µl from the DNA extract of whey, plasma or BMCs were mixed and a PCR was run on Thermal Cycler MJ Research PTC-200 (MJ Research, Inc., Waltham, MA, USA) as described in Table 18. The second round followed with 44 µl mastermix 2 or 2*, 1.3 µl Taq-polymerase and 5 µl template of the first round. The PCR program was run as described in Table 18, but without the initial denaturation step.

Table 18: nested PCR program

Step	Temperature [°C]	time	Cycles (1. round)	Cycles (2. round)
Initial denaturation	93	5 min		-
Denaturation	91	30 sec	20x	30x
Annealing	56	1 min		
Elongation	72	1 min		
Final elongation	72	10 min		

4.2.4.5 Gel electrophoresis

Agarose gels were used for detection of DNA amplificates. A 3% gel was generated using 1.5 g SeaKemLE agarose (Lonza Group AG, Basel, Switzerland) in 50 ml 1xTBE buffer (10x, Carl Roth GmbH + Co. KG, Karlsruhe, Germany) and heated in the microwave until the agarose melted. 1.5 µl Midori Green Advance DNA Stain (Nippon Genetics Europe GmbH, Dueren, Germany) were added and the solution was poured into a gel chamber with either eight or 15 comb slots. After 30 min the gel was cold and used in a horizontal gel electrophoresis chamber (HB710 Hybaid, Teddington, UK). 10 µl of DNA amplificate was mixed with 2 µl loading dye (see Table 5: Buffers and solutions) and added to each slot. A 123 bp DNA ladder (Sigma) was diluted four-fold and 10 µl were mixed with 2 µl loading dye. The gel was run at 400 mA and 100 Volt for 45 min. Documentation was done on a ChemiDoc XRS$^+$ (Bio-Rad Laboratories, Inc., Hercules, CA, USA) and analyzed with Image Lab software (also from Bio-Rad).

4.2.4.6 UL10 to 13 PCR / Restriction Fragment Length Polymorphism

The gene region UL10 until UL13 of HCMV was amplified in a half-nested PCR to gain insights of the HCMV strains present in milk whey or urine with Restriction Fragment Length Polymorphism (RFLP). This protocol followed the instructions from Prix et al. [271]. In the first amplification round, DNA extracted from either milk whey of the mother or urine from the infant was used with PWO Master (Roche, Basel, Switzerland) after the manufacturer's instruction. Additionally 20 pmol of pg1up (forward primer) and pg3do (outer reverse primer) (Table 15) was added. The PCR protocol was run as described in Table 19 and the amplificate had a length of 2137 bp.

Table 19: UL10-13 PCR program

Step	Temperature [°C]	Time [min]	Cycles
Initial denaturation	95	10	
Denaturation	94	1	35x
Annealing	58	1	
Elongation	72	2	

Final elongation	72	7	

For the second amplification round, the PWO Master was used with the same forward primer (pg1up) but this time with another inner reverse primer (pg2do) (Table 15) and 5 µl of the first round as DNA template. The same PCR protocol was used (Table 19). The resulting amplification length was at 1967 bp. Samples were run on a 1% horizontal agarose gel in TBE buffer (see 4.2.4.5). Gel extraction was performed for the band with the size of 1967 bp after the manufacturer's instruction of the Nucleo spin Gel and PCR clean up kit (Macherey-Nagel, Dueren, Germany). The DNA was then digested either with 0.5 µl RsaI or 0.5 µl Hin6I, 1 µl of cut smart buffer and 5 µl DNA as well as 3.5 µl H_2O at 37° C over night. Another 1% agarose gel in TBE buffer was run and analyzed.

4.2.4.7 HCMV UL83 (pp65) quantitative real-time (q) PCR

Quantitative HCMV DNA results of milk whey and cells were generated by using a qPCR of target gene UL83 (encodes pp65) with the CMV R-gene®Kit (BioMérieux, Marcy-l'Étoile, France, Limit of detection (LOD): 600 copies/ml). Results were given in copies/ml. Color compensation for 530 nm and 640 nm from Roche was used.

4.2.4.8 HCMV UL55 (gB) quantitative real-time (q) PCR

300 µl of a glycerin stock of an E.coli JM109 population which was transformed with a pGEM plasmid containing the gB region (performed by Steffen Hartleif) was cultivated overnight in 300 ml LB-broth and a plasma midi preparation was performed after the manufacturer's instructions (Plasmid DNA purification, NucleoBond® Xtra Midi, Macherey-Nagel, Dueren, Germany). The purified plasmid was diluted in 1 ml and linearized with ScaI. Therefore, 900 µl plasmid, 100 µl NE buffer and 10 µl ScaI were mixed and incubated at 37°C for 4 h. With part of the purified plasmid a gB qualitative PCR was performed as described in Table 20 and run as described in Table 21 for sequence checking.

Table 20: gB PCR

	Final concentration	**Amount [µl] per sample**
gB-F primer [100 pmol/µl]	2 µM	1
gB-R primer [100 pmol/µl]	2 µM	1
10x PCR buffer [100 mM Tris-CL pH 9.6, 500 mM KCL]	1x	5
$MgCl_2$ [25 mM]	2.5 mM	5
dNTP [25 mM]	250 µM	0.5
Taq-polymerase [1U/µl]	1 U	1
Template		5
H_2O		31.5

Table 21: gB PCR cycles

Step	Temperature	Time	Cycles
Initial denaturation	94°	5 min	
Denaturation	94°	30 s	35x
Annealing	55°	60 s	
Elongation	72°	30 s	
Terminal elongation	72°	7 min	

After a band size control with gel electrophoresis and a following purification step with NucleoSpin PCR cleanup kit (Macherey-Nagel), the DNA concentration was measured and sent for sequencing (100 ng/µl template, 5 pmol/µl primer gB-F, add 10 µl H_2O) to GATC Biotech AG (Konstanz, Germany).

The DNA concentration of the rest of the correct, linearized plasmid was measured. The amount of copies/µl was determined by photo spectroscopy [g/µl] and Equation 1.

Equation 1: Calculation of the number of gB plasmid copies

$$\frac{6 * 10^{23}\left[\frac{copies}{mol}\right] * DNA\ concentration\left[\frac{g}{\mu l}\right]}{molecular\ weight\ \frac{g}{mol}} = amount\frac{copies}{\mu l}$$

The molecular weight of the plasmid was calculated with equation 2:

Equation 2: Calculation of the molecular weight of the plasmid

$$(pGEM\ plasmid\ [bp] + gB\ insert[bp]) * average\ molecular\ weight\ of\ one\ base\ pair\ \left[\frac{g}{mol}\right]$$

The pGEM plasmid had 3015 bp and the gB gene insert 254 bp. The average molecular weight of one base pair equals 650 g/mol. Therefore, the molecular weight for the gB plasmid is at 2,124,850 g/mol.

Real time qPCR was performed as described earlier [272]. A standard curve for a real-time gB PCR was prepared, diluting the gB plasmid in five dilution steps from 10^7 to 10^3 copies/µl. The qPCR was performed with the LightCycler Master HybProbes kit (Roche, Basel, Switzerland) and primers gB-F, gB-R, as well as probes from TIB Molbiol (Berlin, Germany) (Table 14). 18 µl of the PCR mix, shown in Table 22, were distributed into Light Cycler capillaries and 2 µl of either DNA template or standard curve aliquots were added.

Table 22: q real time gB PCR

	Final concentration	Amount [µl]/sample
gB-F [10 pmol/µl]	0.6 µM	1.2
gB-R [10 pmol/µl]	0.6 µM	1.2
Fluorescein-probe [2 µM]	0.2 µM	2
LightCycler Red-640 [2 µM]	0.2 µM	2
MasterHyb probes kit [10x]	1x	2
$MgCl_2$ [25 mM]	3.5 mM	2.8
H_2O		6.8

After short centrifugation at 0.8 g, the capillaries were put into the carousel of the LightCycler 2.0 (Roche, Basel, Switzerland) and the program described as in Table 23 was started.

Table 23: Light Cycler gB PCR program

Segment	Temperature [°C]	Time [s]	Temperature change [°C/s]	Detection mode
Denaturation **1 cycle:**				
1	95	600	20	-
Amplification **50 cycles:**				
1	95	10	20	-
2	55	15	20	Single
3	72	15	20	-
Melting curve **1 cycle:**				
1	95	0	20	-
2	45	15	20	-
3	95	0	0.1	Continuous
Cooling **1 cycle**:				
1	40	30	20	-

4.2.4.9 Neutralization assay

Neutralization assays of plasma and milk whey samples were conducted on ARPE-19 cells as described earlier [273, 274]. ARPE-19 cells were seeded on the previous day with $2x10^4$ cells/well in a 96-well microtiter plate. Whey and plasma samples were complement inactivated with an incubation step at 56°C for 30 min, followed by a centrifugation step at 2,000 g for 10 min, where only the supernatant was used for further experiments. Milk whey predilutions (1:16 to 1:1024) or plasma predilutions (1:200 to 1:3200) in DMEM were generated. Equal volumes of the whey/plasma-predilutions and a cell-free virus (H2497-11) solution (diluted to infectivity of approximately 100 plaques of 7 IEA stained nuclei per well) were mixed. Therefore, end dilutions for the test were 1:32 to 1:2048 for whey and 1:400 to 1:6400 for plasma. The virus-whey or virus-plasma mix was incubated for 90 min at 37°C in 5% CO_2. Afterwards, the mix was inoculated onto ARPE-19 cells and incubated for 5 days at 37°C in 5% CO_2. Staining of IE1 positive nuclei was performed as described in 4.2.4.2. Over or equal to 7 IE1-stained neighboring nuclei were counted as one plaque.

As positive control and for calibration of the seropositive samples, a hyperimmunoglobulin (HIG) (Cytotect®, Biotest®Pharma; charge B797033, 50 mg/mL) preparation (4725 U/ml, 150.3 Paul-Ehrlich-Institute (PEI) units/ml) was prediluted to the same concentrations as the mean ECLIA level of either plasma (720 U/ml, HIG diluted 1:6.5) or whey pools (6.4 U/ml, HIG diluted 1:700).

Unspecific neutralization was very high in both seropositive and -negative mothers' milk whey. Several procedures were used to prevent these unspecific neutralization effects:

4.2.4.9.1 Ultrafiltration

In order to concentrate IgG antibodies and exclude milk proteins out of milk whey, a 100k Amicon®Ultra device (Merck Millipore, Burlington, Massachusetts, USA) was used after the manufacturer's instructions. The retained concentrated IgG-solution was used in relative amounts for the same dilutions in the neutralization assays.

4.2.4.9.2 Anti-IgA-depletion

Anti-IgA pure human antibody (MACS Miltenyi Biotec) was diluted 1:10 in PBS and 100 µl were incubated on Nunc high absorbance microtiter plates (Thermo Fisher Scientific, Waltham, Massachusetts, USA) overnight on a shaker. The plate was washed three times with PBS containing 0.05% Tween20 and blocking solution of 4% BSA was incubated for 2 h. After three washing steps, milk whey was added and incubated overnight on a shaker. The following day, the whey was used in neutralization assays.

However, the neutralization assays were mostly conducted with pools of milk whey or plasma, and the HCMV-seronegative whey pools were used as the 100% references for NT-capacity calculations.

4.2.4.10 Electrochemiluminescence immunoassay

The electrochemiluminescence immunoassay (ECLIA)-Elecsys CMV-panel was performed on the cobas6000 module e601 (Roche, Basel, Switzerland) for breast milk whey and plasma samples to receive quantitative HCMV-specific IgG results. The immunoglobulins bound to one ruthenium-coupled and one biotin-coupled antigen and were then bound to a surface with streptavidin coated magnetic beads. Detection was guaranteed by electrochemiluminescence. For IgM, p150 and p52 recombinant antigens were used and the output was a cut-off index (COI) with non-reactive results for results under 0.7 COI, indeterminate for results between 0.7 and 1.0 COI and reactive for results over 1.0 COI. For IgG, pp28, pp150, p52 and p38 recombinant antigens were used and the results were given in U/ml: non-reactive under 0.5 U/ml, indeterminate between 0.5-1.0 U/ml and reactive over 1.0 U/ml. Spike and recovery experiments were performed for milk whey. The HIG Cytotect® in a 100-fold dilution was used for spiking milk whey and a recovery rate of 88.3% was achieved.

4.2.4.11 RecomLine immunoblots

IgG and IgM RecomLine blots (Mikrogen Diagnostik, Neuried, Germany) were used to detect six different antigen specific antibodies from plasma and whey. The six immobilized recombinant proteins on the strip were: IE1, an important immediate early protein; CM2 a

fusion protein of a single-strand DNA binding protein (UL57) and a processivity factor for the viral DNA-polymerase (pUL44); p150 (UL32), an important immunogenic phosphoprotein of the tegument; p65 (UL83), another phosphoprotein of the tegument, against which high T cell reactivity is known; gB1, which consists of AD1 (amino acid positions 550 to 640 of gp58) and AD2 (amino acids 28 to 84 of gp116) and gB2, a fusion protein of AD2 of the strains AD169 and Towne. RecomLine blots were performed as described in the manufacturer's manual, with the following difference: plasma was used as recommended in a 100-fold dilution, whereas whey was only diluted two-fold [274]. HIG-spiked milk whey displayed the same intensities for the phosphoproteins p150 and p65. Slight, but not interfering, decreases in intensities were observed for gB1 and gB2, IE1 and CM2. Reactivity scores were described as (nr) – non-reactive, (+/-) – around cut-off level, (+) – one-fold, (++) – two-fold or (+++) – three-fold higher than cut-off limit.

4.2.4.12 Cytokine analysis of milk whey

The analysis of cytokines in human breast milk whey was performed by Olink (Upsala, Sweden), using multiplex analysis of inflammation markers. 20 µl/well of whey were placed in microtiter plates on dry ice. The inflammatory cytokine panel was chosen. Olink performed a proximity extension assay: In an immunoassay two antibodies coupled with nucleic acids bind to one protein at different sites. The two nucleic acids can then align, and the next steps are extension as well as preamplification. In a final step, detection by microfluidic qPCR is performed (Figure 13).

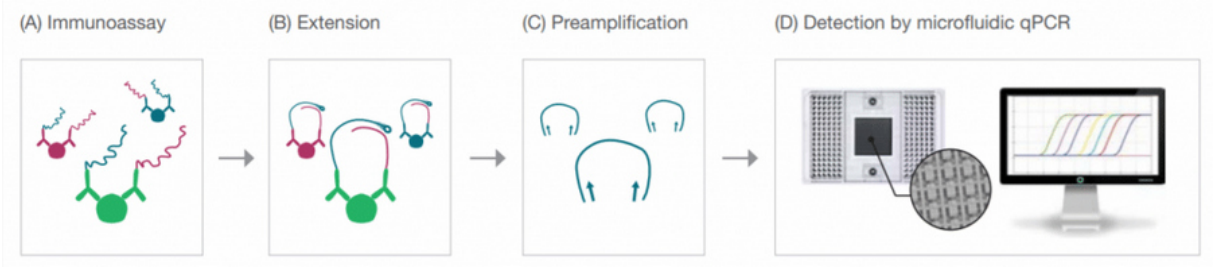

Figure 13: Proximity extension assay by Olink
In an immune assay (A), two antibodies coupled with nucleic acids bind to one cytokine. The nucleic acids can align and a first extension (B) follows. After a preamplification (C) the detection is managed by microfluidic qPCR (D).

4.2.5 Experiments with BMCs and PBMCs

4.2.5.1 Cytospin preparations

BMCs were isolated as described in 4.2.2 and up to $1.5x10^5$ cells were centrifuged on a microscope slide using the Cytospin 3 centrifuge according to manufacturer's instruction at 28 g (500 rpm) for 5 min at RT. Panoptic staining was performed as follows: Giemsa's azur eosin

methylene blue solution and May-Gruenwald's solution (both from Merck, Darmstadt, Germany) were filtrated with two rotilabo®-folded filter (type 113P, Carl Roth, Karlsruhe, Germany). The cell spot on the microscope slide was encircled with a fat pen (liquid blocker super PAP-pen, Science Services, Munich, Germany) and 100 µl of the May-Gruenwald's solution were added for 3 min. The same amount of dH_2O was added, and it was incubated for 1 min. The microscope slide was washed with dH_2O several times. Giemsa solution was diluted 33-fold with dH_2O before use and 200 µl were added on top of the cell spot and incubated for 17 min at RT. After an additional washing step, the cell spots were air dried. Analysis was done using a microscope (Olympus DP71, Olympus, Shinjuku, Tokyo, Japan) with 600-fold magnification.

The α-naphthyl acetate esterase kit (Non-specific esterase, Sigma-Aldrich, St. Louis, Missouri, USA) was used according to the manufacturer's instruction. The incubation time with the staining solution was set to 30 min instead of 15 min.

4.2.5.2 Cryopreservation and thawing of biological controls for flow cytometry assays

Cryopreservations of PBMCs were used as biological control, which was carried along every day a FACS measurement took place. Therefore, PBMCs were isolated from leukaphereses or buffy coats with a Ficoll-gradient centrifugation (see 4.2.3). PBMCs were then resuspended in RPMI with 40% FCS. For each vial, 500 µl of the cell suspension (with 2.5-5x10^6 cells in total) and 250 µl of RPMI with 20% DMSO were mixed and incubated for 5 min. Then, 250 µl of RPMI with 20% DMSO were added and the samples quickly stored at -80°C. The following day, the samples were transferred to liquid nitrogen until usage. On each day of measurement, one vial of the same prepared control batch was thawed in a 37°C water bath and added to the equal volume of 4°C RPMI. After 5 min of incubation the same amount of RPMI was added and centrifuged at 300 g for 5 min. The supernatant was discarded, the pellet resuspended in 10 ml of RPMI and cells were counted under a trypan blue staining. After an additional centrifugation step, the cells were used for the FACS staining protocol below in a 1x10^6 cells/ml concentration.

4.2.5.3 Flow cytometry

The monitoring of immune cells via flow cytometry was performed in cooperation with AG Kilian Wistuba-Hamprecht (Division of Dermatooncology, Department of Dermatology) and Graham Pawelec (Department of Immunology).

A monoclonal antibody panel of 11 different markers was established: EMA was used as a life/dead marker. Since breast milk only has around 2% leukocytes, CD45 was included as a

general marker of leukocytes. Monocytes/macrophages are an important component of breast milk. Therefore, CD14 was included in the panel. For distinguishing the lymphocyte population, antibodies against CD3 and CD56 were included to be able to determine T cells, NK cells and $CD56^+$ T cells. To analyze T cells further anti-CD4 and anti-CD8 antibodies were added to the panel. The memory phenotypes were distinguished using anti-CCR7 and anti-CD45RA antibodies. As activation marker of T cells anti-HLA-DR and anti-CD38 were incorporated. The whole panel was designed under consideration of the spectral overlap of different fluorophores and the flow cytometer LSR II configuration (laser and filter in Table 25). All antibodies for flow cytometry assays were titrated using cryopreserved PBMCs. Therefore, the recommended amount from the manufacturer was used and four dilution steps with two-fold dilutions downwards were additionally measured. The amount showing the best separation between the positive and the negative cell population was used (Table 24).

Fluorescent minus one (FMO) controls for BMCs and PBMCs were stained for all established panels. The staining was performed as described below but excluding one color at a time.

For the immunophenotyping in the BlooMil study, fresh PBMCs ($1x10^6$ cells/sample) and BMCs ($0.2\text{-}3x10^6$ cells/sample), a thawed biological control, as well as compensation controls (see below) were used on every day of measurement and stained in FACS tubes (BD Falcon 5 ml round bottom, BD Biosciences, San Jose, California, USA) with final staining volumes of 100 µl (50 µl of mastermix and 50 µl of residual buffer): In a first step, buffer was exchanged from the cell suspension in RPMI (PBMCs) or PBS (BMCs) to the flow cytometry staining buffer (PBS with 2% FCS, 2 mM EDTA and 0.01% sodium azide, termed PFEA) with equal volumes of cell suspension and PFEA. After a centrifugation step at 300 g for 5 min at RT, the supernatant was discarded. A master mix with 1 µl 1% Ethidium Monoazide Bromide (EMA, Biotium, Hayward, California, USA, diluted in PFEA) for life/dead staining and 49 µl 1% GAMUNEX per sample (10% GAMUNEX, Grifols, Barcelona, Spain, prediluted in PFEA) as an Fc-receptor-blocker was prepared and the cell pellets were resuspended. Negative controls were only incubated with 50 µl of GAMUNEX. Samples were incubated for 20 min at RT under UV-light due to required photolysis of EMA to covalently bind DNA, followed by a washing step with 1 ml of PFEA at 300 g for 5 min at RT. Next, the CCR7 biotin antibody was prediluted in PFEA (Table 24) and 50 µl were added to each sample. An incubation step of 20 min at RT in the dark followed. The streptavidin BV510 was centrifuged at 15,000 g for 5 min at 4°C to eliminate complexes and prediluted in PFEA for usage (1:10). After a washing step of the cells, a mastermix with 1 µl of the prediluted streptavidin BV510 and 49 µl PFEA per sample were prepared and 50 µl of this master mix were added to each sample. After another incubation and washing step, a final mastermix with CD45 BV421, CD14 PE-CY7, CD3 A700, CD4 BV605, CD8 APC-H7, CD45RA APC, CD56 FITC, CD38 PE and HLA-DR PerCP-Cy5.5 in Brilliant stain buffer (BD Biosciences) was prepared using a final volume of 50 µl for each

sample (Table 24). An incubation step and two washing steps, as described above were applied, and the samples were finally resuspended in 120 µl PFEA for acquisition.

Table 24: BlooMil-antibodies amounts per sample.
For antibody details refer to Table 8 in Materials.

Target	Fluorophore	Clone	Lot	µl/sample
EMA			11E0611	1
CCR7	primary antibody CCR7-biotin secondary streptavidin BV510	G043H7	B247211 B239818	0.5 0.1
HLA-DR	PerCP-Cy5.5	G46-6	7235979	3
CD3	A700	UCHT1	7145618	1
CD4	BV605	OKT-4	B244137	1.5
CD8	APC-H7	SK1	7354859	2
CD45	BV421	HI30	B240853/B258289	1.5/1
CD14	PE-Cy7	M5E2	B231081	0.5
CD38	PE	HB-7	B216325/B241817	0.5
CD56	FITC	HCD56	B237911	1
CD45RA	APC	HI100	B238560	1.5

Compensation beads (BD™ CompBeads anti-mouse Ig, κ / negative Control compensation particle set, BD Biosciences, of both one droplet per sample) were stained with each fluorophore-coupled antibody separately and incubated on ice for 20 min in the dark. The compensation controls were only used at two sequential days. If not applicable, they were made new each day of measurement.

All samples were diluted in 120 µl PFEA and acquired with a BD™ LSR II (BD Biosciences) with filter settings as shown in Table 25. The flow rate for acquisition was around 5,000 events per second. The compensation of spectral overlap of each channel was calculated by BD FACSDiva™ and was performed every day of measurement. Compensation between the channels did not exceed 20%.

Analysis was performed with FlowJo (version 10.6.1, FlowJo LLC, Ashland, OR, USA). Only daughter populations with a parental population over 120 events were included in the analysis.

Table 25: Specifications of the LSRII

Fluorochrome	Laser	Detector	Dichroic long pass filter	Bandpass filter
PE-Cy7	Blue laser (488 nm)	A	735	780/60
PerCP-Cy5.5		B	685	695/40
EMA		D	600	610/20
PE		E	550	575/25
FITC		F	505	530/30
SSC		G	-	488/10
BV421	Violet laser (405 nm)	E	-	450/50
BV510		D	545	561/14
PO				
BV605		C	600	610/20
BV711		A	685	700/13
APC-H7	Red laser (633 nm)	A	735	780/60
Alexa Fluor 700		B	710	730/45
APC		C	-	660/20

The longitudinal courses of BMCs and PBMCs of mother C and D were stained with the markers in Table 26 for flow cytometry analysis. The live/dead staining with EMA and GAMUNEX was performed as above, but on ice, since CCR7 (in this panel) was a directly fluorophore coupled antibody and not a biotin-streptavidin binding, which needed RT (see above). Therefore, all staining steps for this panel were performed on ice. After a washing step, a mastermix with 20 µl purified Mouse Anti-Human TCR γ/δ and 30 µl PFEA per sample was applied, followed by an incubation step on ice for 20 min and a washing step. 5 µl of a secondary rabbit anti-mouse antibody coupled with PO (predilution 1:10) were mixed with 45 µl PFEA and added to each sample. After an incubation and washing step, 50 µl mouse serum per sample were added and samples were incubated for 20 min on ice in the dark. A master mix with Vδ1 TCR FITC, Vδ2 TCR PerCP, CD3 A700, CD4 BV711, CD8 APC-H7, CD45 BV421, CD14 PE-Cy7, CCR7 PE, CD45RA APC was prepared with the amounts indicated in Table 26 and 25 µl Brilliant Stain Buffer per sample. After incubation and two washing steps, the samples were diluted in 120 µl PFEA and acquired with the LSR II. Compensation controls were prepared and measured as described above.

Frozen biological controls, which should theoretically stay constant over time due to aliquots of the same PBMCs, were analyzed using the same gating strategy as for all other samples. Within same cell subsets, the highest frequency difference over time of the biological control were used to create upper and lower error bars for the corresponding cell subsets of the mothers. Therefore, the error bars indicate the fluctuation over time due to staining and flow cytometry fluctuations.

Table 26: Antibody amounts for individual courses of mothers C and D.
For antibody details refer to Table 8 in Materials

Target	Fluorophore	Clone	Lot	µl/ sample
EMA			11E0611	1
Mouse serum			NG1900341	50
Pan γδ TCR	primary antibody secondary antibody PO	11F2	7137893 1847388	20 0.5
Vδ1	FITC	TS8.2	RG234822	1
Vδ2	PerCP	B6	B193574	1
CD3	A700	UCHT1	5067104	1
CD4	BV711	OKT4	B181032	1
CD8	APC-H7	SK1	4002507	2
CD45	BV421	HI30	B240853	2
CD14	PE-Cy7	M5E2	B218299	2
CCR7	PE	150503	39033	10
CD45RA	APC	HI100	275395	5

4.2.5.4 Tetramer staining

Tetramer staining's were performed with selected HLA-A*02:01 positive mothers, recruited at the Neonatology Department. Their HLA-A types were identified through an antibody staining of whole blood. Therefore, 100 µl whole EDTA-blood were added to 2 ml of 1x Red Blood Cell (RBC) lysis buffer (Biolegend, diluted in autoclaved demineralized water). After incubation in the dark for 15 min at RT a centrifugation step followed. Then three washing steps by adding 4 ml PFEA to the cell pellet and centrifuging were performed. The pellet was stained with a mix of 1.5 µl anti-human HLA-A2 PE (Biolegend, San Diego, CA, USA) and 48.5 µl PFEA per sample for 20 min on ice in the dark. Cells were acquired with the LSR II to evaluate the HLA-A*02 status of the mothers.

At each day of measurement for the tetramer analysis with IE1 (VLEETSVML) and pp65 (NLVPMVATV) peptides, fresh EDTA-blood and breast milk was collected and cells isolated (see 4.2.2 and 4.2.3). $2x10^6$ PBMCs and $1\text{-}6x10^6$ BMCs, as well as an HLA-A*02:01 positive biological control with $CD8^+$ T cells specific for IE1 peptide VLEETSVML and pp65 peptide

NLVPMVATV were used for the tetramer staining. At first, the live/dead staining with 1 µl 1% EMA and 49 µl 1% GAMUNEX per sample was incubated for 20 min under light at RT. After a washing step with PFEA, the samples were double stained for each peptide (IE1 and pp65): the NLVPMVATV-pp65-tetramer was either coupled with APC or PE (of each 3 µl) and VLEETSVML-IE1-tetramer was either coupled with APC or BV510 (of each 5 µl) (Table 12) and diluted in PBS with a final volume of 50 µl per sample and incubated for 15 min at 37°C. The following washing step was performed at RT. A master mix with CD45 BV421, CD14 PE-Cy7, CD3 A700, CD4 BV605 and CD8 APC-H7 (amounts used as indicated in Table 24) in add 50 µl brilliant stain buffer was added per sample and incubated for 30 min in darkness on ice. Up to $6x10^6$ events were recorded on the flow cytometer for BMCs. Compensation controls for each fluorophore were stained at each day of measurement (see above).

4.2.6 Statistical analysis

All statistical tests were conducted with SPSS (version 25.0.0.1, IBM, Armonk, USA).
Within one cohort, kinetics were analyzed with the Friedman test followed by Dunn-Bonferroni post-hoc tests (termed just post-hoc test in the following) with correction for multiple testing by Bonferroni. Single time ranges (T's) were compared with Wilcoxon matched-pairs signed rank tests (Wilcoxon) and corrected for multiple testing with Bonferroni correction.
Differences between HCMV-seropositive and -seronegative cohorts (of blood or breast milk) were analyzed with the Mann-Whitney U test at the counterpart of each time range (T1 with T1, mentioned in the text as T1's), whereas for an analysis of differences between the kinetics of HCMV-seropositive and –seronegative mothers a linear mixed model was used.
Specimens of different body sites (breast milk or blood) were compared with the Wilcoxon matched-pairs signed rank test with Bonferroni correction for multiple testing on the counterpart of each time range (T1's, T2's, etc.).
All correlations were conducted as Spearman correlations. Rho is given as r. Correlations were only mentioned when r was between 0.6-1.0 (moderate to strong correlation according to [275]) and $p<0.05$.
Probit analysis was performed for the NT-50 values of the neutralization assays.
The significance level in this thesis was set below $p<0.05$.

5 Results

The following results are structured in three parts. At first, longitudinal case studies were used to gain first insights into HCMV reactivation in breast milk and to establish a first flow cytometry antibody panel. The second part is about the clinical-virological study termed BlooMil, where IgG antibodies and immune cells (with a slightly adjusted antibody panel) were monitored. Additionally, HCMV-specific $CD8^+$ T cells were monitored in breast milk and blood of four mothers. The third part is an initial step towards the cytokine analysis in breast milk (multiplex analysis of 92 inflammatory cytokines), which were the basis for another project (Tabea Rabe).

5.1 Long-term case studies

In preparation of the BlooMil study, different clinical-virological aspects of individual longitudinal courses of four mothers were closely monitored during the first two to three months after birth. Mother A and B (Table 27) were included for detection of BMC counts, prolactin levels, total protein concentrations, staining of BMCs on cytospin preparations, breast milk viral load and HCMV-specific IgGs. Both mothers were 27 years old, but their newborns had different GAs at delivery: mother A (HCMV-seropositive) had the infant at GA 30 6/7 weeks, while mother B (HCMV-seronegative) gave birth at a GA of 26 3/7 weeks, both preterm infants. Mothers C and D were observed for breast milk viral loads and flow cytometry data including monocyte, T cell, γδ T cell and Vδ1 and 2 frequencies. Both mothers were 41 years old. However, only mother C had a preterm infant at GA 29 weeks, while the seronegative mother D had a term infant (GA 39 4/7 weeks).

Table 27: Demographics of individual longitudinal courses of mothers A, B, C and D.

Mother	HCMV-IgG	Age [years]	GA [weeks]	BW [g]	number of births	multi-births	country of origin
A	pos	27	30 6/7	1050	1	no	Portugal
B	neg	27	26 3/7	810	1	no	Germany
C	pos	41	29	1170	3	no	Germany
D	neg	41	39 4/7	3430	2	no	Germany

5.1.1 Individual courses of Mother A and B: implications on histology, cell count, prolactin, HCMV-IgG and total protein

The case reports of mother A and mother B were conducted from January 2017 to June 2017. The HCMV detection in breast milk of mother A was observed using two different techniques. Breast milk whey was either inoculated on fibroblasts (HFF) to detect infectious particles via immunostaining of IE1 (virolactia), or the DNA from milk whey was extracted and qualitative

PCR of IE1 (nested PCR), and quantitative PCR for UL83 (pp65) or UL55 (gB) (real-time PCRs) was performed (DNAlactia). Figure 14 shows the breast milk viral load of mother A. Both real-time PCRs (target genes UL83 Figure 14 A and UL 55 Figure 14 B) had similar unimodal courses, although the amount of copies/ml differed by almost one log-scale. The milk whey of mother A showed DNAlactia and virolactia (8 nuclei) already on day 3 p.p. Therefore the onset of viral shedding was calculated to 36 h after birth. Peak viral load was detected in both real time PCRs on day 19 p.p., while the peak of the microculture assays was identified on day 23 p.p. BMCs were only positive on day 23 (nPCR), day 25 (nPCR, UL55 qPCR) and day 27 (UL83 qPCR). Virus could not be isolated from BMCs during the observation period.

A

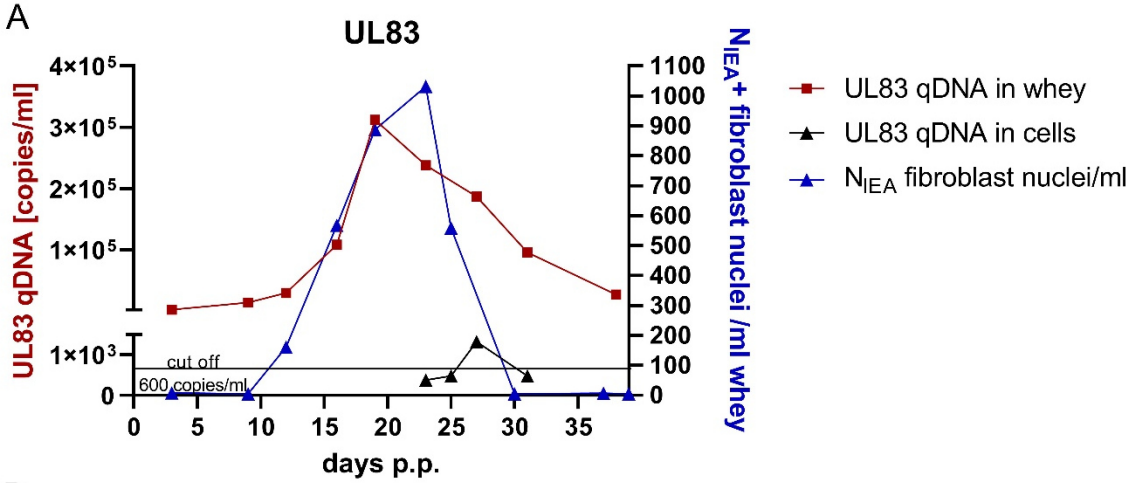

B

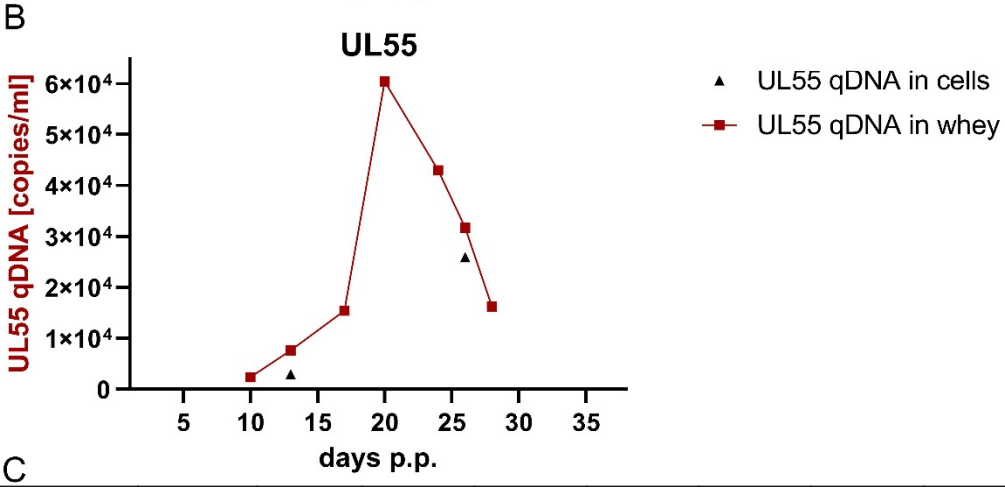

C

	day 3	day 9	day 12	day 16	day 19	day 23	day 25	day 27	day 31
Long-term culture	positive	positive	positive	positive	positive	positive	positive	positive	positive
nPCR whey	positive	positive	positive	positive	positive	positive	positive	positive	positive
nPCR cells	-	-	negative	negative	negative	positive	positive	negative	negative

Figure 14: Viral load in breast milk of HCMV-seropositive mother A.
qPCR results of either gene region (A) UL83 (pp65) or (B) UL55 (gB) of milk whey and breast milk cells. (A) The numbers of immediate early 1 (NIE1) stained nuclei in microculture assays are shown on the right y-axis. (C) nested PCR results of whey or breast milk cell extracts and long-term culture from milk whey. The area marked in grey highlights the days, where the breast milk cells were positive for HCMV DNA.

Cytospin preparations of $1.5x10^5$ BMCs were stained with either a panoptic staining according to Pappenheim or with an α-naphthyl acetate esterase staining (Figure 15, left and right

respectively). Neutrophils (Figure 15 A, black arrow) displayed in the panoptic staining a dark purple stained nucleus lobed into three segments. Eosinophils were distinguishable from neutrophils (Figure 15 A, blue arrow) by the red granulated cytoplasm. Granulocytes demonstrated no cytoplasm staining with α-naphthyl acetate esterase staining, but a purple nucleus was visible due to the hematoxylin counter stain. The panoptic staining of monocytes/macrophages is shown in Figure 15 B (black arrows). The α-naphthyl acetate esterase exists in monocytes and macrophages, therefore these cell types were stained black. Lactocytes and other epithelial cells (Figure 15 B, blue arrow) were difficult to distinguish from monocytes/macrophages, since both cell types presented with many vacuoles. Epithelial cells also appeared to slightly stain for α-naphthyl acetate esterase. Presumable skin epithelial cells are shown in Figure 15 C. BMCs with two nuclei were also detected (Figure 15 D). Lymphocytes are small cells with large nuclei and almost no cytoplasm (Figure 15 E, black arrow). It is important to mention that α-naphthyl acetate esterase slightly stains lymphocytes. However, no further distinguishing of lymphocytes into B, T, or NK cells was possible.

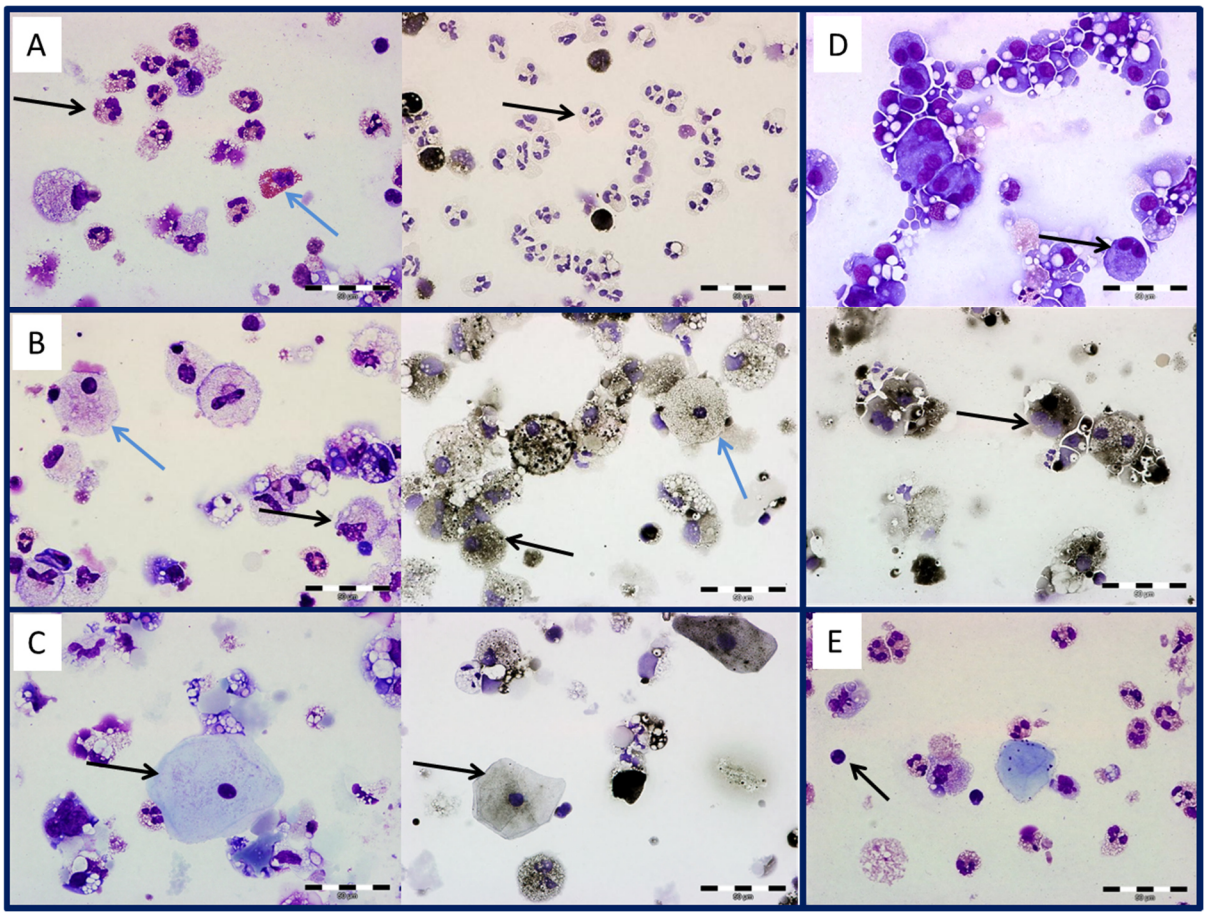

Figure 15: Breast milk cells on cytospin preparations.
Breast milk cells (1.5x10^5) immobilized on microscope slides were either stained with panoptic staining according to Pappenheim (on the left) or for α-naphthyl acetate esterase (on the right). The black arrows show (A) granulocytes, (B) monocytes/macrophages, (C) epithelial cells, (D) breast milk cells with two nuclei, (E) lymphocytes. The blue arrows show (A) eosinophils and (C) presumably lactocytes. All images were taken with 600-fold magnification using an Olympus BX51 TF microscope. Scale bar equals 50 µm.

The HCMV-seropositive mother A showed high HCMV-specific IgGs (ECLIA) in colostrum, followed by a sharp decrease in transient milk. The HCMV-specific IgG increased again slightly after breast milk peak viral load (Figure 16 A). Still, the total protein content in milk whey constantly decreased from colostrum to mature milk (Figure 16 A). RecomLine blot analysis showed that especially anti-CM2 and anti-p150 IgGs were increasing after peak viral load (Figure 16 B). Prolactin in milk whey of the seropositive mother had higher levels in transient milk (40-45 µg/L, concurrent with high viral loads) than the HCMV-seronegative mother (26-28 µg/L) (Figure 16 C). The total trypan blue stained cell counts of the HCMV-seropositive mother A were high compared to the cell counts of the seronegative mother B (Figure 16 D). Both cell counts decreased over time.

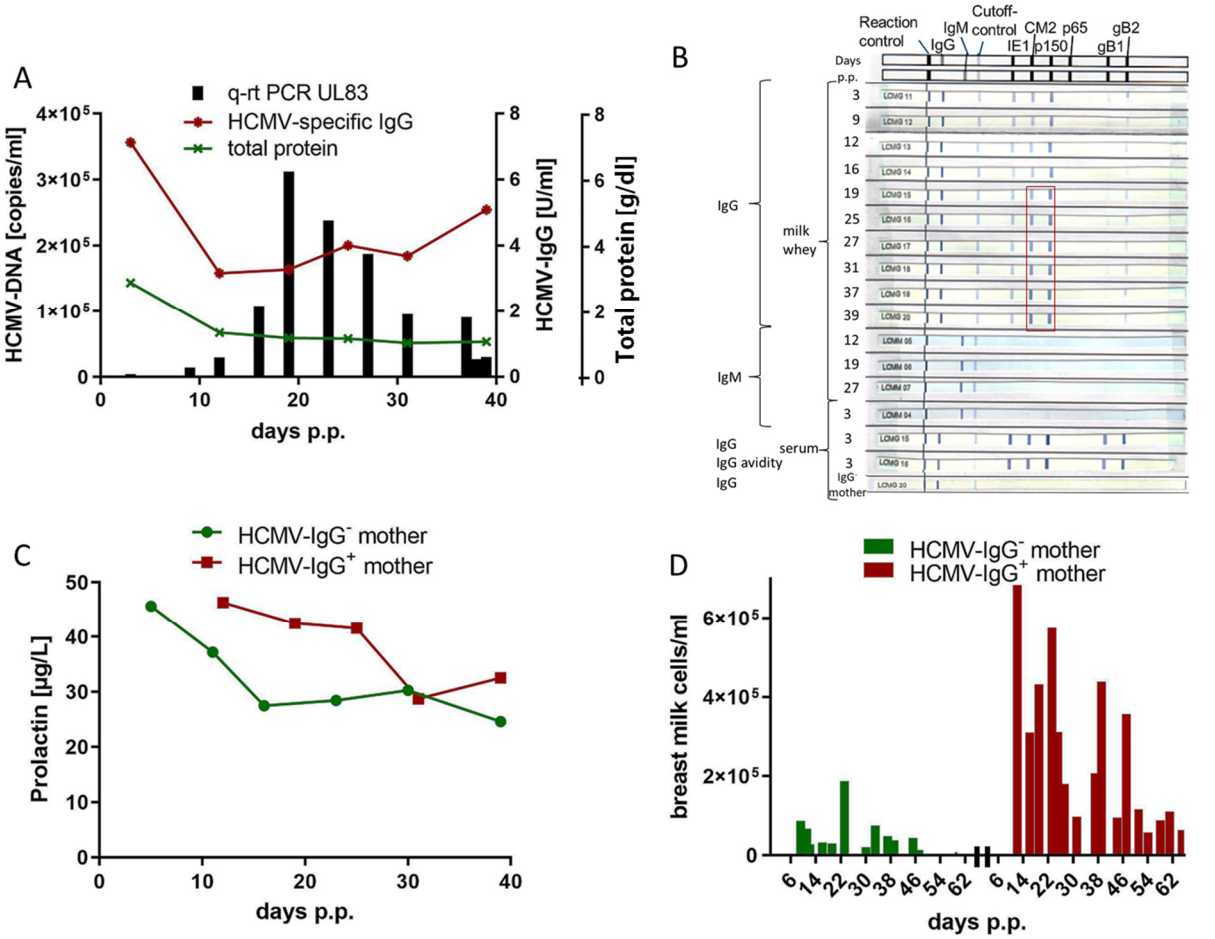

Figure 16: Longitudinal data from milk fractions of the HCMV-seropositive mother A and -seronegative mother B.
(A) Kinetics of HCMV DNA in milk-whey of the seropositive mother A (qPCR of UL83 as target gene) and HCMV-specific IgG-concentration [U/ml] measured with ECLIA, as well as total protein concentrations [g/dl]. (B) RecomLine blots of the seropositive mother's milk whey (two-fold dilution) and serum (100-fold dilution). (C) Prolactin concentrations in milk-whey [ng/L] measured with ADVIA Centaur® XPT. Limit of detection (LOD) = 2.7 ng/L. (D) total breast milk cell counts/ml of both mothers evaluated with trypan blue staining.

5.1.2 Longitudinal courses of Mother C and D: breast milk viral load and immune cell monitoring including γδ T cells

In cooperation with AG Kilian Wistuba-Hamprecht (Division of Dermatooncology, Department of Dermatology) and Graham Pawelec (Department of Immunology) another HCMV-seropositive and seronegative pair of mothers (mothers C and D, see Table 27) was studied for their longitudinal immunophenotypes in breast milk and blood.

The breast milk viral load of the HCMV-seropositive mother C is shown in Figure 17. The virolactia measured by microculture assays was mostly concordant with the HCMV DNAlactia. Peak viral loads differed from qPCR results (day 38 p.p.) to microculture assay results (day 31 p.p.). The measurements were only three to four days apart and high variations over time were observed.

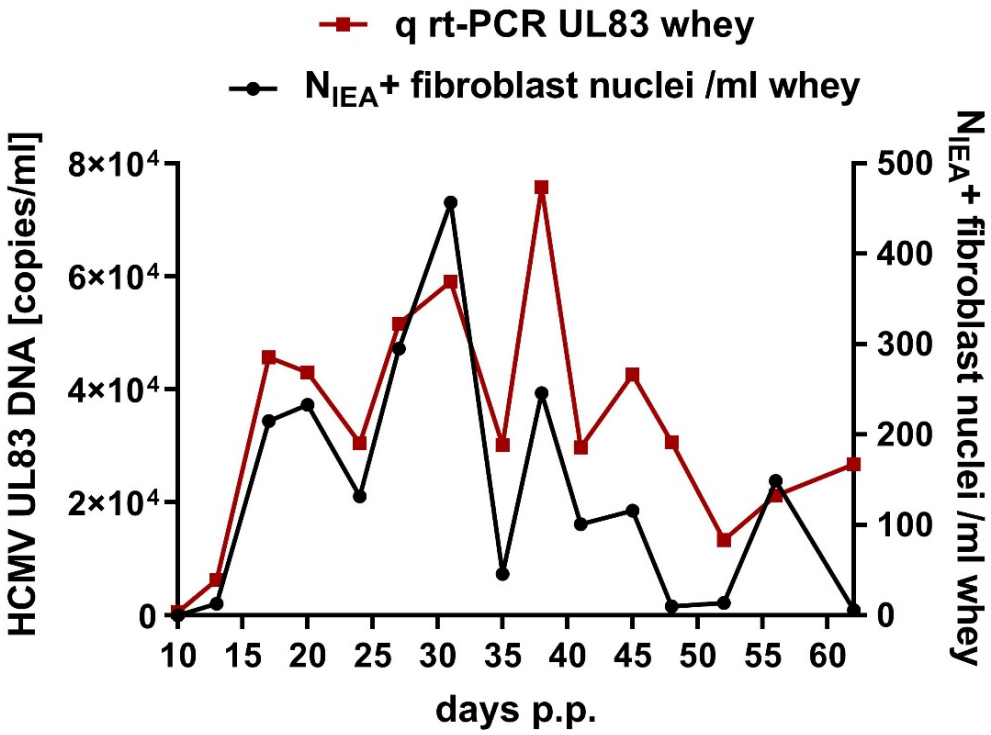

Figure 17: HCMV DNA and short-term microculture immediate early-positive nuclei counts of mother C.
Milk whey of mother C was either used for qPCR with the target gene UL83 (left y-axis) or for quantitative short-term microculture (right y-axis).

BMCs of mother C were only positive for HCMV DNA on day 20 and 27 p.p. (Table 28). In addition to breast milk, the HCMV-seropositive mother donated EDTA-blood on days 13, 20, 27, 35, 41, 48, 56 and 62 p.p. The HCMV-seronegative mother D donated breast milk and EDTA-blood on days 4, 12, 22, 28, 36, 50 and 57 p.p. nPCRs and microculture assays from breast milk samples of mother D were all tested negative for HCMV.

Table 28: nested PCR results of milk whey and cells.
Flow cytometry was applied on the days marked in red. N.d. stands for no data available; all breast milk cells were used for flow cytometry.

Days p.p.	10	13	17	20	24	27	31	35	38	41	45	48	52	56	62
whey	-	+	+	+	+	+	+	+	+	+	+	+	+	+	+
cells	-	-	-	+	-	+	-	-	-	n.d.	-	n.d.	-	n.d.	n.d.

Fresh BMCs and corresponding PBMCs were analyzed by flow cytometry with the following markers (Table 26): a live/death marker (EMA), pan γδ TCR with a secondary antibody coupled to pacific orange, Vδ1-FITC, Vδ2-PerCP, CD3-A700, CD4-BV711, CD8- APC-H7, CD14-PE-Cy7, CD45-BV421, CCR7-PE and CD45RA-APC.

In a first step of the gating strategy, exclusion of potential contamination with prior samples, as well as the continuous flow over time were assured by a plot of time against side scatter (SSC)-area (A) (Figure 18 A). Only singlets were included in further analysis. This was achieved by plotting SSC-height (H) against SSC-A, using only the cells in the diagonal (Figure 18B). Another exclusion of doublets was performed using the same strategy on the forward scatter (FSC) channel (Figure 18 C). In a next step, dead cells were excluded by selecting only EMA negative cells (Figure 18 D). Living cells were further separated by a CD45-leukocyte marker (Figure 18 E). The following morphological gate (FSC vs SSC) was used to cut off particles that were smaller than the lymphocyte population, such as debris and fat globules (Figure 18 F). The next plot discriminated $CD14^+$ monocytes/macrophages (Figure 18 G). The CD14-negtive population was utilized to obtain the lymphocyte population in a morphological gate (Figure 18H). The lymphocytes were distinguished into $CD3^+$ T cells (I) and further separated into γδ TCR positive and negative cells (Figure 18 J). The γδ TCR positive cells were discriminated into Vδ1 and Vδ2 γδ TCR isoform expressing cells (Figure 18L), while the γδ TCR negative cells (termed αβ T cells in the following) were divided into $CD4^+$ and $CD8^+$ T cells (Figure 18 K).

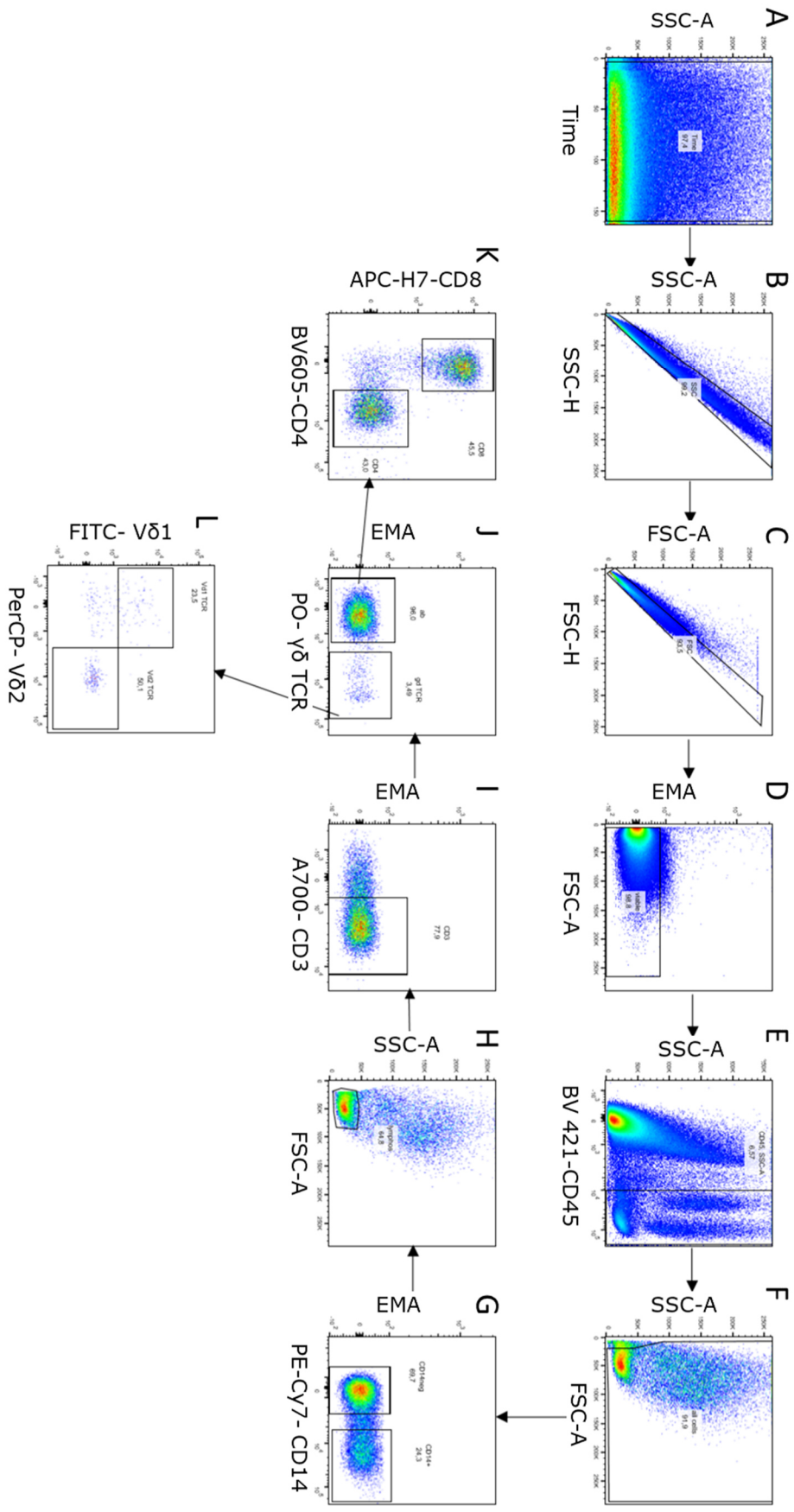

Figure 18: Gating strategy of γδ T cells.*Breast milk cells of mother C at day 41 p.p. are shown.Gating strategy is explained in the text above.*

BMCs mainly consist of epithelial cells. Other cells like leukocytes, which are the focus in this thesis, are rare. In Figure 19, only 1.07% of all BMCs are leukocytes, while the corresponding PBMC sample consisted of 96% leukocytes. Therefore, up to $6x10^6$ total BMCs and only $1x10^6$ PBMC were acquired in the flow cytometer to analyze the leukocyte population.

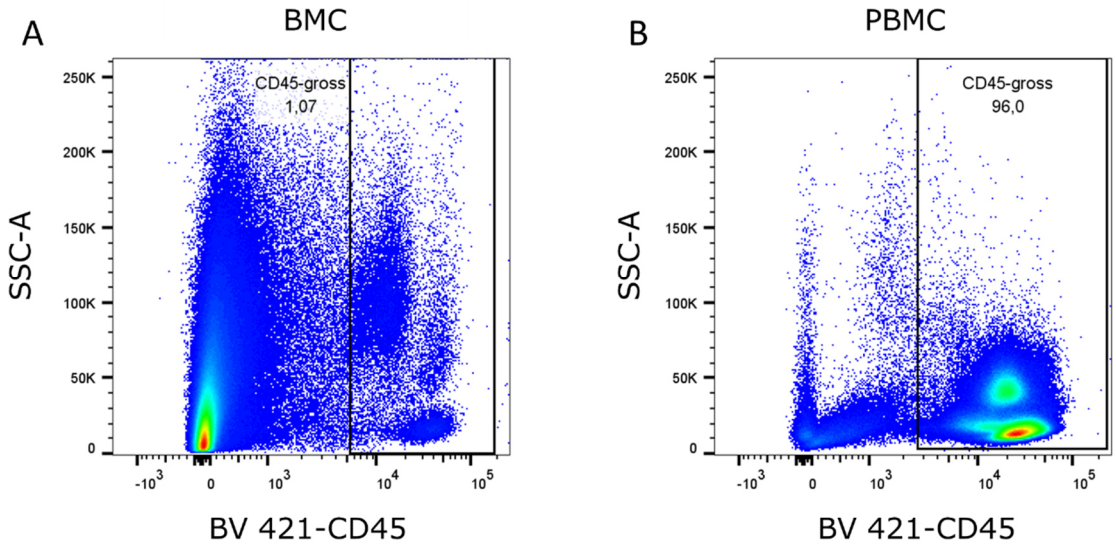

Figure 19: CD45⁺ leukocytes of breast milk and blood.
(A) Breast milk cells (BMC) and (B) Peripheral blood mononuclear cells (PBMC) of mother C day 48 p.p. in a plot with anti-human CD45 against SSC-A.

The BMCs and PBMCs of both mothers were analyzed by flow cytometry over almost 9 weeks p.p. Breast milk CD14⁺ monocytes/macrophages of both mothers represented a higher frequency of total leukocytes compared to PBMCs in early milk (Figure 20 A). However, high time point dependent variations of cells were detectable in the HCMV-seropositive and -seronegative mother. Nevertheless, the frequency of monocytes seemed to decrease into mature breast milk.

Blood CD14⁺ monocytes of Mother D (HCMV-seronegative) showed a frequency of around 20 to 25% during the whole observation period (Figure 20 A). Mother C (HCMV-seropositive) had higher blood monocyte frequencies after birth, decreasing over time and staying constant at about 10% subsequently.

CD3⁺ T cell frequencies were lower in breast milk of both mothers (2-23%) compared to blood (~60%) (Figure 20 B). Interestingly, the last measured time point of mother C revealed higher CD3⁺ T cell frequencies of all leukocytes in breast milk than in blood in comparison to the other time points. The percentages of αβ T cells of all CD3⁺ T cells in breast milk and blood were comparable and around 95% over the whole observed lactation period (Figure 20 C). Accordingly, the γδ T cell frequency was also constant in both mothers in breast milk and blood over time with around 5% of all CD3⁺ T cells (Figure 20 D).

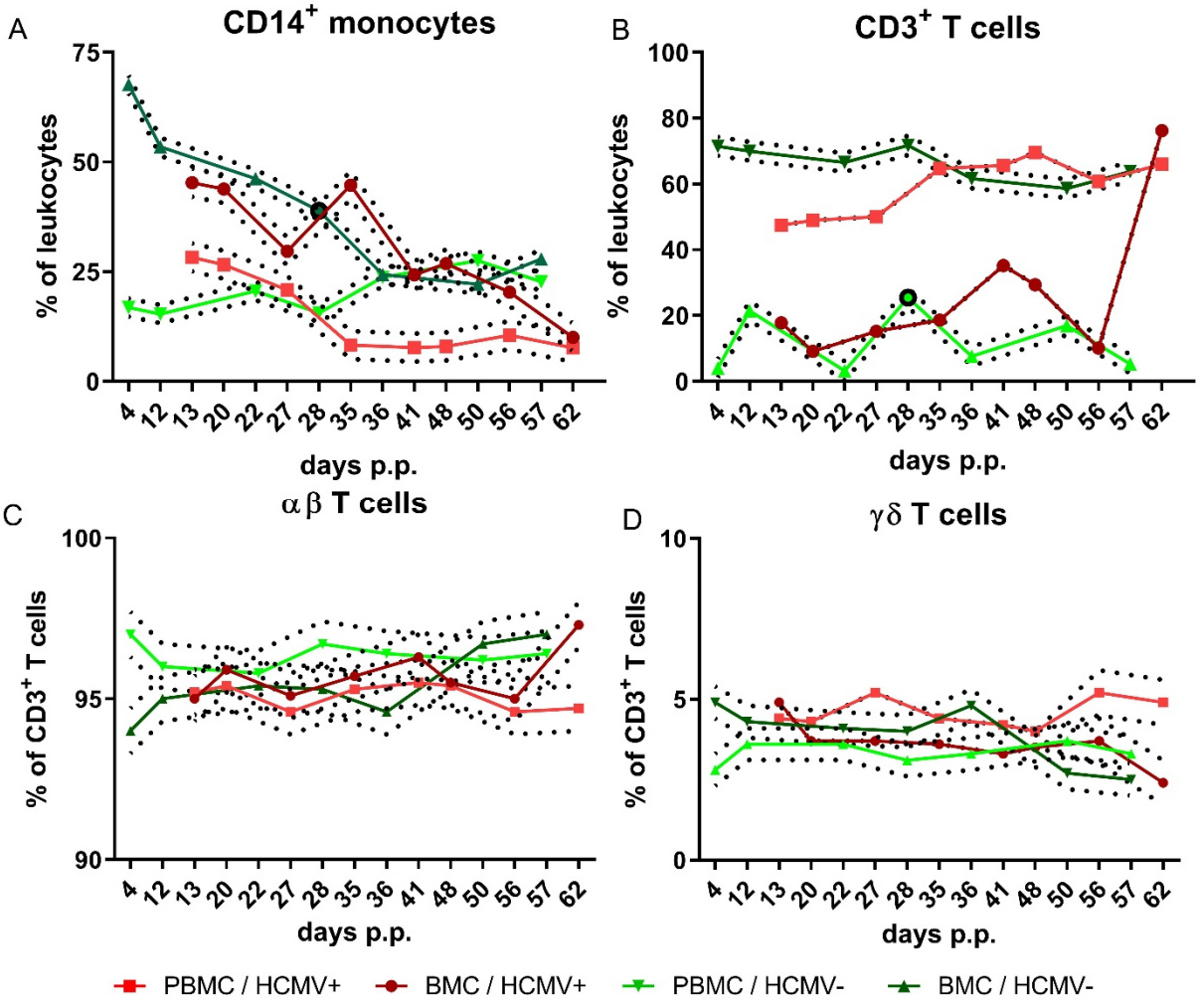

Figure 20: Individual courses of an HCMV-seropositive and a -negative mother's breast milk and peripheral blood cells.
Peripheral blood mononuclear cells (PBMC) and breast milk cells (BMC) of mother C (HCMV$^+$) and D (HCMV-). Frequencies of (A) CD14$^+$ monocytes, (B) CD3$^+$ T cells, (C) αβ T cells and (D) γδ T cells are shown. The black circle indicates a time point where the breast milk cell pellet was slightly red indicating erythrocytes in the milk, what may come from mastitis. The difference in the cell subset-frequencies of the biological control over time was used here as upper and lower error (black dotted line) for the same cell subset of the mothers.

The CD4$^+$ T cell frequency of all αβ T cells of both, blood and breast milk, was higher in mother D (HCMV-seronegative) than mother C (HCMV-seropositive). A tendency to higher CD4$^+$ T cell frequencies in breast milk compared to blood was also visible for both mothers (Figure 21 A). Otherwise, there was no meaningful variation over time. The CD8$^+$ T cell frequencies showed also no changes over time and were higher in mother C (seropositive) in both body fluids (Figure 21 B).

The CD8⁺ T cell frequency of all CD3⁺ T cells in breast milk was slightly lower compared to blood in both mothers.

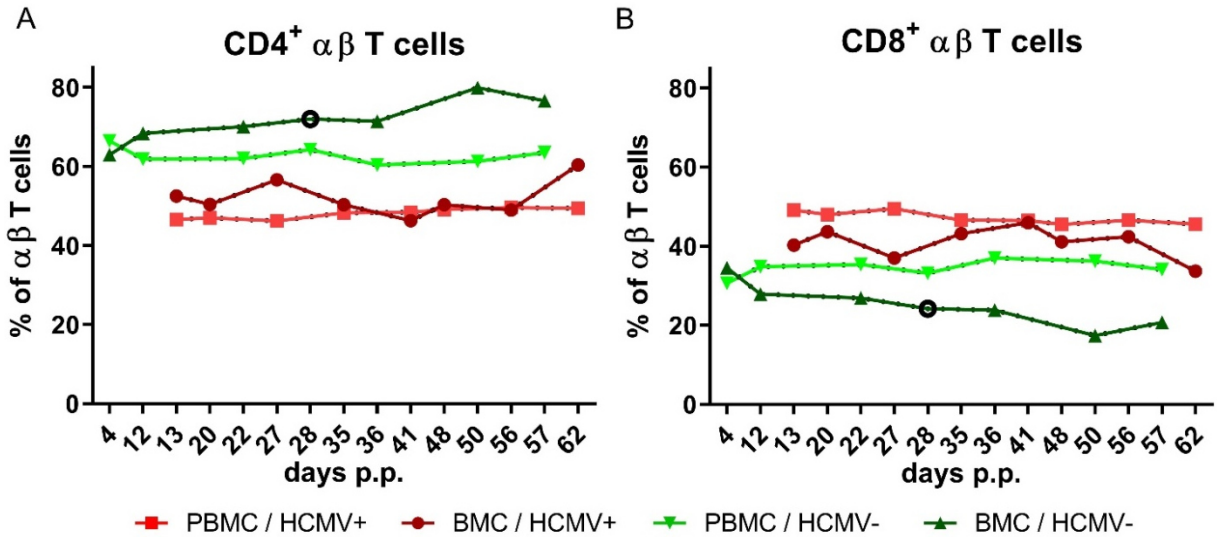

Figure 21: CD4⁺ and CD8⁺ T cells of mother C and D.
Peripheral blood mononuclear cells (PBMC) and breast milk cells (BMC) of mother C (HCMV⁺) and D (HCMV-). The frequencies of (A) CD4⁺ T cells and (B) CD8⁺ T cells are shown. The black circle indicates a time point where the breast milk cell pellet was slightly red indicating erythrocytes in the milk, what may come from mastitis. The black dotted lines show upper and lower boundaries indicating the difference in the subset-frequencies of the biological control over time.

The γδ T cells were further discriminated after expression of a Vδ1 or Vδ2 TCR carrying cell subset. The HCMV-seropositive mother C showed around 20% more Vδ1⁺ T cells in blood, compared to her breast milk frequencies (Figure 22 A). The seronegative mother D had 20-30% less Vδ1⁺ γδ T cells in blood compared to breast milk. The blood frequencies differed highly comparing the mothers between each other. In detail, mother D had around 10% Vδ1⁺ T cells, while the HCMV-seropositive mother C displayed frequencies around 40% over the whole observation period (Figure 22 A). Interestingly, the seropositive mother had a lower Vδ1⁺ γδ T cell frequency in breast milk, while the seronegative mother had a higher Vδ1⁺ γδ T cell frequency in breast milk compared to blood. Therefore, both breast milk Vδ1⁺ frequency courses had more similar frequencies to each other than their blood courses. Additionally, the breast milk Vδ1 frequencies seemed to slightly decrease at the end of the observation period in both mothers.

Vδ2⁺ T cell frequencies also differed highly between the mothers (Figure 22 B). The seronegative mother D had around 70% Vδ2⁺ T cells of all γδ T cells in their blood, while the Vδ2 frequency of the seropositive mother C was at around 30%. Both breast milk samples were more equivalent in their Vδ2⁺ frequencies than blood. The Vδ2 frequencies seemed to increase in both mothers at the end of the observed lactation period in breast milk (Figure 22 B).

Data was not generated at all experiments, as in some γδ T cell populations less than 120 counts were acquired. Therefore, data displaying breast milk Vδ1⁺ and Vδ2⁺ γδ T cell frequencies are based on fewer data points than the comparative blood samples.

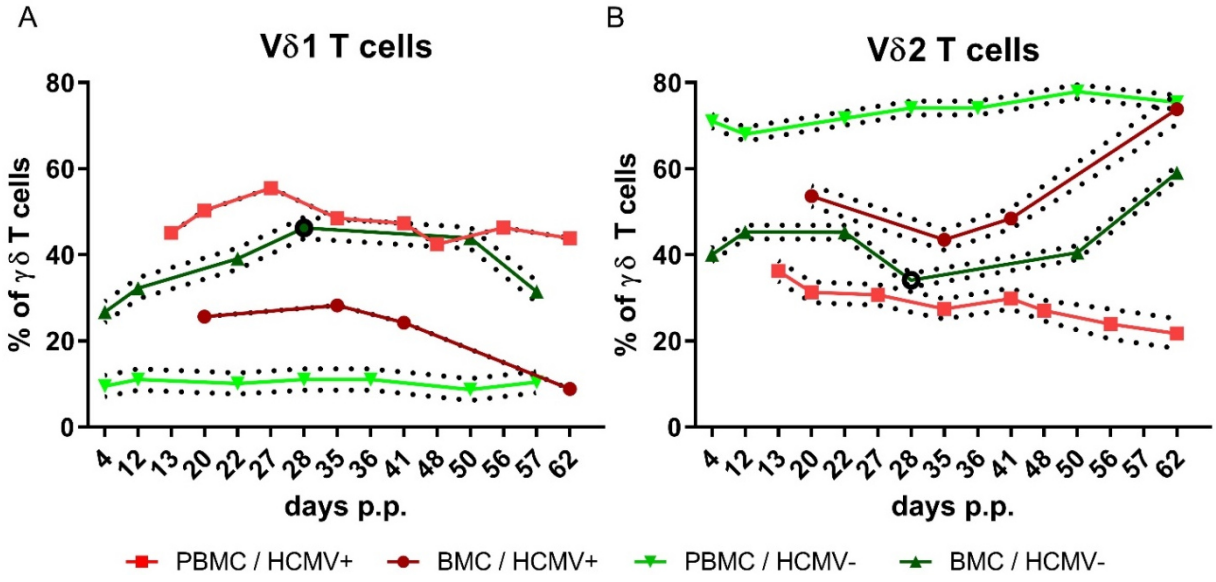

Figure 22: Vδ1 and Vδ2 T cells of mother C and D.
Peripheral blood mononuclear cells (PBMC) and breast milk cells (BMC) of mother C (HCMV⁺) and D (HCMV⁻). The frequencies of (A) Vδ1 T cells and (B) Vδ2 T cells are shown. The black circle indicates a time point where the breast milk cell pellet was slightly red indicating erythrocytes in the milk, what may come from mastitis. The black dotted lines show upper and lower boundaries indicating the difference in the subset-frequencies of the biological control over time.

The developed FACS panel, which was used to investigate BMCs and PBMCs of mother C and D, included markers for the memory phenotypes of T cells (CD45RA and CCR7, Figure 23 E).

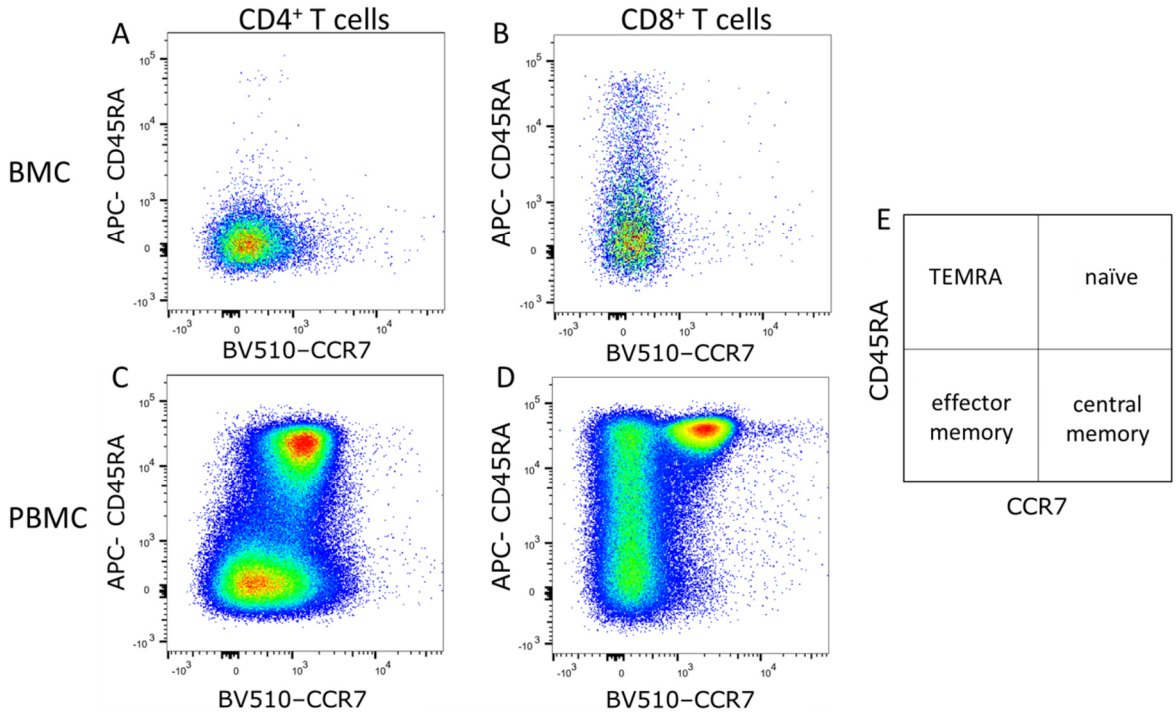

Figure 23: Pseudocolor plots of CCR7 against CD45RA.
Breast milk cells (BMC) A) CD4⁺ T cells and B) CD8⁺ T cells, as well as peripheral blood mononuclear cells (PBMC) C) CD4⁺ T cells and D) CD8⁺ T cells are separated with the memory phenotype markers CCR7 and CD45RA (E).

However, the anti-human CCR7-PE antibody displayed a poor separation of positive and negative populations, mostly in CD4⁺ T cells (Figure 23). Breast milk seemed to have a lower overall CCR7 expression, although it was difficult to analyze (Figure 23 A and B). Since no definite results could be drawn, memory subset identification was not performed.

5.2 Neutralization experiments

Antibodies in breast milk were investigated for their NT-capacity against the clinical isolate H2497-11 from amniotic fluid. Experiments showed that the unspecific neutralization in milk whey was very high. Several experiments were conducted to identify which components were responsible for the unspecific neutralization. In a first approach, milk whey was depleted of IgA. Results of an IgA depletion experiment followed by a neutralization assay are displayed in Figure 24 A. No differences were found between the depleted and the undepleted milk whey in either the seropositive (C) or the seronegative mother (D) in all dilutions. However, the depletion of IgA was not controlled via total IgA determination.

Another strategy was to remove milk whey proteins, like lactoferrin (around 80 kDa) and lysozyme (around 15 kDa) with a 100k Amicon®Ultra device. It concentrates proteins over 100

kDa and was used to retain IgG (about 150 kDa). The neutralization assay after the IgG ultrafiltration experiment exhibited high variations and inconsistent results in all dilutions probably due to the formation of aggregates in the filter unit (Figure 24 B).

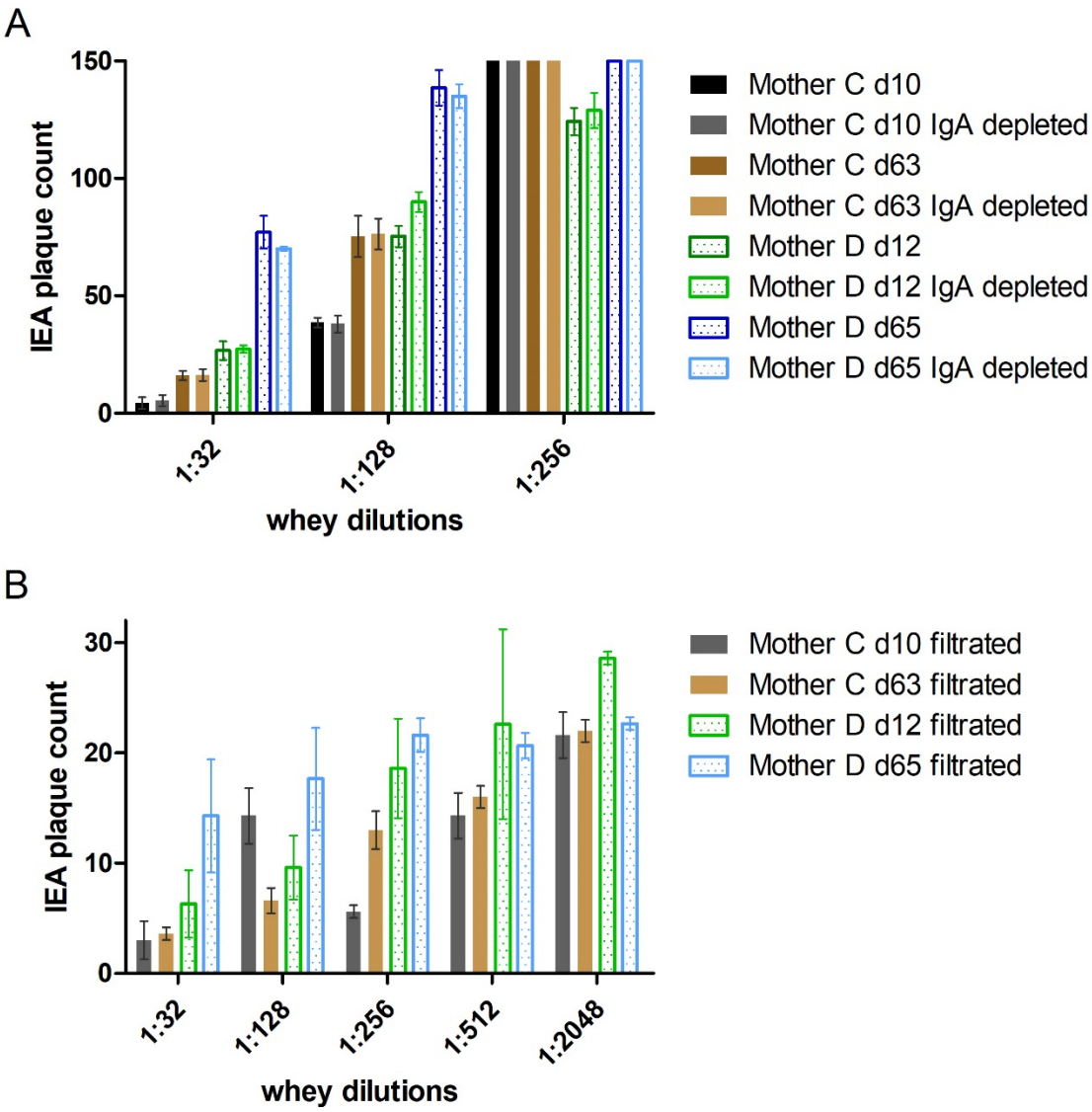

Figure 24: IgA depletion and filtration experiment.
Breast milk whey was depleted of IgA and used in a plaque reduction assay in different dilution steps (A). The dilution steps higher than 1:256 are not shown, since the plaque counts of the virus control with 150 plaques was not reduced anymore. The HCMV-seropositive mother C and the seronegative mother D are shown.

HCMV-specific plaque reduction in milk whey or plasma was read out as plaque numbers following a five day incubation period before IE1 staining. NT-capacity was either calculated with reference to the virus control (see below) or pools were created to minimize inter-individual variability and set in comparison to the HCMV-seronegative pools (see BlooMil study).

5.2.1 Heat-inactivation: impact on HCMV neutralizing antibodies

HCMV inactivation in breast milk is an important step before feeding preterm infants, whose immune system is still developing. Therefore, pasteurization methods can be performed. Short-term pasteurization is a very gentle method, where breast milk is only heated for 5 sec to 62°C. The short heating time is accomplished by producing a thin milk film in the flask. The Holder pasteurization heats up samples to 62.5°C for 30 min. It is an open question, whether virus inactivation methods reduce HCMV-specific neutralization capacity.

The neutralization assays for the comparison of different pasteurization methods were performed without prior IgA depletion or IgG retaining, since only HCMV-seropositive milk of the same mothers were used.

Short-term and holder pasteurized breast milk samples of four mothers were compared in neutralization assays. From two additional mothers, raw milk was either compared to Holder or short-term pasteurized milk. The results of one of the experiments are shown exemplarily in Figure 25 [276]. Holder pasteurized milk whey displayed very high plaque counts (Figure 25 a) and therefore very low NT-capacity compared to raw milk whey (Figure 25 b). The NT-capacity at a 32-fold dilution was already only half as effective as that of raw milk whey. When native milk was compared to short-term pasteurized milk whey (Figure 25 d and e), only minimal differences were observed in plaque counts and neutralization capacities.

The differently treated milks were also used for recomLine blots. A loss of antigen binding was found for Holder pasteurized milk (Figure 25 c), whereas after short-term pasteurization, antibodies were still detectable to the same degree as in native milk whey (Figure 25 f).

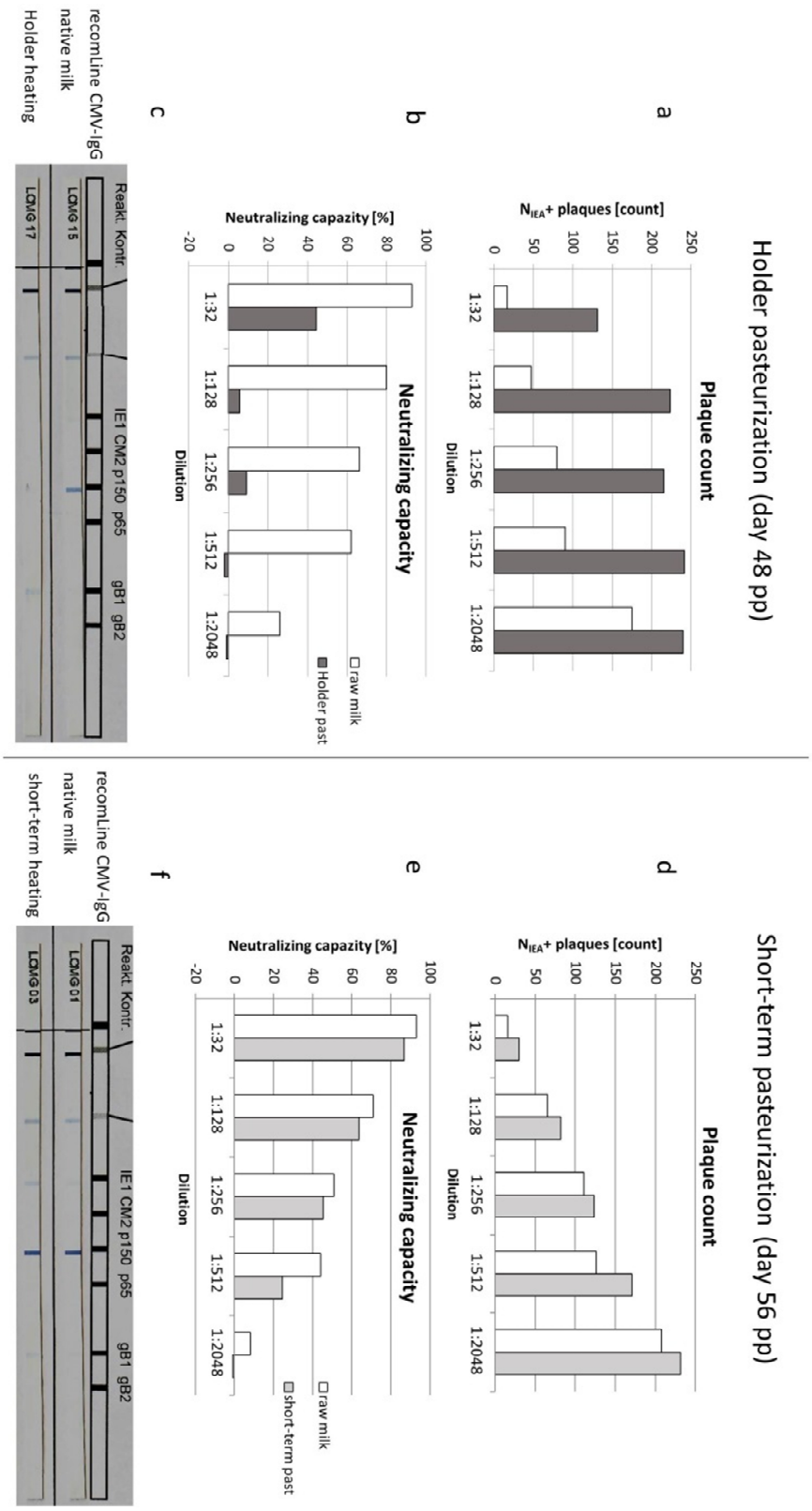

Figure 25: Neutralization assays with different methods of pasteurization[276].
Breast milk short-term and Holder pasteurized milk with corresponding raw milk of one mother at two time points (day 48 and 56 p.p.). a) shows the plaque count of Holder pasteurized and native breast milk samples in a neutralization assay at 48 days p.p. b) shows the corresponding neutralization capacity calculated with the virus control as reference. RecomLine Blots of the native and Holder pasteurized milk whey is displayed in c). d), e) and f) show the same for short-term pasteurized milk and native milk 56 days p.p.

5.3 BlooMil study

5.3.1 Study design

In cooperation with the Neonatology Department of the University Hospital Tuebingen, the AG Kilian Wistuba-Hamprecht (Division of Dermatooncology, Department of Dermatology) and Graham Pawelec (Department of Immunology) a study named BlooMil study was inaugurated. Mothers of mostly preterm infants were invited to join the study between April 2018 and April 2019 for the main BlooMil study of breast milk viral load, HCMV-specific IgG and phenotypical leukocyte subset analysis. Between September 2019 and February 2020 an adjunct BlooMil study cohort was asked to participate for the analysis of HCMV-specific T cells (tetramer analysis). In total, 45 mothers were recruited and gave their informed written consent. The study was approved by the Clinical Ethics Committee at the University Hospital Tuebingen (project number: 804/2015-BO2).

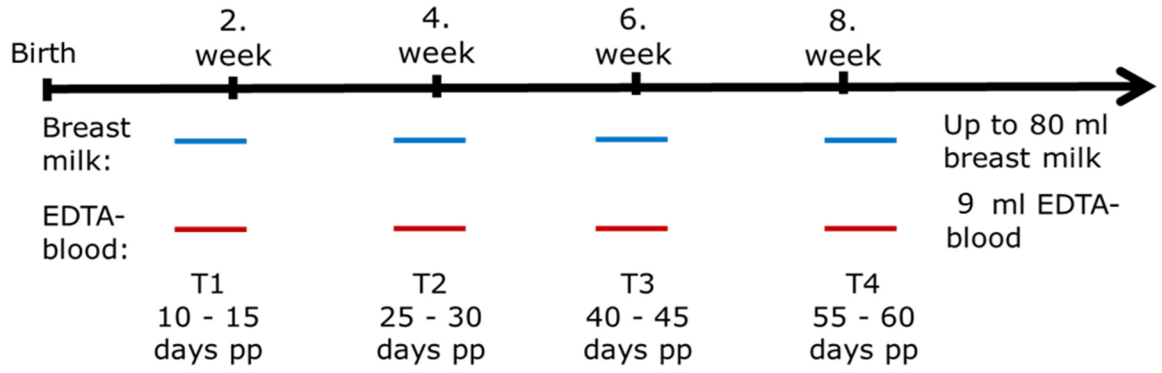

Figure 26: BlooMil study design.
Mothers were asked to donate blood and breast milk at four time ranges (T) after birth (T1 - 10 to 15, T2 - 25 to 30, T3 - 40 to 45 and T4 - 55 to 60 days p.p.).

36 mothers participated in the main BlooMil study, but eight had to be excluded due to too less milk during the longitudinal observation of the study or transfer to other hospitals. The remaining 28 mothers were sampled at four time ranges (T): T1 - 10 to 15, T2 - 25 to 30, T3 - 40 to 45 and T4 - 55 to 60 days p.p. (Figure 26). At each time range up to 80 ml of freshly pumped breast milk and up to 9 ml of EDTA-blood were donated by each mother. Separating the group into HCMV-seropositive and –seronegative mothers resulted in 18 seropositive and ten seronegative mothers (Figure 27). All seropositive mothers were latently infected (detectable IgG with high avidity, ECLIA). Only one mother was persistently expressing a low IgM, all other mothers were IgM negative (ECLIA).

This one mother (mother 12, Table 29) was excluded from the analysis of PBMCs and BMCs, since she had a primary infection during her pregnancy and participated in the HIG-study Tuebingen and got five treatment cycles with Cytotect®.

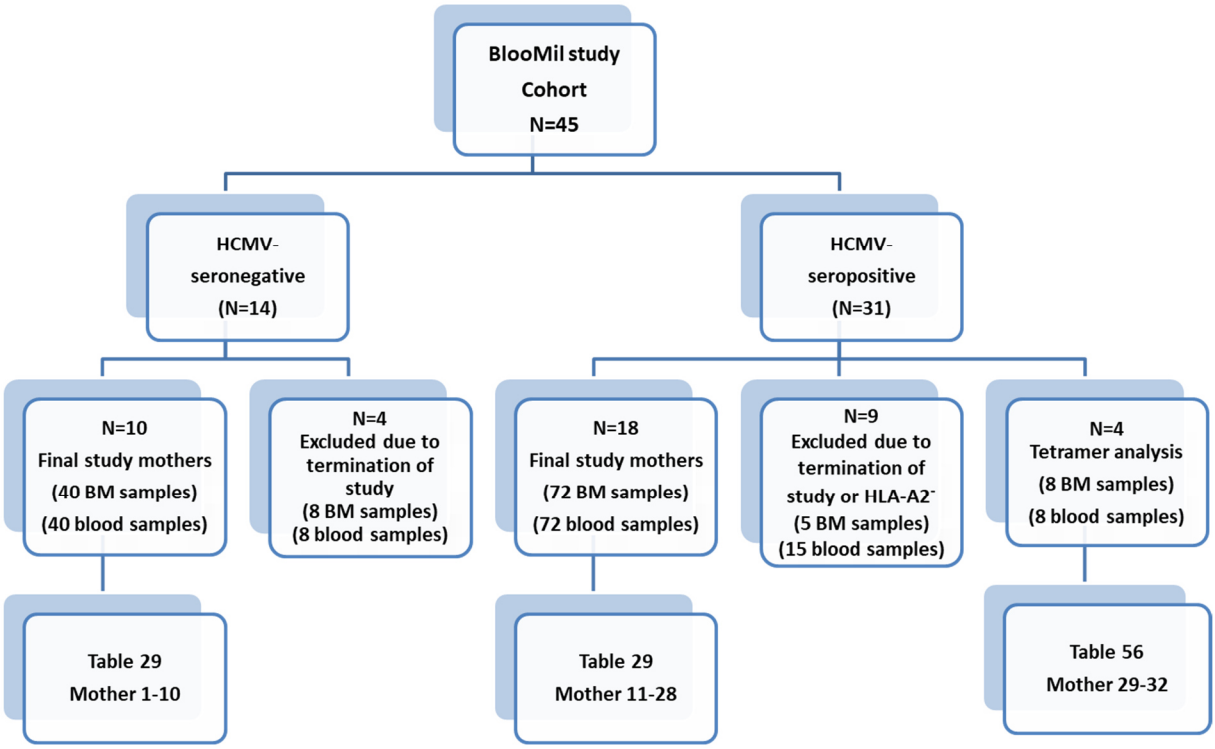

Figure 27: BlooMil study organigram.
The BlooMil study cohort consisted of 45 mothers, which were further distinguished by their HCMV-serostatus. After exclusion of mothers, who terminated the study, the final study mothers for the main BlooMil study and the mothers for adjunct BlooMil study cohort for tetramer analysis remained.

After the main BlooMil study, an additional four out of nine mothers were found to be HLA-A*02:01 positive and were participants of the adjunct BlooMil study cohort for tetramer analysis of HCMV-specific $CD8^+$ T cells. The same amounts, as mentioned above for breast milk and blood samples, were analyzed at T1 and T3. One out of the four mothers could only participate at T1, due to too less milk at T3.

5.3.2 Study cohorts

The study cohort of the main BlooMil study is shown in Table 29. The HCMV-seropositive mothers were on average 34 ± 5.1 years old and their GA was on average at 30.15 ± 4.3 weeks, whereas the HCMV-seronegative mothers were on average 32.2 ± 2.7 years old and had a mean GA of 30.75 ± 4.9 weeks. All seronegative mothers had their country of origin in Germany, while for the HCMV-seropositive mothers only 55.5% stated Germany. Five HCMV-seropositive mothers had multi-births with twins or triplets.

Table 29: Demographics of the BlooMil study mothers

Mother	HCMV-IgG	Age [years]	GA [weeks]	BW [g]	number of births	multi-births	country of origin	color-coding of figures
1	neg	27	27 2/7	940	first	no	Germany	black
2	neg	37	27 0/7	745	third	no	Germany	black
3	neg	31	26 2/7	515	second	no	Germany	black
4	neg	33	33 3/7	1990	first	no	Germany	black
5	neg	34	33 4/7	1800	first	no	Germany	black
6	neg	31	29 5/7	1840	first	no	Germany	black
7	neg	33	24 5/7	550	second	no	Germany	black
8	neg	31	34 2/7	2100	first	no	Germany	black
9	neg	31	40 6/7	3470	first	no	Germany	black
10	neg	34	30 3/7	1180	first	no	Germany	black
11	pos	36	25 4/7	860	first	no	Germany	dark blue
12	pos	33	39 2/7	3100	second	no	Germany	red
13	pos	30	23 6/7	625	third	no	Italy	green
14	pos	33	24 2/7	580^{+}780	first	no	Bosnia-Herzegovina	purple
15	pos	30	30 2/7	1165	second	no	Russia	orange
16	pos	33	28 5/7	1340	second	no	Italy	black
17	pos	28	33 0/7	2600	first	no	Syria	pink
18	pos	33	29 1/7	1190	first	no	Germany	beige
19	pos	39	38 1/7	3000	third	no	Germany	bright brown
20	pos	38	31 5/7	1540	second	no	Germany	dark red
21	pos	27	28 4/7	970^{+}1170	first	twins	Germany	brown
22	pos	32	27 2/7	920^{+}485^{+}945	second	triplets	Germany	dark green
23	pos	49	27 6/7	880^{+}1250	first	twins	Germany	blue
24	pos	36	34 2/7	2430	second	no	Italy	bright green
25	pos	31	31 4/7	1790	first	no	Sri Lanka	grey
26	pos	37	30 6/7	990^{+}1410	first	twins	Macedonia	bright blue
27	pos	30	25 5/7	915	fourth	no	Germany	bright purple
28	pos	38	32 4/7	1970^{+}2065	first	twins	Germany	yellow

5.3.3 Dynamics of viral reactivation

The DNA from milk whey was extracted and a quantitative PCR was performed to describe the dynamics of HCMV reactivation in breast milk. Almost all HCMV-seropositive BlooMil study mothers (17 of 18, 94.4%) had HCMV DNA in their breast milk (Figure 28). Only mother 19 showed no reactivation of HCMV at all measured time ranges (one of 18, 5.6%). Another three of 18 (16.7%) mothers did not reactive at T1, but later at T2 (mother 17), T3 (mother 20) or T4 (mother 16). Therefore, HCMV in breast milk reactivated in 83.3% of the mothers between birth and T1. The calculated mean onset of all mothers was at 11.5 days p.p. Mother 27 only showed virus shedding at T1 and T2 and mother 15 had no viral shedding at T4. After onset, all other mothers (12 of 18, 66.7%) displayed viral shedding over the whole observed period.

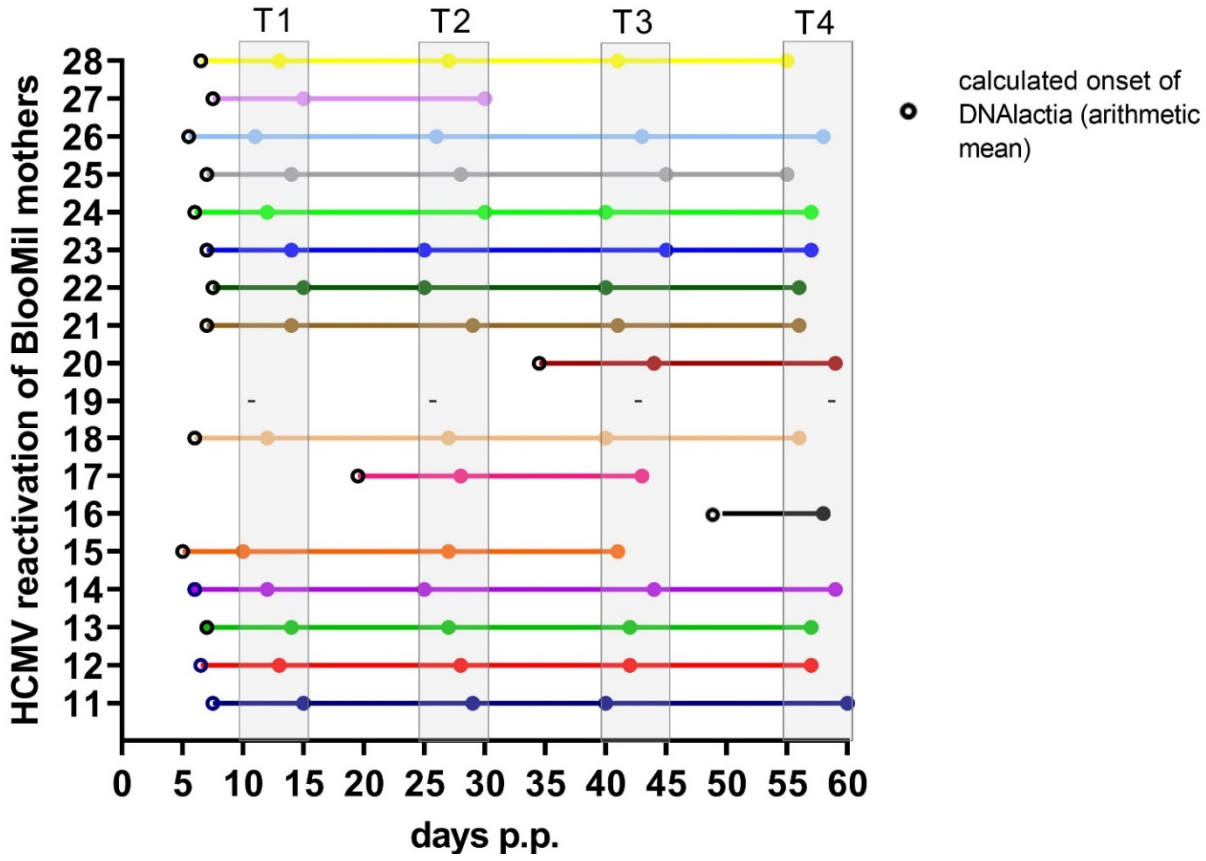

Figure 28: Calculated onset and course of quantitative DNAlactia of BlooMil study mothers. *The numbers of the y-axis match the mothers of Table 29.The time ranges were T1 - 10 to 15, T2 - 25 to 30, T3 - 40 to 45 and T4 - 55 to 60 days p.p. Mother 19 did not reactivate HCMV in breast milk at the measured time points (-). Onset is calculated by the arithmetic mean between the first measured positive sample and the last negative sample or time of birth. Three mothers reactivated HCMV late (16, 17, 20) and initial HCMV PCR was negative. The last positive result marks the last data point connected with a line; no calculations were done for the end of shedding. Individual color-coding is applied.*

Most of the mothers (15 of 18, 83.3%) displayed a unimodal course of DNAlactia with peak viral load at T2 (11 of 18, 61.1%) or T3 (four of 18, 22.2%, Figure 29). Two mothers showed

slight increases towards the end of the observation range. The peak viral load varied highly from mother to mother. The highest viral load detected was from mother 14 with $2.6x10^6$ copies/ml. Other mothers had very low peak viral loads (mother 17 with $1.1x10^4$ copies/ml), but still showed unimodal courses.

The plasma samples of BlooMil mothers were also monitored for HCMV DNA with nPCR. All plasma samples had no detectable HCMV DNA at any time point.

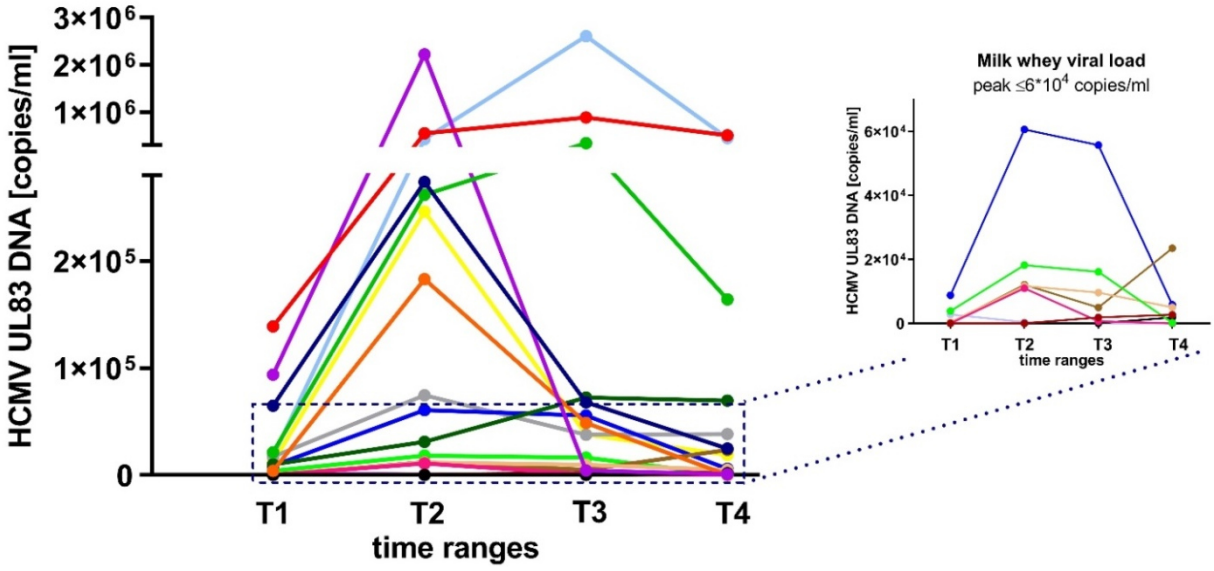

Figure 29: DNAlactia in milk whey of HCMV-seropositive BlooMil study mothers[274].
Results of the qPCR using target gene UL83 are shown. The time ranges are T1 - 10 to 15, T2 - 25 to 30, T3 - 40 to 45 and T4 - 55 to 60 days p.p. The insert shows milk whey viral loads with a peak level lower than $6x10^4$. Mother 19 did not reactivate the virus and is not shown in this graph. Individual color-coding is applied.

Virolactia was measured with microculture assays and similar, but varying to the corresponding DNA quantities, courses were found (Figure 30). Still, the virolactia and DNAlactia revealed strong correlations. At T1 with Spearman's R (r) =0.714; T2 with r=0.675, T3 with r=0.482 and T4 with r=0.785.

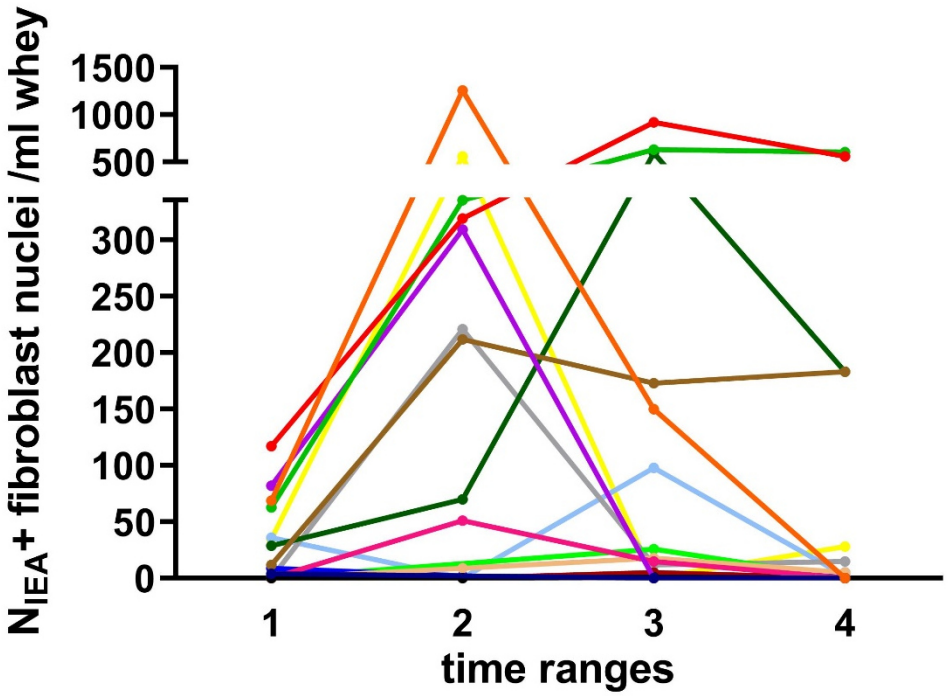

Figure 30: Virolactia in milk whey of HCMV-seropositive BlooMil study mothers.
Results of the short-term microculture assays are shown. The time ranges are T1 - 10 to 15, T2 - 25 to 30, T3 - 40 to 45 and T4 - 55 to 60 days p.p. Viral isolates were obtained from all mothers. Only Mother 19 did not reactivate the virus. Individual color-coding applies.

All breast milk samples of HCMV-seronegative mothers were negative in microculture and nPCR tests.

5.3.4 Humoral immune response (HCMV-specific IgG)

5.3.4.1 ECLIA

HCMV-specific IgGs were analyzed in milk whey and plasma of the seropositive cohort of the BlooMil study with ECLIA (Figure 31). The plasma levels of all 18 mothers widely differed from 40 to 4532 U/ml (Figure 31 A). The two mothers with very high HCMV-IgG levels in plasma (purple and bright blue), had also very high peak viral loads in milk whey (>1x10^6). However, using all samples, correlations between breast milk viral load and HCMV-specific IgGs in plasma were not found. An increase of plasma HCMV-IgG was detectable over all four time ranges after birth. The mean levels increased from T1 (604 U/ml) to T4 (831 U/ml) by 227 U/ml. Friedman test confirmed a significant increase (p=0.00018) and the Dunn Bonferroni post-hoc test with correction for multiple testing after Bonferroni revealed a significant increase from T1 to T3 (p=0.0029) and from T1 to T4 (p=0.00022). Mother 12 (red, primary infection during pregnancy) had very low plasma HCMV-IgG levels.

In milk whey, only ten of 18 mothers (55.6%) were positive for ECLIA HCMV-IgG and an additional three mothers showed borderline levels (16.6%) (Figure 31 B). The overall amount of HCMV-specific IgGs in milk whey was about 275-fold lower than in plasma. Six of 18 mothers (33.3%) displayed a sharp increase by three- to eight-fold from T1 to either T3 or T4, depending on the mother. Mothers 14 and 26, who had high milk whey viral loads, had a higher HCMV-specific-IgG titer and revealed an increase over time in milk whey. However, correlations with viral loads were not found. Friedman test of all positive samples showed no significant changes over time (p=0.15), but Wilcoxon test without corrections revealed a significant increase between T2 and T4 (p=0.037) in milk whey. When Friedman test was only performed on the six increasing samples in milk whey, a significant increase was detected (p=0.042).

A Spearman correlation from plasma to whey HCMV-IgG was found (Figure 31 C, D), but the correlation at T1 was stronger and higher significant than at T4, indicating an unproportional increase of HCMV-IgGs in milk whey.

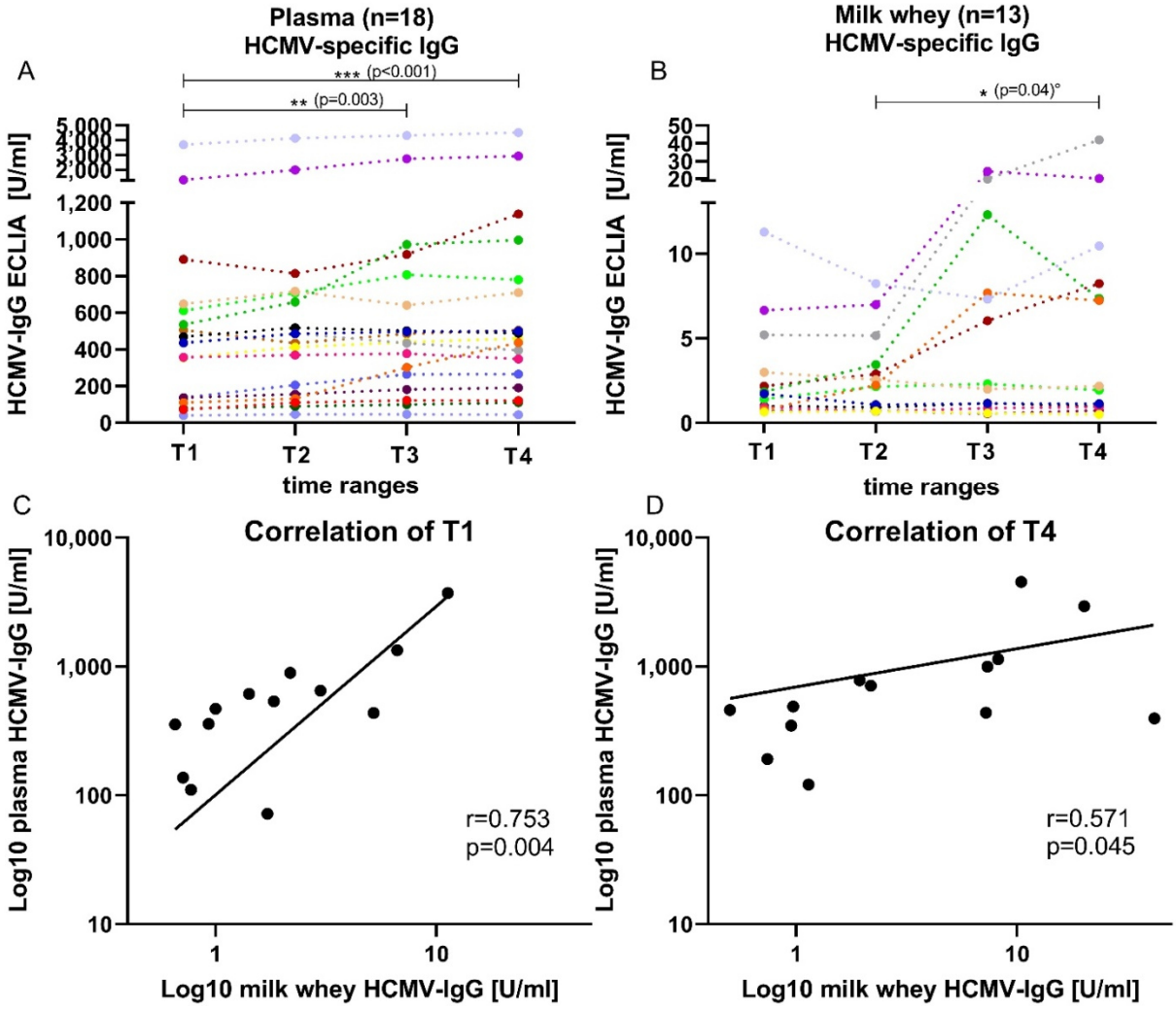

Figure 31: HCMV-specific IgG titers in plasma and whey of the BlooMil study mother[274]. *HCMV-specific IgG ECLIA values are shown in A) plasma and B) milk whey of all seropositive BlooMil study mothers. The time ranges are T1 - 10 to 15, T2 - 25 to 30, T3 - 40 to 45 and T4 - 55 to 60 days p.p. The Friedman test was used for both kinetics in plasma (significant) and milk whey (not significant). Dunn-Bonferroni post-hoc test with Bonferroni corrections showed significant changes between T1 and T4 (*** p<0.001) and T1 and T3 (**p=0.003) in plasma. In milk whey, the Wilcoxon matched pairs signed rank test without corrections showed a significant increase from T2 to T4 (°p=0.04). The correlation of blood and milk whey HCMV-IgGs are given with the Spearman correlation and a non-linear regression at C) T1 (r=0.753, p=0.004) and D) T4 (r=0.571, p=0.045).*

5.3.4.2 RecomLine blot

In an additional approach to investigate HCMV-specific IgGs, recomLine blots analyzing reactivities against six different antigens were performed with samples of T1 (10-15 days p.p.) and T3/T4 (40-60 days p.p.).

Anti-IE1-IgGs were found in 12/18 plasma samples (66.6%) with differing intensities at T1 (Figure 32 A). However, only two of 18 mothers (11.1%) showed IgG antibodies against IE1 in milk whey (Figure 32 A), one of them only detected around cut-off level. At T3/T4 three mothers displayed a seroconversion against IE1 in plasma (Figure 32 B). In whey, five additional mothers had reactivities against IE1. Overall the intensities increased in plasma and in milk whey from T1 to T3/4.

For anti-CM2-IgG similar intensities were depicted (Figure 32 C, D). Also, three mothers had seroconversions against CM2 in plasma at T3/T4, but only two developed reactivity against CM2 in milk whey. Again, an increase in intensities was observed from T1 to T3/4. In milk whey, one mother showed a very strong increase with high intensities (+++) at the later time range (Figure 32 D).

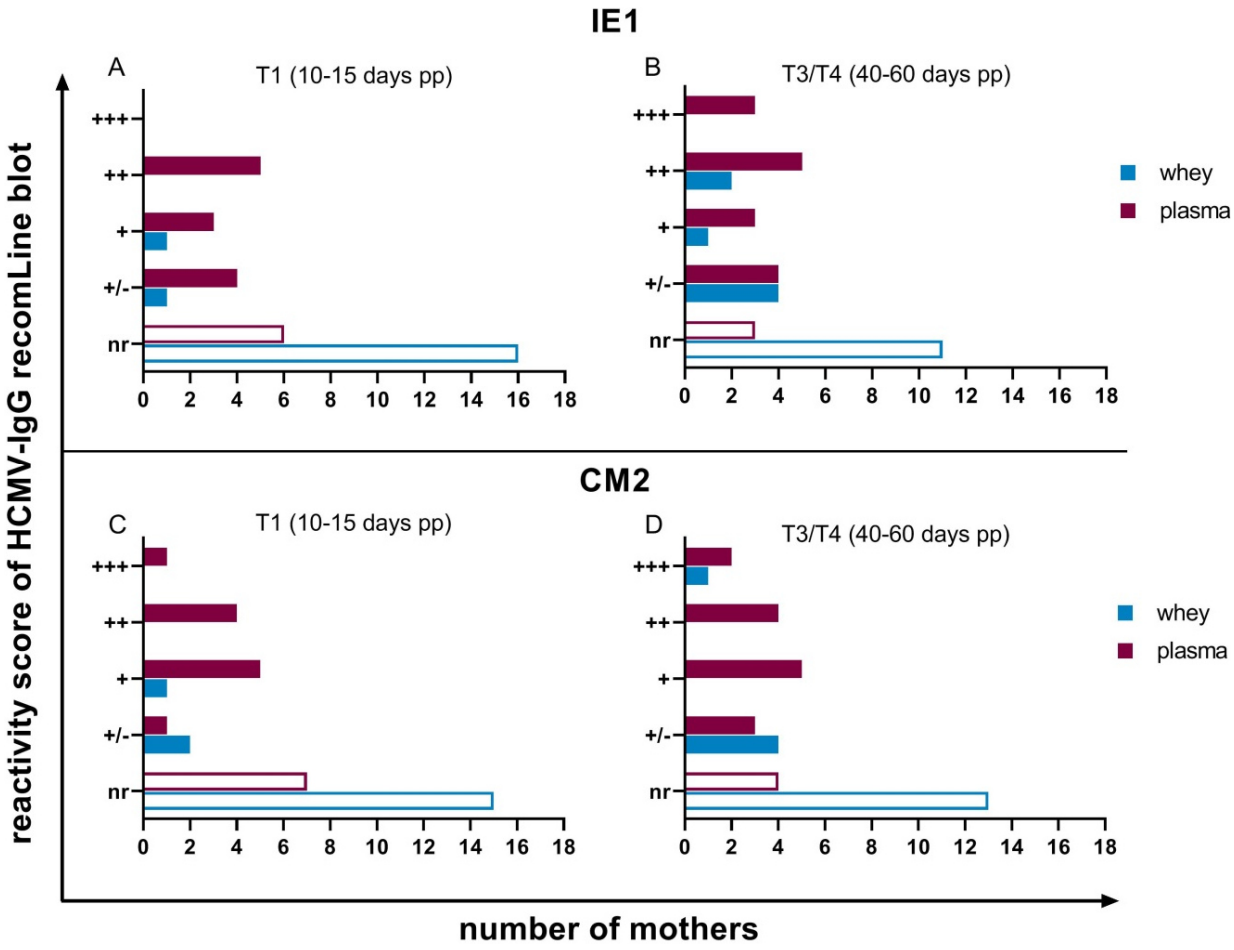

Figure 32: RecomLine blot reactivity scores of anti-rec IE1 and anti-rec CM2 IgG[274].
Plasma and whey IgGs at A) T1 (10-15 days p.p.) and B) T3/T4 (40-60 days p.p.) against recombinant immediate early 1 (IE1) and at C) T1 (10-15 days p.p.) and D) T3/T4 (40-60 days p.p.) against recombinant CM2. The number of mothers expressing the scores is shown on the x-axis. Scoring on the y-axis was performed as followed: (nr) – non-reactive, (+/-) – around cut-off level, (+) – one-fold, (++) – two-fold or (+++) – three-fold higher than cut-off limit. Plasma was diluted 100-fold, milk whey two-fold.

Two important phosphoproteins of the tegument, p150 and p65, were also analyzed for the humoral immunogenicity (Figure 33). All mothers expressed anti-p150-IgGs constitutively in plasma, showing very high intensities (Figure 33 A and B). All mothers also exhibited reactivities against p150 in milk whey, but five of them had only reactivities around cut-off level (Figure 33 A). Some mothers revealed increased intensities to the later time range T3/4 in milk whey (Figure 33 B).

Anti-p65-IgG highly varied in intensities between the mothers. Lower intensities were observed in milk whey than in plasma (Figure 33 C and D). Seroconversion from T1 to T3/T4 was only found in plasma of one mother. However, generally increased intensities were also found for anti-p65 IgGs in both body fluids at the later time range.

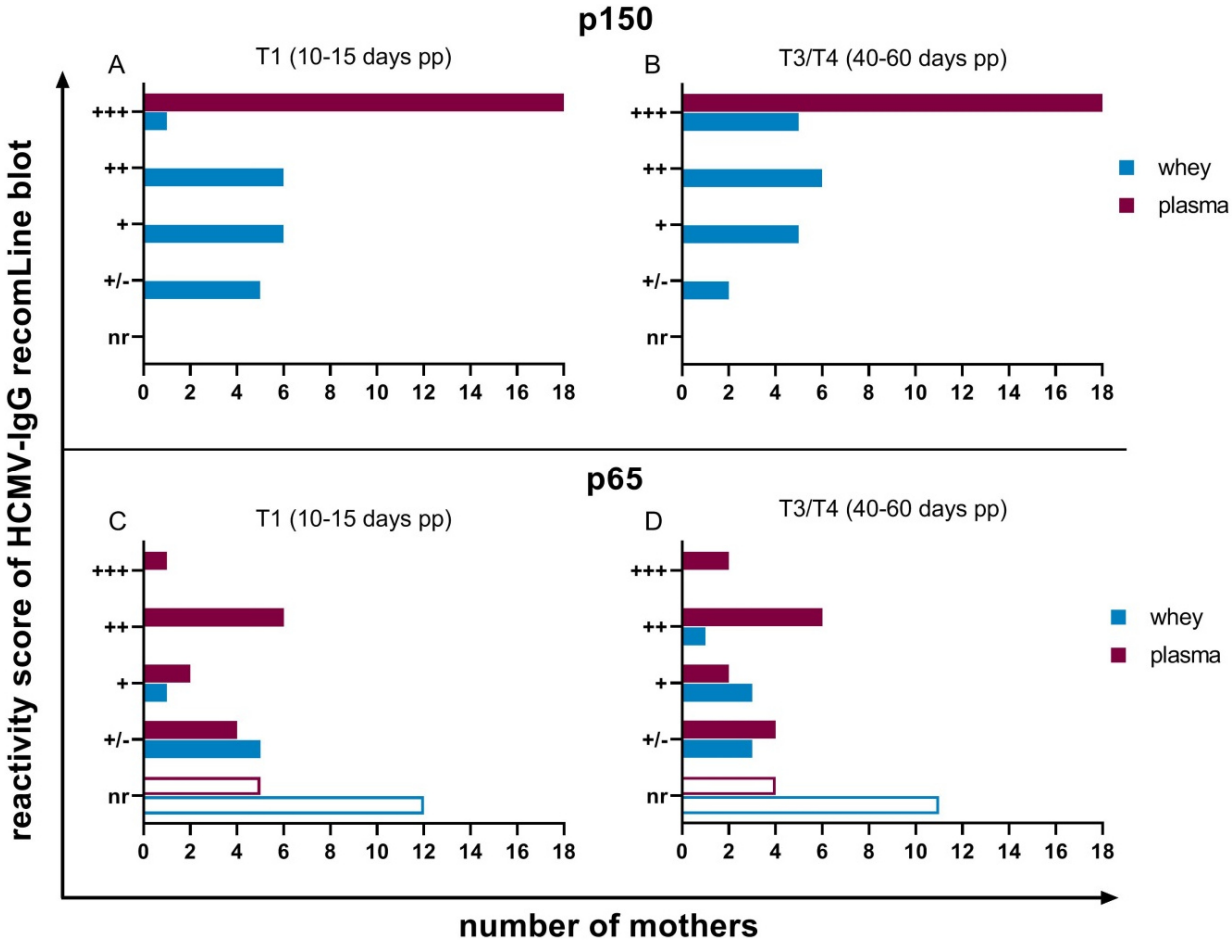

Figure 33: RecomLine blot reactivity scores of anti-rec p150 and anti-rec p65 IgG[274].
Plasma and whey IgGs at A) T1 (10-15 days p.p.) and B) T3/T4 (40-60 days p.p.) against recombinant p150 protein and at C) T1 (10-15 days p.p.) and D) T3/T4 (40-60 days p.p.) against recombinant p65. The number of mothers expressing the scores is shown on the x-axis. Scoring on the y-axis was performed as followed: (nr) – non-reactive, (+/-) – around cut-off level, (+) – one-fold, (++) – two-fold or (+++) – three-fold higher than cut-off limit. Plasma was diluted 100-fold, milk whey two-fold.

Anti-gB1-IgGs in plasma were detected in all mothers in varying intensities, but all above cut-off levels (Figure 34 A). At T1 in whey, five mothers showed levels around cut-off, while all others were non-reactive for anti-gB1 (13 of 18, 72.2%). An increase of the intensities from T1 to T3/4 was observed in plasma and milk whey. Three mothers developed higher intensities than cut-off level in milk whey (Figure 34 B).

Anti-gB2-IgG was variably expressed in plasma and only showed slight increases over time. However, no seroconversions were found (Figure 34 C, D). Nevertheless, a high number of mothers (15 of 18, 83.3%) was positive in their plasma for anti-gB2-IgG. Only five of 18 mothers (27.7%) expressed IgGs against gB2 in milk whey. An increase of intensities over time was also detectable for milk whey anti-gB2 IgGs (Figure 34 D).

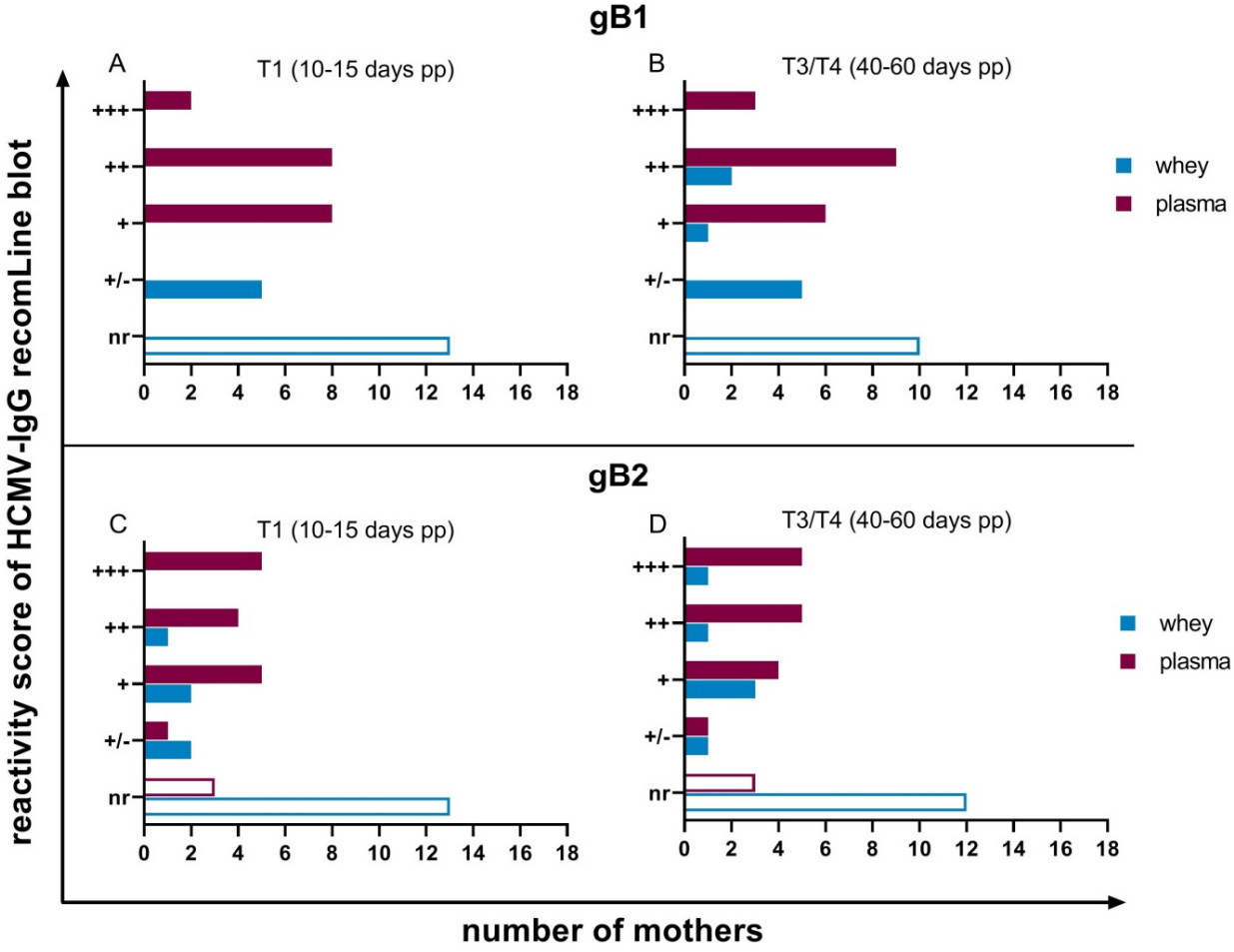

Figure 34: RecomLine blot reactivity scores of anti-rec gB1 and anti-rec gB2 IgG[274].
Plasma and whey IgGs at A) T1 (10-15 days p.p.) and B) T3/T4 (40-60 days p.p.) against recombinant gB1 and at C) T1 (10-15 days p.p.) and D) T3/T4 (40-60 days p.p.) against recombinant gB2. The number of mothers expressing the scores is shown on the x-axis. Scoring on the y-axis was performed as followed: (nr) – non-reactive, (+/-) – around cut-off level, (+) – one-fold, (++) – two-fold or (+++) – three-fold higher than cut-off limit. Plasma was diluted 100-fold, milk whey two-fold.

5.3.4.3 Neutralization capacity of plasma and whey

Neutralization assays were performed to see if the increase of HCMV-IgG ECLIA values and the higher intensities of recomLine blots at T3/4 were also visible in the neutralizing capacity of breast milk whey from T1 to T4. The clinical isolate H2497-11 form amnion fluid was incubated with either whey or plasma pools and was afterwards incubated on ARPE-19 cells for five days to stain for plaque forming IEA nuclei.

Pools of all BlooMil HCMV-seropositive or –seronegative mothers' whey or plasma samples were generated of either T1 or T4. Plaque counts were obtained and are shown in Figure 35 A and B of plasma and milk whey pools, respectively.

The plasma pool of HCMV-seronegative mothers displayed similar high plaque counts as the virus control in all dilution steps (Figure 35 A). The reduced number of plaque counts in HCMV-seropositive plasma pools showed the high neutralization capacity of HCMV-specific IgGs (Figure 35 A, C). Plaque counts (=infectivity) at T1 were higher compared to T4 of HCMV-seropositive mothers' plasma pools resulting in lower neutralizing capacity at T1 versus T4. The HIG positive control was prediluted to possess the same HCMV-IgG concentration as the mean of HCMV-seropositive plasma pools T1 and T4. Therefore, it showed plaque counts between the one of T1 and T4 plasma pools (Figure 35 A).

In contrast, whey pools of seronegative mothers revealed unspecific neutralization (Figure 35 B), as the pools were tested negative for HCMV-specific IgGs. Nevertheless, HCMV-seronegative mothers' whey pools showed still higher plaque counts than the whey pools of HCMV-seropositive mothers at T1 and T4 (Figure 35 B). HIG, diluted to the concentration of mean ECLIA IgG values of all breast milk pools with DMEM:F12 (see 4.2.4.9) revealed higher plaque counts than both HCMV-positive whey pools.

The actual NT-capacity was calculated by using the plaque counts of the seronegative pools as the reference value. Due to this procedure, the unspecific neutralization activity was excluded from the seropositive samples. NT-capacity was higher at the later time range in breast milk, however, the NT50-values differed not as highly as in plasma (Figure 35 D).

In accordance with the plaque count results, the NT capacity of seropositive pools at T1 (Probit-analysis: NT-50 of plasma 1:3,000 and of whey 1:86) was lower than at T4 (Probit-analysis: NT-50 of plasma: 1:4,000 and of whey: 1:100) in plasma (Figure 35 C) and in milk whey (Figure 35 D). The NT-50 was about 40 fold lower in milk whey compared to plasma.

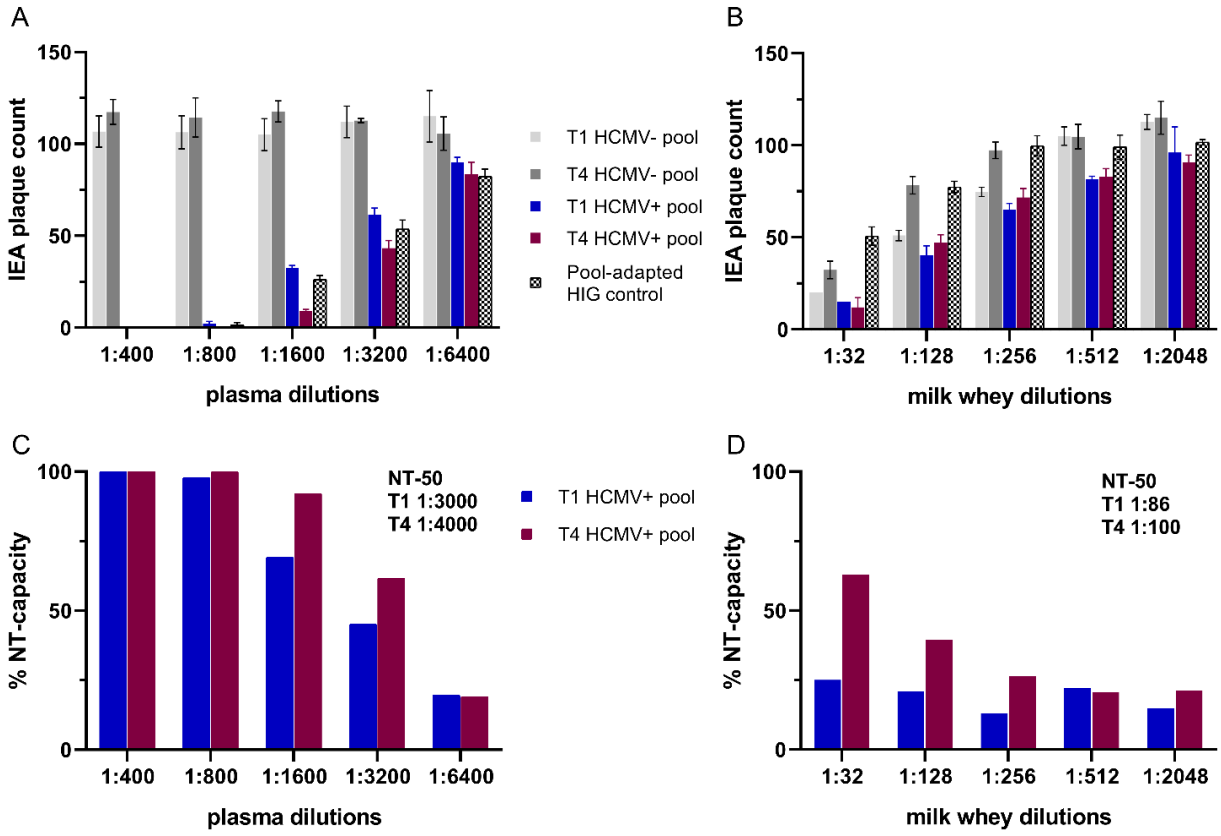

Figure 35: Neutralization assays of plasma and milk whey pools of BlooMil-study mothers[274]. *Immediate early antigen (IEA) plaque counts (>6 nuclei equals one plaque) of neutralization assays on ARPE-19 cells with A) plasma and B) milk whey pools. The mean with standard deviation (SD) of triplicates is displayed. Hyperimmunoglobulin (HIG) was used as positive control. Neutralization capacity (NT-capacity) was calculated with the seronegative plaque counts as reference for C) plasma and D) milk whey pools. NT-50 values were calculated with the Probit analysis. Time ranges used for pool generation are T1 – 10 to 15 and T4 – 55 to 60 days p.p.*

5.3.5 Immune cell monitoring

5.3.5.1 BlooMil study gating strategy

After collecting data about the humoral IgG-immune response to HCMV in milk whey and plasma, the focus was set on the cellular components in cooperation with AG Kilian Wistuba-Hamprecht (Division of Dermatooncology, Department of Dermatology) and Graham Pawelec (Department of Immunology). Phenotypical analysis of leukocyte populations in breast milk was compared to corresponding blood leukocytes in HCMV-seropositive and negative mothers using flow cytometry. A gating strategy was developed and is shown in Figure 36 (A to Q) of BMCs and in Figure 37 (A to Q) of PBMCs:
For the steps A to F, the same gating strategy was used as for the γδ T cell-panel (see 5.1.2). In a next step, the cells were divided by CD14 and HLA-DR (G) and gates were set on the CD14-positive and HLA-DR negative to dim population for M-MDSCs. This gate was adapted from the gating of PBMCs onto BMCs (Figure 37 and Figure 36, respectively). After several different approaches due to lower cell counts and high variations in the HLA-DR expression on monocytes in breast milk, this was established as the best way to assure a consistent gating strategy. The gated population from F was also used in a next step (H) to further distinguish $CD14^+$ monocytes in general from the rest of cells with a CD14 vs EMA chart (H). The CD14-negative cells were used to gate lymphocytes in a morphological gate (I). The next CD3 vs CD56 graph shows the lymphocyte population split into $CD3^+$ T cells, $CD3^+CD56^+$ T cells and $CD56^+$ NK cells (J). Only the $CD3^+$ T cells were further subgrouped, due to too less $CD56^+$ T cells or NK cells in many of the breast milk samples. The $CD3^+$ T cells were divided into $CD8^+$ or $CD4^+$ T cells (K) and both were examined for either CD38 (L and O), HLA-DR (M and P) or the memory phenotypes by CCR7 or CD45RA (N and Q) expression for naïve ($CCR7^+$,$CD45RA^+$), central memory ($CCR7^+$, $CD45RA^-$), effector memory ($CCR7^-$, $CD45RA^-$) and TEMRA ($CCR7^-$, $CD45RA^+$) subsets. CD38 gates were set close to the negative population due to difficulties in breast milk to define distinct populations with high CD38 expression.

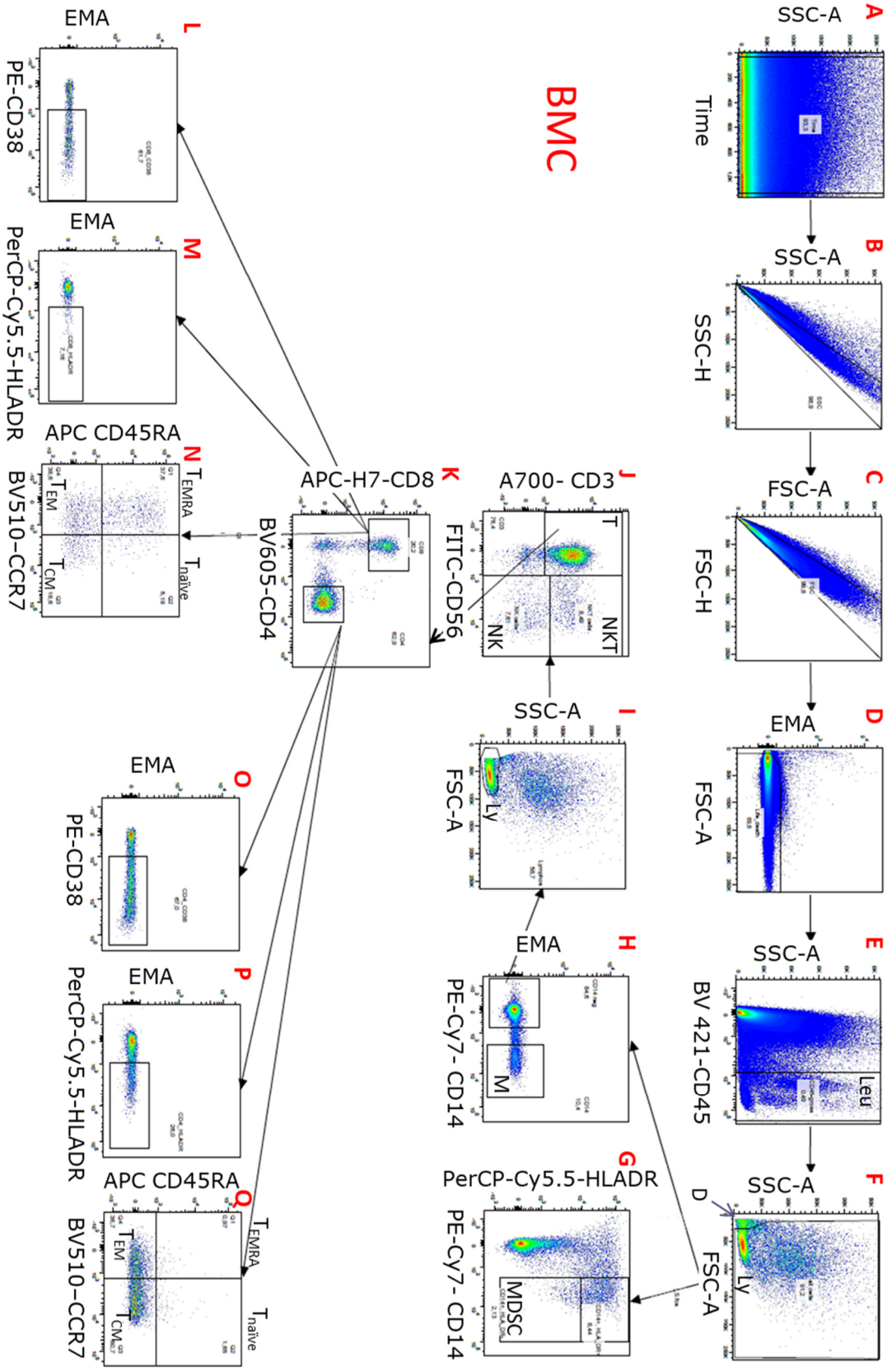

Figure 36: Example of the breast milk cell gating strategy for the BlooMil study.
Breast milk cell gating is shown and explained in the text above. Leu: leukocytes, D: debris, Ly: lymphocytes, MDSC: monocytic myeloid suppressor cells, M: monocytes, T: CD3⁺ T cells, NKT: CD56⁺ T cells, NK: natural killer cells, T_{EMRA}: TEMRA cells, $T_{naïve}$: naïve T cells, T_{EM}: effector memory T cells, T_{CM}: central memory T cells.

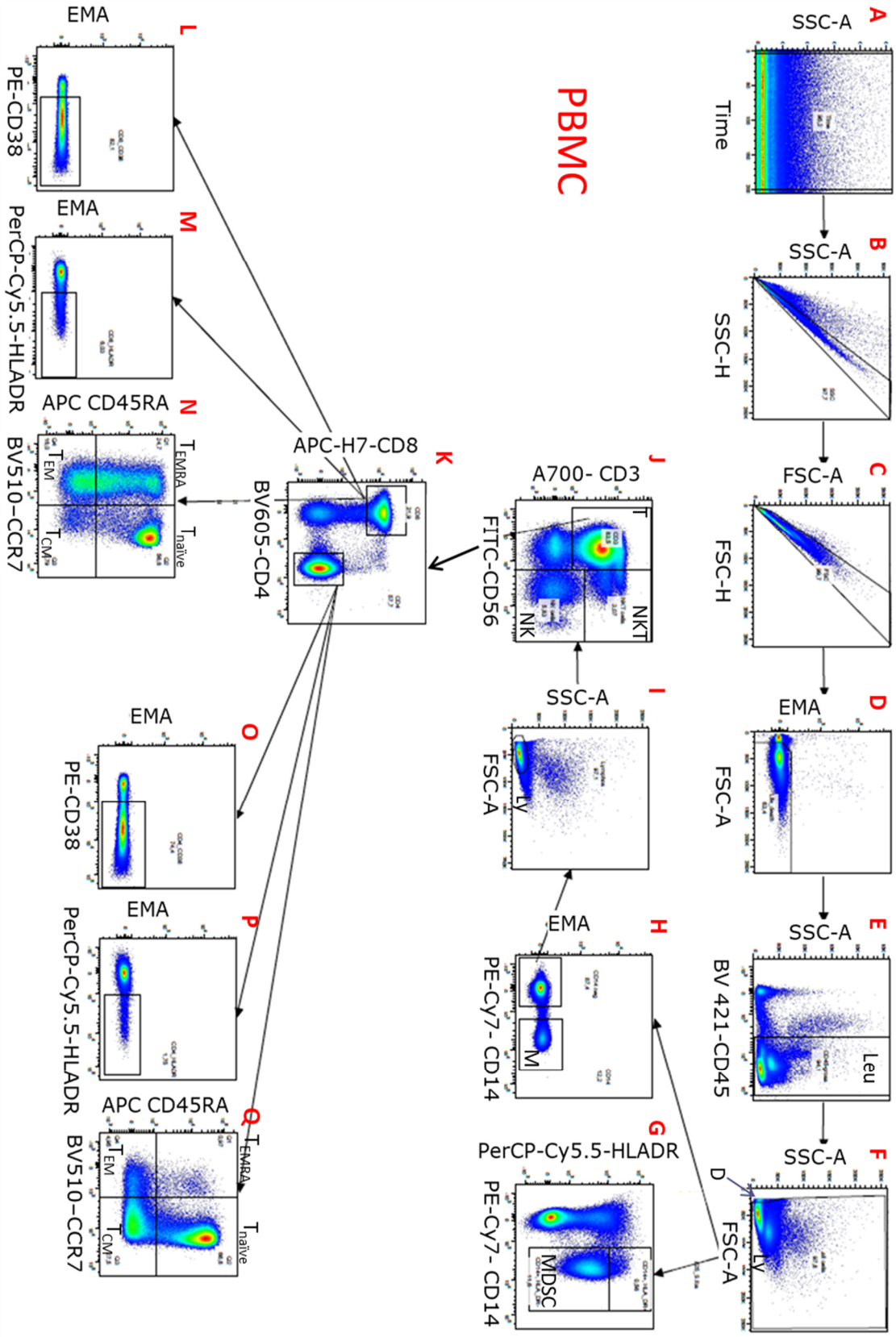

Figure 37: Example of the blood cell gating strategy for the BlooMil study.
Peripheral blood mononuclear cells (PBMC) gating is shown as explained in the text above. Leu: leukocytes, D: debris, Ly: lymphocytes, MDSC: monocytic myeloid suppressor cells, M: monocytes, T: CD3⁺ T cells, NKT: CD56⁺ T cells, NK: natural killer cells, T_{EMRA}: TEMRA cells, $T_{naïve}$: naïve T cells, T_{EM}: effector memory T cells, T_{CM}: central memory T cells.

The average number of total cells in breast milk, counted by a trypan blue staining, was at T1 around $1.2x10^5$ cells/ml with a decrease to T4 with $0.6x10^5$ cells/ml. PBMC counts per ml blood were in general higher and constantly remained around $9x10^5$ PBMC/ml. The analyzed leukocyte subset frequencies by flow cytometry are shown in detail in the following. A synopsis of the average frequencies (mean and SD) at each time point are given in Supplement table 1. All immune cell subsets did not show correlations with viral load.

5.3.5.2 Monocytes/Macrophages ($CD14^+$)

$CD14^+$ monocytes/macrophages were biweekly analyzed during the first two months after birth in breast milk and blood samples of HCMV-seropositive and –seronegative mothers of the BlooMil study (Figure 38).

$CD14^+$ monocyte frequencies **in blood** were consistently over time around 10-25% of all leukocytes regardless of HCMV-serostatus and time ranges (Figure 38 A and B, Table 30).

Monocyte frequencies in **breast milk** highly varied from 8 to over 60% of all leukocytes at T1. Mean breast milk monocyte frequencies showed a significant decrease from 27.0 ± 11.7% at T1 to 15.8 ± 11.0% at T4 in HCMV-seropositive mothers (p=0.0038, Figure 38 D) and from 25.1 ± 17.4% at T1 to 15.9 ± 8.8% at T4 in seronegative mothers (p=0.045, Friedman test in Table 31) (Figure 38 C). However, post-hoc test with corrections indicated only significant decreases in breast milk of seropositive but not seronegative mothers between T1 and T3, as well as between T1 and T4 (Table 31).

Monocytes of HCMV-seropositive mothers showed a tendency (p=0.067) towards higher frequencies in **breast milk** at T1 compared to **blood** frequencies. However, at T3, the breast milk frequencies were significantly lower (Wilcoxon test p=0.034, Table 31) than in blood. HCMV-seronegative mothers showed no differences between blood and breast milk frequencies (Figure 38 B, D).

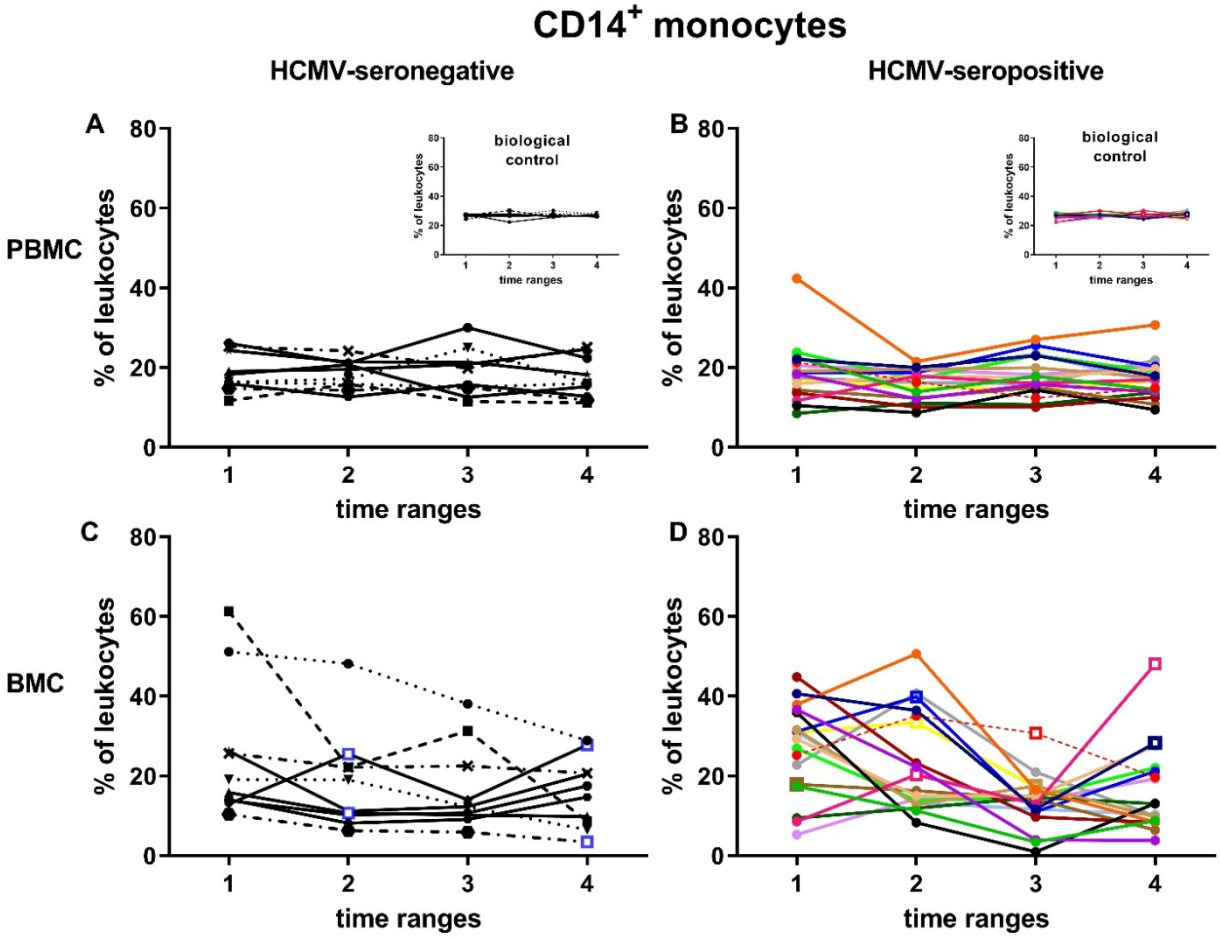

Figure 38: CD14⁺ monocyte kinetics in blood and breast milk of the BlooMil study mothers. *CD14⁺ monocyte frequencies acquired by flow cytometry are shown of peripheral blood mononuclear cells (PBMC) in (A) HCMV-seronegative mothers and (B) seropositive mothers. CD14⁺ monocyte frequency of breast milk cells (BMC) is displayed of (C) HCMV-seronegative and (D) seropositive mothers. The inserts in (A) and (B) show the biological control over all experimental days. Individual color-coding as described in Table 29 is applied. Mother 12 (red, dotted line) was excluded from statistical analysis due to HCMV-primary infection during pregnancy. The time ranges are T1 - 10 to 15, T2 - 25 to 30, T3 - 40 to 45 and T4 - 55 to 60 days p.p. Square data point symbols instead of round symbols indicate a time point where the breast milk cells showed a slightly red color in the cell pellet (presumably an indicator for mastitis).*

Table 30: Mean CD14⁺ monocyte/macrophage frequencieswith standard deviation (SD).

Cell subset	Mate-rial	HCMV	T1 [% mean ± SD]	T2 [% mean ± SD]	T3 [% mean ± SD]	T4 [% mean ± SD]
CD14⁺ monocytes	PBMC	IgG⁺	18.6 ± 7.5	16.0 ± 3.9	18.1 ± 4.9	17.2 ± 4.9
		IgG-	18.8 ± 4.9	18.3 ± 3.7	18.7 ± 5.8	17.4 ± 5.1
	BMC	IgG⁺	**27.0 ± 11.7**	**22.6 ± 12.7**	**12.3 ± 5.3**	**15.8 ± 11.0**
		IgG-	**25.1 ± 17.4**	**18.4 ± 12.4**	**16.6 ± 10.6**	**15.9 ± 8.8**

In short, monocyte frequencies showed no changes in blood over time, but in breast milk the monocyte frequency decreased from T1 to T4, especially in HCMV-seropositive mothers.

Table 31: Statistical analysis of CD14⁺ monocytes *The p-values are given and significant digits are bold and marked in grey. Friedman test was used to look for differences in the kinetics followed by a Dunn-Bonferroni post-hoc test with Bonferroni (B.) correction comparing single time ranges. The linear mixed model was used to show differences in the courses over time between HCMV-seropositive and seronegative mothers. Mann-Whitney U showed no differences between the single time ranges of seropositive or negative mothers (p>0.7, not shown). The Wilcoxon test with B. correction was used to compare single time ranges (T's) of blood and breast milk.*

CD14⁺ monocytes	PBMC HCMV pos	PBMC HCMV neg	BMC HCMV pos	BMC HCMV neg
Friedman test	0.20	0.29	**0.0038**	**0.045**
Dunn-Bonferroni post-hoc test with B. correction	-	-	T1 to T2: 1.0 T1 to T3: **0.013** T1 to T4: **0.032** T2 to T3: 0.14 T2 to T4: 0.28 T3 to T4: 1.0	T1 to T2: 0.15 T1 to T3: 0.15 T1 to T4: 0.092 T2 to T3: 1.0 T2 to T4: 1.0 T3 to T4: 1.0
Linear mixed model	0.437		0.212	
Wilcoxon with B. correction	PBMC HCMV pos	BMC HCMV pos	PBMC HCMV neg	BMC HCMV neg
T1's	0.067		1.0	
T2's	0.45		1.0	
T3's	**0.034**		1.0	
T4's	1.0		1.0	

5.3.5.3 M-MDSC

Monocytic myeloid derived suppressor cells (M-MDSC), defined as $CD45^+$, $CD14^+$, $HLA\text{-}DR^{-/dim}$, were gated in breast milk with the same gates as in blood. M-MDSC-frequencies referring to the total leukocyte population in either blood or breast milk are shown in Figure 39.

Frequencies around 10-20% were detected **in blood** (mean frequencies in Table 32) and did not change significantly over time regardless to HCMV-serostatus (Table 33, Figure 39 A, B).

In breast milk, the M-MDSC frequencies mostly were under 10% of total leukocytes (Figure 39 C and D). HCMV-seropositive mothers' mean frequencies slightly decreased from T1 with 3.1 ± 3.1% to T4 with 1.0 ± 0.8% (Friedman test with post-hoc test in Table 33).

When **blood and breast milk was compared** the data revealed that in breast milk the M-MDSC frequencies were significantly lower than in blood regardless to the HCMV-serostatus (Wilcoxon test in Table 33, Figure 39).

The frequency of MDSCs with the monocytes as parental population (data not shown) revealed also no significant changes over time and had low mean frequencies around 13%.

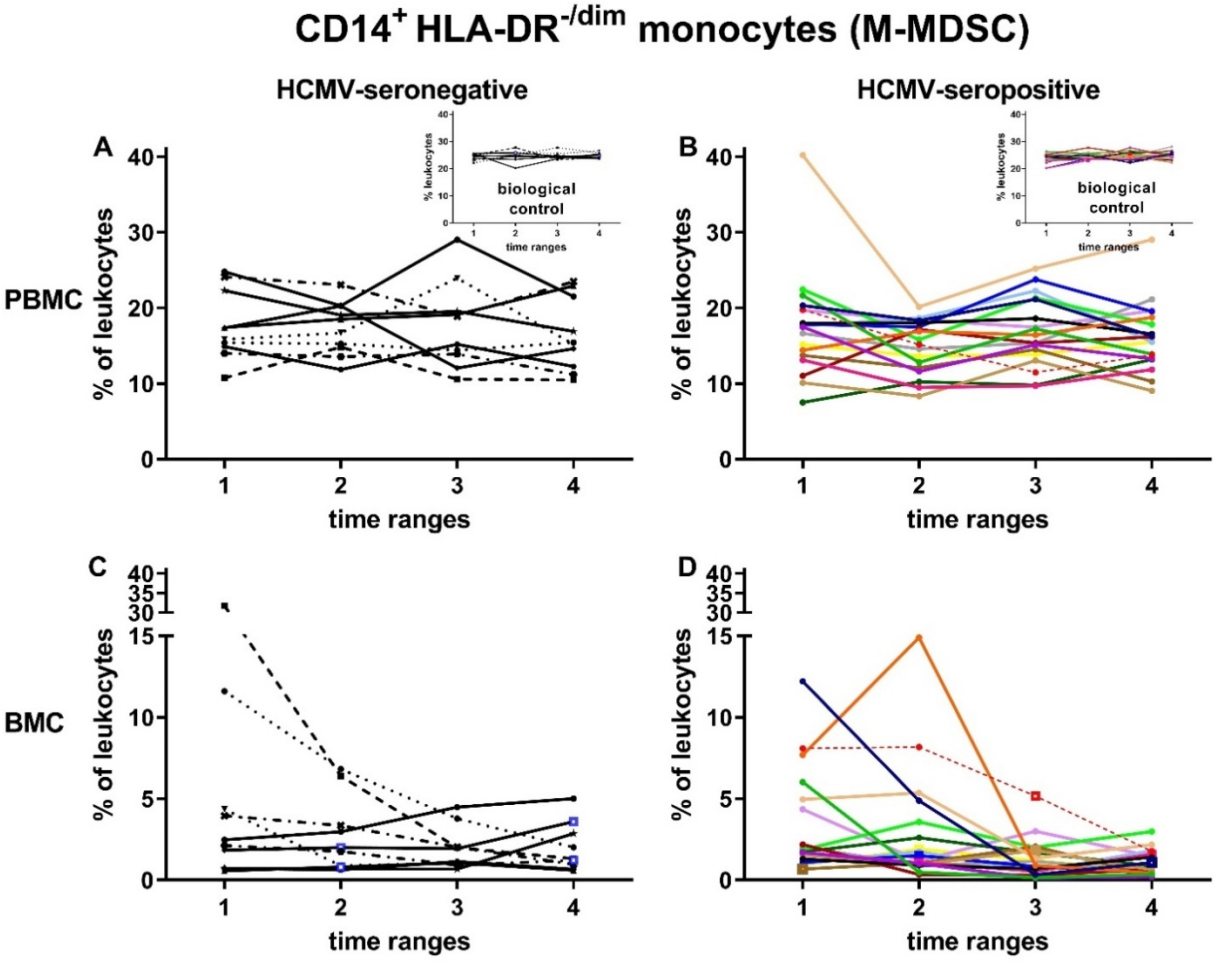

Figure 39: CD14⁺, HLADR $^{low/intermediate}$ myeloid derived suppressor cells (MDSC) in blood and breast milk of the BlooMil study mothers.
MDSC frequencies acquired by flow cytometry are shown of peripheral blood mononuclear cells (PBMC) in (A) HCMV-seronegative mothers and (B) seropositive mothers. MDSC frequency of breast milk cells (BMC) is displayed of (C) HCMV-seronegative and (D) seropositive mothers. The inserts in (A) and (B) show the biological control over all experimental days. Individual color-coding as described in Table 29 is applied. Mother 12 (red dotted line) was excluded from statistical analysis due to HCMV-primary infection during pregnancy. The time ranges are T1 - 10 to 15, T2 - 25 to 30, T3 - 40 to 45 and T4 - 55 to 60 days p.p. Square data point symbols instead of round symbols indicate a time point where the breast milk cells showed a slightly red color in the cell pellet (presumably an indicator for mastitis).

Table 32: Mean M-MDSC frequencies of T1 to T4 with standard deviation (SD).

Cell subset	Mate-rial	HCMV	T1 [% mean ± SD]	T2 [% mean ± SD]	T3 [% mean ± SD]	T4 [% mean ± SD]
CD14⁺, HLA-DR$^{-/dim}$ MDSC	PBMC	IgG⁺	*17.5 ± 7.1*	*14.9 ± 3.6*	*17.1 ± 4.5*	*16.3 ± 4.7*
		IgG-	17.7 ± 4.6	17.3 ± 3.5	17.7 ± 5.7	16.3 ± 4.8
	BMC	IgG⁺	**3.1 ± 3.1**	**2.6 ± 3.5**	**1.1 ± 0.8**	**1.0 ± 0.8**
		IgG-	6.0 ± 9.6	2.6 ± 2.3	1.9 ± 1.3	1.9 ± 1.5

In summary, M-MDSC frequencies showed no changes in blood over time, but in breast milk, some HCMV-seropositive mothers had a decrease from T1 to T4. M-MDSC frequencies were generally lower in breast milk compared to blood.

Table 33: Statistical analysis of M-MDSCs. *The p-values are given and significant digits are bold and marked in grey. Friedman test was used to look for differences in the kinetics followed by a Dunn-Bonferroni post-hoc test with Bonferroni (B.) correction comparing single time ranges. The linear mixed model was used to show differences in the courses over time between HCMV-seropositive and seronegative mothers. Mann-Whitney U showed no differences between the single time ranges of seropositive or negative mothers (p>0.26, not shown).The Wilcoxon test with B. correction was used to compare single time ranges (T's) of blood and breast milk.*

$CD14^+$ $HLA\text{-}DR^{-/dim}$ MDSC	PBMC HCMV pos	PBMC HCMV neg	BMC HCMV pos	BMC HCMV neg
Friedman test	0.078	0.43	**0.0088**	0.67
Dunn-Bonferroni post-hoc test with B. correction	-	-	T1 to T2: 1.0 **T1 to T3: 0.047** T1 to T4: 0.070 T2 to T3: 0.14 T2 to T4: 0.20 T3 to T4: 1.0	-
Linear mixed model	0.34		0.59	
Wilcoxon with B. correction	PBMC HCMV pos	BMC HCMV pos	PBMC HCMV neg	BMC HCMV neg
T1's	**0.0012**		0.188	
T2's	**0.0012**		**0.020**	
T3's	**0.0012**		**0.020**	
T4's	**0.0012**		**0.020**	

5.3.5.4 Total T cells ($CD3^+$), $CD4^+$ and $CD8^+$ T cells

$CD3^+$ T cell frequencies **in blood** were constantly around 50-70% of all leukocytes (mean frequencies in Table 34) and did not change over time in individual blood samples of HCMV-seronegative (Figure 40 A) or -seropositive mothers (Figure 40 B, Table 35).

In breast milk of seronegative mothers (Figure 40 C), the frequencies of $CD3^+$ T cells had high inter-individual variability, but were constantly between 10 to 40% of all breast milk leukocytes (mean with SD in Table 34). However, HCMV-seropositive mothers had a significant increase of T cell frequencies (Figure 40 D) from T1 (25.1 ± 14.4%) to T4 (43.7 ± 15.1%, Table 34) in breast milk (Friedman test p=0.0078, post-hoc test with corrections significant for T1-T4 and T2-T4, Table 35). Consequently, the mean T cell frequencies showed an increase by over 18%. Therefore, a significant increase of the breast milk kinetics of HCMV-seropositive compared to the seronegative mothers was found (linear mixed model p=0.043, Table 35).

Despite the increase, **breast milk** $CD3^+$ T cell frequencies were still significantly lower than **blood** frequencies of HCMV-seropositive mothers (Wilcoxon test in Table 35). Unsurprisingly, HCMV-seronegative mothers had also lower frequencies in breast milk compared to blood (Wilcoxon test in Table 35).

The HCMV-seropositive mother 16 (color code: black) had a very low T cell frequency in breast milk at T3 (Figure 40 D). This was due to a comparatively high number of other leukocyte populations at this time point (presumably granulocytes).

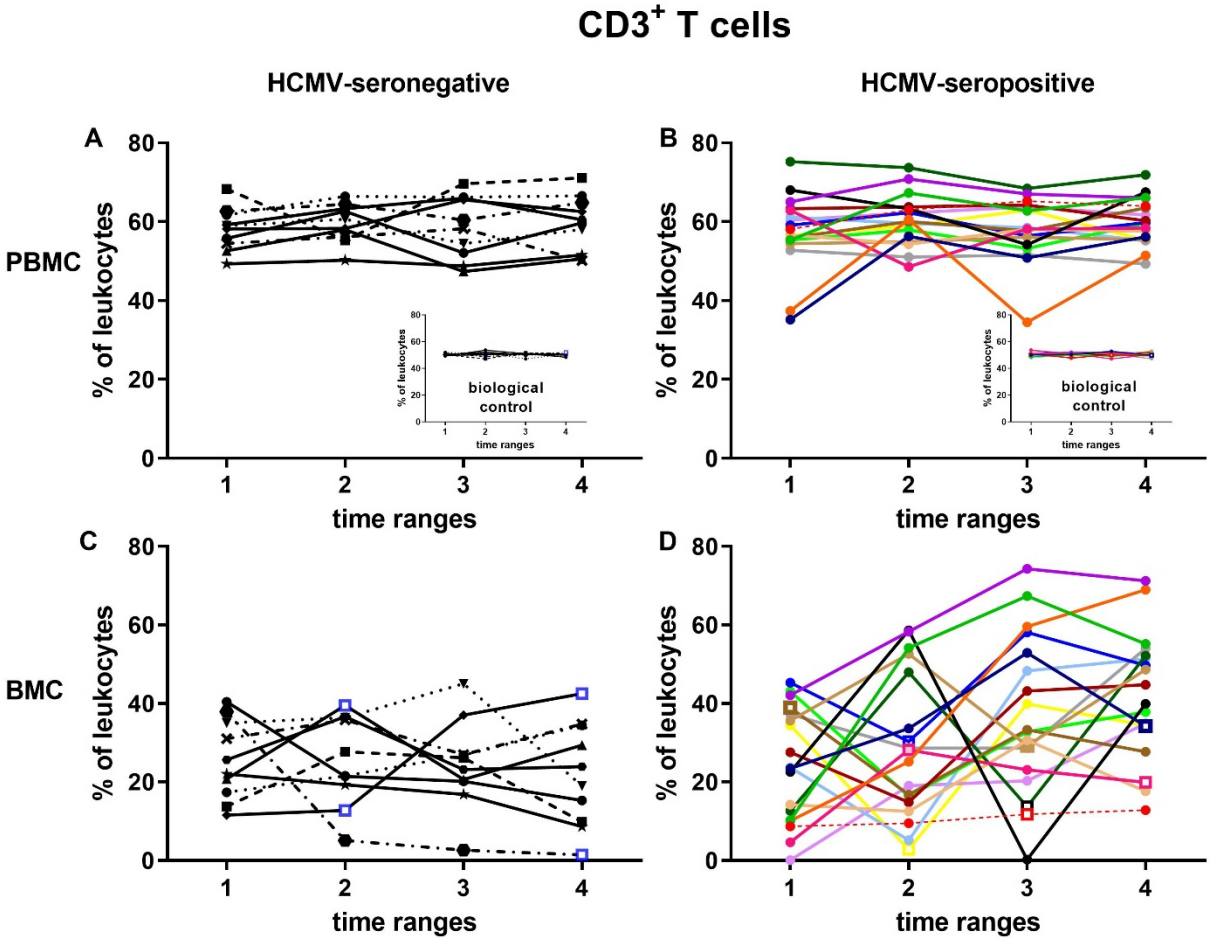

Figure 40: CD3⁺ T cell kinetics in blood and breast milk of BlooMil study mothers.
CD3⁺ T cell frequencies acquired by flow cytometry are shown of peripheral blood mononuclear cells (PBMC) in (A) HCMV-seronegative mothers and (B) seropositive mothers. CD3⁺ T cell frequency of breast milk cells (BMC) is displayed of (C) HCMV-seronegative and (D) seropositive mothers. The inserts in (A) and (B) show the biological control over all experimental days. Individual color-coding as described in Table 29 is applied. Mother 12 (red, dotted line) was excluded from statistical analysis due to HCMV-primary infection during pregnancy. The time ranges are T1 - 10 to 15, T2 - 25 to 30, T3 - 40 to 45 and T4 - 55 to 60 days p.p. Square data point symbols instead of round symbols indicate a time point where the breast milk cells showed a slightly red color in the cell pellet (presumably an indicator for mastitis).

Table 34: Mean CD3⁺ T cell frequenciesof T1 to T4 with standard deviation (SD).

Cell subset	Mate-rial	HCMV	T1 [% mean ± SD]	T2 [% mean ± SD]	T3 [% mean ± SD]	T4 [% mean ± SD]
CD3⁺ T cells	PBMC	IgG⁺	57.3 ± 9.7	60.3 ± 6.5	57.6 ± 7.9	59.7 ± 5.9
		IgG-	58.1 ± 5.4	59.5 ± 4.9	58.9 ± 7.9	59.6 ± 7.1
	BMC	IgG⁺	**25.1 ± 14.4**	**29.7 ± 18.5**	**38.6 ± 19.7**	**43.7 ± 15.1**
		IgG-	25.6 ± 10.2	25.6 ± 11.5	24.6 ± 11.4	21.9 ± 13.3

In summary, blood CD3$^+$ T cell frequencies were constant over time and were in general higher as in breast milk. The HCMV-seropositive mothers' breast milk T cell frequency strongly increased over time.

Table 35: Statistical analysis of CD3$^+$ T cells *The p-values are given and significant digits are bold and marked in grey. Friedman test was used to look for differences in the kinetics followed by a Dunn-Bonferroni post-hoc test with Bonferroni (B.) correction comparing single time ranges. The linear mixed model was used to show differences in the courses over time between HCMV-seropositive and seronegative mothers. Mann-Whitney U indicated differences between the single time ranges of seropositive and negative mothers. The Wilcoxon test with B. correction was used to compare single time ranges (T's) of blood and breast milk.*

CD3$^+$ T cells	PBMC HCMV pos	PBMC HCMV neg	BMC HCMV pos	BMC HCMV neg
Friedman test	0.51	0.16	**0.0078**	0.22
Dunn-Bonferroni post-hoc test with B. correction	-	-	T1 to T2: 1.0 T1 to T3: 0.20 **T1 to T4: 0.032** T2 to T3: 0.28 **T2 to T4: 0.047** T3 to T4: 1.0	-
Linear mixed model	0.83		**0.043**	
Mann-Whitney U with B. correction				
T1's	1.0		1.0	
T2's	1.0		1.0	
T3's	1.0		0.16	
T4's	1.0		**0.0057**	
Wilcoxon with B. correction	PBMC HCMV pos	BMC HCMV pos	PBMC HCMV neg	BMC HCMV neg
T1's	**0.0012**		**0.020**	
T2's	**0.0012**		**0.020**	
T3's	**0.034**		**0.020**	
T4's	**0.011**		**0.020**	

CD4$^+$ T cells

The CD3$^+$ T cell populations were further discriminated into CD4$^+$ and CD8$^+$ T cells. The CD4$^+$ T cell frequencies in **blood** reached around 55-75% of all CD3$^+$ T cells (Table 36) and did not differ between HCMV-seronegative (Figure 41 A) and -seropositive (Figure 41 B) mothers over time (linear mixed model in Table 37). CD4$^+$ T cell frequencies in blood slightly decreased in HCMV-seropositive mothers (Friedman test, Table 37).

In **breast milk**, the kinetics did not change over time (Table 37), but inter-individual variability was higher than in blood (Figure 41 C and D). The CD4$^+$ T cell frequencies of HCMV-seropositive mothers were between 25-63% (Figure 41 D) and for HCMV-seronegative mothers around 37-76% of all CD3$^+$ T cells in breast milk (Figure 41 C). Therefore, the frequencies were slightly lower in HCMV-seropositive mothers' compared to seronegative mothers' breast milk (Table 36; mean frequencies at T4: 49.4 ± 9.1% and 65.9 ± 6.5%, respectively, Mann-Whitney U test with corrections in Table 37).

Seronegative mothers showed no differences between their **blood and breast milk** frequencies. However, seropositive mothers had significantly lower CD4⁺ T cell frequencies in breast milk (e.g. at T1: 51.8 ± 9.3, Table 36) compared to corresponding blood (T1: 62.6 ± 7.5%, Wilcoxon test in Table 37).

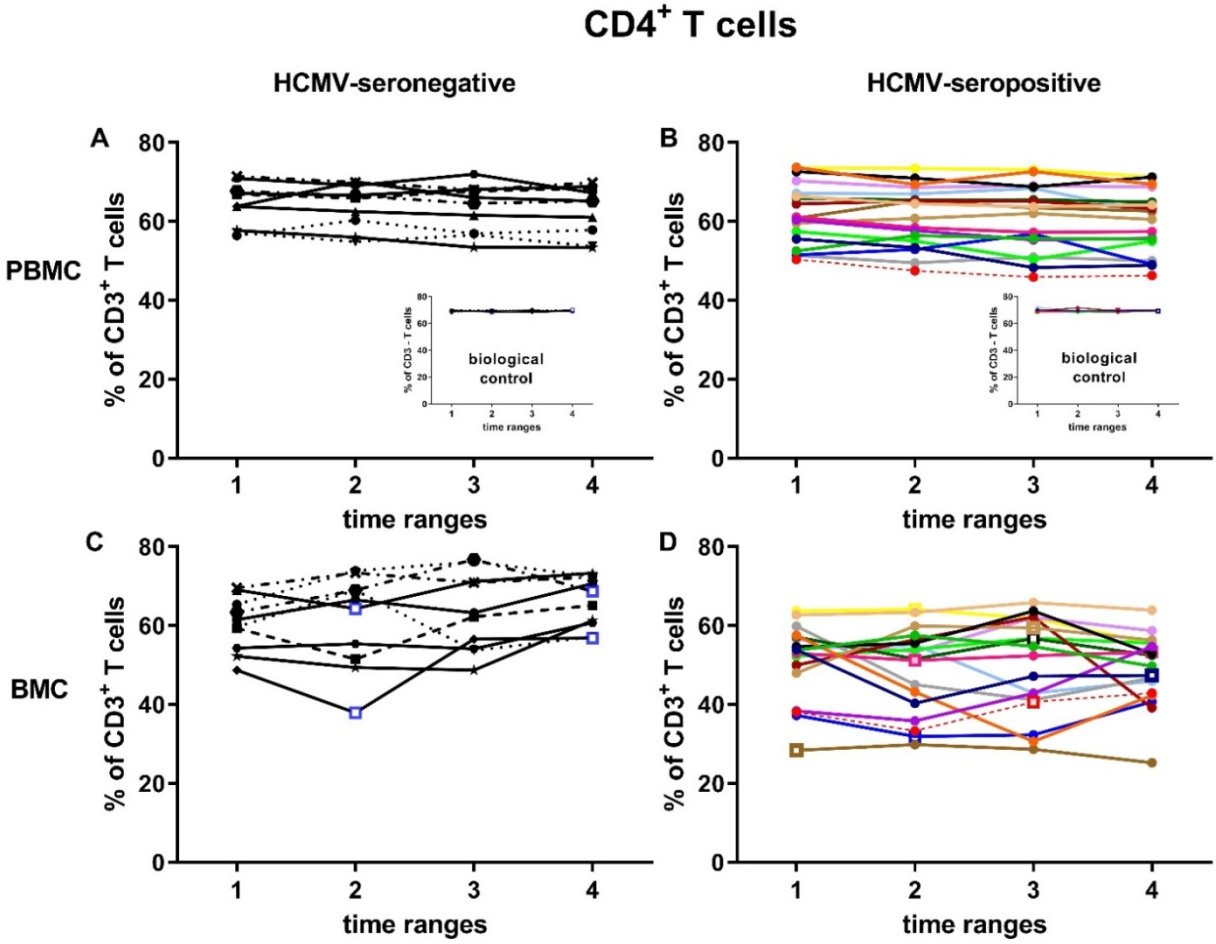

Figure 41: CD4⁺ T cell kinetics in blood and breast milk of BlooMil study mothers.
CD4⁺ T cell frequencies acquired by flow cytometry are shown of peripheral blood mononuclear cells (PBMC) in (A) HCMV-seronegative mothers and (B) seropositive mothers. CD4⁺ T cell frequency of breast milk cells (BMC) is displayed of (C) HCMV-seronegative and (D) seropositive mothers. The inserts in (A) and (B) show the biological control over all experimental days. Individual color-coding as described in Table 29 is applied. Mother 12 (red, dotted line) was excluded from statistical analysis due to HCMV-primary infection during pregnancy. The time ranges are T1 - 10 to 15, T2 - 25 to 30, T3 - 40 to 45 and T4 - 55 to 60 days p.p. Square data point symbols instead of round symbols indicate a time point where the breast milk cells showed a slightly red color in the cell pellet (presumably an indicator for mastitis).

Table 36: Mean CD4⁺ T cell frequenciesof T1 to T4 with standard deviation (SD).

Cell subset	Mate-rial	HCMV	T1 [% mean ± SD]	T2 [% mean ± SD]	T3 [% mean ± SD]	T4 [% mean ± SD]
CD4⁺ T cells	PBMC	IgG⁺	**62.6 ± 7.5**	**62.0 ± 7.1**	**61.6 ± 7.8**	**60.6 ± 7.5**
		IgG-	64.3 ± 5.6	64.2 ± 5.6	63.5 ± 6.1	63.1 ± 6.2
	BMC	IgG⁺	51.8 ± 9.3	49.9 ± 10.5	50.6 ± 12.3	49.4 ± 9.1
		IgG-	*60.3 ± 7.0*	*61.0 ± 11.9*	*63.3 ± 10.0*	*65.9 ± 6.5*

In short, CD4⁺ T cell frequencies of CD3⁺ T cells showed no strong changes over time in either blood or breast milk, but frequencies in breast milk of seropositive mothers were in general slightly lower than in the corresponding blood samples and in the breast milk of seronegative mothers.

Table 37: Statistical analysis of CD4⁺ T cells *The p-values are given for different tests and significant digits are bold and marked in grey. Friedman test was used to look for differences in the kinetics followed by a Dunn-Bonferroni post-hoc test with Bonferroni (B.) correction comparing single time ranges. The linear mixed model was used to show differences in the courses over time between HCMV-seropositive and seronegative mothers. Mann-Whitney U indicated differences between the single time ranges of seropositive and negative mothers. The Wilcoxon test with B. correction was used to compare single time ranges (T's) of blood and breast milk.*

CD4⁺ T cells	PBMC HCMV pos	PBMC HCMV neg	BMC HCMV pos	BMC HCMV neg
Friedman test	**0.015**	0.56	0.86	0.077
Dunn-Bonferroni post-hoc test with B. correction	T1 to T2: 1.0 T1 to T3: 0.51 **T1 to T4: 0.0086** T2 to T3: 1.0 T2 to T4: 0.28 T3 to T4: 0.86			
Linear mixed model	0.90		0.14	
Mann-Whitney U with B. correction				
T1's	1.0		0.11	
T2's	1.0		0.11	
T3's	1.0		0.092	
T4's	1.0		**0.000028**	
Wilcoxon with B. correction	PBMC HCMV pos	BMC HCMV pos	PBMC HCMV neg	BMC HCMV neg
T1's	**0.0040**		0.68	
T2's	**0.0020**		1.0	
T3's	**0.0077**		1.0	
T4's	**0.0017**		1.0	

CD8⁺ T cells

CD8⁺ T cells showed frequencies of around 20-40% of all CD3⁺ T cells **in blood** (mean with SD in Table 38). There were no significant changes detectable over time in blood of either HCMV-seropositive or seronegative mothers (Figure 42 A and B, Friedman in Table 39).

Looking at single time ranges, the CD8⁺ T cell frequency was significantly higher in **breast milk** of HCMV-seropositive mothers compared to negative mothers at T2, 3 and 4 (Mann-Whitney U in Table 39).The mean frequencies of HCMV-seropositive mothers' breast milk CD8⁺ T cells slightly increased from T1 (33.7 ± 6.0%) to T4 (37.5 ± 6.9%, Friedman test not significant), while seronegative mothers' frequencies slightly decreased from T1 (27.1 ± 6.6%,) to T4 (22.7 ± 6.4%, Friedman not significant in Table 39). These changes led to a significant difference between the kinetics of HCMV-seronegative and seropositive mothers in breast milk (Figure 42 C and D, linear mixed model, p=0.028, Table 39).

Between blood and breast milk frequencies, no differences were detected in HCMV-seronegative mothers, but the seropositive mothers' breast milk CD8⁺ T cell frequencies were slightly higher at T2 (Table 38) and T4 (Wilcoxon test in Table 39) than their corresponding blood samples.

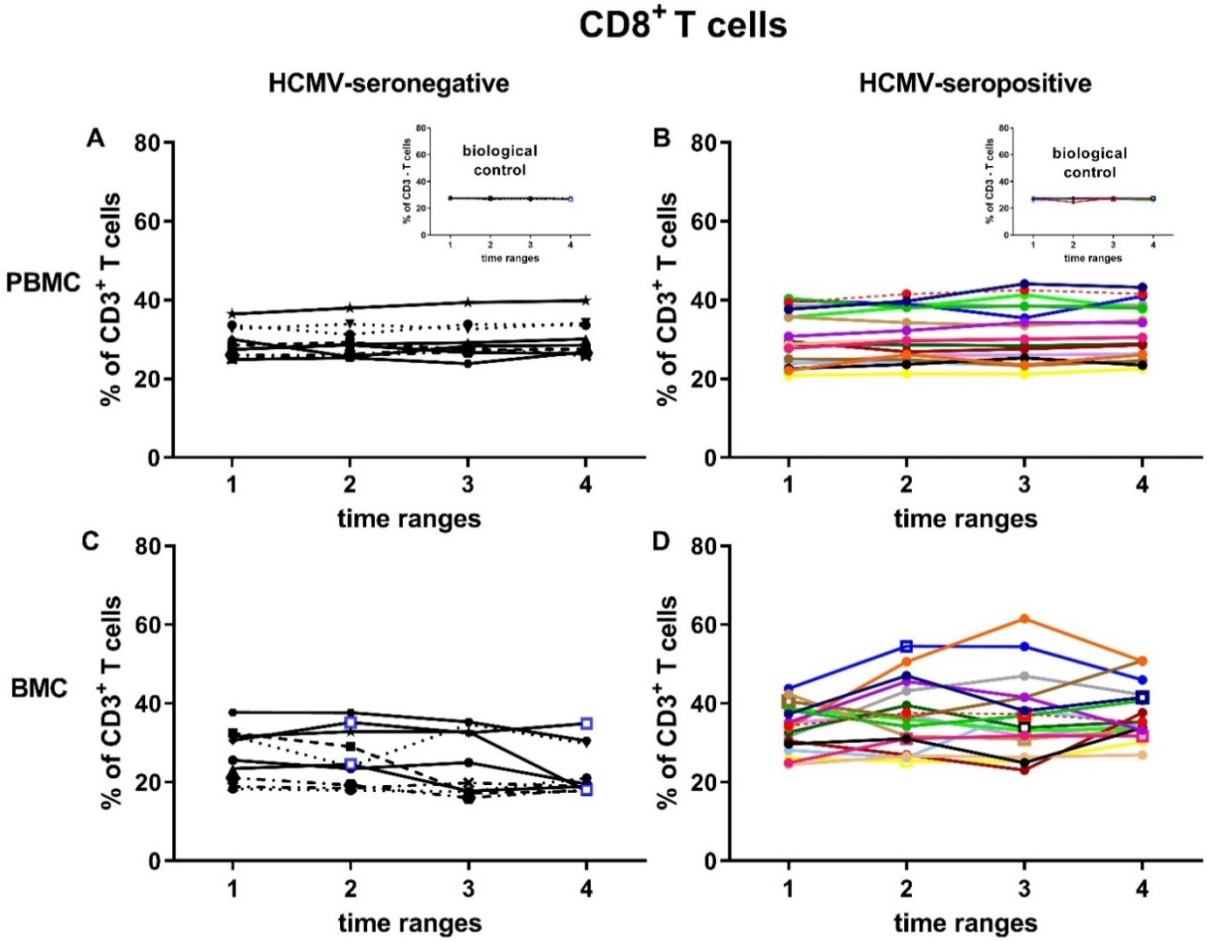

Figure 42: CD8⁺ T cell kinetics in blood and breast milk of BlooMil study mothers.
CD8⁺ T cell frequencies acquired by flow cytometry are shown of peripheral blood mononuclear cells (PBMC) in (A) HCMV-seronegative mothers and (B) seropositive mothers. CD8⁺ T cell frequency of breast milk cells (BMC) is displayed of (C) HCMV-seronegative and (D) seropositive mothers. The inserts in (A) and (B) show the biological control over all experimental days. Individual color-coding as described in Table 29 applied. Mother 12 (red, dotted line) was excluded from statistical analysis due to HCMV-primary infection during pregnancy. The time ranges are T1 - 10 to 15, T2 - 25 to 30, T3 - 40 to 45 and T4 - 55 to 60 days p.p. Square data point symbols instead of round symbols indicate a time point where the breast milk cells showed a slightly red color in the cell pellet (presumably an indicator for mastitis).

Table 38: Mean CD8⁺ T cell frequencies of T1 to T4 with standard deviation (SD).

Cell subset	Material	HCMV	T1 [% mean ± SD]	T2 [% mean ± SD]	T3 [% mean ± SD]	T4 [% mean ± SD]
CD8⁺ T cells	PBMC	IgG⁺	*30.1 ± 6.7*	*30.7 ± 6.2*	*30.9 ± 6.9*	*31.5 ± 6.5*
		IgG-	29.2 ± 3.9	29.3 ± 4.1	29.6 ± 4.5	29.9 ± 4.6
	BMC	IgG⁺	33.7 ± 6.0	36.6 ± 8.9	36.5 ± 10.5	37.5 ± 6.9
		IgG-	27.1 ± 6.6	26.2 ± 7.1	24.9 ± 8.1	22.7 ± 6.4

In summary, $CD8^+$ T cells showed no changes over time in blood. However, breast milk $CD8^+$ T cells of HCMV-seropositive mothers had higher frequencies than the corresponding blood samples and the seronegative mothers' breast milk.

Table 39: Statistical analysis of $CD8^+$ T cells *The p-values are given for different tests and significant digits are bold and marked in grey. Friedman test was used to look for differences in the kinetics followed by a Dunn-Bonferroni post-hoc test with Bonferroni (B.) correction comparing single time ranges. The linear mixed model was used to show differences in the courses over time between HCMV-seropositive and seronegative mothers. Mann-Whitney U indicated differences between the single time ranges of seropositive and negative mothers. The Wilcoxon test with B. correction was used to compare single time ranges (T's) of blood and breast milk.*

$CD8^+$ T cells	PBMC HCMV pos	PBMC HCMV neg	BMC HCMV pos	BMC HCMV neg
Friedman test	0.089	0.67	0.18	0.36
Dunn-Bonferroni post-hoc test with B. correction	-	-	-	-
Linear mixed model	0.85		**0.028**	
Mann-Whitney U with B. correction				
T1's	1.0		0.11	
T2's	1.0		**0.019**	
T3's	1.0		**0.037**	
T4's	1.0		**0.00026**	
Wilcoxon with B. correction	PBMC HCMV pos	BMC HCMV pos	PBMC HCMV neg	BMC HCMV neg
T1's	0.11		0.68	
T2's	**0.040**		0.96	
T3's	0.37		0.68	
T4's	**0.045**		0.26	

The parental population ($CD3^+$ T cells) in breast milk of HCMV-seropositive mothers increased and the $CD4^+$ and $CD8^+$ T cells stayed more or less constant over time, when referred to the parental $CD3^+$ T cell population. Supplement figure 1 shows the $CD4^+$ and $CD8^+$ T cell frequency of all leukocytes in breast milk of HCMV-seronegative and seropositive mothers. As expected, both cell subsets revealed significant increases in the HCMV-seropositive mothers (Friedman test: $CD4^+$ T cells $p=0.0073$; $CD8^+$ T cells $p=0.010$). However, when the kinetics of HCMV-seropositive to negative mothers' was compared, only the $CD8^+$ T cell frequency displayed a significant increase in HCMV-seropositive mothers in comparison to the seronegative mothers (linear mixed model $CD4^+$ T cells $p=0.11$, $CD8^+$ T cells $p=0.032$).

The $CD4^+/CD8^+$ T cell ratio is an established marker for assessing the competence of the immune system. In **blood** (Figure 43 B), the ratio was constantly around 2 (Table 40) in HCMV-seropositive and -seronegative mothers.

In **breast milk**, the $CD4^+/CD8^+$ T cell ratio was significantly lower in HCMV-seropositive compared to -seronegative mothers at T2 and T4 (Figure 43 A, Mann-Whitney U test in Table 41), due to both lower $CD4^+$ and higher $CD8^+$ T cell frequencies. Mean $CD4^+/CD8^+$ T cell ratios increased in HCMV-seronegative ($CD4^+$ T cells increased, Table 36, and $CD8^+$ T cells slightly decreased, Table 38) and slightly decreased in seropositive mothers' breast milk and led to a significant difference between their kinetics (linear mixed model: p=0.0092).

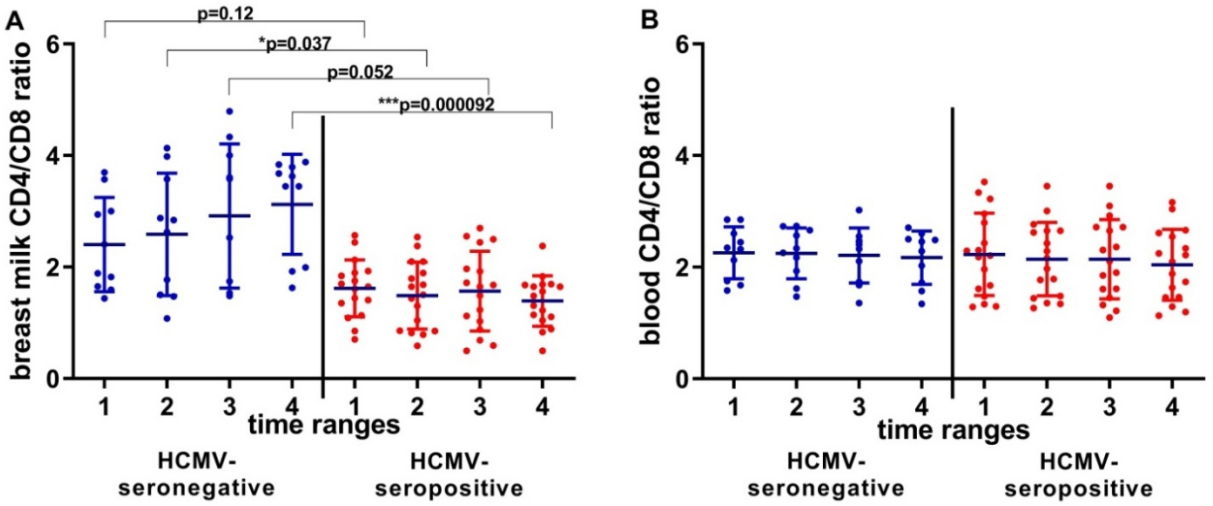

Figure 43: $CD4^+/CD8^+$ T cell ratio.
The $CD4^+/CD8^+$ T cell ratio is shown in (A) breast milk and (B) blood. The mean levels with standard deviation (SD) are displayed. Mann Whitney-U tests with Bonferroni corrections were performed for comparing the time ranges between the serostatus. The time ranges are T1 - 10 to 15, T2 - 25 to 30, T3 - 40 to 45 and T4 - 55 to 60 days p.p.

Table 40: Mean $CD4^+/CD8^+$ T cell ratio of T1 to T4 with standard deviation (SD).

Cell subset	Mate-rial	HCMV	T1 [mean ± SD]	T2 [mean ± SD]	T3 [% mean ± SD]	T4 [mean ± SD]
$CD4^+/CD8^+$ T cell ratio	PBMC	IgG^+	2.2 ± 0.7	2.1 ± 0.7	2.1 ± 0.7	2.0 ± 0.7
		IgG-	2.3 ± 0.5	2.2 ± 0.5	2.2 ± 0.5	2.2 ± 0.5
	BMC	IgG^+	1.6 ± 0.5	1.5 ± 0.6	1.5 ± 0.7	1.4 ± 0.4
		IgG-	2.4 ± 0.8	2.6 ± 1.1	2.9 ± 1.3	3.1 ± 0.9

Comparing the **blood and breast milk** $CD4^+/CD8^+$ T cell ratio, the breast milk ratio of HCMV-seropositive mothers was significantly lower as in corresponding blood samples (Wilcoxon test with correction in Table 41). However, for the HCMV-seronegative mothers the breast milk ratio was not lower but even showed a tendency towards higher levels as in blood at T4's (p=0.087).

Table 41: Statistical analysis of CD4⁺/CD8⁺ T cell ratio *The p-values are given for different tests. Significant digits are bold and marked in grey. Friedman test was used to look for differences in the kinetics followed by a Dunn-Bonferroni post-hoc test with Bonferroni (B.) correction comparing single time ranges. The linear mixed model was used to show differences in the courses over time between HCMV-seropositive and seronegative mothers. Mann-Whitney U indicated differences between the single time ranges of seropositive and negative mothers. The Wilcoxon test with B. correction was used to compare single time ranges (T's) of blood and breast milk.*

CD4⁺/CD8⁺ T cell ratio	PBMC HCMV pos	PBMC HCMV neg	BMC HCMV pos	BMC HCMV neg
Friedman test	**0.031**	0.67	0.36	0.095
Dunn-Bonferroni post-hoc test with B. correction	T1 to T2: 1.0 T1 to T3: 1.0 **T1 to T4: 0.021** T2 to T3: 1.0 T2 to T4: 0.38 T3 to T4: 0.38	-	-	-
Linear mixed model	0.73		**0.0092**	
Mann-Whitney U with B. correction				
T1's	1.0		0.12	
T2's	1.0		**0.037**	
T3's	1.0		0.052	
T4's	1.0		**0.000092**	
Wilcoxon with B. correction	PBMC HCMV pos	BMC HCMV pos	PBMC HCMV neg	BMC HCMV neg
T1's	**0.022**		1.0	
T2's	**0.0066**		1.0	
T3's	0.087		0.81	
T4's	**0.017**		0.087	

5.3.5.4.1 Activation markers on CD4⁺ and CD8⁺ T cells (CD38, HLA-DR)

Activation markers can provide information about the status of a cell. If no prior activation took place, no direct functionality can follow. If activation markers are found on a T cell, the cell is most likely antigen experienced and can directly act upon contact with their antigen. In this thesis, CD38 and HLA-DR were chosen as activation markers.

The CD38 expression on CD4⁺ T cells is shown in Figure 44. **In blood**, high frequencies with around 60 to 80% of all CD4⁺ T cells expressing CD38 (mean with SD in Table 42) were found in seropositive and seronegative mothers (Figure 44 A, B). HCMV-seropositive mothers' blood frequencies slightly decreased over time (Friedman test, Table 43).

High inter-individual variances were found in **breast milk** with CD38⁺ frequencies around 20 to 72% of CD4⁺ T cells independent of the HCMV-serostatus (Figure 44 C and D). Additionally, no changes were observed over time (Friedman test in Table 43), but some seropositive mothers revealed an increase of frequency in breast milk.

CD38 is known to be expressed in low intensities on naïve T cells. The best gating for consistency along all samples was chosen and resulted in a strategy, where the gates were set close to the negative population. Breast milk was shown to have few naïve cells, while

blood usually has high frequencies. Therefore, the differences between breast milk and blood CD38 expression were not compared (6.3.3.1).

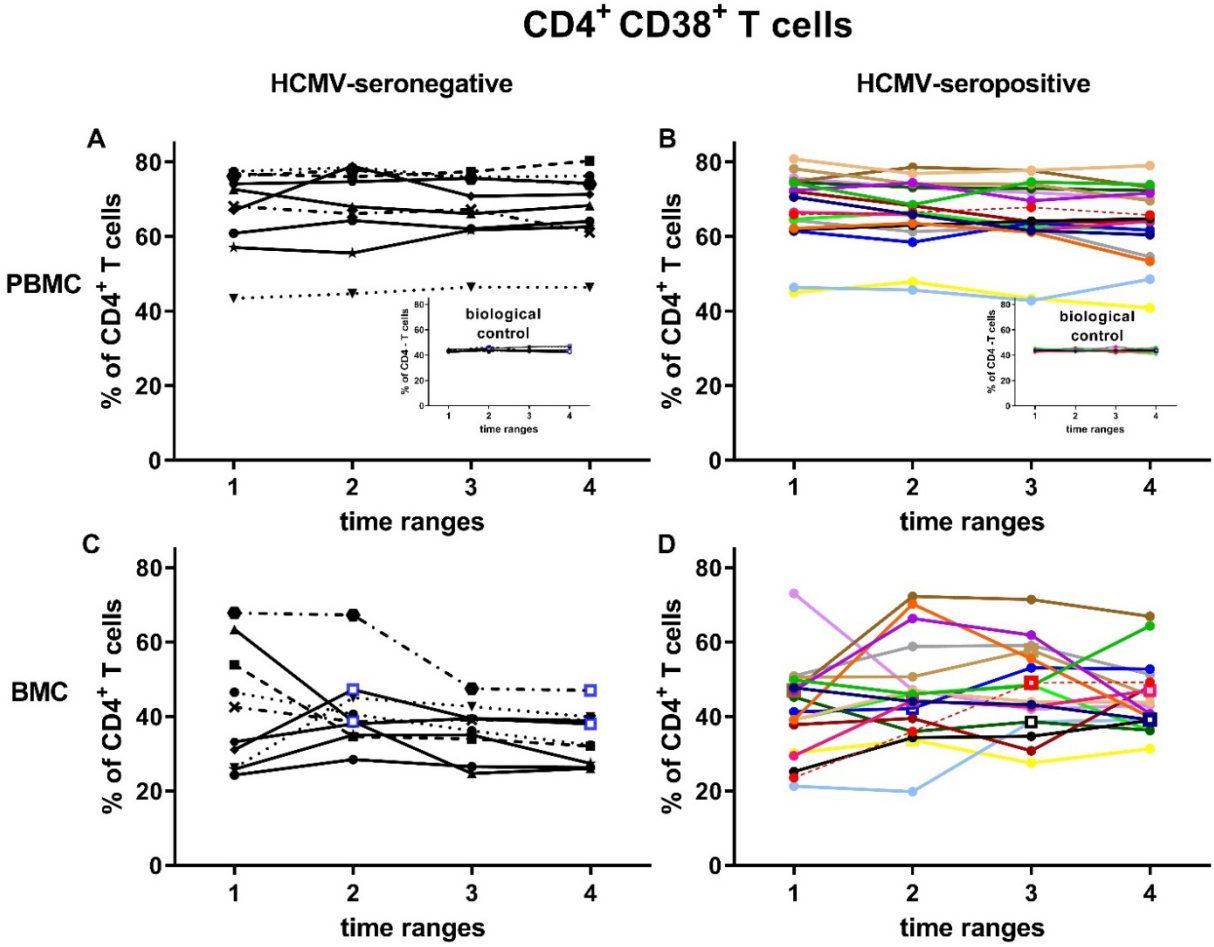

Figure 44: CD4⁺ CD38⁺ T cell kinetics in blood and breast milk of BlooMil study mothers. *CD4⁺ CD38⁺ T cell frequencies acquired by flow cytometry are shown of peripheral blood mononuclear cells (PBMC) in (A) HCMV-seronegative mothers and (B) seropositive mothers. CD4⁺ CD38⁺ T cell frequency of breast milk cells (BMC) is displayed of (C) HCMV-seronegative and (D) seropositive mothers. The inserts in (A) and (B) show the biological control over all experimental days. Individual color-coding as described in Table 29 is applied. Mother 12 (red, dotted line) was excluded from statistical analysis due to HCMV-primary infection during pregnancy (). The time ranges are T1 - 10 to 15, T2 - 25 to 30, T3 - 40 to 45 and T4 - 55 to 60 days p.p. Square data point symbols instead of round symbols indicate a time point where the breast milk cells showed a slightly red color in the cell pellet (presumably an indicator for mastitis).*

Table 42: Mean CD4+ CD38+ T cell frequencies of T1 to T4 with standard deviation (SD).

Cell subset	Mate-rial	HCMV	T1 [% mean ± SD]	T2 [% mean ± SD]	T3 [% mean ± SD]	T4 [% mean ± SD]
CD4⁺ CD38⁺ T cells	PBMC	IgG⁺	**67.4 ± 10.1**	**66.2 ± 9.2**	**65.0 ± 10.1**	**63.8 ± 10.0**
		IgG-	67.4 ± 10.9	68.5 ± 11.3	67.9 ± 9.5	67.9 ± 9.8
	BMC	IgG⁺	42.0 ± 12.1	47.0 ± 13.7	46.9 ± 11.7	45.0 ± 9.6
		IgG-	41.5 ± 16.0	41.3 ± 10.5	36.5 ± 6.9	34.7 ± 7.0

Table 43: Statistical analysis of CD4⁺ CD38⁺ T cells *The p-values are given for different tests and significant digits are bold and marked in grey. Friedman test was used to look for differences in the kinetics followed by a Dunn-Bonferroni post-hoc test with Bonferroni (B.) correction comparing single time ranges. The linear mixed model was used to show differences in the courses over time between HCMV-seropositive and seronegative mothers. Mann-Whitney U indicated differences between the single time ranges of seropositive and negative mothers. The Wilcoxon test with B. correction was used to compare single time ranges (T's) of blood and breast milk.*

CD4⁺ CD38⁺ T cells	PBMC HCMV pos	PBMC HCMV neg	BMC HCMV pos	BMC HCMV neg
Friedman test	**0.0060**	0.84	0.26	0.29
Dunn-Bonferroni post-hoc test with B. correction	T1 to T2: 1.0 T1 to T3: 0.14 **T1 to T4: 0.0054** T2 to T3: 1.0 T2 to T4: 0.14 T3 to T4: 1.0			
Linear mixed model	0.29		0.35	
Mann-Whitney U with B. correction				
T1's	1.0		1.0	
T2's	1.0		0.82	
T3's	1.0		0.81	
T4's	1.0		**0.027**	
Wilcoxon with B. correction	PBMC HCMV pos	BMC HCMV pos	PBMC HCMV neg	BMC HCMV neg
T1's	**0.0012**		**0.020**	
T2's	**0.0020**		**0.028**	
T3's	**0.0012**		**0.020**	
T4's	**0.0012**		**0.020**	

CD8⁺ T cells were also analyzed for their CD38 expression in blood and in breast milk of seropositive and seronegative mothers (Figure 45). 40-83% of the CD8⁺ T cells expressed CD38 (mean with SD in Table 44) **in blood** irrespective to HCMV-serostatus (Table 45). Seropositive mothers' blood frequencies slightly decreased over time, as already seen for the CD4⁺ T cells (Friedman test, Table 45).

In breast milk (Figure 45 C and D), the frequencies were also found around 40-80% of all CD8⁺ T cells (mean with SD in Table 44) and did not show strong changes over time. Some mothers displayed an increase over time, which led to a tendency towards an increase of the CD38⁺ CD8⁺ T cell frequencies in breast milk of HCMV-seropositive mothers (Friedman test p=0.083).

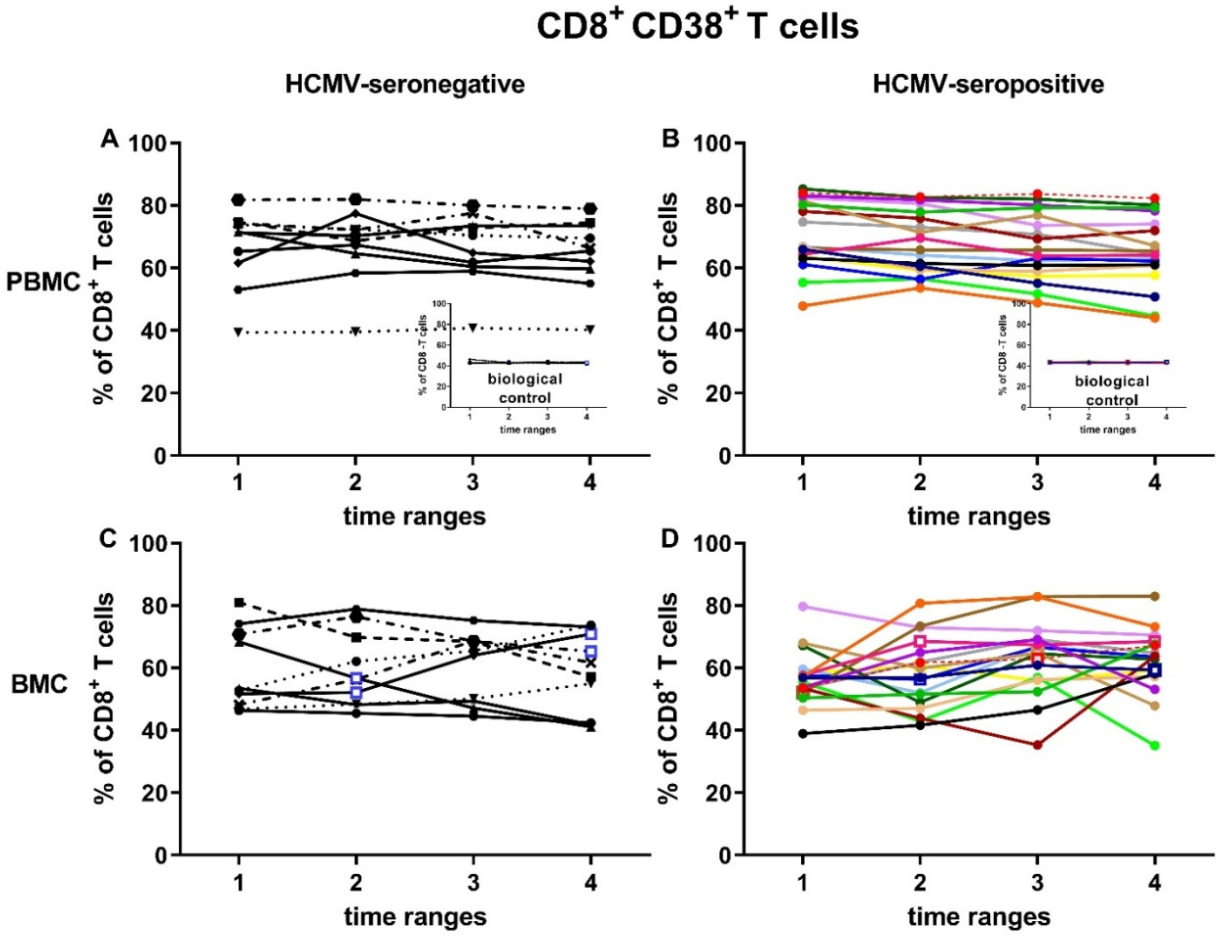

Figure 45: CD8⁺ CD38⁺ T cell kinetics in blood and breast milk of BlooMil study mothers. *CD8⁺ CD38⁺ T cell frequencies acquired by flow cytometry are shown of peripheral blood mononuclear cells (PBMC) in (A) HCMV-seronegative mothers and (B) seropositive mothers. CD8⁺ CD38⁺ T cell frequency of breast milk cells (BMC) is displayed of (C) HCMV-seronegative and (D) seropositive mothers. The inserts in (A) and (B) show the biological control over all experimental days. Individual color-coding as described in Table 29 is applied. Mother 12 (red, dotted line) was excluded from statistical analysis due to HCMV-primary infection during pregnancy. The time ranges are T1 - 10 to 15, T2 - 25 to 30, T3 - 40 to 45 and T4 - 55 to 60 days p.p. Square data point symbols instead of round symbols indicate a time point where the breast milk cells showed a slightly red color in the cell pellet (presumably an indicator for mastitis).*

Table 44: Mean CD8⁺ CD38⁺ frequenciesof T1 to T4 with standard deviation (SD).

Cell subset	Mate-rial	HCMV	T1 [% mean ± SD]	T2 [% mean ± SD]	T3 [% mean ± SD]	T4 [% mean ± SD]
CD8⁺ CD38⁺ T cells	PBMC	pos	**69.8 ± 10.7**	**67.7 ± 9.7**	**65.9 ± 10.1**	**64.1 ± 10.9**
		neg	66.7 ± 12.5	67.3 ± 11.7	66.1 ± 11.5	64.5 ± 11.2
	BMC	pos	*56.8 ± 9.0*	*57.9 ± 11.6*	*63.0 ± 12.0*	*61.8 ± 10.6*
		neg	59.4 ± 12.8	59.5 ± 12.0	60.2 ± 11.1	58.2 ± 13.0

Overall, CD38 frequencies in blood were high (up to 70% on average). Both, CD4⁺ and CD8⁺ T cells, showed a slight decrease over time of CD38 frequencies in blood of HCMV-seropositive mothers.

Breast milk CD38 frequencies showed no significant changes over time, despite individual increases of frequencies in some mothers (in both $CD4^+$ and $CD8^+$ T cells). $CD8^+$ T cells had higher CD38 frequencies than $CD4^+$ T cells in breast milk.

Table 45: Statistical analysis of $CD8^+$ $CD38^+$ T cells *The p-values are given for different tests and significant digits are bold and marked in grey. Friedman test was used to look for differences in the kinetics followed by a Dunn-Bonferroni post-hoc test with Bonferroni (B.) correction comparing single time ranges. The linear mixed model was used to show differences in the courses over time between HCMV-seropositive and seronegative mothers. Mann-Whitney U showed no differences between the single time ranges of seropositive or negative mothers (p>1.0, not shown). The Wilcoxon test with B. correction was used to compare single time ranges (T's) of blood and breast milk.*

$CD8^+$ $CD38^+$ T cells	PBMC HCMV pos	PBMC HCMV neg	BMC HCMV pos	BMC HCMV neg
Friedman test	**0.000011**	0.70	0.083	0.70
Dunn-Bonferroni post-hoc test with B. correction	T1 to T2: 0.38 **T1 to T3: 0.00040** **T1 to T4: 0.00004** T2 to T3: 0.20 **T2 to T4: 0.047** T3 to T4: 1.0			
Linear mixed model	0.50		0.60	
Wilcoxon with B. correction	PBMC HCMV pos	BMC HCMV pos	PBMC HCMV neg	BMC HCMV neg
T1's	**0.0056**		0.56	
T2's	**0.045**		0.46	
T3's	1.0		0.56	
T4's	1.0		0.96	

When T cells are activated, HLA-DR is upregulated. Therefore, HLA-DR expression was investigated as an activation marker on $CD4^+$ and $CD8^+$ T cells.

Expression of HLA-DR on $CD4^+$ T cells was very low in all **blood samples** regardless to HCMV-serostatus (0.8-4% of all $CD4^+$ T cells, mean with SD in Table 46). Additionally, no changes during the observation period were noticed (Figure 46 A and B, Table 47).

Regarding **breast milk**, again high inter-individual variability was observed (Figure 46 C and D). HCMV-seronegative mothers had no change in mean frequencies over time (around 15%, Table 46). However, seropositive mothers' breast milk frequencies of HLA-DR expressing $CD4^+$ T cells (Figure 46 D) increased significantly from T1 to T4 by 8.5% (Friedman test, p=0.00045, Table 47). Post-hoc test with corrections revealed significant increases between T1 and T3, as well as between T1 and T4 (Table 47).

Mean CD4⁺ HLA-DR⁺ T cell frequencies were 4.8 to 9.2 fold higher (mean frequencies in Table 46) in **breast milk than in blood** independent of HCMV-serostatus (significant with Wilcoxon test, Table 47).

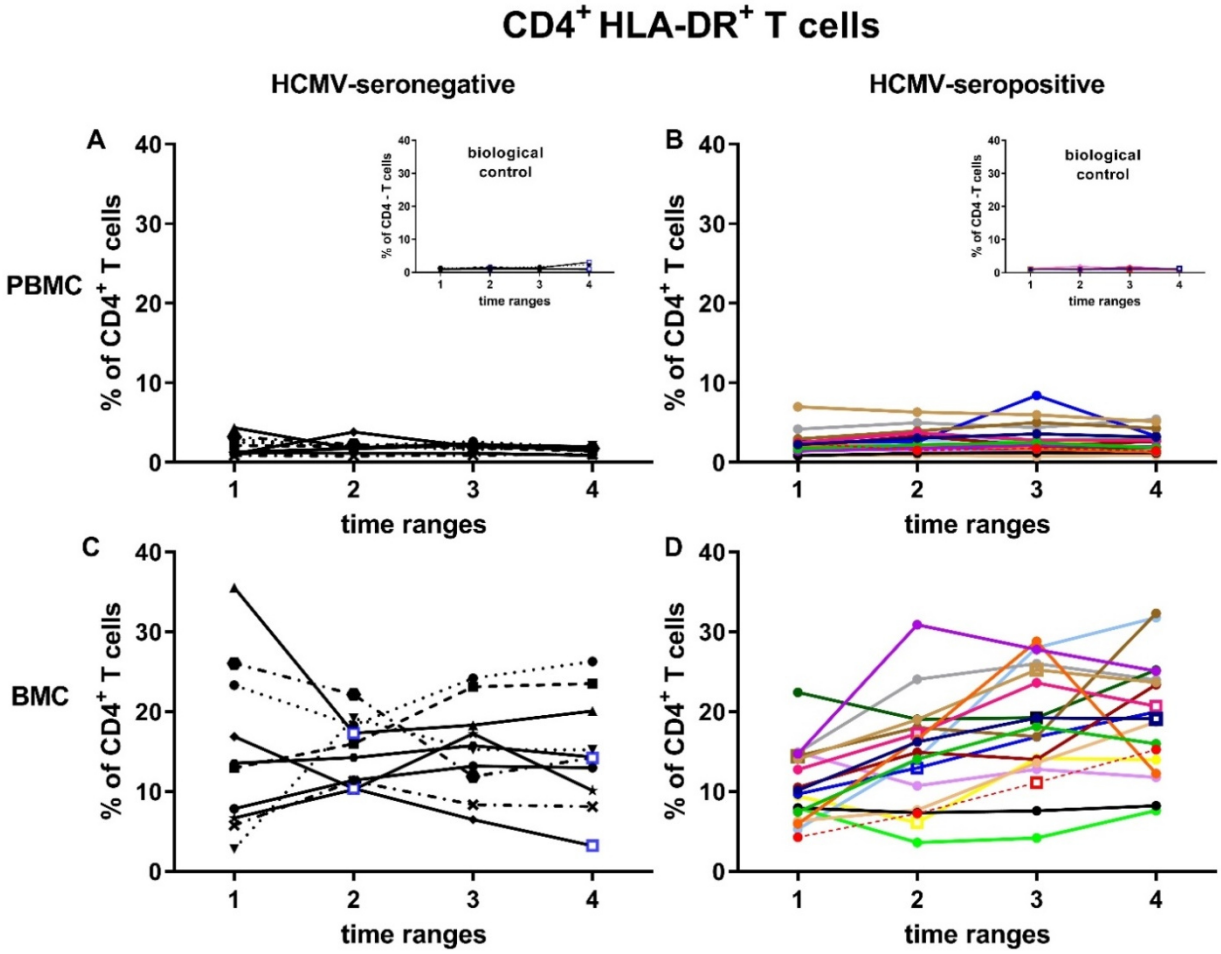

Figure 46: CD4⁺ HLA-DR⁺ T cell kinetics in blood and breast milk of BlooMil study mothers. *CD4⁺ HLA-DR⁺ T cell frequencies acquired by flow cytometry are shown of peripheral blood mononuclear cells (PBMC) in (A) HCMV-seronegative mothers and (B) seropositive mothers. CD4⁺ HLA-DR⁺ T cell frequency of breast milk cells (BMC) is displayed of (C) HCMV-seronegative and (D) seropositive mothers. The inserts in (A) and (B) show the biological control over all experimental days. Individual color-coding as described in Table 29 is applied. Mother 12 (red, dotted line) was excluded from statistical analysis due to HCMV-primary infection during pregnancy. The time ranges are T1 - 10 to 15, T2 - 25 to 30, T3 - 40 to 45 and T4 - 55 to 60 days p.p. Square data point symbols instead of round symbols indicate a time point where the breast milk cells showed a slightly red color in the cell pellet (presumably an indicator for mastitis).*

Table 46: Mean CD4⁺ HLA-DR⁺ T cell frequencies of T1 to T4 with standard deviation (SD).

Cell subset	Mate-rial	HCMV	T1 [% mean ± SD]	T2 [% mean ± SD]	T3 [% mean ± SD]	T4 [% mean ± SD]
CD4⁺ HLA-DR⁺ T cells	PBMC	IgG⁺	*2.3 ± 1.4*	*2.7 ± 1.4*	*3.0 ± 2.0*	*2.7 ± 1.3*
		IgG-	2.1 ± 1.2	2.0 ± 0.8	1.9 ± 0.5	1.6 ± 0.4
	BMC	IgG⁺	**11.1 ± 4.4**	**14.9 ± 6.8**	**18.6 ± 7.2**	**19.6 ± 7.3**
		IgG-	15.1 ± 10.4	15.1 ± 4.2	15.4 ± 5.7	14.8 ± 7.0

Table 47: Statistical analysis of CD4⁺ HLA-DR⁺ T cells *The p-values are given for different tests and significant digits are bold and marked in grey. Friedman test was used to look for differences in the kinetics followed by a Dunn-Bonferroni post-hoc test with Bonferroni (B.) correction comparing single time ranges. The linear mixed model was used to show differences in the courses over time between HCMV-seropositive and seronegative mothers. Mann-Whitney U showed no differences between the single time ranges of seropositive or negative mothers (p>0.08, not shown). The Wilcoxon test with B. correction was used to compare single time ranges (T's) of blood and breast milk.*

CD4⁺ HLA-DR⁺ T cells	PBMC HCMV pos	PBMC HCMV neg	BMC HCMV pos	BMC HCMV neg
Friedman test	0.057	0.45	**0.00045**	0.47
Dunn-Bonferroni post-hoc test with B. correction			T1 to T2: 1.0 **T1 to T3: 0.0054** **T1 to T4: 0.0033** T2 to T3: 0.10 T2 to T4: 0.070 T3 to T4: 1.0	
Linear mixed model	0.44		0.11	
Wilcoxon with B. correction	PBMC HCMV pos	BMC HCMV pos	PBMC HCMV neg	BMC HCMV neg
T1's T2's T3's T4's	**0.0012** **0.0012** **0.0012** **0.0012**		**0.028** **0.020** **0.020** **0.020**	

The activation marker HLA-DR was weakly expressed on CD8⁺ T cells **in blood** of HCMV-seronegative mothers (1-6.4%, Figure 47 A). Interestingly, HCMV-seropositive mothers (Figure 47 B) had in blood a significantly elevated HLA-DR expression on CD8⁺ T cells (e.g. at T1: 7.1 ± 3.6%) compared to seronegative mothers (T1: 2.5 ± 1.2%, Table 48) (Mann-Whitney U in Table 49). Still, both kinetics of CD8⁺ HLA-DR⁺ T cells in blood (Figure 47 A and B) did not show variations over time (Friedman test in Table 49).

Regardless of serostatus, **breast milk** HLA-DR frequencies ranged between 2 and 30% of all CD8⁺ T cells at T1 (mean with SD in Table 48) and showed high inter-individual variation (Figure 47 C and D). In seronegative mothers no significant changes were observed over time in breast milk, but HCMV-seropositive mothers had a strong increase of activated T cells from 15.3 ± 8.1% at T1 to 25.1 ± 9.2% at T4 (Friedman test, p=0.0012, Post-hoc test with correction significant for T1-T3 and T1-T4, Table 49).

Comparing breast milk to blood frequencies, significantly higher proportions of HLA-DR$^+$ CD8$^+$ T cells were found in breast milk regardless of serostatus (Wilcoxon test in Table 49). Correlations of HCMV-seronegative mothers' breast milk and blood CD8$^+$ HLA-DR$^+$ T cells were strong at T2 (r=0.76, Supplement figure 2), however, it appeared to have no relevant implications. All other correlations were under r=0.6 or not significant (Supplement figure 2).

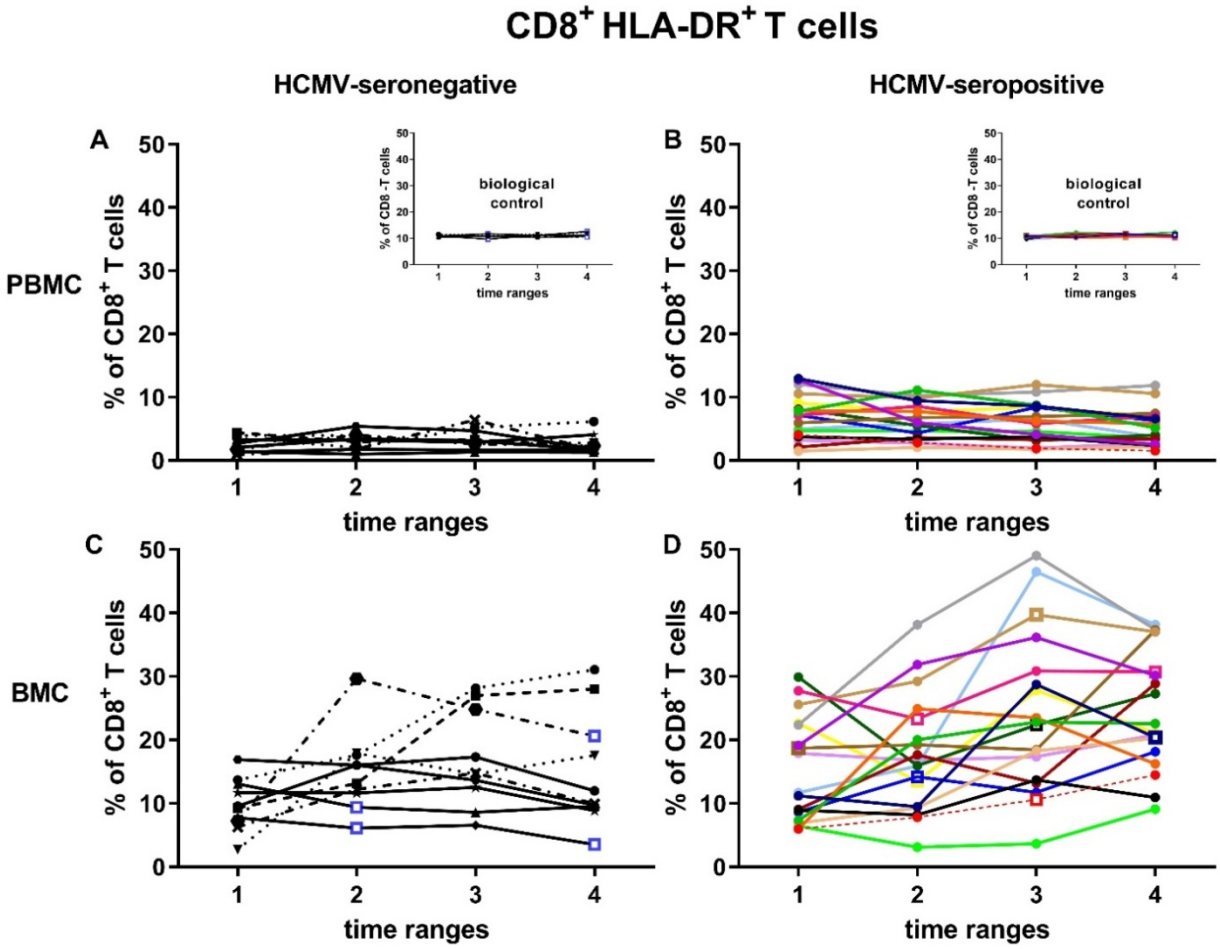

Figure 47: CD8$^+$ HLA-DR$^+$ T cell kinetics in blood and breast milk of BlooMil study mothers. *CD8$^+$ HLA-DR$^+$ T cell frequencies acquired by flow cytometry are shown of peripheral blood mononuclear cells (PBMC) in (A) HCMV-seronegative mothers and (B) seropositive mothers. CD8$^+$ HLA-DR$^+$ T cell frequency of breast milk cells (BMC) is displayed of (C) HCMV-seronegative and (D) seropositive mothers. The inserts in (A) and (B) show the biological control over all experimental days. Individual color-coding as described in Table 29 is applied. Mother 12 (red, dotted line) was excluded from statistical analysis due to HCMV-primary infection during pregnancy. The time ranges are T1 - 10 to 15, T2 - 25 to 30, T3 - 40 to 45 and T4 - 55 to 60 days p.p. Square data point symbols instead of round symbols indicate a time point where the breast milk cells showed a slightly red color in the cell pellet (presumably an indicator for mastitis).*

Table 48: Mean CD8$^+$ HLA-DR$^+$ frequencies of T1 to T4 with standard deviation (SD).

Cell subset	Mate-rial	HCMV	T1 [% mean ± SD]	T2 [% mean ± SD]	T3 [% mean ± SD]	T4 [% mean ± SD]
CD8$^+$ HLA-DR$^+$ T cells	PBMC	IgG$^+$	7.1 ± 3.6	6.4 ± 2.8	6.2 ± 3.0	5.4 ± 2.8
		IgG-	2.5 ± 1.2	3.0 ± 1.3	3.4 ± 1.6	2.6 ± 1.5
	BMC	IgG$^+$	**15.3 ± 8.1**	**18.3 ± 9.1**	**24.9 ± 12.5**	**25.1 ± 9.2**
		IgG-	9.8 ± 4.1	15.0 ± 6.4	16.8 ± 7.5	15.1 ± 9.0

Table 49: Statistical analysis of CD8⁺HLA-DR⁺ T cells *The p-values are given for different tests and significant digits are bold and marked in grey. Friedman test was used to look for differences in the kinetics followed by a Dunn-Bonferroni post-hoc test with Bonferroni (B.) correction comparing single time ranges. The linear mixed model was used to show differences in the courses over time between HCMV-seropositive and seronegative mothers. Mann-Whitney U indicated differences between the single time ranges of seropositive and negative mothers. The Wilcoxon test with B. correction was used to compare single time ranges (T's) of blood and breast milk.*

CD8⁺ HLA-DR⁺ T cells	PBMC HCMV pos	PBMC HCMV neg	BMC HCMV pos	BMC HCMV neg
Friedman test	0.089	0.62	**0.0012**	0.49
Dunn-Bonferroni post-hoc test with B. correction	-	-	T1 to T2: 1.0 **T1 to T3: 0.013** **T1 to T4: 0.013** T2 to T3: 0.070 T2 to T4: 0.070 T3 to T4: 1.0	-
Linear mixed model	0.38		0.33	
Mann-Whitney U with B. correction				
T1's	**0.0014**		0.75	
T2's	**0.0029**		1.0	
T3's	**0.044**		0.33	
T4's	**0.0046**		0.060	
Wilcoxon with B. correction	PBMC HCMV pos	BMC HCMV pos	PBMC HCMV neg	BMC HCMV neg
T1's	**0.0066**		**0.028**	
T2's	**0.0017**		**0.020**	
T3's	**0.0014**		**0.020**	
T4's	**0.0012**		**0.020**	

In short, HLA-DR expression on CD8⁺ T cells is elevated in HCMV-seropositive mothers' compared to HCMV-seronegative mothers' blood. Otherwise no changes over time were detectable in the frequency on neither CD4⁺ nor CD8⁺ T cells.
Breast milk harbors higher HLA-DR⁺ T cell frequencies than blood. Interestingly, in breast milk, the HLA-DR expression on both CD4⁺ and CD8⁺ T cells highly increased over time in HCMV-seropositive, but not in seronegative mothers.

5.3.5.4.2 Memory phenotyping (using CCR7, CD45RA)

Memory phenotyping gives insights about naïve and antigen-experienced T cell frequencies. Memory T cells are an important part of the immune response against HCMV, protecting against virus reactivations.
Here, CD4⁺ T cells were investigated for their memory phenotype expressions. The mean levels (Table 50) at T1 are displayed in pie charts in Figure 48. In blood, frequency differences between the HCMV-serostatus of the mothers were detectable. HCMV-seropositive mothers had more TEMRA cells and less naïve T cells than HCMV-seronegative mothers (Figure 48 A and C) (significances explained in the next paragraph).

In breast milk samples, the separation of CCR7 and, therefore, especially central memory and effector memory subsets, was poor and populations difficult to determine. Therefore, the cross gates in the flow cytometry analysis for the memory subsets were set in the blood setting, where CCR7-staining showed good separations and were finally copied to breast milk samples (Figure 48 E and F). Thus, breast milk results of the memory phenotypes should be interpreted with caution (see 6.3.3.2). Hence, the statistical analysis of breast milk frequencies is given in Supplement table 3, but is not discussed in the text.

The memory phenotype frequencies did not show strong differences between the HCMV-serostatus' in breast milk (Figure 48 B, D). The main subsets of breast milk $CD4^+$ T cells were central and effector memory T cells, whereas in blood, naïve and central memory T cells represented the main population.

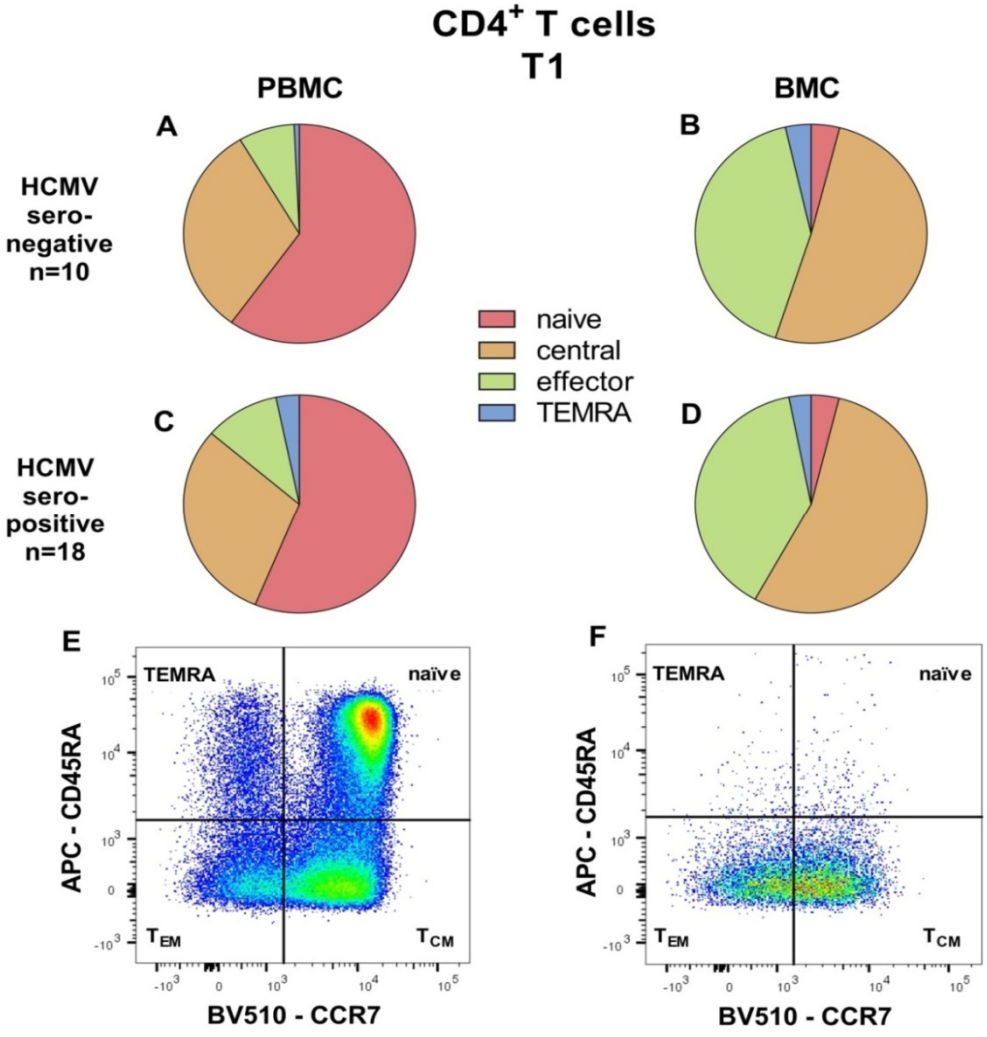

Figure 48: Memory subtypes of $CD4^+$ T cells at T1.
$CD4^+$ T cells were divided into naïve ($CCR7^+$, $CD45RA^+$), central memory ($CCR7^+$, CD45RA-), effector memory ($CCR7^-$, $CD45RA^-$) and TEMRA ($CCR7^-$, $CD45RA^+$) cells and displayed HCMV-seronegative mothers in (A) peripheral blood mononuclear cells (PBMCs) and (B) breast milk cells (BMCs). Seropositive mothers' distribution of memory phenotypes is shown in (C) for PBMCs and in (D) for BMCs. (E) and (F) demonstrate the pseudocolor plots of the FACS-analysis of PBMC or BMC, respectively. T1 is at 10 to 15 days p.p.

Surprisingly, in an observational time range of only two months, the **naïve CD4$^+$ T cells in blood** (CCR7$^+$, CD45RA$^+$) of HCMV-seropositive mothers demonstrated slight decreases of the mean frequencies from T1 (56.5 ± 10.6%) to T4 (51.7 ± 10.5) with around 4.8% (Friedman test p=0.0083, Supplement table 2; Figure 49 C). Post-hoc tests with corrections revealed significant decreases between T1 and T4 (p=0.005). The HCMV-seronegative mothers constantly had around 61% mean naïve CD4$^+$ T cell frequencies in blood (Figure 49 A). Therefore, a significant decrease of the seropositive in comparison to the seronegative mothers' kinetics were detected (linear mixed model p=0.025, Supplement table 2). Since the parental population (CD4$^+$ T cells) showed also a slight decrease over time, this indicated in general a decrease in the frequency of naïve T cells in HCMV-seropositive mothers' blood. **In breast milk**, naïve CD4$^+$ T cell frequencies were very low with mean frequencies around 2-4% of all CD4$^+$ T cells (Figure 49 B and D). Consequently, when **comparing blood and breast milk samples**, less naïve CD4$^+$ T cells were found in breast milk (Supplement table 2).

Mean **central memory CD4$^+$ T cell** (CCR7$^+$, CD45RA$^-$) frequencies were around 29-31% of all CD4$^+$ T cells independent of HCMV-serostatus and time (Figure 49 A and C, Supplement table 2). However, **in breast milk** the central memory CD4$^+$ T cell frequencies were the main subset together with effector memory CD4$^+$ T cells and showed a decrease in mean frequencies in HCMV-seropositive mothers from T1 with 55.0 ± 7.0% to T4 with 46.8 ± 7.9% (Figure 49 D, Table 50). The seronegative mothers' frequencies constantly stayed around 50-52% (Figure 49 B). **Breast milk** contained, therefore, more central memory CD4$^+$ T cells than **blood** (Supplement table 2).

Mean **blood effector memory T cell** frequencies (CCR7$^-$, CD45RA$^-$) were around 10-13% of all CD4$^+$ T cells in HCMV-seropositive and significantly lower with around 7-8% in seronegative mothers (Figure 49 A and C, Table 50, Mann-Whitney U in Supplement table 2). In **breast milk** of HCMV-seropositive mothers an increase was detectable from mean frequencies at T1 (38.4 ± 6.4%) to T4 (47.9 ± 7.6%) (Figure 49 D, Table 50). Conclusively, the decrease of breast milk central memory CD4$^+$ T cells showed therefore strong negative correlations with the increasing effector memory CD4$^+$ T cells in HCMV-seropositive mothers (Spearman: T1's and T2's r=-0.85, T3's and T4's r=-0.89). However, this effect was not observed in HCMV-seronegative mothers, where effector memory CD4$^+$ T cell frequencies constantly stayed around 40-42% (Figure 49 B). **Comparing blood and breast milk**, effector memory CD4$^+$ T cell frequencies were always higher in breast milk regardless to serostatus (Table 50, Supplement table 2).

As expected, **blood CD4$^+$ TEMRA cells** (CCR7-, CD45RA$^+$) displayed no significant changes over time and constantly were at mean frequencies of 0.7-0.8% for HCMV-seronegative and 3-3.6% of all CD4$^+$ T cells for seropositive mothers (Figure 49 A and C). This resulted in

significantly less TEMRA cell frequencies at the single time ranges in blood of HCMV-seronegative compared to seropositive mothers (Mann-Whitney U test with corrections for all T's $p<0.003$, Supplement table 2). **Breast milk** TEMRA cell frequencies of either HCMV-serostatus showed no changes over time (Figure 49 B and D) and were around 2.2 to 3.6% of all $CD4^+$ T cells. HCMV-seronegative mothers had less TEMRA cells in **blood** than in the corresponding **breast milk samples**, while no differences between blood and breast milk were found in HCMV-seropositive mothers (Supplement table 2).

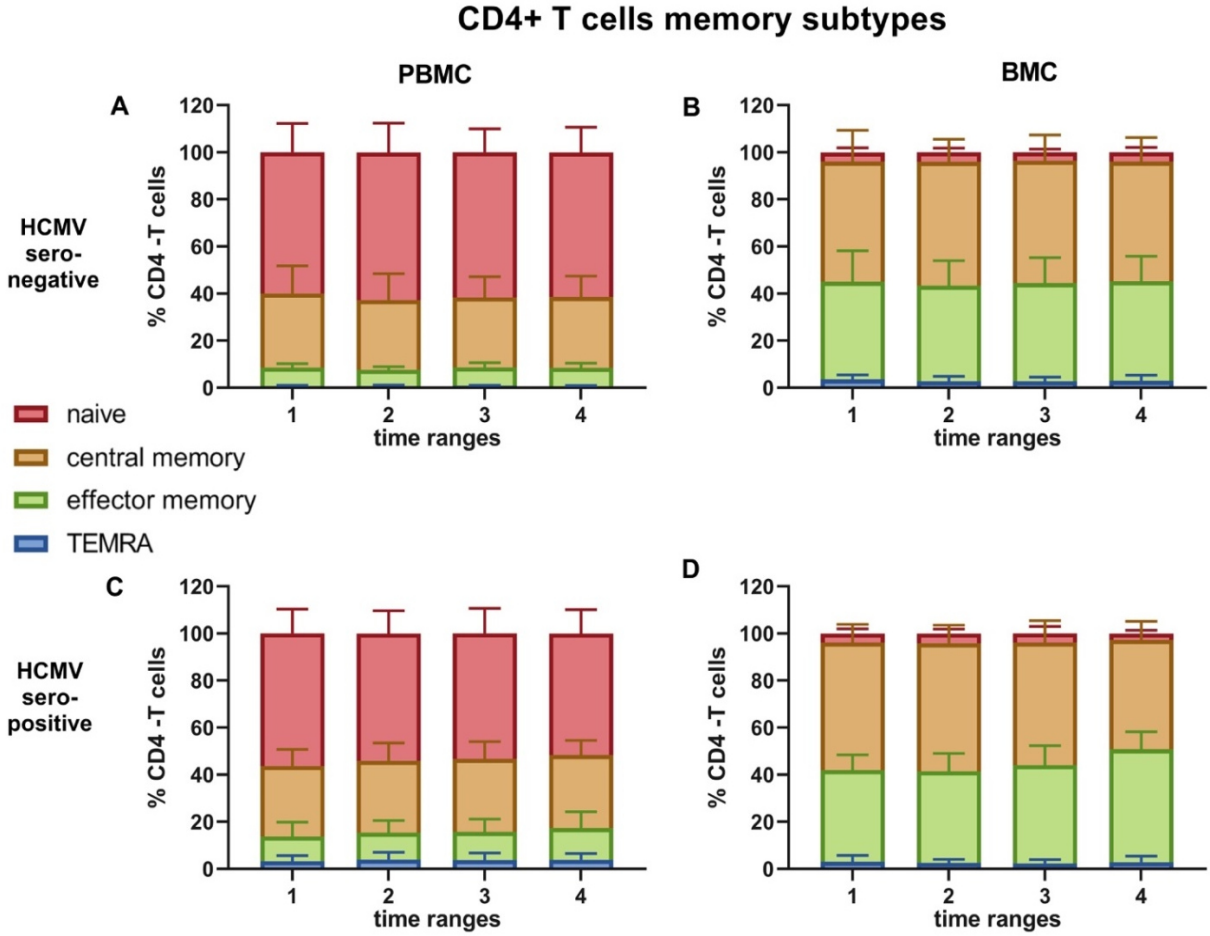

Figure 49: Longitudinal memory subtypes of $CD4^+$ T cells.
Mean levels of naïve ($CCR7^+$, $CD45RA^+$), central memory ($CCR7^+$, CD45RA-), effector memory (CCR7-, CD45RA-) and TEMRA (CCR7-, $CD45RA^+$) $CD4^+$ T cells are displayed with standard deviation (SD) in HCMV-seronegative mothers in (A) peripheral blood mononuclear cells (PBMCs) and (B) breast milk cells (BMCs). The same results are shown in (C) PBMCs and (D) BMCs for HCMV-seropositive mothers. T1 – 10 to 15, T2 – 25 to 30, T3 – 40 to 45 and T4 – 55 to 60 days p.p.

Table 50: Mean CD4⁺ T cell memory subtype frequencieswith standard deviation (SD).

Cell subset	Mate-rial	HCMV	T1 [% mean ± SD]	T2 [% mean ± SD]	T3 [% mean ± SD]	T4 [% mean ± SD]
CD4⁺ T_N	PBMC	IgG⁺	**56.5 ± 10.6**	**54.1 ± 9.9**	**53.3 ± 11.0**	**51.7 ± 10.5**
		IgG-	60.0 ± 12.2	62.7 ± 12.3	61.6 ± 10.0	61.5 ± 10.7
	BMC	IgG⁺	**3.8 ± 2.0**	**4.1 ± 1.9**	**3.9 ± 3.0**	**2.6 ± 1.3**
		IgG-	4.0 ± 1.8	4.0 ± 1.8	3.6 ± 1.3	3.9 ± 2.0
CD4⁺ T_{CM}	PBMC	IgG⁺	30.1 ± 7.2	30.9 ± 7.6	31.2 ± 7.5	31.2 ± 6.3
		IgG-	31.5 ± 11.7	29.6 ± 11.2	29.7 ± 8.8	30.1 ± 8.9
	BMC	IgG⁺	**55.0 ± 7.0**	**54.4 ± 7.9**	**52.3 ± 9.6**	**46.8 ± 7.9**
		IgG-	51.0 ± 13.4	52.7 ± 9.6	51.9 ± 10.9	50.9 ± 10.2
CD4⁺ T_{EM}	PBMC	IgG⁺	**10.5 ± 6.3**	**11.5 ± 5.4**	**12.0 ± 5.6**	**13.6 ± 7.1**
		IgG-	**7.8 ± 1.7**	**6.9 ± 1.3**	**7.9 ± 1.9**	**7.7 ± 2.0**
	BMC	IgG⁺	**38.4 ± 6.4**	**39.1 ± 7.8**	**41.6 ± 8.6**	**47.9 ± 7.6**
		IgG-	41.4 ± 13.1	40.6 ± 10.6	41.8 ± 10.7	42.3 ± 10.6
CD4⁺ T_{EMRA}	PBMC	IgG⁺	3.0 ± 2.2	3.6 ± 3.0	3.4 ± 2.6	3.6 ± 2.6
		IgG-	0.7 ± 0.3	0.8 ± 0.3	0.8 ± 0.3	0.7 ± 0.3
	BMC	IgG⁺	2.7 ± 2.2	2.4 ± 1.5	2.2 ± 1.6	2.6 ± 2.5
		IgG-	3.6 ± 1.9	2.7 ± 2.1	2.7 ± 1.8	3.0 ± 2.4

$CD8^+$ T cell memory subtypes at T1 from HCMV seropositive and -negative mothers' blood and breast milk samples are shown in Figure 50. The pie charts show that the differentiation signature of $CD8^+$ T cells **in blood** differs between the HCMV serostatus. In accordance with literature, HCMV-seropositive mothers had higher frequencies of TEMRA and lesser frequencies of naïve T cells in blood than seronegative mothers (Table 51, statistical evaluation is described in the next paragraph).

Despite the different distributions in blood, **breast milk** frequencies did not show strong differences between HCMV-seropositive and negative mothers (Figure 50 B and D). Frequencies of naïve T cells were low, but interestingly higher than in $CD4^+$ T cells. In controversy to $CD4^+$ T cells, where the main subsets of breast milk were central and effector memory T cells, $CD8^+$ T cells mainly consisted of TEMRA and effector memory cells.

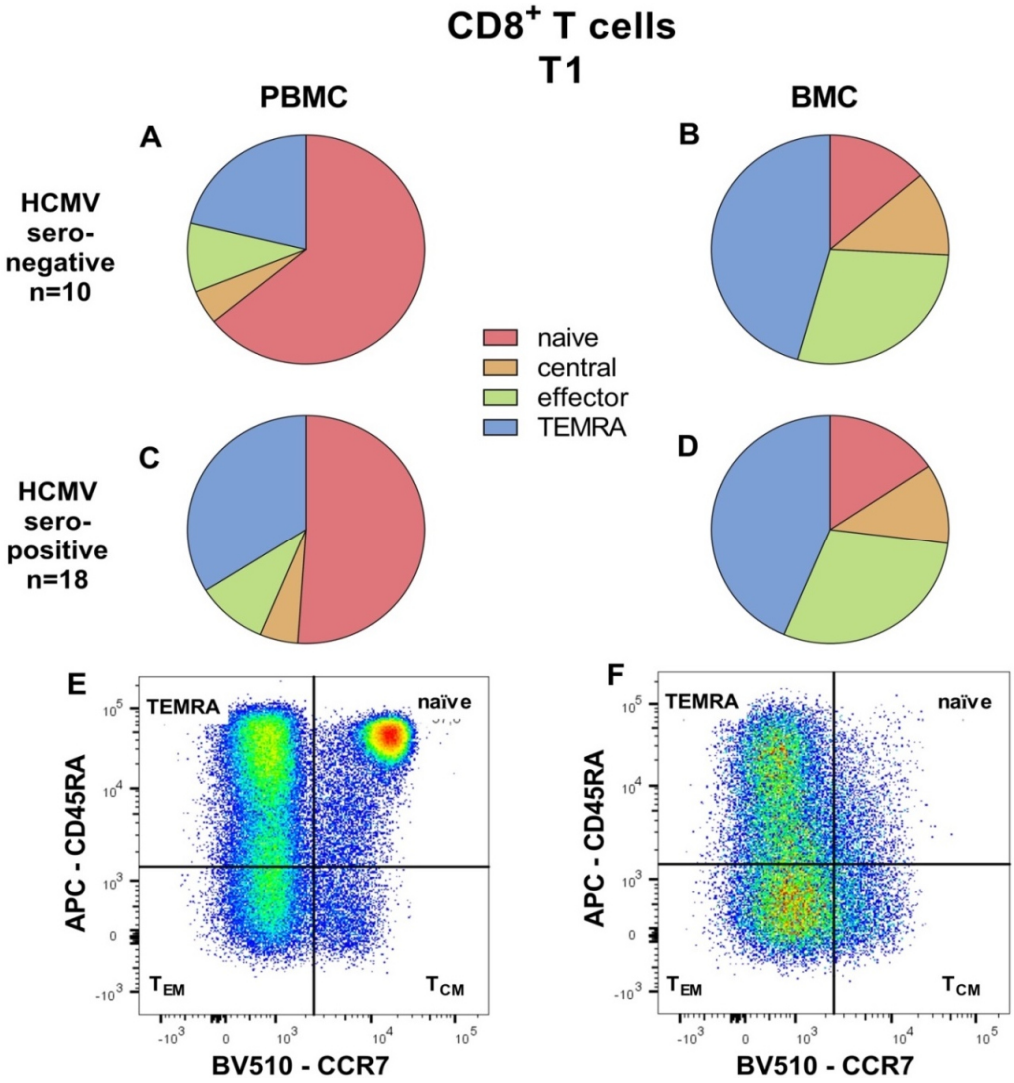

Figure 50: Memory subtypes of CD8⁺ T cells at T1.
CD8⁺ T cells were divided into naïve (CCR7⁺, CD45RA⁺), central memory (CCR7⁺, CD45RA-), effector memory (CCR7-, CD45RA-) and TEMRA (CCR7-, CD45RA⁺) cells and displayed HCMV-seronegative mothers in (A) peripheral blood mononuclear cells (PBMCs) and (B) breast milk cells (BMCs). Seropositive mothers' distribution of memory phenotypes is shown in (C) for PBMCs and in (D) for BMCs. (E) and (F) demonstrate the pseudocolor plots of the FACS-analysis of PBMCs or BMCs, respectively. T1 is at 10 to 15 days p.p.

The mean levels with SD of CD8⁺ T cell memory subset frequencies are shown over all four time ranges in Figure 51 and Table 51.

In blood, an unexpected slight decrease from 51.6 ± 11.7% at T1 to 45.2 ± 12.6% at T4 of **naïve CD8⁺ T cells** (CCR7⁺, CD45RA⁺) was observed in HCMV-seropositive mothers over only a two months range (Friedman, p=0.00046, Supplement table 3) (Figure 51 C), no changes in the parental population of CD8⁺ T cells was observed. Post-hoc tests with corrections indicated the main decrease between T1 and T4 (p=0.0004), as well as between T2 and T4 (p=0.009, Supplement table 3). HCMV-seronegative mothers revealed no changes over the observation period in naïve CD8⁺ T cells of blood (Figure 51 A). Interestingly, when comparing the HCMV-serostatus, seropositive mothers had significantly less naïve T cells (T4: 45.2 ± 12.6%) than seronegative mothers (T4: 62.7 ± 11.1%, Table 51) at later time ranges

(Mann-Whitney U test with corrections: T1's p=0.094, T2's 0.013, T3's p=0.015 and T4's p=0.027, Supplement table 3). The decreasing naïve blood $CD8^+$ T cell frequencies in seropositive mothers compared to constant seronegative mothers' frequencies over time resulted in significant differences of the kinetics of HCMV-seropositive and negative mothers (linear mixed model p=0.043, Supplement table 3). **In breast milk**, the already low naïve T cell frequencies of HCMV-seropositive mothers showed a mean decrease of 5.2% from T1 to T4 (Table 51, Figure 51 D). Naïve $CD8^+$ T cell frequencies from HCMV-seronegative mothers' breast milk exhibited no changes over time (Figure 51 B). Higher naïve $CD8^+$ T cell frequencies were found in **blood** (e.g. HCMV-seronegative at T1: 63.2 ± 10.7%) **compared to breast milk** (e.g. HCMV-seronegative at T1: 13.7 ± 6.4, Table 51).

The **central memory $CD8^+$ T cell** ($CCR7^+$, $CD45RA^-$) frequencies **in blood** were the smallest population of all four subsets with mean frequencies around 4-5% of $CD8^+$ T cells (Table 51) and stayed constant over time in HCMV-seropositive and negative mothers (Supplement table 3). **In breast milk**, the central memory $CD8^+$ T cell frequencies did also not change over time (Figure 51 D and B). However, with mean frequencies around 10-13% of $CD8^+$ T cells (Table 51), the central memory frequencies were higher in **breast milk** than in **blood** (Supplement table 3).

Effector memory T cells ($CCR7^-$, $CD45RA^-$) displayed mean frequencies around 9-13% of $CD8^+$ T cells **in blood** of HCMV-seronegative and seropositive mothers (Table 51, Figure 51 A and C). **In breast milk**, mean frequencies at T1 were at 28.5% for seronegative and 30% of $CD8^+$ T cells for seropositive mothers. Both groups showed a mean increase of effector memory $CD8^+$ T cell frequencies over time, the HCMV-seronegative by 6.4% and the seropositive mothers by 5.8% (Figure 51 B and D, Table 51). **Breast milk** displayed with around 18-24% higher frequencies of effector memory $CD8^+$ T cells than **blood** (Table 51).

$CD8^+$ TEMRA cell (CCR7-, $CD45RA^+$) frequencies **in blood** showed no significant changes over time independent of HCMV-serostatus (Supplement table 3, Figure 51 A and C). However, a significantly higher TEMRA cell frequency in blood of HCMV-seropositive (e.g. T4: 36.8 ± 11.2%) compared to seronegative mothers (T4: 22.1 ± 7.8%; Table 51) was observed (Mann-Whitney U tests with corrections all T's p<0.03, Supplement table 3). **Breast milk** TEMRA cell frequencies were the most frequent of all memory subsets and had mean frequencies of around 41-46% of all $CD8^+$ T cells disregarding the HCMV-serostatus of the mothers (Figure 51 B and D). But, due to the higher TEMRA cell frequency in blood of HCMV-seropositive mothers, only the HCMV-seronegative mothers showed higher TEMRA cell frequencies **in breast milk compared to blood** (Supplement table 3).

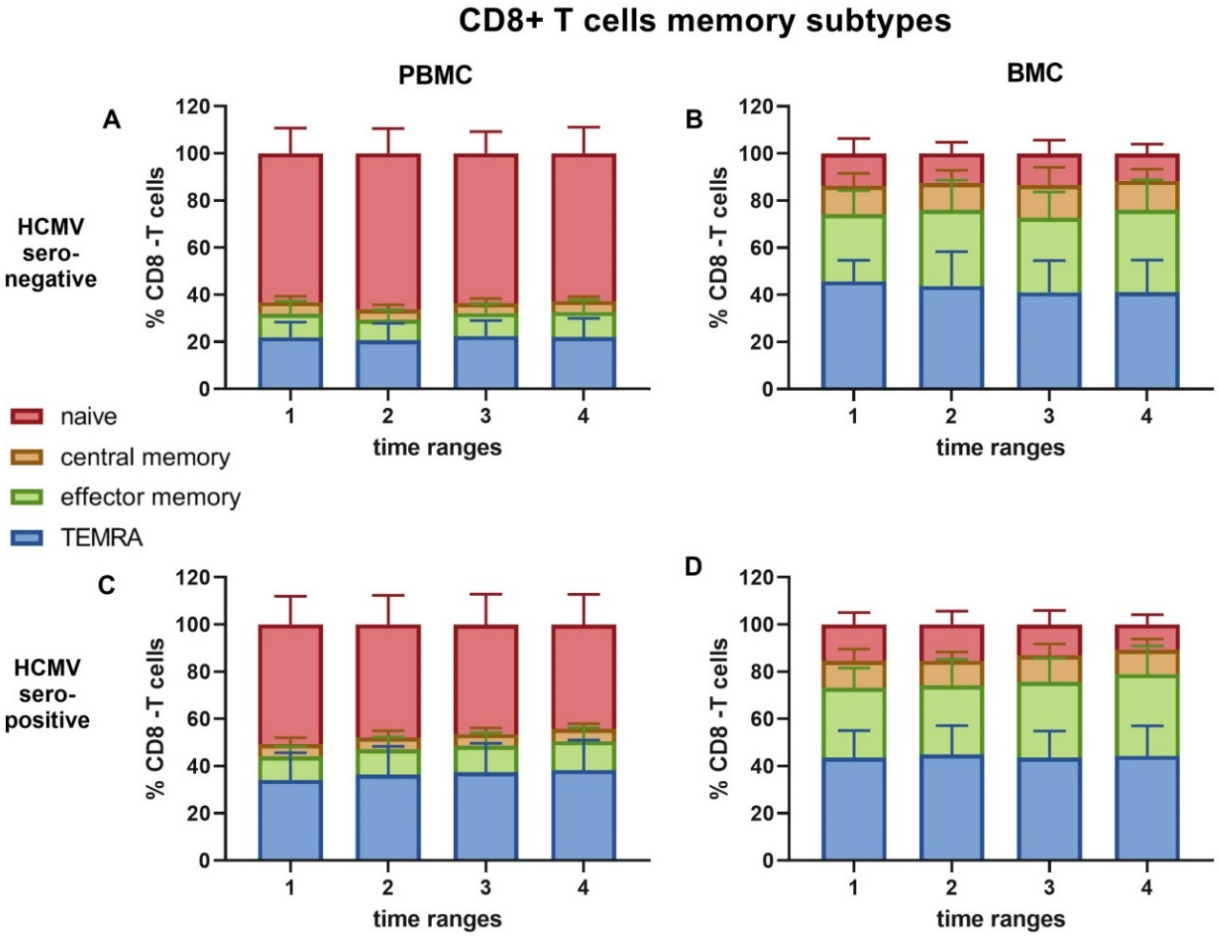

Figure 51: Longitudinal memory subtypes of CD8⁺ T cells.
Mean frequencies of naïve (CCR7⁺, CD45RA⁺), central memory (CCR7⁺, CD45RA-), effector memory (CCR7-, CD45RA-) and TEMRA (CCR7-, CD45RA⁺) CD8⁺ T cells are displayed with standard deviation (SD) in HCMV-seronegative mothers in (A) peripheral blood mononuclear cells (PBMCs) and (B) breast milk cells (BMCs). The same results are shown in (C) PBMCs and (D) BMCs for HCMV-seropositive mothers. T1 – 10 to 15, T2 – 25 to 30, T3 – 40 to 45 and T4 – 55 to 60 days p.p.

Table 51: Mean CD8⁺ T cell memory subset frequenciesof T1 to T4 with standard deviation (SD).

Cell subset	Mate-rial	HCMV	T1 [% mean ± SD]	T2 [% mean ± SD]	T3 [% mean ± SD]	T4 [% mean ± SD]
CD8⁺ T_N	PBMC	IgG⁺	**51.6 ± 11.7**	**48.9 ± 11.9**	**47.4 ± 12.4**	**45.2 ± 12.6**
		IgG-	63.2 ± 10.7	66.3 ± 10.6	63.5 ± 9.2	62.7 ± 11.1
	BMC	IgG⁺	**15.8 ± 5.0**	**15.3 ± 5.9**	**13.1 ± 6.1**	**10.6 ± 4.3**
		IgG-	13.7 ± 6.4	12.5 ± 4.7	13.4 ± 5.6	11.7 ± 4.0
CD8⁺ T_{CM}	PBMC	IgG⁺	5.4 ± 2.8	5.2 ± 2.8	5.1 ± 2.5	5.3 ± 2.1
		IgG-	4.9 ± 2.5	4.3 ± 2.0	4.3± 1.8	4.7 ± 1.8
	BMC	IgG⁺	11.6 ± 5.1	10.7 ± 3.7	11.3 ± 5.0	10.7 ± 4.5
		IgG-	12.1 ± 5.3	11.5 ± 5.4	13.8 ± 7.6	12.3 ± 5.0
CD8⁺ T_{EM}	PBMC	IgG⁺	**10.3 ± 4.1**	**11.1 ± 5.0**	**11.8 ± 5.2**	**12.8 ± 5.4**
		IgG-	10.0 ± 5.3	8.7 ± 4.1	9.7 ± 4.0	10.6 ± 5.0
	BMC	IgG⁺	**30.0 ± 8.3**	**30.0 ± 10.9**	**33.0 ± 9.6**	**35.8 ± 11.1**
		IgG-	**28.5 ± 10.0**	**32.3 ± 12.7**	**31.7 ± 10.9**	**34.9 ± 12.7**

CD8⁺ T_{EMRA}	PBMC	IgG⁺	*32.7 ± 9.9*	*34.8 ± 10.1*	*35.7 ± 10.2*	*36.8 ± 11.2*
		IgG-	21.9 ± 6.4	20.7 ± 7.1	22.5 ± 6.5	22.1 ± 7.8
	BMC	IgG⁺	42.6 ± 10.8	44.1 ± 12.0	42.6 ± 11.0	42.9 ± 11.5
		IgG-	45.7 ± 8.9	43.7 ± 14.7	41.0 ± 13.6	41.2 ± 13.6

5.3.5.5 NK cells (CD56⁺)

NK cell frequencies (CD56⁺) **in blood** showed higher inter-individual variability in seropositive mothers than in seronegative mothers. However, the NK cell frequencies in blood did not change significantly over time (Friedman test in Table 53) and constantly were around mean frequencies of 9-11% of all lymphocytes (Table 52, Figure 52 B).

In breast milk, mean NK cell frequencies varied between 3.5 and 6.3% without regard to the serostatus and time (Table 52, Figure 52 C and D).

When **comparing blood and breast milk** samples, seropositive mothers had significantly higher frequencies over all four time ranges in blood (Wilcoxon in Table 53). Seronegative mothers showed significant elevations in breast milk compared to blood between T1's, T2's and T4's (Wilcoxon in Table 53).

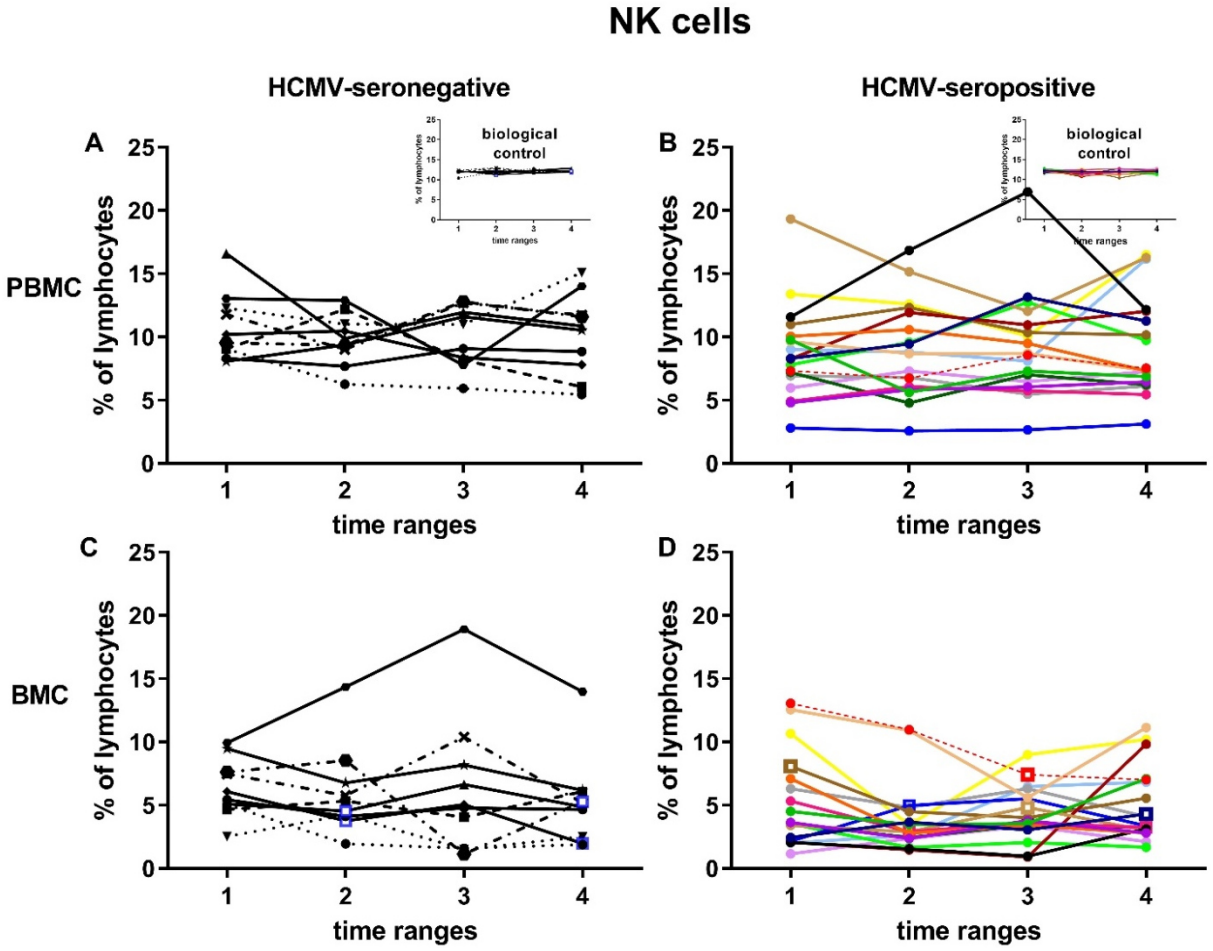

Figure 52: NK cell kinetics in blood and breast milk of the BlooMil study mothers.
NK cell frequencies acquired by flow cytometry are shown of peripheral blood mononuclear cells (PBMC) in (A) HCMV-seronegative mothers and (B) seropositive mothers. NK cell frequency of breast milk cells (BMC) is displayed of (C) HCMV-seronegative and (D) seropositive mothers. The inserts in (A) and (B) show the biological control over all experimental days. Individual color-coding as described in Table 29 is applied. Mother 12 (red dotted line) was excluded from statistical analysis due to HCMV-primary infection during pregnancy. The time ranges are T1 - 10 to 15, T2 - 25 to 30, T3 - 40 to 45 and T4 - 55 to 60 days p.p. Square data point symbols instead of round symbols indicate a time point where the breast milk cells showed a slightly red color in the cell pellet (presumably an indicator for mastitis).

Table 52: Mean NK cell frequencies of T1 to T4 with standard deviation (SD).

Cell subset	Mate-rial	HCMV	T1 [% mean ± SD]	T2 [% mean ± SD]	T3 [% mean ± SD]	T4 [% mean ± SD]
CD56⁺ NK cells	PBMC	IgG⁺	8.9 ± 3.8	9.1 ± 3.8	9.3 ± 4.2	9.4 ± 4.1
		IgG-	10.8 ± 2.6	9.8 ± 2.0	9.9 ± 2.4	10.2 ± 3.2
	BMC	IgG⁺	**4.7 ± 3.2**	**3.5 ± 2.2**	**4.1 ± 2.0**	**5.0 ± 3.0**
		IgG-	6.3 ± 2.3	5.9 ± 3.5	6.2 ± 5.4	5.3 ± 3.5

Overall, NK cell frequencies did not show high variances over time in all compartments. Frequencies in breast milk were lower than in blood.

Table 53: Statistical analysis of NK cells *The p-values are given for different tests and significant digits are bold and marked in grey. Friedman test was used to look for differences in the kinetics followed by a Dunn-Bonferroni post-hoc test with Bonferroni (B.) correction comparing single time ranges. The linear mixed model was used to show differences in the courses over time between HCMV-seropositive and seronegative mothers. The Wilcoxon test with B. correction was used to compare single time ranges (T's) of blood and breast milk.*

NK cells	PBMC HCMV pos	PBMC HCMV neg	BMC HCMV pos	BMC HCMV neg
Friedman test	0.96	0.62	**0.028**	0.23
Dunn-Bonferroni post-hoc test with B. correction			**T1 to T2: 0.032** T1 to T3: 1.0 T1 to T4: 1.0 T2 to T3: 0.20 T2 to T4: 0.14 T3 to T4: 1.0	
Linear mixed model	0.70		0.29	
Wilcoxon with B. correction	PBMC HCMV pos	BMC HCMV pos	PBMC HCMV neg	BMC HCMV neg
T1's	**0.004**		**0.028**	
T2's	**0.0047**		**0.037**	
T3's	**0.004**		0.24	
T4's	**0.0077**		**0.028**	

5.3.5.6 CD56⁺ T cells

Blood CD56⁺ T cell (CD3⁺, CD56⁺) frequencies remained constant over time (Friedman test in (Table 55) at mean frequencies of around 4-5% of all lymphocytes regardless to HCMV-serostatus (Table 54, Figure 53 A and B). Seropositive mothers had higher inter-individual variabilities than seronegative mothers. However, one HCMV-seronegative mother (mother 6) showed relatively high CD56⁺ T cell frequencies (10-13%) in blood compared to all other seronegative mothers (around and fewer than 6%).

Breast milk CD56⁺ T cell mean frequencies were around 3-5% of all lymphocytes regardless to serostatus (Table 54). The seropositive mothers 21 and 23 showed elevated frequencies at T2 with almost 15 and 10%, respectively. These two mothers had also high blood CD56⁺ T cell frequencies. All other seropositive mothers had frequencies around and fewer than 6% (Figure 53 D). The seronegative mothers had in general high inter-individual variability with frequencies around 0.5 to 10% (Figure 53 C).

When **breast milk and blood was compared**, only the seropositive cohort showed significantly higher frequencies in blood compared to breast milk at T4's (Wilcoxon in Table 55) Moderate to strong correlations were found between blood and breast milk CD56⁺ T cells at T1 (r=0.6, p=0.01) and T2 (r=0.79, all other time ranges in Supplement figure 3) of HCMV-seropositive mothers. CD56⁺ T cells from blood and breast milk of HCMV-seronegative

mothers showed only at T4 a moderate correlation (r=0.66, all other time ranges in Supplement figure 3).

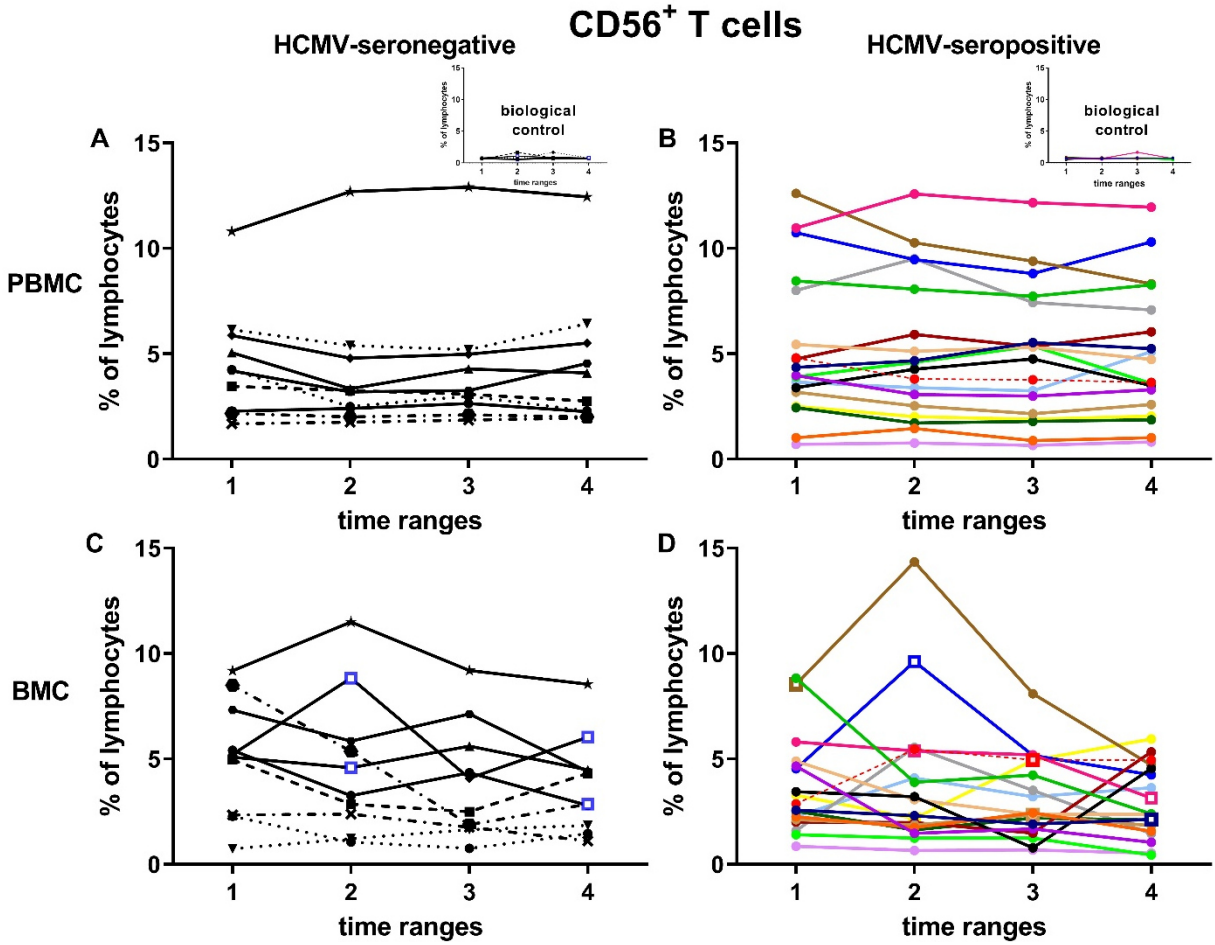

Figure 53: CD56⁺ T cell kinetics in blood and breast milk of the BlooMil study mothers.
CD56⁺ T cell frequencies acquired by flow cytometry are shown of peripheral blood mononuclear cells (PBMC) in (A) HCMV-seronegative mothers and (B) seropositive mothers. CD56⁺ T cell frequency of breast milk cells (BMC) is displayed of (C) HCMV-seronegative and (D) seropositive mothers. The inserts in (A) and (B) show the biological control over all experimental days. Individual color-coding as described in Table 29 is applied. Mother 12 (red dotted line) was excluded from statistical analysis due to HCMV-primary infection during pregnancy. The time ranges are T1 - 10 to 15, T2 - 25 to 30, T3 - 40 to 45 and T4 - 55 to 60 days p.p. Square data point symbols instead of round symbols indicate a time point where the breast milk cells showed a slightly red color in the cell pellet (presumably an indicator for mastitis).

Table 54: Mean CD56⁺ T cell frequenciesof T1 to T4 with standard deviation (SD).

Cell subsets	Mate-rial	HCMV	T1 [% mean ± SD]	T2 [% mean ± SD]	T3 [% mean ± SD]	T4 [% mean ± SD]
CD3⁺ CD56⁺ T cells	PBMC	IgG⁺	5.3 ± 3.6	5.3 ± 3.5	5.0 ± 3.3	5.1 ± 3.2
		IgG-	4.6 ± 2.7	4.1 ± 3.2	4.3 ± 3.2	4.4 ± 3.2
	BMC	IgG⁺	**3.6 ± 2.3**	**3.8 ± 3.5**	**3.0 ± 2.0**	**2.8 ± 1.7**
		IgG-	5.1 ± 2.7	4.7 ± 3.4	3.9 ± 2.7	3.8 ± 2.3

In short, CD56$^+$ T cells showed in general high inter-individual variances and stayed relatively constant over time in blood and in breast milk.

Table 55: Statistical analysis of CD56$^+$ T cells *The p-values are given for different tests and significant digits are bold and marked in grey. Friedman test was used to look for differences in the kinetics followed by a Dunn-Bonferroni post-hoc test with Bonferroni (B.) correction comparing single time ranges. The linear mixed model was used to show differences in the courses over time between HCMV-seropositive and seronegative mothers. Mann-Whitney U showed no differences between the single time ranges of seropositive or negative mothers (p>0.46, not shown). The Wilcoxon test with B. correction was used to compare single time ranges (T's) of blood and breast milk.*

CD56$^+$ T cells	PBMC HCMV pos	PBMC HCMV neg	BMC HCMV pos	BMC HCMV neg
Friedman test	0.25	0.29	**0.025**	0.22
Dunn-Bonferroni post-hoc test with B. correction			T1 to T2: 0.86 T1 to T3: 0.67 **T1 to T4: 0.013** T2 to T3: 1.0 T2 to T4: 0.67 T3 to T4: 0.86	
Linear mixed model	0.42		0.91	
Wilcoxon with B. correction	PBMC HCMV pos	BMC HCMV pos	PBMC HCMV neg	BMC HCMV neg
T1's	0.14		1.0	
T2's	0.18		1.0	
T3's	**0.052**		1.0	
T4's	**0.045**		1.0	

5.3.5.7 Analysis of HCMV-specific CD8$^+$ T cells in breast milk and blood

The presence of HCMV-specific CD8$^+$ T cells was investigated in samples from HLA-A*02:01 positive mothers recruited at the Neonatology Department. Breast milk and blood samples from T1 and T3 were investigated for pp65 (NLVPMVATV) and IE1 (VLEETSVML) antigen specific CD8$^+$ T cells. The demographics of the participating mothers of the adjunct BlooMil study are shown in Table 56. Mother 31 could only participate at T1.

Table 56: Demographics of tetramer mothers

Mother	HCMV-IgG	Age [years]	GA [weeks]	BW [g]	number of births	multi-births	country of origin
29	pos	33	27 5/7	920$^+$905	3	twins	Germany
30	pos	29	27 4/7	940	3	no	Rumania
31	pos	35	25 2/7	520	1	no	Germany
32	pos	21	28 1/7	1120	1	no	Germany

For the populations from A to I the same gating strategy as already established for the main BlooMil study was used (see 5.3.5.1). After the CD3$^+$ T cells were split into CD8$^+$ and CD4$^+$ T cells, the CD8$^+$ T cells were further separated into both (IE1 and pp65) tetramers coupled to APC versus tetramer IE1- BV510 (Figure 54 K). The pp65-PE tetramer did not work in one sample and was therefore not used to evaluate tetramer frequencies in the entire gating-strategy to warrant comparability between all samples. Therefore, double positive populations were IE1 tetramer positive; while the APC positive and BV510 negative population revealed the pp65 tetramer positive population.

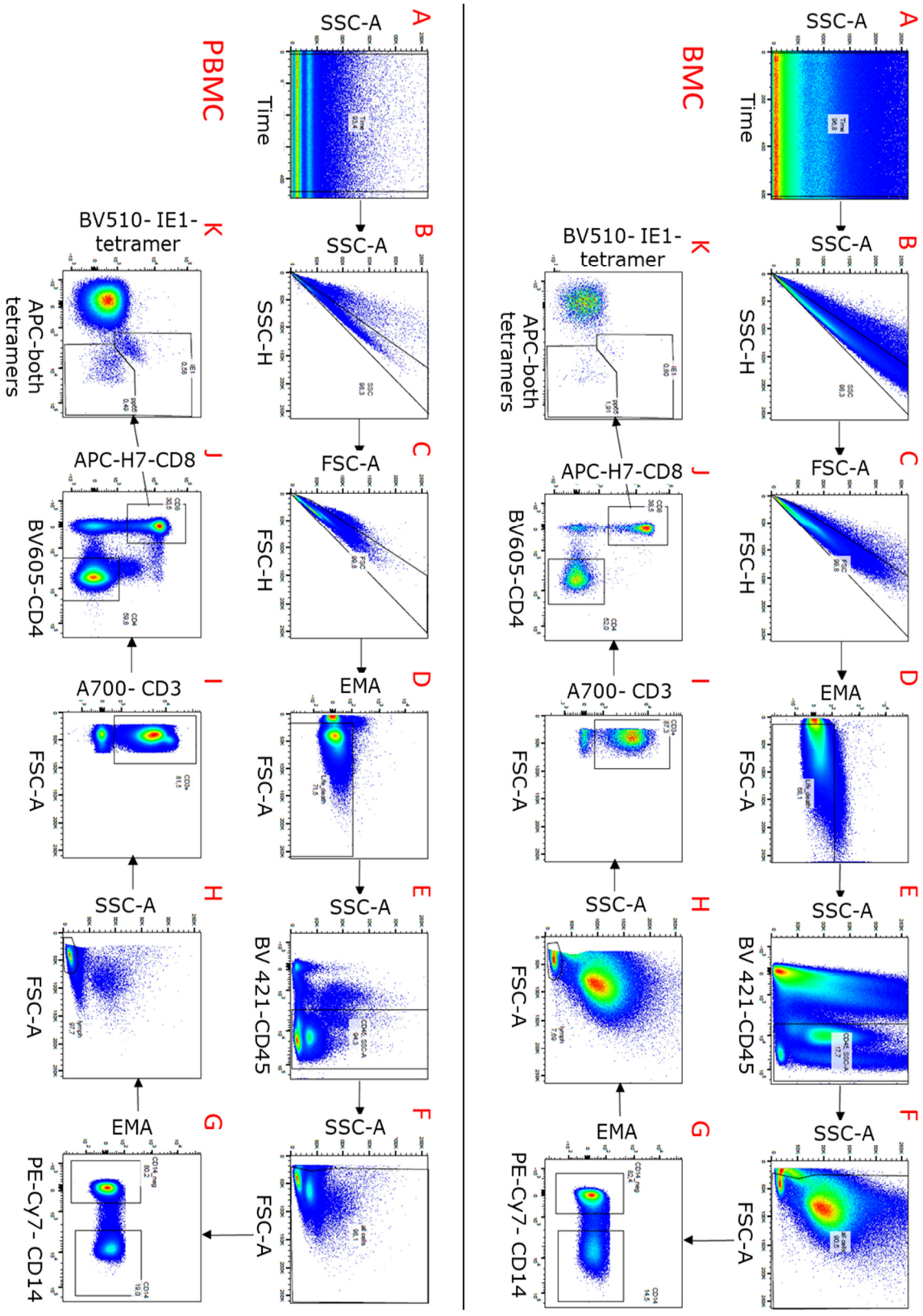

Figure 54: Tetramer gating strategy.
Breast milk cells (BMC, top) and peripheral blood mononuclear cells (PBMC, bottom) of mother 32 at T1.

Samples of the four included mothers showed blood frequencies of $CD3^+$ T cells (52-71%), $CD8^+$ T cells (21-50%), $CD4^+$ T cells (39-74%) and $CD14^+$ monocytes (7-19%, Table 57) similar to the range of the BlooMil study mothers' frequencies.

Table 57: Immune phenotyping of mothers participating in the tetramer study.

Mothers	Cells	$CD14^+$ monocytes [%]		$CD3^+$ T cells [%]		$CD4^+$ T cells [%]		$CD8^+$ T cells [%]	
		T1	T3	T1	T3	T1	T3	T1	T3
29	PBMC	15.2	15.7	70.4	68.9	46.6	39.6	44.2	50.1
	BMC	62.6	19.0	20.6	18.0	39.9	52.2	46.8	36.9
30	PBMC	15.1	7.5	66.5	52.7	58.1	57.5	32.8	33.6
	BMC	20.5	15.8	60.2	23.3	54.9	46.6	36.4	36.1
31	PBMC	16.7		63.1		74.3		21.3	
	BMC	81.7		2.6		54.0		38.0	
32	PBMC	19.0	10.4	63.8	71.2	59.7	58.5	30.5	30.6
	BMC	14.5	71.0	5.5	13.3	50.2	57.3	38.5	27.7

In breast milk, as seen before, high variations occurred. Frequencies of monocytes ranged between 20.5 to 81.6% at T1 and were decreasing to 15-18% at T3, following the same trends as the BlooMil mothers did (Table 57). However, mother 32 displayed abnormally high monocyte frequencies at T3 (71%, Table 57).

Breast milk $CD3^+$ T cells were high in mother 30 at T1 (60%), but all other mothers showed similar frequencies to the BlooMil study mothers. This was also the case for the frequencies of $CD4^+$ and $CD8^+$ T cells (Table 57).

Pp65-specific $CD8^+$ T cells were found in blood as well as in breast milk (Figure 55). However, statistical analysis was not performed, due to the low number of participants. All mothers, despite mother 31, reactivated HCMV in breast milk (Table 58). Mother 31 donated breast milk only at T1, where HCMV was not detectable. Interestingly, the two seropositive mothers with no detectable HCMV at T1 showed also lower pp65-specific T cell frequencies than the two mothers with low but detectable viral loads at T1 (Figure 55 C).

The difference in the biological control frequencies over time was similar to the increase or decrease in the frequencies seen over time in the pp65-specific T cell frequencies (Figure 55 A and B). Therefore, no further interpretation of this data is given.

When comparing breast milk to corresponding blood samples at T1 (Figure 55 C), mother 32 displayed higher frequencies in breast milk than in blood (3.9 fold). Mother 30 had also higher pp65-specific $CD8^+$ T cells in breast milk compared to blood (2.3 fold); while mother 31 showed frequencies close to zero in both body fluids but still with a 1.3 fold higher frequency in breast

milk. Mother 29 had slightly higher pp65-specific T cell frequencies in blood than in breast milk at T1 (1.1 fold) and T3 (1.2 fold) (Figure 55 C and D).

Table 58: Breast milk viral load of mother participating in the tetramer study
n.d. stands for no data available.

Mother	Breast milk viral load [copies/ml]	
	T1	T3
29	852	16,400
30	0	24,100
31	0	n.d.
32	220 (<600)	17,900

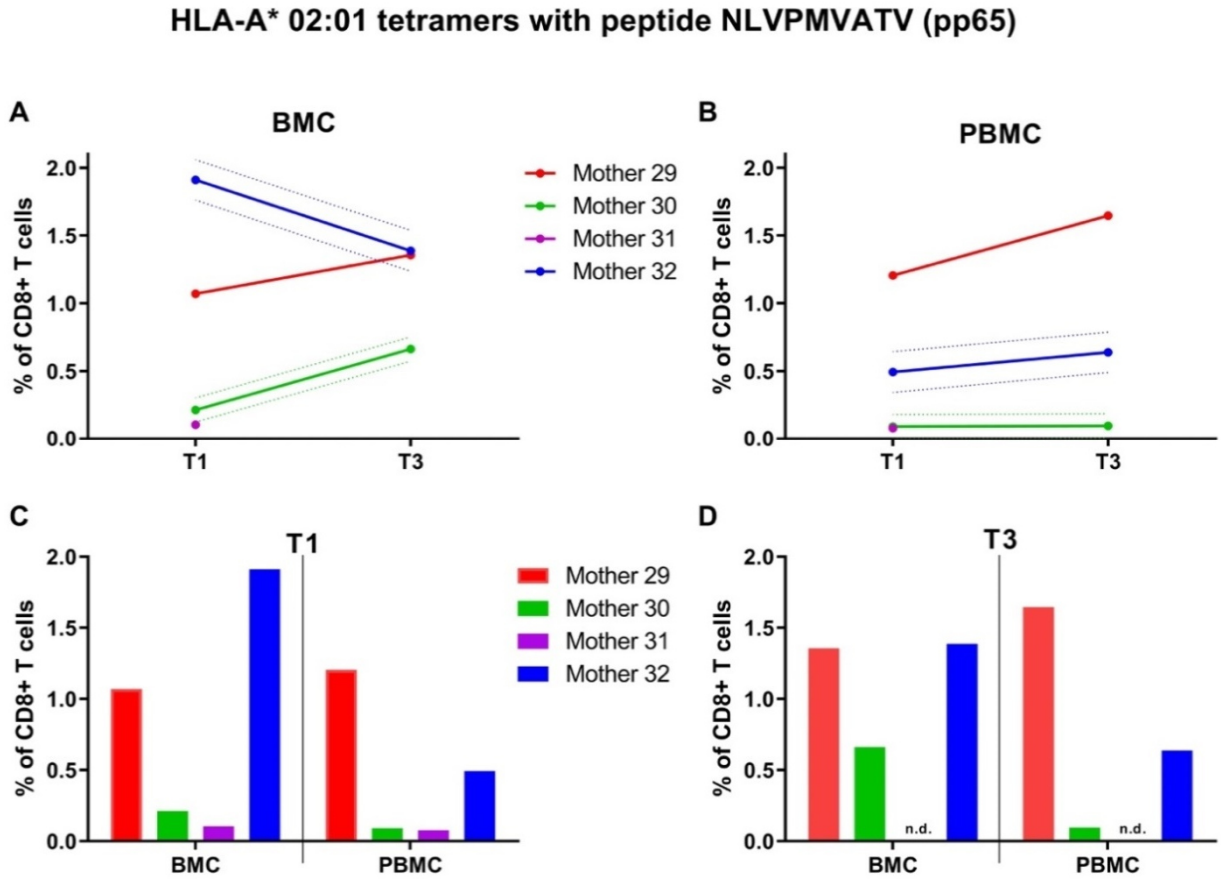

Figure 55: Tetramer analysis with pp65 peptide NLVPMVATV.
Changes in (A) breast milk over time (T1 – 10 to 15 days p.p. and T3 – 40 to 45 days p.p.) and (B) blood over time (T1-T3) as well as the differences between breast milk and corresponding blood samples at (C) T1 and (D) T3 are displayed. The dotted line equals the difference in frequencies of pp65-specific CD8⁺ T cells of the biological control between the two measurement days at T1 and T3.

IE1-specific CD8⁺ T cells were only found in two mothers (30 and 32) at lower frequencies (under 1%) than pp65 -specific CD8⁺ T cells. The analysis of changes during the lactation period concerning IE1-specific CD8⁺ T cells in breast milk (Figure 56 A) and blood (Figure 56 B) samples was difficult, due to high differences of the biological control between T1 and T3 (dotted line).

When comparing breast milk with corresponding blood samples at T1 (same day of measurement) only mother 32 expressed obvious amounts of IE1-specific $CD8^+$ T cells. The frequencies were slightly higher in breast milk than in blood (Figure 56 C). At T3, mother 30 had almost no IE1-specific T cell frequencies in blood, but a 23.1 fold higher frequency in breast milk when compared to blood (Figure 56 D).

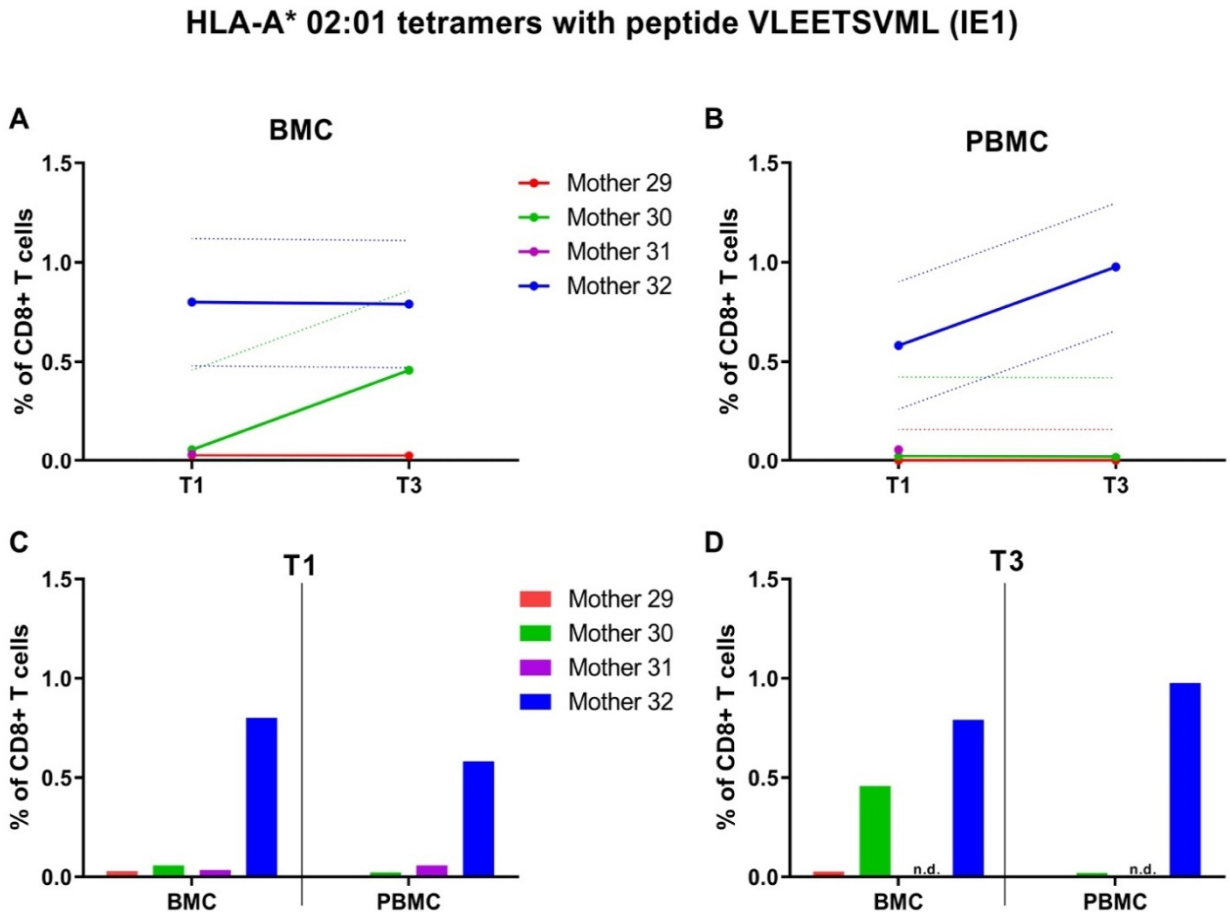

Figure 56: Tetramer analysis with IE1 peptide VLEETSVML.
Changes in (A) breast milk over time (T1 – 10 to 15 days p.p. and T3 – 40 to 45 days p.p.) and (B) blood over time (T1-T3), as well as the differences between breast milk and corresponding blood samples at (C) T1 and (D) T3 are displayed. The dotted line equals the difference in frequencies of IE1-specific $CD8^+$ T cells of the biological control between the two measurement days at T1 and T3.

5.3.6 Molecular analysis of HCMV transmission via RFLP

The preterm infant of mother 13 showed an HCMV infection five weeks after birth. The possibility of congenital transmission was excluded by negative urine and throat swab samples one week p.p. The route of transmission was unclear, since the mother's breast milk was usually pasteurized. Restriction length polymorphism was used to compare the HCMV strains in the mother's breast milk and the infant's urine (Figure 57). The breast milk and urine HCMV DNA was amplified for gene region UL10-13, followed by a digestion with Hin6I or RsaI. Both samples showed identical DNA fragment patterns after digestion indicating an infection of the infant via breast milk. The mother's breast milk showed weaker bands as the urine sample of the infant, due to lower HCMV-DNA levels.

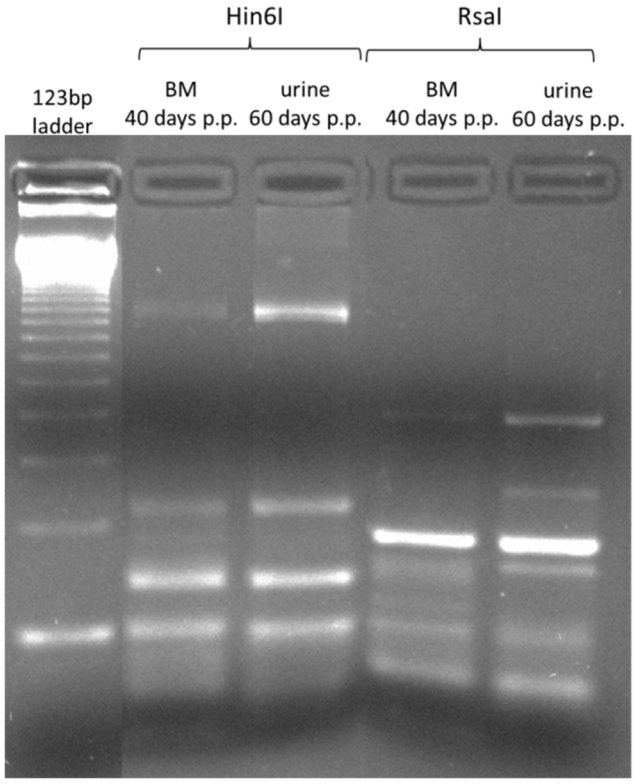

Figure 57: Restriction fragment length polymorphism (RFLP) of breast milk and urine HCMV DNA (mother 13).
Breast milk and urine extracts were first amplified with a UL10-13 PCR, gel extracted and then digested with Hin6I and RsaI. The figure shows a 1% agarose gel.

5.4 Cytokine analysis of milk whey

Milk whey samples of seven mothers (mother A, B, 3, 7, 14, 15 and 17) were analyzed for 92 inflammatory cytokines using proximity extension assays (Olink, Upsala, Sweden). Comparing HCMV-seropositive and -seronegative mothers, it was clearly visible that the mothers shedding HCMV into their milk had also higher cytokine levels. Almost all the evaluable cytokines (74/92) showed distinct elevations (Figure 58 and Figure 59). However, a decrease of most cytokines over the observed lactation period was detected in both seropositive and seronegative mothers.

Interestingly, IFNγ was not detected in breast milk samples, probably due to the low half-life of the interferon.

Two heat maps were used to display the mothers, since two different runs were performed with different baselines. Especially CCL19 ($p=0.007$, evaluated with the linear mixed effect ANOVA for HCMV only, statistical analysis performed by Olink), CXCL9 ($p=0.007$), CXCL11 ($p=0.007$), IL8 ($p=0.012$), IL17C ($p=0.018$), CCL20 ($p=0.02$), CXCL10 ($p=0.02$), CD5 ($p=0.024$), MCP-2 ($p=0.032$) and TNFSF 14 ($p=0.047$) were significantly higher in seropositive mothers' milk whey compared to seronegative mothers' (Figure 59, red box).

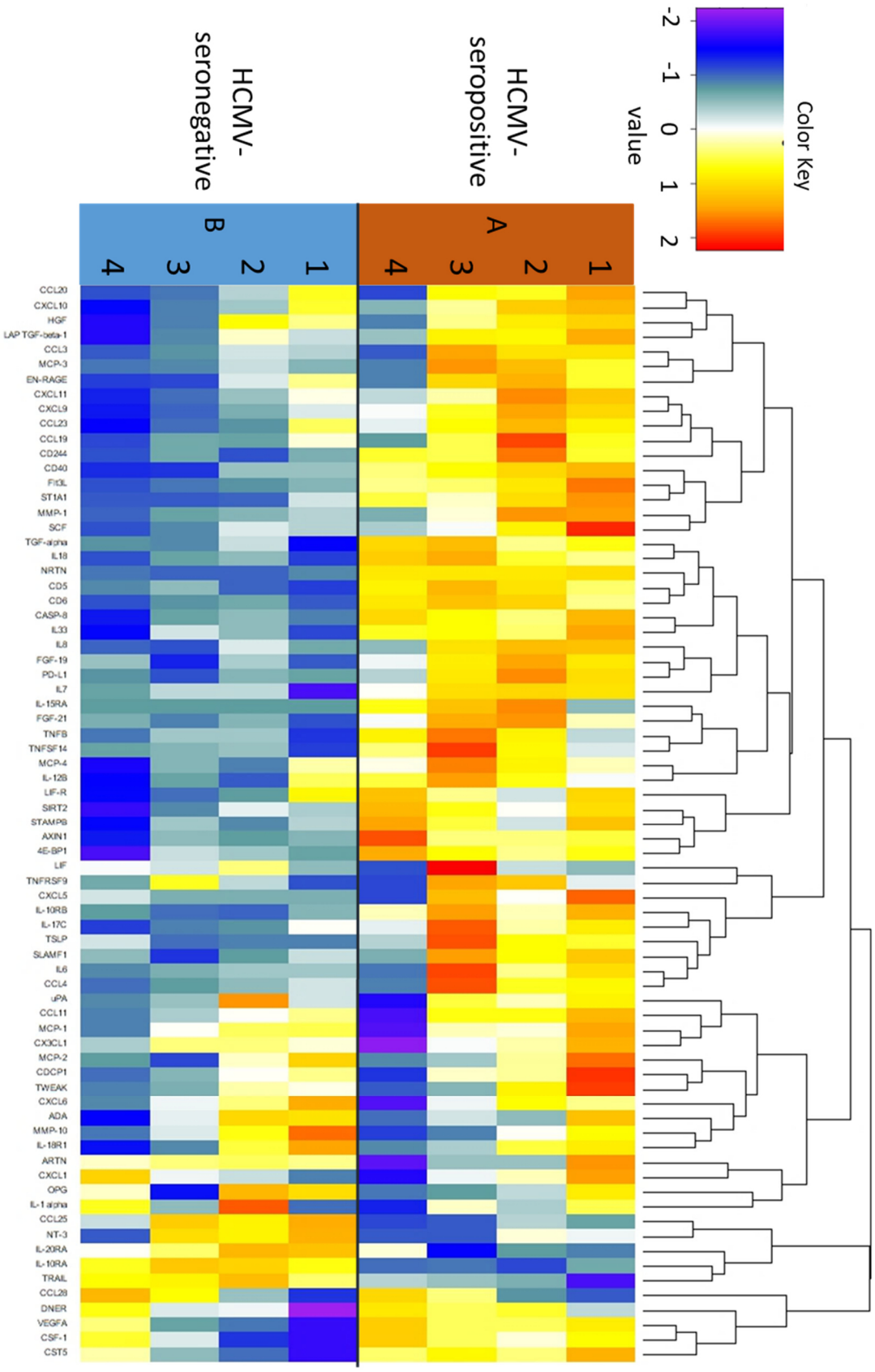

Figure 58: Heat map of 74 cytokines measured in breast milk of mother A and B (modified after [277]).
Cytokines were measured with the proximity extension assay and heat maps generated by Olink. Time ranges are: 1 – 10 to 15, 2 – 25 to 30, 3 – 40 to 45 and 4 – 55 to 60 days p.p. Breast milk whey was used.

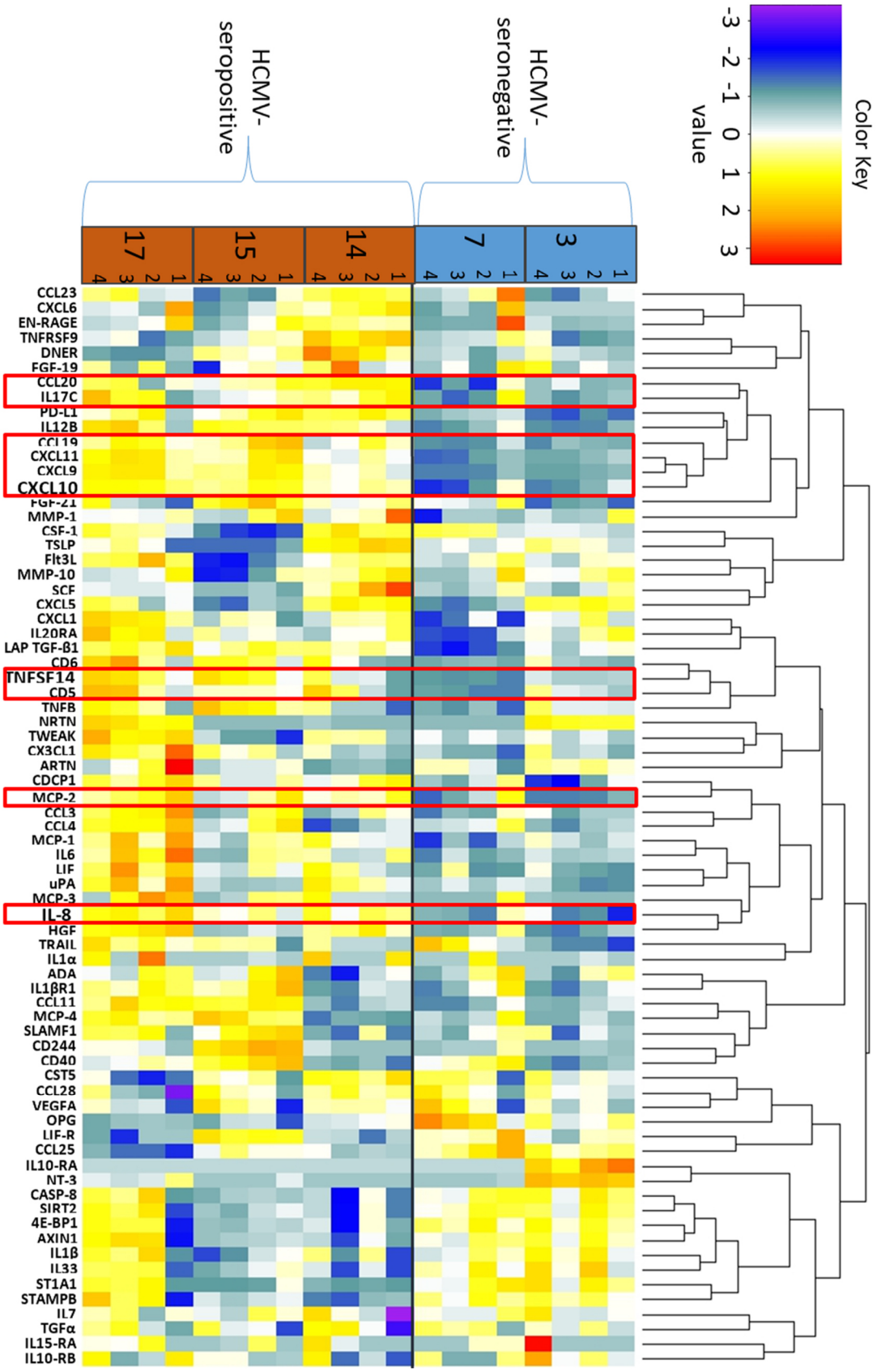

Figure 59: Heat map of 74 cytokines measured in breast milk.
Cytokines were measured with the proximity extension assay of mothers 3, 7, 14, 15 and 17. Heat map was generated by Olink. Time ranges were 1 – 10 to 15, 2 – 25 to 30, 3 – 40 to 45 and 4 – 55 to 60 days p.p. Breast milk whey was used. Cytokines marked in red showed significant differences over the HCMV-serostatus with a linear mixed effect ANOVA (Olink).

The linear mixed model showed significantly differing kinetics between the HCMV-serostatus for IL-12B (p=0.006), TNFSF14 (p=0.02), MCP-4 (p=0.021), CXCL10 (p=0.021), CCL23 (p=0.032), ARTN (p=0.04) and LIF-R (p=0.048). TNFSF14, for example, can bind the herpesvirus entry mediator (HVEM) and can attribute to the proliferation of T cells. TNFSF14 levels are shown in detail in Figure 60. The four seropositive mothers showed an increase over time, while the three seronegative mothers constantly remained at around 3 NPX (normalized protein expression) (Figure 60 A). NPX is a logarithm with base 2. When the antilogarithm was used to display the data of the TNFSF14, mother 17 expressed low levels, close to the level of seronegative mothers' milk whey (Figure 60 B). Mother 17 had only low levels of HCMV DNA in breast milk (peak level of $1.1x10^4$ copies/ml). The other three mothers showed increasing TNFSF14 levels (breast milk peak viral loads: $1.8x10^5$-$2.2x10^6$).

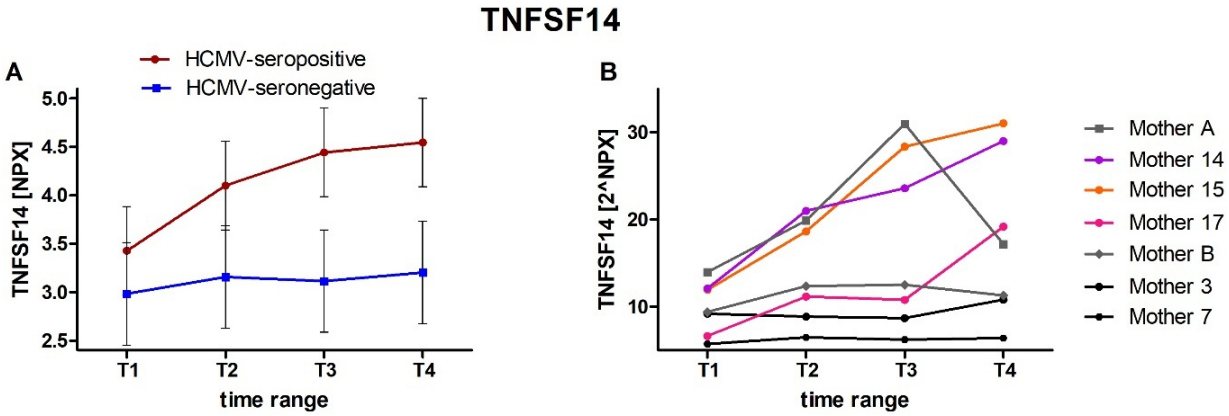

Figure 60: TNFSF14 levels in breast milk of HCMV-seropositive and negative mothers (modified according to [277]). *Mean normalized protein expressions (NPX, base 2 logarithm) of TNFSF14 with 95% confidence interval are shown in (A). The antilogarithm 2^NPX is shown in (B). The time ranges are T1 - 10 to 15, T2 - 25 to 30, T3 - 40 to 45 and T4 - 55 to 60 days p.p.*

Another cytokine, which showed significant differences in the kinetics between serostatus was CXCL10 or also called IP10 (see above, linear mixed model p=0.021). Both, the seropositive and seronegative milk whey levels of CXCL10 decreased over time (Figure 61). However, the decrease of the seropositive mothers' CXCL10 levels was only visible after a slight plateau at T2. All four investigated mothers also had their peak viral load at T2. HCMV-seropositive mothers showed also higher levels than seronegative mothers during the whole observation period (post-hoc test T1's: p=0.71; T2's p=0.014; T3's p=0.013; T4's p=0.0083).

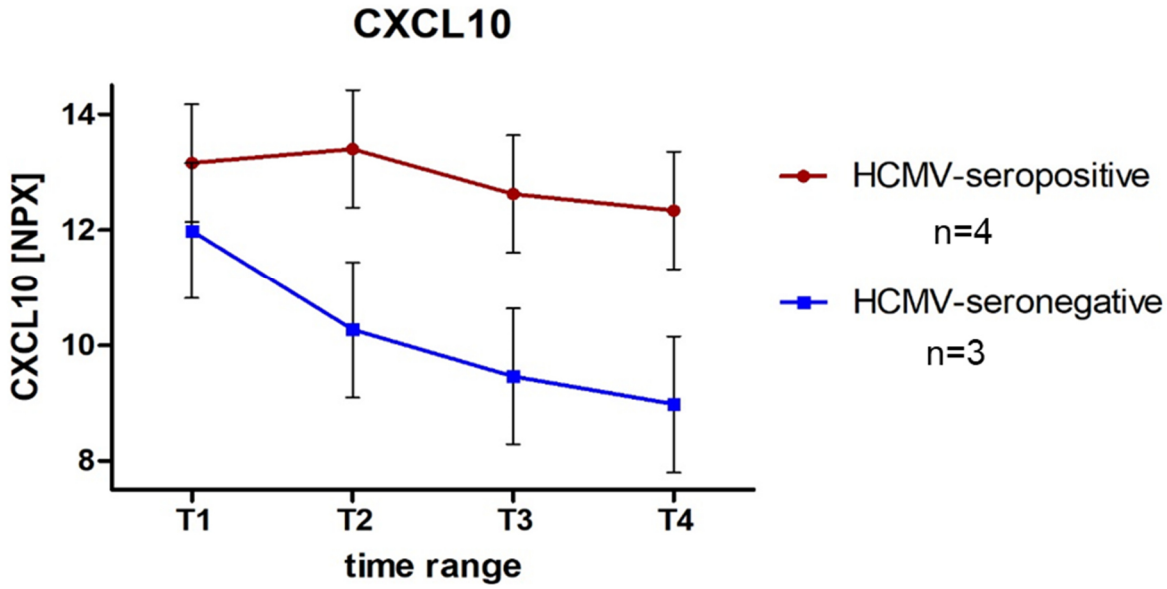

Figure 61: CXCL10 levels in breast milk of HCMV-seropositive and negative mothers(modified after [277]). *Mean normalized protein expressions (NPX, base 2 logarithm) of CXCL10 with 95% confidence interval are shown. The time ranges are T1 - 10 to 15, T2 - 25 to 30, T3 - 40 to 45 and T4 - 55 to 60 days p.p.*

6 Discussion

The local HCMV reactivation process and the influence on the immune signatures in blood and breast milk were monitored over two month's p.p. At first, the viral reactivation pattern in breast milk will be discussed, followed by the observations of humoral immune response and phenotypic immune cell profiling during reactivation. Finally, inflammatory cytokines in breast milk will be discoursed.

6.1 Dynamics of viral reactivation

The analytical performance of different qPCR protocols in context of identical milk fractionation resulting in cell- and fat-free milk whey, as well as an identical DNA extraction method, documented the impact of two target gene regions for viral DNA amplification. The usage of the commercial UL83 qPCR versus the in-house UL55 (gB) PCR protocol [272] showed up to one log step variation, but otherwise concordant longitudinal courses. For standardization, the commercially available UL83 qPCR was used for all other breast milk viral load determinations. A typical longitudinal course of HCMV reactivation in breast milk was observed during lactation in mother A. The calculated onset of viral reactivation was 36 hours after birth. In contrast, mother C had still no HCMV reactivation at 10 days p.p., which was confirmed by nPCR, qPCR and microculture assays of milk whey. However, the calculated onset for this mother was at 11.5 days p.p. During the BlooMil study, 83.3% of the mothers reactivated HCMV before T1 (10-15 days p.p.) and also displayed a mean calculated onset of 11.5 days p.p. [274]. Since the BlooMil study started at day 10 p.p. at the earliest, the viral shedding into colostrum was not monitored. However, mother A's very early onset is not unusual. Other studies were able to detect between 35 and 54% HCMV-positive colostrum samples [278-280].

Only one of the 18 BlooMil study mothers (5.6%) did not reactivate the virus in all four measured time points. This observation was in accordance with previously published reactivation rates of about 96% of all HCMV-seropositive mothers [251].

The start and end point criteria for the BlooMil study provided suitable results of HCMV reactivation courses in breast milk. Most of the mothers had a unimodal course of virolactia and DNAlactia without detection of HCMV DNA in plasma. Closely observed longitudinal cases (mother A and C) showed fluctuations, but the overall course of low viral shedding into breast milk in the beginning, followed by an increase to peak viral load and a decrease afterwards, was still detectable. These findings are in accordance with other groups, which also reported unimodal courses in the first two to three months p.p. [269, 281, 282]. The high differences in peak viral loads of breast milk from BlooMil study mothers (10^4 to 10^6 copies/ml) were also consistent with previous reports [258, 283].

Despite the DNA-positivity in whey, the BMCs were positive on only a few days (mother A: 23, 25 and 27 days p.p., mother C: 20 and 27 days p.p.) The incidence of sporadically positive BMCs was reported before and might coincide with peak viral load [251, 284].
In this thesis, an effort was made to find reasons for this strictly self-limited, unimodal course of HCMV-shedding by analyzing differences in immune signatures between HCMV-seropositive and –negative mothers.

6.2 Humoral immune response

6.2.1 HCMV-IgG

HCMV-seropositive BlooMil study mothers were analyzed for their HCMV-specific IgGs in plasma and milk whey. Using ECLIA as detection method, only 55.6% (ten of 18) of breast milk samples were positive for HCMV-specific IgGs. In addition, three mothers displayed borderline levels. When using recomLine blots against six recombinant antigens (IE1, CM2, p65, p150, gB1, gB2), anti-p150 IgGs were found in breast milk of all mothers at least around cut-off level [274]. The differences in HCMV-IgG detection in milk whey might be due to the sensitivity of the test systems and the different antigens used. ECLIA uses pp28, pp150, p52 and p38 recombinant antigens providing a single read out of quantitative HCMV-IgG (U/ml), while in recomLine blots all antigens are separately detectable and intensities are perceived visually. In contrast, Kassim et al. [285] found only 20% (six of 30) of breast milk samples positive for HCMV IgGs with an in-house ELISA according to Voller and Bidwell [286].
Mother A displayed an increase of total ECLIA HCMV-specific IgGs in breast milk, specifically of anti-CM2 and anti-p150 antibodies determined by recomLine blots, while the total protein concentration showed constant levels. Six of the ten (60%) BlooMil study mothers, who showed positive ECLIA HCMV-IgG results in milk whey, also had a strong increase in their HCMV-IgG concentration after peak viral load. The three borderline samples and the negative samples did not increase over time. Comparable studies, which investigated HCMV-specific IgGs in breast milk, used only one sample during lactation, disregarding dynamic changes over time in the concentration [285, 287]. Milk whey HCMV-IgGs did not correlate with milk viral load. Similar results were reported earlier [287], however, the BlooMil study design allowed to detect a delayed increase after peak viral load in some mothers.
It is noteworthy that plasma HCMV-IgGs significantly increased over time in all seropositive BlooMil study mothers (on average 227 U/ml from T1 to T4, [274]). This result was unexpected, since the reactivation of HCMV is believed to be local in the mammary gland without a systemic infection [250, 253]. The plasma samples of all BlooMil mothers were negative for HCMV DNA and, therefore, viral DNAemia for all mothers could be excluded. Another reason might be found in the transmission of IgG-antibodies from mother to the fetus during pregnancy [231].

Umbilical cord blood had in 75% of cases higher HCMV-IgG concentrations than the maternal serum [288]. Accordingly, the mothers' total IgG-levels, without reflecting the HCMV-specific IgG, were observed to decrease, especially between the second and last trimesters [289-291]. Another reason for low total IgG levels might be the fact that pregnant women were shown to have higher plasma volumes with up to one liter more than non-pregnant women [292]. Thus, the increases of HCMV-IgG found in this thesis might partially reflect a stabilization of IgG levels to pre-pregnancy levels. However, no pre-pregnancy levels were measured in the BlooMil study.

Only plasma anti-p150 IgGs showed very high intensities in all HCMV-seropositive mothers of the BlooMil study. Anti-gB1 IgGs were also present in all mothers, but with varying intensities. Both antibodies were previously reported to be the most frequent IgGs against HCMV [110, 111]. Anti-gB2 IgGs were found in the plasma of 83.3% of seropositive BlooMil mothers, which is similar to the 82% frequency reported in the literature [293, 294].

When comparing plasma and milk whey HCMV-IgGs, 275-fold lower concentrations were found on average in milk whey of BlooMil study mothers using ECLIA results. However, a report from Ehlinger et al. [287] also showed that total IgG concentrations were lower in breast milk than in plasma, but if normalized to the total IgG concentration, breast milk harbors more HCMV-IgGs than plasma.

Anti-p150 IgGs were found in plasma and milk whey of all mothers, but continuously expressed anti-gB1 IgGs were found only in plasma of all mothers [274]. At T1 in milk whey, 13 of 18 mothers had no anti-gB1 IgG and the remaining five displayed intensities around the cut-off level. Since anti-gB IgGs are reported to be neutralizing antibodies [295], a reason for the lower intensities of gB1 IgGs might be the presence of virus in breast milk. The antibodies might have already bound to HCMV and therefore might not be detectable with the immunoblot test system. Interestingly, this pattern of gB1 and gB2 IgG antibodies in breast milk is comparable to the pattern in serum of pregnant women with a primary infection [296].

Very important neutralizing IgGs, which were not analyzed during the BlooMil study, but should be mentioned here, are pentamer-specific IgGs [297]. These antibodies are highly neutralizing, however, this thesis focused on the neutralizing anti-gB IgG antibodies.

The correlation between breast milk and blood HCMV-IgGs was stronger at T1 than at T4, which highlighted the disproportionally high increase of HCMV-IgG in milk whey of some mothers. A study by Ehlinger et al. [287] reported correlations between neutralizing titers of HCMV-IgGs in blood and breast milk and suggested that no compartmentalization occurred. However, the HCMV-IgGs in this thesis revealed a high correlation at T1, but only a moderate correlation at T4 after HCMV reactivation, suggesting some kind of compartmentalization. Interestingly, a compartmentalization was also reported for HIV-specific IgGs in breast milk compared to blood [298].

One reason for low IgGs in milk whey might be that the local plasma cells are mainly excreting IgA and not IgG. Since it's a mucosal site, the stimuli promote class-switching to IgA and the generally low IgG content might contribute to the low overall intensities found in milk. It might be interesting to include the analysis of HCMV-specific IgA content and if it is increasing over time in investigations of the humoral immune response in breast milk in the future.

6.2.2 Neutralization

The breast milk neutralization assays on epithelial cells showed high unspecific neutralization. Breast milk contains many different components, which can contribute to unspecific neutralizing activity. For instance, lactoferrin exhibits antiviral activities by inhibiting HCMV entry into host cells [299, 300] and breast milk oligosaccharides may also play important roles in antiviral effects [223, 301]. These breast milk components and many others, like sIgA, which is the most abundant immunoglobulin in breast milk, may possibly interfere with the neutralizing test system. Therefore, the breast milk samples were pooled, and the unspecific neutralization observed in HCMV-seronegative mothers was subtracted from the seropositive pools. With this defined procedure, only the intrinsic NT-capacity of the seropositive pools was measured. Pools were used to minimize influences of inter-individual variations. Interestingly, higher plaque counts at all T4 breast milk pools suggested a lower unspecific neutralization in mature milk. This might be explained by high concentrations of many proteins in colostrum [182] and a decrease of them into mature milk. T1 with 10 to 15 days p.p. is still close to colostrum.

Plasma pools of seropositive mothers had higher NT-capacities at T4 compared to T1, which probably mirrors the increase seen in plasma HCMV-IgG concentrations. Breast milk NT-50 values (1:100) were 40-fold lower at T4 compared to plasma NT-50 values (1:4,000). Ehlinger et al. [287] also showed higher neutralizing titers in plasma compared to breast milk, although no attention was payed to the unspecific neutralizing activity in breast milk. In contrast, Donalisio et al. [302] reported high unspecific neutralization activity in HCMV-seronegative mothers using the HCMV strain Towne. They even found no differences in anti-HCMV activity of transitional and mature milk between HCMV-seropositive and -seronegative mothers (12 and six mothers, respectively). These results indicate the necessity to use pools and exclude unspecific neutralization. Both mentioned studies performed the neutralization experiments on fibroblasts.

6.2.2.1.1 Breast milk pasteurization

Holder and short-term pasteurizations were performed to analyze the influence on protein precipitation and therefore on neutralizing capacity. Neutralization assays were done with untreated breast milk, Holder and short-term pasteurized breast milk. Holder pasteurization of

milk had high negative effects on the NT-capacity and seemed to destroy p150 antibodies detected by recomLine blots. In contrast, short-term pasteurized milk displayed NT-capacities close to untreated milk and p150 antibodies were still detectable [276]. In addition, Holder pasteurization seemed to destroy unspecific neutralization. Other studies [302, 303] also showed that Holder pasteurization decreased the NT-capacity of breast milk compared to a short-term pasteurization method (72 °C, 15 sec) from Giribaldi et al. [304]. Interestingly, microwaving was also reported as a successful method for eliminating HCMV in breast milk [305]. However, the influence on antibody stability or reactivity was not analyzed.

6.3 Immune cell monitoring

BMCs consist of many different cells, like epithelial cells, stem cells and leukocytes, and are discussed to protect the mammary gland and the infant from infections [239, 246, 306].
In the BlooMil study, the influence of local HCMV reactivation on breast milk leukocytes was investigated and is discussed in the following. B cells were not included in the panel, due to previous work of Thorsten Kussmann, who found very low frequencies of B cells in breast milk.

6.3.1 Cytospin preparations of BMCs

In this thesis, BMCs immobilized on microscope slides showed many inclusion bodies in the panoptic staining. Fat vacuoles were found in different sizes in almost all cells. In 1979, Ho et al. [307] published electron microscopic pictures of BMCs using different staining methods. Other visualized BMCs are not easy to find in literature, since most studies concentrate on flow cytometric analysis.
The α-naphthyl acetate esterase staining's slightly stained epithelial cells and made the differentiation of monocytes/macrophages and epithelial cells difficult. Nucleus to cytoplasm relations, as well as nucleus morphology was considered. The cytospin preparations of BMCs performed in this thesis, exhibited cells, which seemed to have two nuclei. Like Brooker [308] reported in his study, those cells could be ductal or alveolar epithelial cells, which are still connected with tight junctions. This would be not visible at a 600-fold magnification. Flow cytometry was performed for further analysis and distinguishing of cells.

6.3.2 Monocytes/macrophages

BlooMil blood $CD14^+$ monocytes showed average frequencies of 17.2 ± 4.9% in HCMV-seropositive and 17.4 ± 5.1% -seronegative mothers at T4. Slightly lower frequencies with 14.3 ± 3.4% of leukocytes (whole blood, but parental population was set around lymphocytes and monocytes, granulocytes were excluded) were reported in healthy two months p.p. women [309].

In colostrum, Mother D showed very high monocyte frequencies (day 4 p.p., ~67%). However, the frequencies decreased over time. The same was observed in the BlooMil study, where a significant decrease over time of breast milk monocytes was generally detectable. The results confirmed findings of Trend et al. [245] about decreasing amounts of classical monocytes over the lactation period without regard to the HCMV-serostatus.

Interestingly, the decrease of $CD14^+$ monocytes in the BlooMil study mothers was highest in breast milk of HCMV-seropositive mothers. The decrease of HCMV-seronegative mothers was not significant using post-hoc test with corrections. HCMV-seropositive $CD14^+$ monocyte frequencies in breast milk at T3 were very low, even significantly lower than blood monocyte frequencies. This decreasing course in HCMV-seropositive mothers might implicate some changes of breast milk $CD14^+$ monocyte frequencies related to the (latent/locally reactivated) HCMV infection. The mechanism of reactivation in the mammary gland is unknown. However, monocytes are known to be a persistence site of HCMV and the virus can be reactivated, when monocytes are migrating into tissue and differentiating into macrophages [36]. The migration into the mammary gland, the differentiation into macrophages and additional inflammatory cytokines and hormones present in the restructuring mammary gland might contribute to the reactivation process. The reactivation of HCMV could hypothetically then lead to a lytic cycle destroying the macrophages. However, if this lytic cycle led to the low $CD14^+$ frequency at the time point after peak viral load is only theoretical. It is too less known about the local reactivation mechanism in the mammary gland [251]. Nevertheless, Maschmann et al. [284] found monocytes positive for HCMV DNA and p67 mRNA, after enrichment out of BMCs.

Still, breast tissue samples of healthy, non-lactating women were also discovered to be positive for HCMV DNA in 66% of samples (serostatus was unknown) [310], and 63% of women were positive for HCMV antigens in the glandular epithelium [311]. Therefore, the HCMV reactivation process might possibly also originate from low or chronic HCMV expressing epithelium [27] and not from monocytes.

Monocytes/macrophages are professional phagocytes. The observed decrease in $CD14^+$ cell frequency in the BlooMil study could also be due to a migration of monocytes into the mammary gland and later on, after contact with HCMV, a migration from the mammary gland to lymph nodes, finally resulting in lower frequencies in breast milk. However, usually these immune responses are thought to happen faster than the 30 days from T1 to T3 [312].

Another important factor to take into consideration is the dependency on frequencies. Since T cell frequencies increased in the BlooMil study and both populations, monocytes and T cells, are dependent on the same parental population, the decreasing monocytes in this thesis might also reflect an increase of T cells. However, an alteration of these populations is occurring, which is not detectable in HCMV-seronegative mothers' breast milk. Our results indicate the

importance to evaluate absolute cell counts in future experiments to eliminate the dependency of subsets on parental populations.

6.3.2.1 M-MDSC

M-MDSC frequencies are usually very low with increasing frequencies in cancer or chronic diseases [50]. In blood of the BlooMil mothers, the M-MDSC frequency did not change over time and displayed average frequencies around 16 to 18% of all leukocytes. M-MDSC evaluation using the definition of negative to dim HLA-DR expression and CD14 positivity can highly variate between laboratories due to different cut-offs for HLA-DR expression levels [313]. The frequencies in this thesis are higher compared to reported values in literature, due to the gating strategy, which included also great proportions of dim HLA-DR expression on $CD14^+$ monocytes. However, this gating strategy was necessary to ensure a consistent gating due to low cell numbers and very high HLA-DR expression of corresponding BMCs, on which the same gates were copied.

High frequencies of M-MDSCs might also be due to generally higher frequencies in women after birth. Postpartum women were reported to have a slight, but not significant elevation of M-MDSCs in PBMCs three days p.p. [314]. However, others reported a significant increase during pregnancy, but normal levels five to eight weeks after birth [315].

Most of the monocytes in breast milk were HLA-DR positive. Rivas et al. [316] found that the density of HLA-DR expression on breast milk macrophages was higher than on blood monocytes. The high expression of HLA-DR could result in higher interactions with B and T cells and therefore their activations.

Supportive of that, the M-MDSC mean frequencies in breast milk of the BlooMil study mothers' ranged between 1-6% of all leukocytes. It was reported earlier, that granulocytic MDSCs, but not M-MDSCs, are the main MDSC subset in breast milk [317], confirming our low M-MDSC frequencies. Therefore, the low M-MDSC frequency in breast milk compared to blood might also support the findings that immune cells in breast milk usually are active and motile.

6.3.3 T cells

BlooMil study mothers displayed blood $CD3^+$ T cell frequencies on average around 59.7 ± 5.9% in HCMV-seropositive and 59.6 ± 7.1% in -seronegative mothers at T4 and showed no changes over time. These T cell frequencies were similar to published frequencies of healthy postpartum women with 57.5 ± 5.2% in whole blood at two months after birth [309]. The same was described for $CD4^+$ T cell (BlooMil study average between 60 and 64%; McTiernan et al. [309]: 60.2 ± 8.6%) and $CD8^+$ T cell frequencies (BlooMil study average: 29 to 31%; McTiernan et al. [309]: 28.9 ± 5.6%). Additionally, Kraus et al. [318] reported comparable results with

around 60% $CD4^+$ T cells and around 30% $CD8^+$ T cells of leukocytes in peripheral blood of women six weeks p.p.

No differences of blood $CD4^+$ or $CD8^+$ T cell frequencies between the HCMV-serostatus were noticed in the BlooMil study. Similar results were also observed by Wistuba-Hamprecht et al. [319] for young individuals (23-35 years), which is comparable to the age of BlooMil study mothers ($HCMV^+$ 34.0 ± 5.1 years old, HCMV- 32.2 ± 2.7 years old).

In breast milk of Australian women, a constant level of cytotoxic T/NK lymphocytes and non-cytotoxic T cells over colostrum, transient milk and mature milk was observed [245]. Conversely, in the BlooMil study and despite the constant frequencies in blood, breast milk $CD3^+$ T cell frequencies of HCMV-seropositive mothers increased significantly during the first two months of lactation. These differences might reflect two aspects. First, the Australian study group used different markers for detection (CD45, CD2 and CD294 double positive, CD36 negative and CD16 expression was used for cytotoxic T/NK lymphocytes and CD45, CD2 and CD294 double positive, CD16 negative expression for non-cytotoxic T cells) and, second, no attention was directed to the HCMV-serostatus of the mothers [245].

In this thesis, the overall T cell increase in breast milk of HCMV-seropositive mothers is a remarkable finding and might reflect a protection of the mammary gland from infection and in addition a probable protection provided to the newborn infant, as well as an additional help in the development of the immature immune system.

In the mammary gland, the immune cells translocate to breast milk by a paracellular pathway and can in this way reach the suckling newborn. Several studies in animal models reported that immune cells survive and translocate from the infant's gastrointestinal tract to tissue or blood [320-329]. However, in humans, it is unclear if BMCs reach the infant's circulation. Healthy adults were shown to have maternal leukocytes in low frequencies present in their peripheral blood [330], probably acquired during gestation period [331]. However, BMCs might also play a role in microchimerism [332, 333]. Gut permeability rapidly decreases in newborns during the first seven days of life, interestingly coinciding with high numbers of leukocytes and immunoglobulins in colostrum, also expressed in the first week after birth [333]. Breastfed recipients of renal allografts from their mothers had higher chances of tolerating the allograft than non-breastfed individuals (82% versus 57%, respectively) [334].

$CD4^+$ and $CD8^+$ T cells

In the BlooMil study, HCMV-seropositive mothers had significantly lower $CD4^+$ T cell frequencies in breast milk compared to HCMV-seronegative breast milk samples at T4 and additionally also when compared to their corresponding blood samples. Reciprocally, $CD8^+$ T cell frequencies of HCMV-seropositive mothers were higher in breast milk compared to blood. Additionally, $CD8^+$ T cell frequencies in breast milk showed significant elevations in

seropositive compared to negative mothers with regard to the course of their kinetics. Due to this elevation, as well as the overall parental $CD3^+$ T cell increase, $CD8^+$ T cells seem to be an important component in breast milk for the response to HCMV. Many studies showed that $CD8^+$ T cells play a major role in the defense against HCMV [37, 108, 335, 336]. The phenomenon of an increased $CD8^+$ T cell frequency is also known in blood during HCMV primary infections [337]. Therefore, this slightly elevated level of $CD8^+$ T cells in HCMV-seropositive BlooMil study mothers might be the result of the local HCMV reactivation showing a compartmentalization in breast milk versus blood.

Still, although $CD3^+$ T cells increased over time, only a slightly larger increase of $CD8^+$ T cells over $CD4^+$ T cells was noticed in HCMV-seropositive mothers. BlooMil results showed that the mean ratio of $CD4^+/CD8^+$ T cells revealed a tendency towards an increase in HCMV-seronegative mothers possibly indicating that without HCMV reactivations $CD4^+$ T cell frequencies might be very high compared $CD8^+$ T cell frequencies in mature milk. Therefore, the BlooMil constant level (slight decline) in the mean ratio of HCMV-seropositive mothers' breast milk might reflect a stronger increase of $CD8^+$ T cells then our data suggested.

However, two publications from the nineteen nineties reported the frequencies of $CD4^+$ to $CD8^+$ T cells in breast milk were more equal to each other than in blood [242, 243]. But, neither of them included the HCMV-serostatus and both studies mostly used colostrum samples, hence before T1 of the BlooMil study, where the increase in the $CD4^+/CD8^+$ ratio was found about two months p.p.

Another role of breast milk or breast milk lymphocytes might not only be the protection against pathogens, but also the nurturing of the immature immune system of the infant [338]. In mice, milk $CD4^+$ T cells were found in the pubs thymus and proposed to 'educate' $CD8^+$ T cells [339]. In humans, the thymus was found to be larger in exclusively breastfed infants than in formula-fed infants [340].

On the other hand, one main function of the immune cells is probably to protect the mammary gland from infections [239] and the immune cells in breast milk might just be a bystander effect. Overall, during the HCMV reactivation in the mammary gland $CD8^+$ T cells seem to be more abundant than $CD4^+$ T cells. $CD8^+$ T cells might selectively home into the mammary gland to destroy infected tissue. With viral loads up to 10^6 copies/ml in breast milk, the ductal epithelial cells probably are also infected and contribute to the viral dissemination. Therefore, $CD8^+$ T cells might be fundamental to help control the infection.

6.3.3.1 Activation marker (HLA-DR, CD38)

Regarding the CD38 expression in blood, high frequencies in $CD4^+$ and $CD8^+$ T cells were found in BlooMil study mothers. The frequency of CD38 in blood compared to breast milk was difficult to analyze. Naïve T cells express CD38 to some extent [341]. In order to be able to

apply an equal gating to breast milk and blood samples, the gating was set close to the negative population. As a result, naïve T cells were also included in this gating. However, in breast milk, not many naïve T cells are present [342] and this absent population led to generally lower $CD38^+$ frequencies. Due to this issue, only the kinetics were taken into consideration. However, no strong increases or decreases of CD38 expression on breast milk or blood $CD4^+$ or $CD8^+$ T cells were observed over time. This was unexpected. CD38 was shown to especially be expressed during virus infections: In the HIV setting, HIV-specific $CD8^+$ T cells in blood were found to express high levels of CD38 [343, 344]. For HCMV, Wang et al. [345], [346] reported also higher CD38 expression on peripheral blood $CD8^+$ T cells during active HCMV infection. However, in the BlooMil study, which reflects a cohort of latently infected women after birth, only a few mothers showed slight effects of HCMV reactivation on the frequency of CD38 on T cells in breast milk.

Conclusively, CD38 expression seems to have low significance in the comparative evaluation of T cell profiles and their change over time in the early lactation period.

Still, the frequency of CD38 was generally higher on $CD8^+$ T cells than on $CD4^+$ T cells in breast milk (but not in blood). Since CD38 also functions as an adhesion marker and facilitates migration into tissue [347], this might be a reason for the slightly higher $CD8^+$ T cell frequency in breast milk of HCMV-seropositive mothers.

Regarding the activation marker HLA-DR, the frequency was slightly higher in blood of HCMV-seropositive compared to negative mothers, especially on $CD8^+$ T cells. This might be indicating some sort of systemic reaction to the local HCMV reactivation. However, a significantly increased frequency of HLA-DR expression on $CD8^+$ T cells but not $CD4^+$ T cells was also found by Apoil et al. [348] in peripheral blood of healthy HCMV-seropositive blood donors.

In accordance with the BlooMil study results, the expression of the activation marker HLA-DR on $CD8^+$ and $CD4^+$ T cells was reported to be higher in colostrum or breast milk compared to blood [243, 342, 349]. However, the HCMV-serostatus and kinetics in breast milk were not considered in these earlier reports. Interestingly, only seropositive mothers of the BlooMil study revealed a significant increase of HLA-DR expressing $CD4^+$ and $CD8^+$ T cells up to two months after birth. Conclusively, not only the $CD3^+$ T cell frequency increased over time, but also more activated T cells were found in breast milk of HCMV-seropositive mothers. During the reactivation of HCMV in the mammary gland, selective homing of activated T cells into the mammary gland seems to take place.

HLA-DR seems to be a representative marker in our study and superior for analysis of the activation status in comparison to CD38.

The infants of HCMV-seropositive mothers seem to digest more ready-to-act T cells than infants of seronegative mothers. An analysis of the antigen repertoire could confirm if mostly

HCMV-specific or other pathogen-specific T cells home to the mammary gland. If activated T cells in general increase, an interesting investigation would be to see if infants of HCMV-seropositive mothers show different outcomes or frequencies of typical neonatal diseases or if the development of the immune system is influenced in any way.

Most of the immune cells in breast milk, like monocytes, granulocytes, T and B cells, were found to have activated phenotypes [237, 243, 350-352] and might be able to directly act upon pathogen exposure in breast milk, the upper respiratory tract or probably also in the gastrointestinal tract of the infant. Due to protective factors in milk and high stomach pH in newborns, these cells might survive the acidic environment of the stomach, as shown before in animal studies [320-329].

6.3.3.2 Memory phenotypes (using CCR7, CD45RA)

Pregnancy itself, without regard to HCMV-serostatus was reported to change the peripheral blood T cell memory phenotype profile in women: those, who were pregnant before showed significantly elevated $CD4^+$ and $CD8^+$ effector memory T cells compared to women, who have never been pregnant [353]. Additionally, HCMV infections remodel the memory phenotype of especially $CD8^+$ T cells vastly [354-356]. The terminally differentiated $CD45RA^+$ $CCR7^-$ TEMRA cell phenotype was reported to represent between 22 and 76% of all HCMV-specific $CD8^+$ T cells after primary infections [357]. Accordingly, HCMV-seropositive BlooMil study mothers showed significantly higher TEMRA cell-frequencies of blood $CD8^+$ T cells than seronegative mothers. Similar results were reported before in healthy, HCMV-seropositive, HIV negative individuals by Gómez-Mora et al. [358].

A longitudinal study of pregnant women with an additional data point in the early postpartum phase showed highly reduced naïve $CD8^+$ T cells in HCMV-seropositive women throughout the pregnancy and thereafter [359]. Interestingly, in the BlooMil study, naïve T cell frequencies were also lower in seropositive mothers and, additionally, slightly decreased in $CD4^+$ and $CD8^+$ T cells of blood from HCMV-seropositive mothers during the observation period of only two months. This could be related to some kind of systemic reaction to the local HCMV reactivation in the mammary gland. However, it needs to be kept in mind that cell frequencies and not total cell counts were measured. Slight increases of the other three populations result in the decrease of naïve T cells. Usually, a decrease is expected to occur over years and is seen, therefore, especially in the elderly [360], who are susceptible for several subclinical reactivations over the years [361].

BMCs were described to have low to no CCR7 expression on $CD8^+$ T cells [342], and therefore mainly the phenotype of an effector memory population. In this thesis, similar results were found, since effector memory and TEMRA cells were the main subsets of $CD8^+$ T cells. $CD4^+$ T cells mainly were central and effector memory T cells. The differences in the main subsets

of $CD8^+$ and $CD4^+$ T cells is also reflecting a ready to act $CD8^+$ T cell population, while $CD4^+$ T cells main subpopulation, the central memory T cells, need further activation before they are fully functional.

In this thesis, the CCR7 separation was strongly improved using biotin-streptavidin binding, in comparison to our case reports, where the fluorophore coupled antibody directly bound to CCR7. However, the separation of CCR7 was in breast milk still not as efficient as in blood. This might be due to the already reported lower overall expression of CCR7, but probably also due to higher auto-fluorescence in breast milk compared to blood samples. Another reason could be tissue resident memory cells, which are known to express CCR7 in low intensities [362] and might be present in breast milk.

Still, breast milk memory phenotypes did not show the same differences between HCMV-seropositive and -seronegative mothers as observed in blood, concluding a compartmentalization between blood and breast milk and homing of effector memory cells to the mammary gland (measured via breast milk), disregarding the HCMV-serostatus.

6.3.3.3 HCMV-specific $CD8^+$ T cells

pp65 and IE1 are two of the most immunogenic proteins of HCMV with respect to T cell responses [108, 363]. Interestingly, it was reported that IE1 and pp65 specific T cell responses were lower in postpartum women compared to non-pregnant women [364]. Reports on tetramer analysis of HCMV-specific T cells in breast milk are very rare. A study by Sabbaj et al. [342] investigated one HLA-B*07:02 positive mother for pp65 specific T cells and found slightly elevated frequencies in breast milk compared to blood. Their results were proven by an ELISPOT assay showing similar results. In the extended BlooMil study, pp65 or IE1-specific $CD8^+$ T cells in breast milk were found in four mothers. pp65 and IE1-specific T cells were elevated in breast milk compared to blood in some of the BlooMil mothers, especially when HCMV DNA was present in breast milk. This might indicate a local proliferation in the mammary gland of HCMV-specific effector memory T cells.

Taking antibodies and immune cells together, the breastfed infant might gain a protection against HCMV to some degree, which might result in some sort of basic immunity against HCMV.

With intracellular cytokine staining after pp65 antigen stimulation, another study could also show higher frequencies of HCMV-specific $CD8^+$ T cells in breast milk compared to blood [306]. The site of reactivation or infection seems to more often harbor higher or different immune responses, as also seen in lung transplant patients with seroconversions [135, 365].

As for another virus, HIV-1 specific T cells were also reported to be elevated in breast milk compared to blood, although the HIV load itself usually is lower in breast milk than in blood [342, 366, 367].

Less IE1-specific and more pp65-specific $CD8^+$ T cells were discovered in the BlooMil study mothers. Correspondingly, Kern et al. [363] found that HLA-A2 positive individuals had higher reactivities against pp65 than IE1 peptides.
In conclusion, the results of the BlooMil study might implicate an extra lymphoid active HCMV-specific T cell compartmentalization in breast milk versus blood of HCMV-seropositive mothers during lactation, but the number of participating mothers would have to be increased to confirm. Also, functional experiments with a peptide library should be performed so that all potential epitopes of these proteins can be covered. In addition, other HCMV proteins despite pp65 and IE1 could be used to analyze the general frequency of HCMV-specific T cells.

6.3.3.4 γδ T cells

γδ T cells play an important role in the immune response to HCMV [368]. The longitudinal courses of mothers C and D revealed the same γδ T cell frequencies with around 5% in blood as in breast milk. This finding was unexpected, since other reports found higher γδ T cell frequencies in breast milk compared to blood [369-371]. Only Eglinton et al. [242] could not show significant differences between breast milk and blood γδ T cell frequencies.
HCMV-seropositive individuals were found to display higher $V\delta1^+$ γδ T cells in peripheral blood than seronegative [147, 319, 337]. Similar results were found in the HCMV-seropositive mother C, who had in blood higher Vδ1 frequencies than the seronegative mother D, whose main subset of $V\delta2^+$ T cells was around 70% of all γδ T cells. Breast milk of both mothers demonstrated more equivalent frequencies of $V\delta1^+$ and $V\delta\ 2^+$ T cells compared to blood. The seronegative mother revealed even more Vδ1 γδ T cells in breast milk than the seropositive mother. An elevated frequency of Vδ1 in the γδ T cells of breast milk was found before, without regard to HCMV [369]. This suggested selective homing of γδ T cell subsets into the mammary gland and might implicate more adaptive than innate features of γδ T cells in breast milk. However, analysis of the clonal repertoire in breast milk could give more information about the distribution of innate-like and adaptive-like clones in the future.

6.3.4 NK cells ($CD56^+$)

Maternal NK cell cytotoxicity was reported to be suppressed from after birth to up to six months p.p. [372, 373]. NK cells might, therefore, have a minor role in the ‘fight’ against HCMV reactivation processes in the mammary gland. The BlooMil mothers displayed significantly lower frequencies in breast milk compared to blood. The expected increase of NK cells in HCMV-seropositive mothers due to the significance of NK cells in the elucidation of HCMV infections [374] was not observed in the BlooMil study.
$CD94/NKG2C^+$ NK cells were detected to expand, when interacting with HCMV infected fibroblasts [101]. Whether or not a higher frequency of these cells within the NK cell subset

was occurring in this thesis is unclear, since only the expression of CD56 was used to detect NK cells. Further experiments, including the markers mentioned above, could show if those subsets increase and an HCMV-specific immune response is taking place.
The low NK cell frequency with mean frequencies of 5% of lymphocytes in breast milk might also show that NK cells are not selectively homed to the mammary gland. Regarding the evolution of the mammary gland, it is hypothesized that the immunologic, protective functions were present prior to the nutritive aspects of breast milk [239, 375-377]. Considering this, one aspect of low NK cell frequencies in breast milk might be that the infant has no direct advantages of NK cells, whose cytotoxicity is suppressed after birth in the mother (see above).

6.4 Cytokine analysis of milk whey

In this thesis, the first steps were performed for a longitudinal cytokine analysis in breast milk. Seven mothers, four HCMV-seropositive and three seronegative, were investigated for 92 inflammatory cytokines [277]. Several CC- and CXC-chemokines, such as CXCL10 were increased in breast milk of HCMV-seropositive mothers. These chemokines are known to recruit leukocytes to the site of inflammation and promote a Th1-related T cell response [378-382]. This would be coincident with the weak antibody response in most mothers of the BlooMil study (for example B cells are promoted in Th2 responses [383]) and with the increased T cell frequency in breast milk of seropositive mothers. HCMV is generally known to promote more of a Th1 response [384].
The significantly increased levels of CXCL10 in breast milk of HCMV-seropositive BlooMil study mothers might contribute to the migration of T cells into the mammary gland. CXCL10 was also reported to be elevated in plasma of lung transplant recipients with detectable HCMV DNAemia [385].
TNFSF14 levels were also significantly elevated over time in HCMV-seropositive mothers of the BlooMil study. TNFSF14 binds the herpesvirus entry mediator (HVEM) and acts as a co-stimulating ligand for T cell activation [386]. HVEM can also bind the B and T lymphocyte attenuator (BTLA), which sends T cells inhibitory signals [387, 388]. Interestingly, one of many immune evasion strategies of HCMV is targeting this pathway [389]. HCMV expresses UL144, an orthologue of HVEM, which selectively binds BTLA and therefore, can inhibit T cell activation [390, 391]. This interaction might occur less often if higher TNFSF14 levels are present, as in the breast milk of HCMV-seropositive mothers. Accordingly, more T cells were found to express activation markers in seropositive mothers than in seronegative mothers' breast milk.
The inflammatory milieu might also contribute to HCMV reactivation in the first place [35, 392], since also BlooMil HCMV-seronegative mothers showed elevated levels of inflammatory cytokines in the first time range after birth. Future experiments not only including cytokines but

also hormones could contribute on the influence of the micro environment to HCMV reactivation.

6.5 Limitations

The study cohorts in this thesis are small. Preterm births occur only in 8.7% of cases in Europe [393]. Therefore, the acquisition of participating mothers in the Neonatology Department was difficult. Another criterion was that the mother had to express enough breast milk for the infant and the study; otherwise they were not fulfilling study criteria. Since mothers of preterm infants have problems with initiation of breast milk production and mostly express low volumes, the BlooMil study cohort is small. Furthermore, for longitudinal analysis all mothers had to be available for at least two months after birth.

Statistical analysis was performed for the cohorts of 18 HCMV-seropositive mothers and ten seronegative mothers. The cohort of ten mothers is relatively small, especially because of very heterogeneous immune profiles in both groups, and the relevance of statistical tests must be considered. The inter-individual variance was higher in breast milk compared to blood. Therefore, the scattering of single time points is influencing significances.

In addition, the high inter-individual variability in breast milk influenced by fullness of breast, the diurnal pattern and many other factors [394-396] make a general analysis of breast milk components challenging. However, breast milk samples of the BlooMil study were always taken in the mornings to counteract circadial fluctuations.

Transmission events would give interesting insights on how cellular or humoral immune responses to HCMV in breast milk would protect the infant from HCMV infection. However, breast milk fed to preterm infants at the Neonatology Department is inactivated by short-term heat inactivation to prevent emergence of symptomatic HCMV infections, which might be able to harm the preterm infants seriously [397].

Another aspect of the cellular analysis that needs to be discussed was the different protocols for BMC and PBMC isolations. Frequencies of breast milk leukocytes contain, for instance, granulocytes, while blood granulocytes mostly are lost in the Ficoll-gradient. However, to analyze the breast milk cell content, all cells play an important role. Only around 2% were leukocytes. The small number of cells might have been lost during a gradient centrifugation. Additionally, a biological control of frozen PBMCs was used to assure the consistency of the experiments. Therefore, PBMCs needed to be purified in a Ficoll-gradient.

Additionally, another restriction of this study was that the cellular analysis showed only frequencies and not total cell counts. Therefore, the frequencies depend on other populations such as the granulocyte numbers in breast milk, which are highly variable in the BMCs. Absolute cell counts could show actual increases or decreases of a population, however, the frequencies can relative proportions of a distinct marker.

Breast milk consists of many important nutritive and immunological important components for the infant. The observed differences in HCMV-seropositive compared to negative mothers' breast milk might be due to the protection of the mammary gland itself or for the protection of the suckling infant. Defined breast biopsies of secretory lobule or alveoli including epithelial cell layers and lactocytes during lactation are extremely rare, but- if ethically allowed- could help in the future to further study the mammary gland and its immune system. However, breast milk represents an ideal non-invasive material for longitudinal study of leukocyte changes during HCMV reactivation in immune competent individuals and can also be used to monitor the immune profile changes due to HCMV in the mammary gland to some extent.

6.6 Conclusions

The local reactivation of HCMV in breast milk was documented nearly in all (17 of 18) mothers of mostly preterm infants of the BlooMil study. The unimodal course with highly varying peak viral loads induces the question how the immune system controls HCMV shedding into breast milk.

In this thesis, a modulation of the immune signatures in probable relation to HCMV reactivation in the mammary gland was documented, identified indirectly by analysis of breast milk. A compartmentalization of monocytes, T cells and their subsets as well as viral load and HCMV-specific IgGs were observed in breast milk versus blood in HCMV-seropositive mothers.

Interestingly, defined breast milk HCMV-IgG antibodies, such as potential neutralizing antibodies like anti-gB-IgG, are not existent in a relevant amount in breast milk of most mothers. Only anti-p150 IgGs were found by immunoblot analysis in all milk whey samples. Therefore, this study gave first evidence that HCMV-specific antibodies might only play a minor role in the decrease of viral load during the late phase of local reactivation.

Still, if a gentle inactivation method using short-term heat inactivation (5 sec, 62°C) based on milk film generation was used, the few antibodies present in breast milk were not destroyed and were still capable of binding their antigen, while traditional Holder pasteurization (30 min, 62.5) destroyed the binding capacity of the antibodies and induced a lack of neutralization capacity. This observation has strong clinical relevance in context of the breastfeeding management of preterm infants.

The detected proinflammatory cytokine shift of mostly IFNγ in HCMV-seropositive mothers' breast milk seemed to support a Th1-related T cell response and not Th2 (B cells, antibodies). Conclusively, $CD3^+$ T cell frequencies showed a strong increase in breast milk of HCMV-seropositive mothers. This seemed to not only originate from local proliferation in the mammary gland, although breast milk HCMV-specific $CD8^+$ T cells were slightly elevated compared to blood. Another reason might be induction of migration of T cells into the mammary gland. This would be consistent with the elevated cytokine levels in HCMV-seropositive mothers' breast

milk. Most were chemokines, such as CXCL10, which can attract leukocytes into the mammary gland. Some are also responsible to give activating signals to T cells. Conclusively, in the BlooMil study, the activation marker HLA-DR was expressed significantly higher at later time ranges in breast milk of HCMV-seropositive mothers on $CD4^+$ and $CD8^+$ T cells. These findings in breast milk suggest that especially HCMV-specific $CD8^+$ T cells might help destroy infected monocytes/macrophages or epithelial cells in the mammary gland, whereas IgG antibodies might only play a minor role in the resulting decrease of HCMV loads in breast milk at the late stage of the reactivation kinetics after peak viral load.

No significant changes were found for NK cells or $CD56^+$ T cells in breast milk.

Nevertheless, some humoral systemic reaction to the local HCMV reactivation might take place, since HCMV-IgG antibodies increased in plasma and the memory compartment in blood was modulated slightly.

The influence on the protection of the nursing infant from HCMV infection or other infections in general, as well as the effect on the developing immune system of the infant is unclear. The mechanism of HCMV reactivation in the mammary gland is also not fully understood.

Both might be an important issue to address in the future, since elevated levels of BMCs, antibodies or cytokines, as well as high HCMV viral loads might affect the infant's developing immune system.

In conclusion, the findings of these investigations contribute to a better understanding of the complex relationship between humoral immune signatures and T cell mediated immune responses to HCMV during lactation.

References

1. Roizmann B, Desrosiers RC, Fleckenstein B, Lopez C, Minson A, Studdert M. 1992. The family Herpesviridae: an update. Arch Virol 123:425-449.
2. Ribbert H. 1904. Uber protozoenartige Zellen in der Niere eines syphilitischen Neugeborenen und in der Parotis von Kindern. Zbl Allg Pathol 15:945-948.
3. Ho M. 2008. The history of cytomegalovirus and its diseases. Med Microbiol Immunol 197:65-73.
4. Wyatt JP, Saxton J, Lee R, Pinkerton H. 1950. Generalized cytomegalic inclusion disease. Journal of Pediatrics 36:271-94.
5. Smith MG. 1956. Propagation in tissue cultures of a cytopathogenic virus from human salivary gland virus (SGV) disease. Proc Soc Exp Biol Med 92:424-430.
6. Rowe W. Hartley, J. w. et al.: cytopathogenic agent resernbling human salivary gland virus recovered from tissue cultures of human adenoids, p 418-424. *In* (ed),
7. Weller TH, Macauley J, Craig J, Wirth P. 1957. Isolation of intranuclear inclusion producing agents from infants with illnesses resembling cytomegalic inclusion disease. Proc Soc Exp Biol Med 94:4-12.
8. Weller TH, Hanshaw JB, Scott D. 1960. Serologie Differentiation of Viruses responsible for Cytomegalic Inclusion Disease. J Virology 12:130-32.
9. Reddehase MJ. 2013. Cytomegaloviruses: From Molecular Pathogenesis to Intervention (Two Volume Box Set). Caister Academic Press.
10. Dolan A, Cunningham C, Hector RD, Hassan-Walker AF, Lee L, Addison C, Dargan DJ, McGeoch DJ, Gatherer D, Emery VC. 2004. Genetic content of wild-type human cytomegalovirus. J Gen Virol 85:1301-1312.
11. Gandhi MK, Khanna R. 2004. Human cytomegalovirus: clinical aspects, immune regulation, and emerging treatments. The Lancet infectious diseases 4:725-738.
12. Tomtishen III JP. 2012. Human cytomegalovirus tegument proteins (pp65, pp71, pp150, pp28). Virology journal 9:22.
13. Kalejta RF. 2008. Tegument proteins of human cytomegalovirus. Microbiol Mol Biol Rev 72:249-265.
14. Nguyen CC, Kamil JP. 2018. Pathogen at the gates: human cytomegalovirus entry and cell tropism. Viruses 10:704.
15. Wille PT, Wisner TW, Ryckman B, Johnson DC. 2013. Human cytomegalovirus (HCMV) glycoprotein gB promotes virus entry in trans acting as the viral fusion protein rather than as a receptor-binding protein. MBio 4:e00332-13.
16. Ryckman BJ, Chase MC, Johnson DC. 2008. HCMV gH/gL/UL128–131 interferes with virus entry into epithelial cells: evidence for cell type-specific receptors. Proceedings of the National Academy of Sciences 105:14118-14123.
17. Kalejta R. 2008. Functions of human cytomegalovirus tegument proteins prior to immediate early gene expression, p 101-115, Human cytomegalovirus. Springer.
18. Gibson W. 2008. Structure and formation of the cytomegalovirus virion, p 187-204, Human cytomegalovirus. Springer.
19. Honess RW, Roizman B. 1974. Regulation of herpesvirus macromolecular synthesis I. Cascade regulation of the synthesis of three groups of viral proteins. J Virol 14:8-19.
20. Jean Beltran PM, Cristea IM. 2014. The life cycle and pathogenesis of human cytomegalovirus infection: lessons from proteomics. Expert review of proteomics 11:697-711.
21. Sinclair J. 2010. Chromatin structure regulates human cytomegalovirus gene expression during latency, reactivation and lytic infection. Biochimica et Biophysica Acta (BBA)-Gene Regulatory Mechanisms 1799:286-295.
22. Taylor-Wiedeman J, Sissons JP, Borysiewicz LK, Sinclair J. 1991. Monocytes are a major site of persistence of human cytomegalovirus in peripheral blood mononuclear cells. J Gen Virol 72:2059-2064.
23. Hahn G, Jores R, Mocarski ES. 1998. Cytomegalovirus remains latent in a common precursor of dendritic and myeloid cells. Proceedings of the National Academy of Sciences 95:3937-3942.
24. Mendelson M, Monard S, Sissons P, Sinclair J. 1996. Detection of endogenous human cytomegalovirus in CD34+ bone marrow progenitors. J Gen Virol 77:3099-3102.
25. Kondo K, Xu J, Mocarski ES. 1996. Human cytomegalovirus latent gene expression in granulocyte-macrophage progenitors in culture and in seropositive individuals. Proceedings of the National Academy of Sciences 93:11137-11142.

26. Sinzger C, Digel M, Jahn G. 2008. Cytomegalovirus cell tropism, p 63-83, Human cytomegalovirus. Springer.
27. Goodrum F. 2016. Human cytomegalovirus latency: approaching the Gordian knot. Annual review of virology 3:333-357.
28. Goodrum F, Caviness K, Zagallo P. 2012. Human cytomegalovirus persistence. Cell Microbiol 14:644-655.
29. Reeves M, MacAry P, Lehner P, Sissons J, Sinclair J. 2005. Latency, chromatin remodeling, and reactivation of human cytomegalovirus in the dendritic cells of healthy carriers. Proceedings of the National Academy of Sciences 102:4140-4145.
30. Murphy JC, Fischle W, Verdin E, Sinclair JH. 2002. Control of cytomegalovirus lytic gene expression by histone acetylation. The EMBO journal 21:1112-1120.
31. Saffert RT, Kalejta RF. 2006. Inactivating a cellular intrinsic immune defense mediated by Daxx is the mechanism through which the human cytomegalovirus pp71 protein stimulates viral immediate-early gene expression. J Virol 80:3863-3871.
32. Wright E, Bain M, Teague L, Murphy J, Sinclair J. 2005. Ets-2 repressor factor recruits histone deacetylase to silence human cytomegalovirus immediate-early gene expression in non-permissive cells. J Gen Virol 86:535-544.
33. Reeves MB, Sinclair JH. 2013. Circulating dendritic cells isolated from healthy seropositive donors are sites of human cytomegalovirus reactivation in vivo. J Virol 87:10660-10667.
34. Poole E, Juss JK, Krishna B, Herre J, Chilvers ER, Sinclair J. 2015. Alveolar macrophages isolated directly from human cytomegalovirus (HCMV)–seropositive individuals are sites of HCMV reactivation in vivo. The Journal of infectious diseases 211:1936-1942.
35. Reeves MB, Compton T. 2011. Inhibition of inflammatory interleukin-6 activity via extracellular signal-regulated kinase–mitogen-activated protein kinase signaling antagonizes human cytomegalovirus reactivation from dendritic cells. J Virol 85:12750-12758.
36. Reeves MB. 2020. Cell signaling and cytomegalovirus reactivation: what do Src family kinases have to do with it? Biochem Soc Trans.
37. Manandhar T, Hò G-GT, Pump WC, Blasczyk R, Bade-Doeding C. 2019. Battle between Host Immune Cellular Responses and HCMV Immune Evasion. International journal of molecular sciences 20:3626.
38. Zuhair M, Smit GSA, Wallis G, Jabbar F, Smith C, Devleesschauwer B, Griffiths P. 2019. Estimation of the worldwide seroprevalence of cytomegalovirus: A systematic review and meta-analysis. Rev Med Virol 29:e2034.
39. Lachmann R, Loenenbach A, Waterboer T, Brenner N, Pawlita M, Michel A, Thamm M, Poethko-Müller C, Wichmann O, Wiese-Posselt M. 2018. Cytomegalovirus (CMV) seroprevalence in the adult population of Germany. PLoS One 13.
40. Eggert-Kruse W, Reuland M, Johannsen W, Strowitzki T, Schlehofer JR, sterility. 2009. Cytomegalovirus (CMV) infection—related to male and/or female infertility factors? Fertility 91:67-82.
41. Ljungman P, Boeckh M, Hirsch HH, Josephson F, Lundgren J, Nichols G, Pikis A, Razonable RR, Miller V, Griffiths PD. 2016. Definitions of cytomegalovirus infection and disease in transplant patients for use in clinical trials. Clin Infect Dis:ciw668.
42. Enders G, Daiminger A, Bäder U, Exler S, Enders M. 2011. Intrauterine transmission and clinical outcome of 248 pregnancies with primary cytomegalovirus infection in relation to gestational age. J Clin Virol 52:244-246.
43. Hamprecht K, Jahn G. 2007. Humanes Cytomegalovirus und kongenitale Infektion. Bundesgesundheitsblatt-Gesundheitsforschung-Gesundheitsschutz 50:1379-1392.
44. Kenneson A, Cannon MJ. 2007. Review and meta-analysis of the epidemiology of congenital cytomegalovirus (CMV) infection. Rev Med Virol 17:253-276.
45. Kagan KO, Hamprecht K. 2017. Cytomegalovirus infection in pregnancy. Archives of gynecology and obstetrics 296:15-26.
46. Kotton C. 2013. CMV: prevention, diagnosis and therapy. Am J Transplantation 13:24-40.
47. Arango Duque G, Descoteaux A. 2014. Macrophage cytokines: involvement in immunity and infectious diseases. Frontiers in immunology 5:491.
48. Zhang J-M, An J. 2007. Cytokines, inflammation and pain. International anesthesiology clinics 45:27.
49. Laing KJ, Secombes CJ. 2004. Chemokines. Dev Comp Immunol 28:443-460.
50. Veglia F, Perego M, Gabrilovich D. 2018. Myeloid-derived suppressor cells coming of age. Nat Immunol 19:108-119.
51. Raber PL, Thevenot P, Sierra R, Wyczechowska D, Halle D, Ramirez ME, Ochoa AC, Fletcher M, Velasco C, Wilk A. 2014. Subpopulations of myeloid-derived suppressor cells

impair T cell responses through independent nitric oxide-related pathways. Int J Cancer 134:2853-2864.
52. Umansky V, Blattner C, Gebhardt C, Utikal J. 2016. The role of myeloid-derived suppressor cells (MDSC) in cancer progression. Vaccines 4:36.
53. Jost S, Altfeld M. 2013. Control of human viral infections by natural killer cells. Annu Rev Immunol 31:163-194.
54. Vivier E, Raulet DH, Moretta A, Caligiuri MA, Zitvogel L, Lanier LL, Yokoyama WM, Ugolini S. 2011. Innate or adaptive immunity? The example of natural killer cells. Science 331:44-49.
55. Terabe M, Berzofsky JA. 2008. The role of NKT cells in tumor immunity. Adv Cancer Res 101:277-348.
56. Robertson FC, Berzofsky JA, Terabe M. 2014. NKT cell networks in the regulation of tumor immunity. Frontiers in immunology 5:543.
57. Kumar V, Delovitch TL. 2014. Different subsets of natural killer T cells may vary in their roles in health and disease. Immunology 142:321-336.
58. Bennstein SB. 2018. Unraveling natural killer T-cells development. Frontiers in Immunology 8:1950.
59. Murphy K, Weaver C. 2016. Janeway's immunobiology. Garland science.
60. Hoffman W, Lakkis FG, Chalasani G. 2016. B cells, antibodies, and more. Clinical Journal of the American Society of Nephrology 11:137-154.
61. Schroeder Jr HW, Cavacini L. 2010. Structure and function of immunoglobulins. J Allergy Clin Immunol 125:S41-S52.
62. Parker ME, Ciofani M. 2020. Regulation of γδ T Cell Effector Diversification in the Thymus. Frontiers in Immunology 11.
63. Cresswell P, Ackerman AL, Giodini A, Peaper DR, Wearsch PA. 2005. Mechanisms of MHC class I-restricted antigen processing and cross-presentation. Immunol Rev 207:145-157.
64. Hayday AC. 2019. γδ T Cell Update: Adaptate Orchestrators of Immune Surveillance. The Journal of Immunology 203:311-320.
65. Ravens S, Schultze-Florey C, Raha S, Sandrock I, Drenker M, Oberdörfer L, Reinhardt A, Ravens I, Beck M, Geffers R. 2017. Human γδ T cells are quickly reconstituted after stem-cell transplantation and show adaptive clonal expansion in response to viral infection. Nat Immunol 18:393.
66. Willcox CR, Davey MS, Willcox BE. 2018. Development and selection of the human Vγ9Vδ2+ T-cell repertoire. Frontiers in immunology 9:1501.
67. Davey MS, Willcox CR, Hunter S, Kasatskaya SA, Remmerswaal EB, Salim M, Mohammed F, Bemelman FJ, Chudakov DM, Oo YH. 2018. The human Vδ2+ T-cell compartment comprises distinct innate-like Vγ9+ and adaptive Vγ9-subsets. Nature communications 9:1-14.
68. Fichtner AS, Bubke A, Rampoldi F, Wilharm A, Tan L, Steinbrück L, Schultze-Florey C, Von Kaisenberg C, Prinz I, Herrmann T. 2020. TCR repertoire analysis reveals phosphoantigen-induced polyclonal proliferation of Vγ9Vδ2 T cells in neonates and adults. J Leukocyte Biol.
69. Rigau M, Ostrouska S, Fulford TS, Johnson DN, Woods K, Ruan Z, McWilliam HE, Hudson C, Tutuka C, Wheatley AK. 2020. Butyrophilin 2A1 is essential for phosphoantigen reactivity by γδ T cells. Science 367.
70. Wistuba-Hamprecht K, Frasca D, Blomberg B, Pawelec G, Derhovanessian E. 2013. Age-associated alterations in γδ T-cells are present predominantly in individuals infected with Cytomegalovirus. Immunity & Ageing 10:26.
71. Chien Y-h, Meyer C, Bonneville M. 2014. γδ T cells: first line of defense and beyond. Annu Rev Immunol 32:121-155.
72. Silva-Santos B, Strid J. 2017. γδ T cells get adaptive. Nat Immunol 18:370-372.
73. Fichtner AS, Ravens S, Prinz I. 2020. Human γδ TCR Repertoires in Health and Disease. Cells 9:800.
74. Luckheeram RV, Zhou R, Verma AD, Xia B. 2012. CD4+ T cells: differentiation and functions. Clin Dev Immunol 2012.
75. Chavez-Galan L, Arenas-Del Angel M, Zenteno E, Chavez R, Lascurain R. 2009. Cell death mechanisms induced by cytotoxic lymphocytes. Cellular & molecular immunology 6:15-25.
76. Reddy M, Eirikis E, Davis C, Davis HM, Prabhakar U. 2004. Comparative analysis of lymphocyte activation marker expression and cytokine secretion profile in stimulated human peripheral blood mononuclear cell cultures: an in vitro model to monitor cellular immune function. J Immunol Methods 293:127-142.
77. Caruso A, Licenziati S, Corulli M, Canaris AD, De Francesco MA, Fiorentini S, Peroni L, Fallacara F, Dima F, Balsari A. 1997. Flow cytometric analysis of activation markers on

stimulated T cells and their correlation with cell proliferation. Cytometry: The Journal of the International Society for Analytical Cytology 27:71-76.
78. Quarona V, Zaccarello G, Chillemi A, Brunetti E, Singh VK, Ferrero E, Funaro A, Horenstein AL, Malavasi F. 2013. CD38 and CD157: a long journey from activation markers to multifunctional molecules. Cytometry Part B: Clinical Cytometry 84:207-217.
79. Youngblood B, Hale JS, Ahmed R. 2013. T-cell memory differentiation: insights from transcriptional signatures and epigenetics. Immunology 139:277-284.
80. Opferman JT, Ober BT, Ashton-Rickardt PG. 1999. Linear differentiation of cytotoxic effectors into memory T lymphocytes. Science 283:1745-1748.
81. Henning AN, Roychoudhuri R, Restifo NP. 2018. Epigenetic control of CD8+ T cell differentiation. Nature Reviews Immunology 18:340.
82. Restifo NP, Gattinoni L. 2013. Lineage relationship of effector and memory T cells. Curr Opin Immunol 25:556-563.
83. Sallusto F, Geginat J, Lanzavecchia A. 2004. Central memory and effector memory T cell subsets: function, generation, and maintenance. Annu Rev Immunol 22:745-763.
84. Saule P, Trauet J, Dutriez V, Lekeux V, Dessaint J-P, Labalette M. 2006. Accumulation of memory T cells from childhood to old age: central and effector memory cells in CD4+ versus effector memory and terminally differentiated memory cells in CD8+ compartment. Mechanisms of ageing and development 127:274-281.
85. Larbi A, Fulop T. 2014. From “truly naïve” to “exhausted senescent” T cells: when markers predict functionality. Cytometry Part A 85:25-35.
86. Kumar BV, Connors TJ, Farber DL. 2018. Human T cell development, localization, and function throughout life. Immunity 48:202-213.
87. Förster R, Davalos-Misslitz AC, Rot A. 2008. CCR7 and its ligands: balancing immunity and tolerance. Nature Reviews Immunology 8:362-371.
88. Hermiston ML, Xu Z, Weiss A. 2003. CD45: a critical regulator of signaling thresholds in immune cells. Annu Rev Immunol 21:107-137.
89. Jackson SE, Mason GM, Wills MR. 2011. Human cytomegalovirus immunity and immune evasion. Virus Res 157:151-160.
90. Juckem LK, Boehme KW, Feire AL, Compton T. 2008. Differential initiation of innate immune responses induced by human cytomegalovirus entry into fibroblast cells. The Journal of Immunology 180:4965-4977.
91. Boehme KW, Guerrero M, Compton T. 2006. Human cytomegalovirus envelope glycoproteins B and H are necessary for TLR2 activation in permissive cells. The Journal of Immunology 177:7094-7102.
92. Compton T, Kurt-Jones EA, Boehme KW, Belko J, Latz E, Golenbock DT, Finberg RW. 2003. Human cytomegalovirus activates inflammatory cytokine responses via CD14 and Toll-like receptor 2. J Virol 77:4588-4596.
93. Wills MR, Ashiru O, Reeves MB, Okecha G, Trowsdale J, Tomasec P, Wilkinson GW, Sinclair J, Sissons JP. 2005. Human cytomegalovirus encodes an MHC class I-like molecule (UL142) that functions to inhibit NK cell lysis. The Journal of Immunology 175:7457-7465.
94. Venema H, Van Den Berg AP, Van Zanten C, Van Son WJ, Van Der Giessen M, Hauw T. 1994. Natural killer cell responses in renal transplant patients with cytomegalovirus infection. J Med Virol 42:188-192.
95. Lopez-Vergès S, Milush JM, Schwartz BS, Pando MJ, Jarjoura J, York VA, Houchins JP, Miller S, Kang S-M, Norris PJ. 2011. Expansion of a unique CD57+ NKG2Chi natural killer cell subset during acute human cytomegalovirus infection. Proceedings of the National Academy of Sciences 108:14725-14732.
96. Huard B, Früh K. 2000. A role for MHC class I down-regulation in NK cell lysis of herpes virus-infected cells. Eur J Immunol 30:509-515.
97. Hamprecht K, Steinmassl M. 1994. Low-dose human cytomegalovirus infection of human fibroblast cultures induces lymphokine-activated killer cell resistance: interferon-beta-mediated target cell protection does not correlate with up-regulation of HLA class I surface molecules. Immunology 82:171.
98. Biron CA, Byron KS, Sullivan JL. 1989. Severe herpesvirus infections in an adolescent without natural killer cells. New Engl J Med 320:1731-1735.
99. Wilkinson GW, Tomasec P, Stanton RJ, Armstrong M, Prod’homme V, Aicheler R, McSharry BP, Rickards CR, Cochrane D, Llewellyn-Lacey S. 2008. Modulation of natural killer cells by human cytomegalovirus. J Clin Virol 41:206-212.

100. Béziat V, Dalgard O, Asselah T, Halfon P, Bedossa P, Boudifa A, Hervier B, Theodorou I, Martinot M, Debré P. 2012. CMV drives clonal expansion of NKG2C+ NK cells expressing self-specific KIRs in chronic hepatitis patients. Eur J Immunol 42:447-457.
101. Gumá M, Budt M, Sáez A, Brckalo T, Hengel H, Angulo A, López-Botet M. 2006. Expansion of CD94/NKG2C+ NK cells in response to human cytomegalovirus-infected fibroblasts. Blood 107:3624-3631.
102. Hammer Q, Rückert T, Borst EM, Dunst J, Haubner A, Durek P, Heinrich F, Gasparoni G, Babic M, Tomic A. 2018. Peptide-specific recognition of human cytomegalovirus strains controls adaptive natural killer cells. Nat Immunol 19:453-463.
103. Foley B, Cooley S, Verneris MR, Pitt M, Curtsinger J, Luo X, Lopez-Verges S, Lanier LL, Weisdorf D, Miller JS. 2012. Cytomegalovirus reactivation after allogeneic transplantation promotes a lasting increase in educated NKG2C+ natural killer cells with potent function. Blood, The Journal of the American Society of Hematology 119:2665-2674.
104. Almehmadi M, Flanagan BF, Khan N, Alomar S, Christmas SE. 2014. Increased numbers and functional activity of CD 56+ T cells in healthy cytomegalovirus positive subjects. Immunology 142:258-268.
105. Almehmadi M, Hammad A, Heyworth S, Moberly J, Middleton D, Hopkins M, Hart I, Christmas S. 2015. CD56+ T cells are increased in kidney transplant patients following cytomegalovirus infection. Transplant Infectious Disease 17:518-526.
106. Prince HE, Lapé-Nixon M. 2014. Role of cytomegalovirus (CMV) IgG avidity testing in diagnosing primary CMV infection during pregnancy. Clin Vaccine Immunol 21:1377-1384.
107. Hamprecht K, Bissinger AL, Arellano-Galindo J, Schweinzer K, Jiang X, Göhring K, Mikeler E, Jahn G. 2014. Intrafamilial transmission of human cytomegalovirus (HCMV): long-term dynamics of epitope-specific antibody response in context of avidity maturation. J Clin Virol 60:119-126.
108. Crough T, Khanna R. 2009. Immunobiology of human cytomegalovirus: from bench to bedside. Clin Microbiol Rev 22:76-98.
109. Alberola J, Tamarit A, Igual R, Navarro D. 2000. Early neutralizing and glycoprotein B (gB)-specific antibody responses to human cytomegalovirus (HCMV) in immunocompetent individuals with distinct clinical presentations of primary HCMV infection. J Clin Virol 16:113-122.
110. Bogner E, Pecher G. 2013. Pattern of the epitope-specific IgG/IgM response against human cytomegalovirus in patients with multiple myeloma. Clin Vaccine Immunol 20:1298-1304.
111. Landini M, La Placa M. 1991. Humoral immune response to human cytomegalovirus proteins: a brief review. Comp Immunol, Microbiol Infect Dis 14:97-105.
112. Van Zanten J, Harmsen M, Van der Giessen M, Van der Bij W, Prop J, De Leij L. 1995. Humoral immune response against human cytomegalovirus (HCMV)-specific proteins after HCMV infection in lung transplantation as detected with recombinant and naturally occurring proteins. Clin Diagn Lab Immunol 2:214-218.
113. Britt W, Vugler L, Stephens E. 1988. Induction of complement-dependent and-independent neutralizing antibodies by recombinant-derived human cytomegalovirus gp55-116 (gB). J Virol 62:3309-3318.
114. Tugizov S, Navarro D, Paz P, Wang Y, Qadri I, Pereira L. 1994. Function of human cytomegalovirus glycoprotein B: syncytium formation in cells constitutively expressing gB is blocked by virus-neutralizing antibodies. Virology 201:263-276.
115. Marshall GS, Rabalais GP, Stout GG, Waldeyer SL. 1992. Antibodies to recombinant-derived glycoprotein B after natural human cytomegalovirus infection correlate with neutralizing activity. J Infect Dis 165:381-384.
116. Urban M, Klein M, Britt W, Hassfurther E, Mach M. 1996. Glycoprotein H of human cytomegalovirus is a major antigen for the neutralizing humoral immune response. J Gen Virol 77:1537-1547.
117. Genini E, Percivalle E, Sarasini A, Revello MG, Baldanti F, Gerna G. 2011. Serum antibody response to the gH/gL/pUL128–131 five-protein complex of human cytomegalovirus (HCMV) in primary and reactivated HCMV infections. J Clin Virol 52:113-118.
118. Macagno A, Bernasconi NL, Vanzetta F, Dander E, Sarasini A, Revello MG, Gerna G, Sallusto F, Lanzavecchia A. 2010. Isolation of human monoclonal antibodies that potently neutralize human cytomegalovirus infection by targeting different epitopes on the gH/gL/UL128-131A complex. J Virol 84:1005-1013.
119. Gerna G, Lilleri D, Fornara C, Comolli G, Lozza L, Campana C, Pellegrini C, Meloni F, Rampino T. 2006. Monitoring of human cytomegalovirus-specific CD4+ and CD8+ T-cell immunity in patients receiving solid organ transplantation. Am J Transplantation 6:2356-2364.

120. Sester M, Sester U, Gärtner BC, Girndt M, Meyerhans A, Köhler H. 2002. Dominance of virus-specific CD8 T cells in human primary cytomegalovirus infection. Journal of the American Society of Nephrology 13:2577-2584.
121. Gamadia LE, Remmerswaal EB, Weel JF, Bemelman F, van Lier RA, Ten Berge IJ. 2003. Primary immune responses to human CMV: a critical role for IFN-γ–producing CD4+ T cells in protection against CMV disease. Blood 101:2686-2692.
122. Jackson S, Wills M, Lim Y. 2020. The CD4+ T cell Response to Human Cytomegalovirus in healthy and immunocompromised people.
123. Walter EA, Greenberg PD, Gilbert MJ, Finch RJ, Watanabe KS, Thomas ED, Riddell SR. 1995. Reconstitution of cellular immunity against cytomegalovirus in recipients of allogeneic bone marrow by transfer of T-cell clones from the donor. New Engl J Med 333:1038-1044.
124. Einsele H, Roosnek E, Rufer N, Sinzger C, Riegler S, Löffler J, Grigoleit U, Moris A, Rammensee H-G, Kanz L. 2002. Infusion of cytomegalovirus (CMV)–specific T cells for the treatment of CMV infection not responding to antiviral chemotherapy. Blood 99:3916-3922.
125. Tu W, Chen S, Sharp M, Dekker C, Manganello AM, Tongson EC, Maecker HT, Holmes TH, Wang Z, Kemble G. 2004. Persistent and selective deficiency of CD4+ T cell immunity to cytomegalovirus in immunocompetent young children. The Journal of Immunology 172:3260-3267.
126. Sylwester AW, Mitchell BL, Edgar JB, Taormina C, Pelte C, Ruchti F, Sleath PR, Grabstein KH, Hosken NA, Kern F. 2005. Broadly targeted human cytomegalovirus-specific CD4+ and CD8+ T cells dominate the memory compartments of exposed subjects. The Journal of experimental medicine 202:673-685.
127. Wills MR, Carmichael AJ, Mynard K, Jin X, Weekes MP, Plachter B, Sissons J. 1996. The human cytotoxic T-lymphocyte (CTL) response to cytomegalovirus is dominated by structural protein pp65: frequency, specificity, and T-cell receptor usage of pp65-specific CTL. J Virol 70:7569-7579.
128. Kern F, Surel IP, Faulhaber N, Frömmel C, Schneider-Mergener J, Schönemann C, Reinke P, Volk H-D. 1999. Target structures of the CD8+-T-cell response to human cytomegalovirus: the 72-kilodalton major immediate-early protein revisited. J Virol 73:8179-8184.
129. McLaughlin-Taylor E, Pande H, Forman SJ, Tanamachi B, Li CR, Zaia JA, Greenberg PD, Riddell SR. 1994. Identification of the major late human cytomegalovirus matrix protein pp65 as a target antigen for CD8+ virus-specific cytotoxic T lymphocytes. J Med Virol 43:103-110.
130. Kern F, Bunde T, Faulhaber N, Kiecker F, Khatamzas E, Rudawski I-M, Pruss A, Gratama J-W, Volkmer-Engert R, Ewert R. 2002. Cytomegalovirus (CMV) phosphoprotein 65 makes a large contribution to shaping the T cell repertoire in CMV-exposed individuals. The Journal of infectious diseases 185:1709-1716.
131. Davignon JL, Clement D, Alriquet J, Michelson S, Davrinche C. 1995. Analysis of the Proliferative T Cell Response to Human Cytomegalovirus Major Immediate-Early Protein (IEI): Phenotype, Frequeney and Variability. Scand J Immunol 41:247-255.
132. Elkington R, Walker S, Crough T, Menzies M, Tellam J, Bharadwaj M, Khanna R. 2003. Ex vivo profiling of CD8+-T-cell responses to human cytomegalovirus reveals broad and multispecific reactivities in healthy virus carriers. J Virol 77:5226-5240.
133. Quinnan Jr GV, Kirmani N, Rook AH, Manischewitz JF, Jackson L, Moreschi G, Santos GW, Saral R, Burns WH. 1982. Cytotoxic T cells in cytomegalovirus infection: HLA-restricted T-lymphocyte and non-T-lymphocyte cytotoxic responses correlate with recovery from cytomegalovirus infection in bone-marrow-transplant recipients. New Engl J Med 307:7-13.
134. Reusser P, Riddell SR, Meyers JD, Greenberg PD. 1991. Cytotoxic T-lymphocyte response to cytomegalovirus after human allogeneic bone marrow transplantation: pattern of recovery and correlation with cytomegalovirus infection and disease. Blood, The Journal of the American Society of Hematology.
135. Shlobin OA, West EE, Lechtzin N, Miller SM, Borja M, Orens JB, Dropulic LK, McDyer JF. 2006. Persistent cytomegalovirus-specific memory responses in the lung allograft and blood following primary infection in lung transplant recipients. The Journal of Immunology 176:2625-2634.
136. Reusser P, Cathomas G, Attenhofer R, Tamm M, Thiel G. 1999. Cytomegalovirus (CMV)—specific T cell immunity after renal transplantation mediates protection from CMV disease by limiting the systemic virus load. The Journal of infectious diseases 180:247-253.
137. Bunde T, Kirchner A, Hoffmeister B, Habedank D, Hetzer R, Cherepnev G, Proesch S, Reinke P, Volk H-D, Lehmkuhl H. 2005. Protection from cytomegalovirus after transplantation is correlated with immediate early 1–specific CD8 T cells. The Journal of experimental medicine 201:1031-1036.

138. Riddell S, Watanabe K, Goodrich J, Li C, Agha M, Greenberg P. 1992. Restoration of viral immunity in immunodeficient humans by the adoptive transfer of T cell clones. J Science 257:238-241.
139. Déchanet J, Merville P, Lim A, Retière C, Pitard V, Lafarge X, Michelson S, Méric C, Hallet M-M, Kourilsky P. 1999. Implication of γδ T cells in the human immune response to cytomegalovirus. The Journal of clinical investigation 103:1437-1449.
140. Davey MS, Willcox CR, Joyce SP, Ladell K, Kasatskaya SA, McLaren JE, Hunter S, Salim M, Mohammed F, Price DA. 2017. Clonal selection in the human Vδ1 T cell repertoire indicates γδ TCR-dependent adaptive immune surveillance. Nature communications 8:1-15.
141. Lafarge X, Merville P, Cazin M-C, Bergé F, Potaux L, Moreau J-F, Déchanet-Merville J. 2001. Cytomegalovirus infection in transplant recipients resolves when circulating γδ T lymphocytes expand, suggesting a protective antiviral role. The Journal of infectious diseases 184:533-541.
142. Déchanet J, Merville P, Bergé F, Bone-Mane G, Taupin J-L, Michel P, Joly P, Bonneville M, Potaux L, Moreau J-F. 1999. Major expansion of γδ T lymphocytes following cytomegalovirus infection in kidney allograft recipients. The Journal of infectious diseases 179:1-8.
143. Couzi L, Lafarge X, Pitard V, Neau-Cransac M, Dromer C, Billes MA, Lacaille F, Moreau JF, Merville P, Déchanet-Merville J. 2011. Gamma-delta T cell expansion is closely associated with cytomegalovirus infection in all solid organ transplant recipients. Transplant Int 24:e40-e42.
144. Puig-Pey I, Bohne F, Benítez C, López M, Martínez-Llordella M, Oppenheimer F, Lozano JJ, González-Abraldes J, Tisone G, Rimola A. 2010. Characterization of γδ T cell subsets in organ transplantation. Transplant Int 23:1045-1055.
145. Knight A, Madrigal AJ, Grace S, Sivakumaran J, Kottaridis P, Mackinnon S, Travers PJ, Lowdell MW. 2010. The role of Vδ2-negative γδ T cells during cytomegalovirus reactivation in recipients of allogeneic stem cell transplantation. Blood 116:2164-2172.
146. Scheper W, van Dorp S, Kersting S, Pietersma F, Lindemans C, Hol S, Heijhuurs S, Sebestyen Z, Gründer C, Marcu-Malina V. 2013. γδT cells elicited by CMV reactivation after allo-SCT cross-recognize CMV and leukemia. Leukemia 27:1328-1338.
147. Pitard V, Roumanes D, Lafarge X, Couzi L, Garrigue I, Lafon M-E, Merville P, Moreau J-F, Déchanet-Merville J. 2008. Long-term expansion of effector/memory Vδ2− γδ T cells is a specific blood signature of CMV infection. Blood, The Journal of the American Society of Hematology 112:1317-1324.
148. Wills MR, Poole E, Lau B, Krishna B, Sinclair JH. 2015. The immunology of human cytomegalovirus latency: could latent infection be cleared by novel immunotherapeutic strategies? Cellular & molecular immunology 12:128-138.
149. Van Den Heuvel D, Jansen MA, Dik WA, Bouallouch-Charif H, Zhao D, Van Kester KA, Smits-te Nijenhuis MA, Kolijn-Couwenberg MJ, Jaddoe VW, Arens R. 2016. Cytomegalovirus-and Epstein-Barr Virus–induced T-cell expansions in young children do not impair naive t-cell populations or vaccination responses: The Generation R Study. The Journal of Infectious Diseases 213:233-242.
150. Lidehäll AK, Engman ML, Sund F, Malm G, Lewensohn-Fuchs I, Ewald U, Tötterman TH, Karltorp E, Korsgren O, Eriksson BM. 2013. Cytomegalovirus-Specific CD 4 and CD 8 T Cell Responses in Infants and Children. Scand J Immunol 77:135-143.
151. Kim J, Kim A, Shin E-C. 2015. Cytomegalovirus infection and memory T cell inflation. Immune network 15:186-190.
152. Di Benedetto S, Derhovanessian E, Steinhagen-Thiessen E, Goldeck D, Müller L, Pawelec G. 2015. Impact of age, sex and CMV-infection on peripheral T cell phenotypes: results from the Berlin BASE-II Study. Biogerontology 16:631-643.
153. Lachmann R, Bajwa M, Vita S, Smith H, Cheek E, Akbar A, Kern F. 2012. Polyfunctional T cells accumulate in large human cytomegalovirus-specific T cell responses. J Virol 86:1001-1009.
154. Wikby A, Johansson B, Olsson J, Löfgren S, Nilsson B-O, Ferguson F. 2002. Expansions of peripheral blood CD8 T-lymphocyte subpopulations and an association with cytomegalovirus seropositivity in the elderly: the Swedish NONA immune study. Experimental gerontology 37:445-453.
155. Olsson J, Wikby A, Johansson B, Löfgren S, Nilsson B-O, Ferguson FG. 2001. Age-related change in peripheral blood T-lymphocyte subpopulations and cytomegalovirus infection in the very old: the Swedish longitudinal OCTO immune study. Mechanisms of ageing and development 121:187-201.

156. Vescovini R, Biasini C, Fagnoni FF, Telera AR, Zanlari L, Pedrazzoni M, Bucci L, Monti D, Medici MC, Chezzi C. 2007. Massive load of functional effector CD4+ and CD8+ T cells against cytomegalovirus in very old subjects. The Journal of Immunology 179:4283-4291.
157. Adriaensen W, Derhovanessian E, Vaes B, Van Pottelbergh G, Degryse J-M, Pawelec G, Hamprecht K, Theeten H, Matheï C. 2015. CD4: 8 ratio> 5 is associated with a dominant naive T-cell phenotype and impaired physical functioning in CMV-seropositive very elderly people: results from the BELFRAIL study. Journals of Gerontology Series A: Biomedical Sciences and Medical Sciences 70:143-154.
158. Van Der Heiden M, Van Zelm MC, Bartol SJ, de Rond LG, Berbers GA, Boots AM, Buisman A-M. 2016. Differential effects of Cytomegalovirus carriage on the immune phenotype of middle-aged males and females. Scientific reports 6:26892.
159. Weltevrede M, Eilers R, de Melker HE, van Baarle D. 2016. Cytomegalovirus persistence and T-cell immunosenescence in people aged fifty and older: a systematic review. Experimental gerontology 77:87-95.
160. Derhovanessian E, Maier AB, Hähnel K, Beck R, de Craen AJ, Slagboom EP, Westendorp RG, Pawelec G. 2011. Infection with cytomegalovirus but not herpes simplex virus induces the accumulation of late-differentiated CD4+ and CD8+ T-cells in humans. J Gen Virol 92:2746-2756.
161. Cooper AP. 1840. On the Anatomy of the Breast, vol 1. Longman.
162. Geddes DT. 2007. Inside the lactating breast: the latest anatomy research. Journal of midwifery women's health 52:556-563.
163. Henry G, William P, Bannister L. 1995. Gray's anatomy. ELBS Churchill Livingstone: London, UK.
164. Boron WF, Boulpaep EL. 2016. Medical physiology E-book. Elsevier Health Sciences.
165. Hunziker W, Kraehenbuhl J-P. 1998. Epithelial transcytosis of immunoglobulins. Journal of mammary gland biology and neoplasia 3:287-302.
166. McManaman JL, Neville MC. 2003. Mammary physiology and milk secretion. Adv Drug Del Rev 55:629-641.
167. Monks J, Neville M. 2000. Transcytosis of proteins across the mammary epithelium into milk. Journal of Women's Cancer 2:193-200.
168. Goldman AS, Chheda S, Garofalo R, Schmalstieg FC. 1996. Cytokines in human milk: properties and potential effects upon the mammary gland and the neonate. Journal of mammary gland biology neoplasia 1:251-258.
169. Mather IH, Keenan TW. 1998. Origin and secretion of milk lipids. Journal of mammary gland biology and neoplasia 3:259-273.
170. Hassiotou F, Geddes D. 2013. Anatomy of the human mammary gland: Current status of knowledge. Clin Anat 26:29-48.
171. Tuaillon E, Valea D, Becquart P, Al Tabaa Y, Meda N, Bollore K, Van de Perre P, Vendrell J-P. 2009. Human milk-derived B cells: a highly activated switched memory cell population primed to secrete antibodies. The Journal of Immunology 182:7155-7162.
172. Roux M, Mcwilliams M, Phillips-Quagliata JM, Weisz-Carrington P, Lamm M. 1977. Origin of IgA-secreting plasma cells in the mammary gland. The Journal of experimental medicine 146:1311-1322.
173. Ramsay DT, Kent JC, Owens RA, Hartmann PE. 2004. Ultrasound imaging of milk ejection in the breast of lactating women. Pediatrics 113:361-367.
174. Moberg KU, Prime DK. 2013. Oxytocin effects in mothers and infants during breastfeeding. Infant 9:201-206.
175. Gardner H, Kent JC, Prime DK, Lai CT, Hartmann PE, Geddes DT. 2017. Milk ejection patterns remain consistent during the first and second lactations. Am J Hum Biol 29:e22960.
176. Ramsay DT, Mitoulas LR, Kent JC, Cregan MD, Doherty DA, Larsson M, Hartmann PE. 2006. Milk flow rates can be used to identify and investigate milk ejection in women expressing breast milk using an electric breast pump. Breastfeeding Medicine 1:14-23.
177. Prime DK, Geddes DT, Spatz DL, Robert M, Trengove NJ, Hartmann PE. 2009. Using milk flow rate to investigate milk ejection in the left and right breasts during simultaneous breast expression in women. International Breastfeeding Journal 4:10.
178. van Sadelhoff J, Mastorakou D, Weenen H, Stahl B, Garssen J, Hartog A. 2018. Differences in Levels of Free Amino Acids and Total Protein in Human Foremilk and Hindmilk. Nutrients 10:1828.
179. Saarela T, Kokkonen J, Koivisto M. 2005. Macronutrient and energy contents of human milk fractions during the first six months of lactation. Acta Paediatrica 94:1176-1181.

180. Ballard O, Morrow AL. 2013. Human milk composition: nutrients and bioactive factors. Pediatric Clinics 60:49-74.
181. Bates CJ, Prentice A. 1994. Breast milk as a source of vitamins, essential minerals and trace elements. Pharmacology therapeutics 62:193-220.
182. Andreas NJ, Kampmann B, Le-Doare KM. 2015. Human breast milk: A review on its composition and bioactivity. Early Hum Dev 91:629-635.
183. Miclat NN, Hodgkinson R, Marx GF. 1978. Neonatal gastric pH. Anesthesia and analgesia 57:98-101.
184. Jones JA, Hopper AO, Power GG, Blood AB. 2015. Dietary intake and bio-activation of nitrite and nitrate in newborn infants. Pediatric research 77:173-181.
185. Lönnerdal B. 2016. Bioactive proteins in human milk: health, nutrition, and implications for infant formulas. The Journal of pediatrics 173:S4-S9.
186. Strömqvist M, Falk P, Bergström S, Hansson L, Lönnerdal B, Normark S, Hernell O. 1995. Human milk kappa-casein and inhibition of Helicobacter pylori adhesion to human gastric mucosa. Journal of pediatric gastroenterology and nutrition 21:288-296.
187. Lönnerdal B, Erdmann P, Thakkar SK, Sauser J, Destaillats F. 2017. Longitudinal evolution of true protein, amino acids and bioactive proteins in breast milk: a developmental perspective. The Journal of nutritional biochemistry 41:1-11.
188. Lönnerdal B, Iyer S. 1995. Lactoferrin: molecular structure and biological function. Annu Rev Nutr 15:93-110.
189. Arnold R, Brewer M, Gauthier J. 1980. Bactericidal activity of human lactoferrin: sensitivity of a variety of microorganisms. Infection immunity 28:893-898.
190. Liao Y, Jiang R, Lönnerdal B. 2012. Biochemical and molecular impacts of lactoferrin on small intestinal growth and development during early life. Biochem Cell Biol 90:476-484.
191. Legrand D. 2016. Overview of lactoferrin as a natural immune modulator. The Journal of pediatrics 173:S10-S15.
192. Lönnerdal B. 2013. Bioactive proteins in breast milk. Journal of paediatrics child health 49:1-7.
193. Koenig Á, Diniz EMdA, Barbosa SFC, Vaz FAC. 2005. Immunologic factors in human milk: the effects of gestational age and pasteurization. Journal of Human Lactation 21:439-443.
194. Martin CR, Ling P-R, Blackburn GL. 2016. Review of infant feeding: key features of breast milk and infant formula. Nutrients 8:279.
195. Dror DK, Allen LH. 2018. Overview of nutrients in human milk. Advances in Nutrition 9:278S-294S.
196. Lopez C, Ménard O. 2011. Human milk fat globules: polar lipid composition and in situ structural investigations revealing the heterogeneous distribution of proteins and the lateral segregation of sphingomyelin in the biological membrane. Colloids Surf B Biointerfaces 83:29-41.
197. Yolken RH, Peterson JA, Vonderfecht SL, Fouts ET, Midthun K, Newburg DS. 1992. Human milk mucin inhibits rotavirus replication and prevents experimental gastroenteritis. The Journal of clinical investigation 90:1984-1991.
198. Tanaka K, Hosozawa M, Kudo N, Yoshikawa N, Hisata K, Shoji H, Shinohara K, Shimizu T. 2013. The pilot study: sphingomyelin-fortified milk has a positive association with the neurobehavioural development of very low birth weight infants during infancy, randomized control trial. Brain and Development 35:45-52.
199. Gomez-Gallego C, Garcia-Mantrana I, Salminen S, Collado MC. The human milk microbiome and factors influencing its composition and activity, p 400-405. *In* (ed), Elsevier,
200. Lindberg T, Skude GJP. 1982. Amylase in human milk. Pediatrics 70:235-238.
201. Hernell O, Bläckberg L. 1982. Digestion of human milk lipids: physiologic significance of sn-2 monoacylglycerol hydrolysis by bile salt-stimulated lipase. Pediatric research 16:882.
202. Björck L, Rosen C, Marshall V, Reiter B. 1975. Antibacterial activity of the lactoperoxidase system in milk against pseudomonads and other gram-negative bacteria. Appl Environ Microbiol 30:199-204.
203. Adkins Y, Lönnerdal B. 2002. Mechanisms of vitamin B12 absorption in breast-fed infants. Journal of pediatric gastroenterology nutrition 35:192-198.
204. Chowanadisai W, Lönnerdal B. 2002. α1-Antitrypsin and antichymotrypsin in human milk: Origin, concentrations, and stability. The American journal of clinical nutrition 76:828-833.
205. Ashkar S, Weber GF, Panoutsakopoulou V, Sanchirico ME, Jansson M, Zawaideh S, Rittling SR, Denhardt DT, Glimcher MJ, Cantor H. 2000. Eta-1 (osteopontin): an early component of type-1 (cell-mediated) immunity. Science 287:860-864.
206. Lönnerdal B. 2003. Nutritional and physiologic significance of human milk proteins. The American journal of clinical nutrition 77:1537S-1543S.

207. Gao X, McMahon RJ, Woo JG, Davidson BS, Morrow AL, Zhang Q. 2012. Temporal changes in milk proteomes reveal developing milk functions. Journal of proteome research 11:3897-3907.
208. German JB, Freeman SL, Lebrilla CB, Mills DA. 2008. Human milk oligosaccharides: evolution, structures and bioselectivity as substrates for intestinal bacteria, p 205-222, Personalized nutrition for the diverse needs of infants and children, vol 62. Karger Publishers.
209. Haschke F, Haiden N, Thakkar SK. 2016. Nutritive and bioactive proteins in breastmilk. Annals of Nutrition and Metabolism 69:16-26.
210. Admyre C, Johansson SM, Qazi KR, Filén J-J, Lahesmaa R, Norman M, Neve EP, Scheynius A, Gabrielsson S. 2007. Exosomes with immune modulatory features are present in human breast milk. The Journal of immunology 179:1969-1978.
211. Agostoni C, Carratu B, Boniglia C, Riva E, Sanzini E. 2000. Free amino acid content in standard infant formulas: comparison with human milk. Journal of the American College of Nutrition 19:434-438.
212. Uauy R, Quan R, Gil A. 1994. Role of nucleotides in intestinal development and repair: implications for infant nutrition. The Journal of nutrition 124:1436S-1441S.
213. Witkowska-Zimny M, Kaminska-El-Hassan E. 2017. Cells of human breast milk. Cellular molecular biology letters 22:11.
214. Organization WH. 2003. World Health Organization Global strategy for infant and young child feeding. Geneva: World Health Organization.
215. Duijts L, Jaddoe VW, Hofman A, Moll HA. 2010. Prolonged and exclusive breastfeeding reduces the risk of infectious diseases in infancy. Pediatrics 126:e18-e25.
216. Chantry CJ, Howard CR, Auinger P. 2006. Full breastfeeding duration and associated decrease in respiratory tract infection in US children. Pediatrics 117:425-432.
217. Lamberti LM, Walker CLF, Noiman A, Victora C, Black RE. 2011. Breastfeeding and the risk for diarrhea morbidity and mortality. BMC Public Health 11:S15.
218. Victoria C. 2000. Effect of breastfeeding on infant and child mortality due to infectious diseases in less developed countries: a pooled analysis. The Lancet 355:451-455.
219. Victora CG, Bahl R, Barros AJ, França GV, Horton S, Krasevec J, Murch S, Sankar MJ, Walker N, Rollins NC. 2016. Breastfeeding in the 21st century: epidemiology, mechanisms, and lifelong effect. The Lancet 387:475-490.
220. Kramer MS, Aboud F, Mironova E, Vanilovich I, Platt RW, Matush L, Igumnov S, Fombonne E, Bogdanovich N, Ducruet T. 2008. Breastfeeding and child cognitive development: new evidence from a large randomized trial. Archives of general psychiatry 65:578-584.
221. Mattsby-Baltzer I, Roseanu A, Motas C, Elverfors J, Engberg I, Hanson LÅ. 1996. Lactoferrin or a fragment thereof inhibits the endotoxin-induced interleukin-6 response in human monocytic cells. Pediatric Research 40:257-262.
222. Ward RE, Ninonuevo M, Mills DA, Lebrilla CB, German JB. 2006. In vitro fermentation of breast milk oligosaccharides by Bifidobacterium infantis and Lactobacillus gasseri. Appl Environ Microbiol 72:4497-4499.
223. Triantis V, Bode L, Van Neerven R. 2018. Immunological effects of human milk oligosaccharides. Frontiers in pediatrics 6:190.
224. Palmeira P, Carneiro-Sampaio M. 2016. Immunology of breast milk. Revista da Associação Médica Brasileira 62:584-593.
225. Chirico G, Marzollo R, Cortinovis S, Fonte C, Gasparoni A. 2008. Antiinfective properties of human milk. The Journal of nutrition 138:1801S-1806S.
226. Wheeler TT, Hodgkinson AJ, Prosser CG, Davis SR. 2007. Immune components of colostrum and milk—a historical perspective. Journal of mammary gland biology and neoplasia 12:237-247.
227. Newburg DS. 2005. Innate immunity and human milk. The Journal of nutrition 135:1308-1312.
228. Thai JD, Gregory KE. 2020. Bioactive Factors in Human Breast Milk Attenuate Intestinal Inflammation during Early Life. Nutrients 12:581.
229. Brandtzaeg P. 2010. The mucosal immune system and its integration with the mammary glands. The Journal of pediatrics 156:S8-S15.
230. Cohen IR, Norins LC. 1968. Antibodies of the IgG, IgM, and IgA classes in newborn and adult sera reactive with gram-negative bacteria. The Journal of clinical investigation 47:1053-1062.
231. Roopenian DC, Akilesh S. 2007. FcRn: the neonatal Fc receptor comes of age. Nat Rev Immunol 7:715.
232. Brandtzaeg P. 2003. Mucosal immunity: integration between mother and the breast-fed infant. Vaccine 21:3382-3388.
233. Telemo E, Hanson LA. 1996. Antibodies in milk. J Mammary Gland Biol Neoplasia 1:243-249.

234. Van de Perre P. 2003. Transfer of antibody via mother's milk. Vaccine 21:3374-3376.
235. Hurley WL, Theil PK. 2011. Perspectives on immunoglobulins in colostrum and milk. Nutrients 3:442-474.
236. Goldman AS. 1993. The immune system of human milk: antimicrobial, antiinflammatory and immunomodulating properties. The Pediatric infectious disease journal 12:664-672.
237. Hassiotou F, Geddes DT, Hartmann PE. 2013. Cells in human milk: state of the science. Journal of Human Lactation 29:171-182.
238. Ninkina N, Kukharsky MS, Hewitt MV, Lysikova EA, Skuratovska LN, Deykin AV, Buchman VL. 2019. Stem cells in human breast milk. Human cell:1-8.
239. Hassiotou F, Geddes DT. 2015. Immune Cell–Mediated Protection of the Mammary Gland and the Infant during Breastfeeding. Advances in Nutrition 6:267-275.
240. Hassiotou F, Hepworth AR, Metzger P, Tat Lai C, Trengove N, Hartmann PE, Filgueira L. 2013. Maternal and infant infections stimulate a rapid leukocyte response in breastmilk. Clinical translational immunology 2:e3.
241. Goldman A, Goldblum R. 1997. Transfer of maternal leukocytes to the infant by human milk, p 205-213, Reproductive immunology. Springer.
242. Eglinton BA, Roberton DM, Cummins AG. 1994. Phenotype of T cells, their soluble receptor levels, and cytokine profile of human breast milk. Immunology & Cell Biology 72.
243. Wirt DP, Adkins LT, Palkowetz KH, Schmalstieg FC, Goldman AS. 1992. Activated and memory T lymphocytes in human milk. Cytometry: The Journal of the International Society for Analytical Cytology 13:282-290.
244. Bertotto A, Gerli R, Fabietti G, Crupi S, Arcangeli C, Scalise F, Vaccaro R. 1990. Human breast milk T lymphocytes display the phenotype and functional characteristics of memory T cells. Eur J Immunol 20:1877-1880.
245. Trend S, de Jong E, Lloyd ML, Kok CH, Richmond P, Doherty DA, Simmer K, Kakulas F, Strunk T, Currie A. 2015. Leukocyte populations in human preterm and term breast milk identified by multicolour flow cytometry. PloS one 10:e0135580.
246. Laouar A. 2020. Maternal leukocytes and infant immune programming during breastfeeding. Trends Immunol 41:225-239.
247. LaTuga MS, Stuebe A, Seed PC. A review of the source and function of microbiota in breast milk, p 068-073. *In* (ed), Thieme Medical Publishers,
248. Martín R, Langa S, Reviriego C, Jimínez E, Marín ML, Xaus J, Fernández L, Rodríguez JM. 2003. Human milk is a source of lactic acid bacteria for the infant gut. The Journal of pediatrics 143:754-758.
249. Diosi P, Babusceac L, Nevinglovschi O, Kun-Stoicu G. 1967. Cytomegalovirus infection associated with pregnancy. The Lancet 290:1063-1066.
250. Meier J, Lienicke U, Tschirch E, Krüger DH, Wauer RR, Prösch S. 2005. Human cytomegalovirus reactivation during lactation and mother-to-child transmission in preterm infants. J Clin Microbiol 43:1318-1324.
251. Hamprecht K, Maschmann J, Vochem M, Dietz K, Speer CP, Jahn G. 2001. Epidemiology of transmission of cytomegalovirus from mother to preterm infant by breastfeeding. The Lancet 357:513-518.
252. Numazaki K. 1997. Human cytomegalovirus infection of breast milk. FEMS Immunology Medical Microbiology 18:91-98.
253. Hamprecht K, Witzel S, Maschmann J, Speer CP, Jahn G. 2002. Transmission of Cytomegalovirus Infection Through Breast Milk in Term and Pretern Infants, p 231-239, Short and Long Term Effects of Breast Feeding on Child Health. Springer.
254. Reynolds DW, Stagno S, Hosty TS, Tiller M, Alford Jr CA. 1973. Maternal cytomegalovirus excretion and perinatal infection. New Engl J Med 289:1-5.
255. Azenkot T, Zaniello B, Green ML, Selke S, Huang Ml, Magaret A, Wald A, Johnston C. 2019. Cytomegalovirus shedding from breastmilk and mucosal sites in healthy postpartum women: A pilot study. J Med Virol 91:894-898.
256. Hamprecht K, Maschmann J, Vochem M, Speer CP, Jahn G. 2003. Transmission of cytomegalovirus to preterm infants by breast-feeding. Monogr Virol 24:43-52.
257. Prendergast AJ, Goga AE, Waitt C, Gessain A, Taylor GP, Rollins N, Abrams EJ, Lyall EH, Van de Perre P. 2019. Transmission of CMV, HTLV-1, and HIV through breastmilk. Lancet Child Adolesc Health 3:264-273.
258. Hamprecht K, Goelz R. 2017. Postnatal cytomegalovirus infection through human milk in preterm infants: transmission, clinical presentation, and prevention. Clin Perinatol 44:121-130.

259. Asanuma H, Numazaki K, Nagata N, Hotsubo T, Horino K, Chiba S. 1996. Role of milk whey in the transmission of human cytomegalovirus infection by breast milk. Microbiol Immunol 40:201-204.
260. Maschmann J, Hamprecht K, Dietz K, Jahn G, Speer C. 2001. Cytomegalovirus infection of extremely low—birth weight infants via breast milk. Clin Infect Dis 33:1998-2003.
261. Vochem M, Hamprecht K, Jahn G, Speer CP. 1998. Transmission of cytomegalovirus to preterm infants through breast milk. The Pediatric infectious disease journal 17:53-58.
262. Lanzieri TM, Dollard SC, Josephson CD, Schmid DS, Bialek SR. 2013. Breast milk–acquired cytomegalovirus infection and disease in VLBW and premature infants. Pediatrics 131:e1937-e1945.
263. Goelz R, Hamprecht K, Klingel K, Poets CF. 2016. Intestinal manifestations of postnatal and congenital cytomegalovirus infection in term and preterm infants. J Clin Virol 83:29-36.
264. Novakova V, Hamprecht K, Müller A, Arellano-Galindo J, Ehlen M, Horneff G. 2014. Severe postnatal CMV colitis with an extensive colonic stenosis in a 2-month-old male immunocompetent term infant infected via breast milk. J Clin Virol 59:259-263.
265. Lawrence RM. 2006. Cytomegalovirus in human breast milk: risk to the premature infant. Breastfeeding medicine 1:99-107.
266. Hamprecht K, Maschmann J, Müller D, Dietz K, Besenthal I, Goelz R, Middeldorp JM, Speer CP, Jahn G. 2004. Cytomegalovirus (CMV) inactivation in breast milk: reassessment of pasteurization and freeze-thawing. Pediatric research 56:529-535.
267. Maschmann J, Hamprecht K, Weissbrich B, Dietz K, Jahn G, Speer C. 2006. Freeze-thawing of breast milk does not prevent cytomegalovirus transmission to a preterm infant. Archives of Disease in Childhood-Fetal and Neonatal Edition 91:F288-F290.
268. Forsgren M. 2004. Cytomegalovirus in breast milk: reassessment of pasteurization and freeze-thawing. Pediatric research 56:526-528.
269. Hamprecht K, Witzel S, Maschmann J, Dietz K, Baumeister A, Mikeler E, Goelz R, Speer CP, Jahn G. 2003. Rapid detection and quantification of cell free cytomegalovirus by a high-speed centrifugation-based microculture assay: comparison to longitudinally analyzed viral DNA load and pp67 late transcript during lactation. J Clin Virol 28:303-316.
270. Hamprecht K, Mikeler E, Jahn G. 1997. Semi-quantitative detection of cytomegalovirus DNA from native serum and plasma by nested PCR: influence of DNA extraction procedures. J Virol Methods 69:125-135.
271. Prix L, Kuner R, Speer C, Jahn G, Hamprecht K. 1998. Evaluation of restriction fragment length polymorphism analysis of the UL10-UL13 genomic region for rapid identification of human cytomegalovirus strains. European Journal of Clinical Microbiology and Infectious Diseases 17:525-528.
272. Hartleif S, Göhring K, Goelz R, Jahn G, Hamprecht K. 2016. Quantitative monitoring of HCMV DNAlactia in human milk by real time PCR assay: Implementation of internal control contributes to standardization and quality control. J Virol Methods 237:101-106.
273. Schampera MS, Schweinzer K, Abele H, Kagan KO, Klein R, Rettig I, Jahn G, Hamprecht K. 2017. Comparison of cytomegalovirus (CMV)-specific neutralization capacity of hyperimmunoglobulin (HIG) versus standard intravenous immunoglobulin (IVIG) preparations: Impact of CMV IgG normalization. J Clin Virol 90:40-45.
274. Lazar K, Rabe T, Goelz R, Hamprecht K. 2020. Human Cytomegalovirus Reactivation During Lactation: Impact of Antibody Kinetics and Neutralization in Blood and Breast Milk. Nutrients 12:338.
275. Akoglu H. 2018. User's guide to correlation coefficients. Turkish journal of emergency medicine 18:91-93.
276. Maschmann J, Müller D, Lazar K, Goelz R, Hamprecht K. 2019. New short-term heat inactivation method of cytomegalovirus (CMV) in breast milk: impact on CMV inactivation, CMV antibodies and enzyme activities. Arch Dis Child:fetalneonatal-2018-316117.
277. Rabe T, Lazar K, Cambronero C, Goelz R, Hamprecht K. 2020. Human Cytomegalovirus (HCMV) Reactivation in the Mammary Gland Induces a Proinflammatory Cytokine Shift in Breast Milk. Microorganisms 8:289.
278. Chiavarini M, Bragetti P, Sensini A, Cenci E, Castronari R, Rossi MJ, Fantauzzi A, Minelli L. 2011. Breastfeeding and transmission of cytomegalovirus to preterm infants. Case report and kinetic of CMV-DNA in breast milk. Ital J Pediatr 37:6.
279. Hayashi S, Kimura H, Oshiro M, Kato Y, Yasuda A, Suzuki C, Watanabe Y, Morishima T, Hayakawa M. 2011. Transmission of cytomegalovirus via breast milk in extremely premature infants. J Perinatol 31:440-5.

280. Lombardi G, Garofoli F, Manzoni P, Stronati M. 2012. Breast milk-acquired cytomegalovirus infection in very low birth weight infants. The Journal of Maternal-Fetal & Neonatal Medicine 25:57-62.
281. Yasuda A, Kimura H, Hayakawa M, Ohshiro M, Kato Y, Matsuura O, Suzuki C, Morishima T. 2003. Evaluation of cytomegalovirus infections transmitted via breast milk in preterm infants with a real-time polymerase chain reaction assay. Pediatrics 111:1333-1336.
282. Hamprecht K, Maschmann J, Jahn G, Poets CF, Goelz R. 2008. Cytomegalovirus transmission to preterm infants during lactation. J Clin Virol 41:198-205.
283. Omarsdottir S, Casper C, Zweygberg Wirgart B, Grillner L, Vanpée M. 2007. Transmission of cytomegalovirus to extremely preterm infants through breast milk. Acta Paediatrica 96:492-494.
284. Maschmann J, Goelz R, Witzel S, Strittmatter U, Steinmassl M, Jahn G, Hamprecht K. 2015. Characterization of human breast milk leukocytes and their potential role in cytomegalovirus transmission to newborns. Neonatology 107:213-219.
285. Kassim O, Afolabi O, Ako-Nai K, Torimiro S, Littleton G, Oke O, Grissom F. 1987. Cytomegalovirus antibodies in breast milk and sera of mother-infant pairs. J Trop Pediatr 33:75-77.
286. Voller A, Bidwell D. 1976. Enzyme-immunoassays for antibodies in measles, cytomegalovirus infections and after rubella vaccination. British journal of experimental pathology 57:243.
287. Ehlinger EP, Webster EM, Kang HH, Cangialose A, Simmons AC, Barbas KH, Burchett SK, Gregory ML, Puopolo KP, Permar SR. 2011. Maternal cytomegalovirus-specific immune responses and symptomatic postnatal cytomegalovirus transmission in very low-birth-weight preterm infants. J Infect Dis 204:1672-1682.
288. Chen J, Hu L, Wu M, Zhong T, Zhou Y-H, Hu Y. 2012. Kinetics of IgG antibody to cytomegalovirus (CMV) after birth and seroprevalence of anti-CMV IgG in Chinese children. Virol J 9:304.
289. Maroulis GB, Buckley RH, Younger JB. 1971. Serum immunoglobulin concentrations during normal pregnancy. Am J Obstet Gynecol 109:971-976.
290. Amino N, Tanizawa O, Miyai K, Tanaka F, Hayashi C, Kawashima M, Ichihara K. 1978. Changes of serum immunoglobulins IgG, IgA, IgM, and IgE during pregnancy. Obstetrics and gynecology 52:415-420.
291. Larsson A, Palm M, Hansson L-O, Basu S, Axelsson O. 2008. Reference values for α1-acid glycoprotein, α1-antitrypsin, albumin, haptoglobin, C-reactive protein, IgA, IgG and IgM during pregnancy. Acta Obstet Gynecol Scand 87:1084-1088.
292. De Haas S, Ghossein-Doha C, Van Kuijk S, Van Drongelen J, Spaanderman M. 2017. Physiological adaptation of maternal plasma volume during pregnancy: a systematic review and meta-analysis. Ultrasound Obstetr Gynecol 49:177-187.
293. Rothe M, Hamprecht K, Lang D. 2000. Diagnostic differentiation of primary versus secondary/recurrent infection of human cytomegalovirus by using a recombinant gB ELISA. Biotest Bulletin 6:147-158.
294. Schoppel K, Kropff B, Schmidt C, Vornhagen R, Mach M. 1997. The humoral immune response against human cytomegalovirus is characterized by a delayed synthesis of glycoprotein-specific antibodies. J Infect Dis 175:533-544.
295. Saccoccio FM, Jenks JA, Itell HL, Li SH, Berry M, Pollara J, Casper C, Gantt S, Permar SR. 2019. Humoral Immune Correlates for Prevention of Postnatal Cytomegalovirus Acquisition. J Infect Dis.
296. Kagan K, Enders M, Schampera M, Baeumel E, Hoopmann M, Geipel A, Berg C, Goelz R, De Catte L, Wallwiener D. 2019. Prevention of maternal–fetal transmission of cytomegalovirus after primary maternal infection in the first trimester by biweekly hyperimmunoglobulin administration. Ultrasound Obstetr Gynecol 53:383-389.
297. Vanarsdall AL, Chin AL, Liu J, Jardetzky TS, Mudd JO, Orloff SL, Streblow D, Mussi-Pinhata MM, Yamamoto AY, Duarte G. 2019. HCMV trimer-and pentamer-specific antibodies synergize for virus neutralization but do not correlate with congenital transmission. Proceedings of the National Academy of Sciences 116:3728-3733.
298. Becquart P, Hocini H, Garin B, Sépou A, Kazatchkine MD, Bélec L. 1999. Compartmentalization of the IgG immune response to HIV-1 in breast milk. AIDS 13:1323-1331.
299. Andersen JH, Osbakk SA, Vorland LH, Traavik T, Gutteberg TJ. 2001. Lactoferrin and cyclic lactoferricin inhibit the entry of human cytomegalovirus into human fibroblasts. Antiviral Res 51:141-149.

300. Van der Strate B, Beljaars L, Molema G, Harmsen M, Meijer D. 2001. Antiviral activities of lactoferrin. Antiviral Res 52:225-239.
301. Morozov V, Hansman G, Hanisch FG, Schroten H, Kunz C. 2018. Human milk oligosaccharides as promising antivirals. Mol Nutr Food Res 62:1700679.
302. Donalisio M, Rittà M, Tonetto P, Civra A, Coscia A, Giribaldi M, Cavallarin L, Moro GE, Bertino E, Lembo D, nutrition. 2018. Anti-Cytomegalovirus Activity in Human Milk and Colostrum from Mothers of Preterm Infants. Journal of pediatric gastroenterology nutrition 67:654-659.
303. Donalisio M, Rittà M, Francese R, Civra A, Tonetto P, Coscia A, Giribaldi M, Cavallarin L, Moro GE, Bertino E. 2018. High Temperature—Short Time Pasteurization Has a Lower Impact on the Antiviral Properties of Human Milk Than Holder Pasteurization. Frontiers in pediatrics 6:304.
304. Giribaldi M, Coscia A, Peila C, Antoniazzi S, Lamberti C, Ortoffi M, Moro GE, Bertino E, Civera T, Cavallarin L. 2016. Pasteurization of human milk by a benchtop high-temperature short-time device. Innovative Food Science & Emerging Technologies 36:228-233.
305. Mikawa T, Mizuno K, Tanaka K, Kohda C, Ishii Y, Yamamoto K, Kobayashi S. 2019. Microwave treatment of breast milk for prevention of cytomegalovirus infection. Pediatrics International 61:1227-1231.
306. Moylan DC, Pati SK, Ross SA, Fowler KB, Boppana SB, Sabbaj S. 2017. Breast Milk Human Cytomegalovirus (CMV) Viral Load and the Establishment of Breast Milk CMV-pp65-Specific CD8 T Cells in Human CMV Infected Mothers. The Journal of infectious diseases 216:1176-1179.
307. Ho FC, Wong RL, Lawton JW. 1979. Human Colostral and Breast Milk Cells A Light and Electron Microscopic Study. Acta Paediatrica 68:389-396.
308. Brooker B. 1980. The epithelial cells and cell fragments in human milk. Cell tissue research 210:321-332.
309. McTiernan CF, Morel P, Cooper LT, Rajagopalan N, Thohan V, Zucker M, Boehmer J, Bozkurt B, Mather P, Thornton J. 2018. Circulating T-cell subsets, monocytes, and natural killer cells in peripartum cardiomyopathy: results from the multicenter IPAC study. Journal of cardiac failure 24:33-42.
310. Tsai JH, Tsai CH, Cheng MH, Lin SJ, Xu FL, Yang CC. 2005. Association of viral factors with non-familial breast cancer in Taiwan by comparison with non-cancerous, fibroadenoma, and thyroid tumor tissues. J Med Virol 75:276-281.
311. Harkins LE, Matlaf LA, Soroceanu L, Klemm K, Britt WJ, Wang W, Bland KI, Cobbs CS. 2010. Detection of human cytomegalovirus in normal and neoplastic breast epithelium. Herpesviridae 1:8.
312. Jakubzick CV, Randolph GJ, Henson PM. 2017. Monocyte differentiation and antigen-presenting functions. Nature Reviews Immunology 17:349-362.
313. Mandruzzato S, Brandau S, Britten CM, Bronte V, Damuzzo V, Gouttefangeas C, Maurer D, Ottensmeier C, van der Burg SH, Welters MJ. 2016. Toward harmonized phenotyping of human myeloid-derived suppressor cells by flow cytometry: results from an interim study. Cancer Immunol, Immunother 65:161-169.
314. Köstlin N, Kugel H, Spring B, Leiber A, Marmé A, Henes M, Rieber N, Hartl D, Poets CF, Gille C. 2014. Granulocytic myeloid derived suppressor cells expand in human pregnancy and modulate T-cell responses. Eur J Immunol 44:2582-2591.
315. Pan T, Zhong L, Wu S, Cao Y, Yang Q, Cai Z, Cai X, Zhao W, Ma N, Zhang W. 2016. 17β-Oestradiol enhances the expansion and activation of myeloid-derived suppressor cells via signal transducer and activator of transcription (STAT)− 3 signalling in human pregnancy. Clinical & Experimental Immunology 185:86-97.
316. Rivas RA, El-Mohandes AA, Katona IM. 1994. Mononuclear phagocytic cells in human milk: HLA-DR and FcγR ligand expression. Neonatology 66:195-204.
317. Köstlin N, Schoetensack C, Schwarz J, Spring B, Marmé A, Goelz R, Brodbeck G, Poets CF, Gille C. 2018. Granulocytic myeloid-derived suppressor cells (GR-MDSC) in breast milk (BM); GR-MDSC accumulate in human BM and modulate T-cell and monocyte function. Frontiers in immunology 9:1098.
318. Kraus TA, Engel SM, Sperling RS, Kellerman L, Lo Y, Wallenstein S, Escribese MM, Garrido JL, Singh T, Loubeau M. 2012. Characterizing the pregnancy immune phenotype: results of the viral immunity and pregnancy (VIP) study. J Clin Immunol 32:300-311.
319. Wistuba-Hamprecht K, Haehnel K, Janssen N, Demuth I, Pawelec G. 2015. Peripheral blood T-cell signatures from high-resolution immune phenotyping of γδ and αβ T-cells in younger and older subjects in the Berlin Aging Study II. Immunity & Ageing 12:25.

320. Seelig Jr LL, Head JR. 1987. Uptake of lymphocytes fed to suckling rats. An autoradiographic study of the transit of labeled cells through the neonatal gastric mucosa. J Reprod Immunol 10:285-297.
321. Tuboly S, Bernath S, Glavits R, Kovacs A, Megyeri Z. 1995. Intestinal absorption of colostral lymphocytes in newborn lambs and their role in the development of immune status. Acta Veterinaria Hungarica 43:105-115.
322. Tuboly S, Bernath S. 2002. Intestinal absorption of colostral lymphoid cells in newborn animals, p 107-114, Integrating population outcomes, biological mechanisms and research methods in the study of human milk and lactation. Springer.
323. Cabinian A, Sinsimer D, Tang M, Zumba O, Mehta H, Toma A, Sant'Angelo D, Laouar Y, Laouar A. 2016. Transfer of maternal immune cells by breastfeeding: maternal cytotoxic T lymphocytes present in breast milk localize in the Peyer's patches of the nursed infant. PloS one 11:e0156762.
324. Hanson LÅ, Korotkova M, Håversen L, Mattsby-Baltzer I, Hahn-Zoric M, Silfverdal SA, Strandvik B, Telemo E. 2002. Breast-feeding, a complex support system for the offspring. Pediatrics International 44:347-352.
325. Jain L, Vidyasagar D, Xanthou M, Ghai V, Shimada S, Blend M. 1989. In vivo distribution of human milk leucocytes after ingestion by newborn baboons. Arch Dis Child 64:930-933.
326. Ma LJ, Walter B, DeGuzman A, Muller HK, Walker AM. 2008. Trans-epithelial immune cell transfer during suckling modulates delayed-type hypersensitivity in recipients as a function of gender. PloS one 3.
327. Zhou L, Yoshimura Y, Huang YY, Suzuki R, Yokoyama M, Okabe M, Shimamura M. 2000. Two independent pathways of maternal cell transmission to offspring: through placenta during pregnancy and by breast-feeding after birth. Immunology 101:570-580.
328. Arvola M, Gustafsson E, Svensson L, Jansson L, Holmdahl R, Heyman B, Okabe M, Mattsson R. 2000. Immunoglobulin-secreting cells of maternal origin can be detected in B cell-deficient mice. Biol Reprod 63:1817-1824.
329. Hughes A, Brock J, Parrott D, Cockburn F. 1988. The interaction of infant formula with macrophages: effect on phagocytic activity, relationship to expression of class II MHC antigen and survival of orally administered macrophages in the neonatal gut. Immunology 64:213.
330. Loubiere LS, Lambert NC, Flinn LJ, Erickson TD, Yan Z, Guthrie KA, Vickers KT, Nelson JL. 2006. Maternal microchimerism in healthy adults in lymphocytes, monocyte/macrophages and NK cells. Lab Invest 86:1185-1192.
331. Kinder JM, Stelzer IA, Arck PC, Way SS. 2017. Immunological implications of pregnancy-induced microchimerism. Nature Reviews Immunology 17:483.
332. Molès J-P, Tuaillon E, Kankasa C, Bedin A-S, Nagot N, Marchant A, McDermid JM, Van de Perre P. 2017. Breastfeeding-related maternal microchimerism. Nature Reviews Immunology 17:729-729.
333. Molès JP, Tuaillon E, Kankasa C, Bedin AS, Nagot N, Marchant A, McDermid JM, Van de Perre P. 2018. Breastmilk cell trafficking induces microchimerism-mediated immune system maturation in the infant. Pediatric allergy and immunology 29:133-143.
334. Campbell JD, Lorber M, Sweeton J, Turcotte J, Niederhuber J, Beer A. 1984. Breast feeding and maternal-donor renal allografts. Possibly the original donor-specific transfusion. Transplantation 37:340-344.
335. Klenerman P, Oxenius A. 2016. T cell responses to cytomegalovirus. Nature Reviews Immunology 16:367.
336. Smith CJ, Quinn M, Snyder CM. 2016. CMV-specific CD8 T cell differentiation and localization: implications for adoptive therapies. Frontiers in immunology 7:352.
337. Riou R, Bressollette-Bodin C, Boutoille D, Gagne K, Rodallec A, Lefebvre M, Raffi F, Senitzer D, Imbert-Marcille B-M, Retière C. 2017. Severe symptomatic primary human cytomegalovirus infection despite effective innate and adaptive immune responses. J Virol 91:e02245-16.
338. Hsu PS, Nanan R. 2018. Does breast milk nurture T lymphocytes in their cradle? Frontiers in pediatrics 6.
339. Ghosh MK, Nguyen V, Muller HK, Walker AM. 2016. Maternal milk T cells drive development of transgenerational Th1 immunity in offspring thymus. The Journal of Immunology 197:2290-2296.
340. Hasselbalch H, Jeppesen D, Engelmann M, Michaelsen K, Nielsen M. 1996. Decreased thymus size in formula-fed infants compared with breastfed infants. Acta paediatrica 85:1029-1032.

341. Malavasi F, Deaglio S, Funaro A, Ferrero E, Horenstein AL, Ortolan E, Vaisitti T, Aydin S. 2008. Evolution and function of the ADP ribosyl cyclase/CD38 gene family in physiology and pathology. Physiol Rev 88:841-886.
342. Sabbaj S, Ghosh MK, Edwards BH, Leeth R, Decker WD, Goepfert PA, Aldrovandi GM. 2005. Breast milk-derived antigen-specific CD8+ T cells: an extralymphoid effector memory cell population in humans. The Journal of Immunology 174:2951-2956.
343. Vollbrecht T, Brackmann H, Henrich N, Roeling J, Seybold U, Bogner JR, Goebel FD, Draenert R. 2010. Impact of changes in antigen level on CD38/PD-1 co-expression on HIV-specific CD8 T cells in chronic, untreated HIV-1 infection. J Med Virol 82:358-370.
344. Savarino A, Bottarel F, Malavasi F, Dianzani U. 2000. Role of CD38 in HIV-1 infection: an epiphenomenon of T-cell activation or an active player in virus/host interactions? AIDS 14:1079-1089.
345. Wang Y, Liu Y, Han R, Li Q, Yao Z, Niu W, Yuan Y, Tang Z, Zhu Z, Shen Z. 2010. Monitoring of CD95 and CD38 expression in peripheral blood T lymphocytes during active human cytomegalovirus infection after orthotopic liver transplantation. Journal of gastroenterology and hepatology 25:138-142.
346. Wang Y, Liu Y, Zhang Y, Peng L, Ma J, Tang Z, Gao W, Zhu Z, Yao Z. 2006. The role of the CD95, CD38 and TGFβ1 during active human cytomegalovirus infection in liver transplantation. Cytokine 35:193-199.
347. Suricoc N, Dianzani U, Mehtad K, Malavasi F. 2000. CD38/CD31, a receptor/ligand system ruling adhesion and signaling in human leukocytes. Human CD38 and Related Molecules 75:99-120.
348. Apoil P, Puissant-Lubrano B, Congy-Jolivet N, Peres M, Tkaczuk J, Roubinet F, Blancher A. 2017. Influence of age, sex and HCMV-serostatus on blood lymphocyte subpopulations in healthy adults. Cell Immunol 314:42-53.
349. Peroni DG, Chirumbolo S, Veneri D, Piacentini GL, Tenero L, Vella A, Ortolani R, Raffaelli R, Boner AL. 2013. Colostrum-derived B and T cells as an extra-lymphoid compartment of effector cell populations in humans. The Journal of Maternal-Fetal & Neonatal Medicine 26:137-142.
350. Keeney SE, Schmalstieg FC, Palkowetz KH, Rudloff HE, Le BM, Goldman AS. 1993. Activated neutrophils and neutrophil activators in human milk: increased expression of CD11b and decreased expression of L-selectin. J Leukocyte Biol 54:97-104.
351. Pitt J. 1979. The milk mononuclear phagocyte. Pediatrics 64:745-749.
352. Järvinen K-M, Juntunen-Backman K, Suomalainen H. 1999. Relation between weak HLA-DR expression on human breast milk macrophages and cow milk allergy (CMA) in suckling infants. Pediatric research 45:76-81.
353. Kieffer TE, Faas MM, Scherjon SA, Prins JR. 2017. Pregnancy persistently affects memory T cell populations. J Reprod Immunol 119:1-8.
354. Waller EC, Day E, Sissons JP, Wills MR. 2008. Dynamics of T cell memory in human cytomegalovirus infection. Med Microbiol Immunol 197:83-96.
355. Vieira Braga FA, Hertoghs KM, van Lier RA, van Gisbergen KP. 2015. Molecular characterization of HCMV-specific immune responses: Parallels between CD8+ T cells, CD4+ T cells, and NK cells. Eur J Immunol 45:2433-2445.
356. Fornara C, Lilleri D, Revello MG, Furione M, Zavattoni M, Lenta E, Gerna G. 2011. Kinetics of effector functions and phenotype of virus-specific and γδ T lymphocytes in primary human cytomegalovirus infection during pregnancy. J Clin Immunol 31:1054-1064.
357. Lilleri D, Fornara C, Revello MG, Gerna G. 2008. Human cytomegalovirus-specific memory CD8+ and CD4+ T cell differentiation after primary infection. The Journal of infectious diseases 198:536-543.
358. Gómez-Mora E, García E, Urrea V, Massanella M, Puig J, Negredo E, Clotet B, Blanco J, Cabrera C. 2017. Preserved immune functionality and high CMV-specific T-cell responses in HIV-infected individuals with poor CD4+ T-cell immune recovery. Scientific reports 7:1-13.
359. Lissauer D, Choudhary M, Pachnio A, Goodyear O, Moss PA, Kilby MD. 2011. Cytomegalovirus sero positivity dramatically alters the maternal CD8+ T cell repertoire and leads to the accumulation of highly differentiated memory cells during human pregnancy. Human reproduction 26:3355-3365.
360. Koch S, Solana R, Rosa OD, Pawelec G. 2006. Human cytomegalovirus infection and T cell immunosenescence: a mini review. Mechanisms of ageing and development 127:538-543.
361. Crough T, Burrows JM, Fazou C, Walker S, Davenport MP, Khanna R. 2005. Contemporaneous fluctuations in T cell responses to persistent herpes virus infections. Eur J Immunol 35:139-149.

362. Mueller SN, Mackay LK. 2016. Tissue-resident memory T cells: local specialists in immune defence. Nature Reviews Immunology 16:79.
363. Kern F, Faulhaber N, Frömmel C, Khatamzas E, Prösch S, Schönemann C, Kretzschmar I, Volkmer-Engert R, Volk HD, Reinke P. 2000. Analysis of CD8 T cell reactivity to cytomegalovirus using protein-spanning pools of overlapping pentadecapeptides. Eur J Immunol 30:1676-1682.
364. Reuschel E, Barabas S, Zeman F, Bendfeldt H, Rascle A, Deml L, Seelbach-Goebel B. 2017. Functional impairment of CMV-reactive cellular immunity during pregnancy. J Med Virol 89:324-331.
365. Pipeling MR, West EE, Osborne CM, Whitlock AB, Dropulic LK, Willett MH, Forman M, Valsamakis A, Orens JB, Moller DR. 2008. Differential CMV-specific CD8+ effector T cell responses in the lung allograft predominate over the blood during human primary infection. The Journal of Immunology 181:546-556.
366. Sabbaj S, Edwards BH, Ghosh MK, Semrau K, Cheelo S, Thea DM, Kuhn L, Ritter GD, Mulligan MJ, Goepfert PA. 2002. Human immunodeficiency virus-specific CD8+ T cells in human breast milk. J Virol 76:7365-7373.
367. Lohman BL, Slyker J, Mbori-Ngacha D, Bosire R, Farquhar C, Obimbo E, Otieno P, Nduati R, Rowland-Jones S, John-Stewart G. 2003. Prevalence and magnitude of human immunodeficiency virus (HIV) type 1–specific lymphocyte responses in breast milk from HIV-1–seropositive women. The Journal of infectious diseases 188:1666-1674.
368. Khairallah C, Déchanet-Merville J, Capone M. 2017. γδ T cell-mediated immunity to cytomegalovirus infection. Frontiers in immunology 8:105.
369. Lindstrand A, Smedman L, Gunnlaugsson G, Troye-Blomberg M. 1997. Selective compartmentalization of γσ-T lymphocytes in human breastmilk. Acta Paediatrica 86:890-891.
370. Bedin AS, Molès JP, Rutagwera D, Nagot N, Kankasa C, Tylleskär T, Valverde-Villegas JM, Durand M, Van de Perre P, Tuaillon E. 2019. MAIT cells, TCR γδ+ cells and ILCs cells in human breast milk and blood from HIV infected and uninfected women. Pediatric Allergy and Immunology 30:479-487.
371. Gibson C, Eglinton B, Penttila I, Cummins A. 1991. Phenotype and activation of milk-derived and peripheral blood lymphocytes from normal and coeliac subjects. Immunol Cell Biol 69:387-393.
372. Groer M, El-Badri N, Djeu J, Harrington M, Van Eepoel J. 2010. Suppression of natural killer cell cytotoxicity in postpartum women. Am J Reprod Immunol 63:209-213.
373. Groer MW, El-Badri N, Djeu J, Williams SN, Kane B, Szekeres K. 2014. Suppression of natural killer cell cytotoxicity in postpartum women: time course and potential mechanisms. Biological research for nursing 16:320-326.
374. López-Botet M, Muntasell A, Vilches C. The CD94/NKG2C+ NK-cell subset on the edge of innate and adaptive immunity to human cytomegalovirus infection, p 145-151. *In* (ed), Elsevier,
375. Vorbach C, Capecchi MR, Penninger JM. 2006. Evolution of the mammary gland from the innate immune system? Bioessays 28:606-616.
376. Goldman AS. 2002. Evolution of the mammary gland defense system and the ontogeny of the immune system. Journal of mammary gland biology and neoplasia 7:277-289.
377. McClellan HL, Miller SJ, Hartmann PE. 2008. Evolution of lactation: nutrition v. protection with special reference to five mammalian species. Nutrition research reviews 21:97-116.
378. Baggiolini M, Dewald B, Moser B. 1997. Human chemokines: an update. Annu Rev Immunol 15:675-705.
379. Schoenborn JR, Wilson CB. 2007. Regulation of interferon-γ during innate and adaptive immune responses. Adv Immunol 96:41-101.
380. Tokunaga R, Zhang W, Naseem M, Puccini A, Berger MD, Soni S, McSkane M, Baba H, Lenz H-J. 2018. CXCL9, CXCL10, CXCL11/CXCR3 axis for immune activation–a target for novel cancer therapy. Cancer treatment reviews 63:40-47.
381. Bonecchi R, Bianchi G, Bordignon PP, D'Ambrosio D, Lang R, Borsatti A, Sozzani S, Allavena P, Gray PA, Mantovani A. 1998. Differential expression of chemokine receptors and chemotactic responsiveness of type 1 T helper cells (Th1s) and Th2s. The Journal of experimental medicine 187:129-134.
382. Campbell JD, Gangur V, Simons FER, HayGlass KT. 2004. Allergic humans are hyporesponsive to a CXCR3 ligand-mediated Th1 immunity-promoting loop. The FASEB Journal 18:329-331.
383. Romagnani S. 2000. T-cell subsets (Th1 versus Th2). Ann Allergy, Asthma Immunol 85:9-21.

384. van de Berg PJ, Heutinck KM, Raabe R, Minnee RC, Young SL, van Donselaar-van der Pant KA, Bemelman FJ, van Lier RA, ten Berge IJ. 2010. Human cytomegalovirus induces systemic immune activation characterized by a type 1 cytokine signature. The Journal of infectious diseases 202:690-699.
385. Weseslindtner L, Nachbagauer R, Kundi M, Jaksch P, Kerschner H, Simon B, Hatos-Agyi L, Scheed A, Aberle J, Klepetko W. 2011. Human cytomegalovirus infection in lung transplant recipients triggers a CXCL-10 response. Am J Transplantation 11:542-552.
386. Cheung TC, Humphreys IR, Potter KG, Norris PS, Shumway HM, Tran BR, Patterson G, Jean-Jacques R, Yoon M, Spear PG. 2005. Evolutionarily divergent herpesviruses modulate T cell activation by targeting the herpesvirus entry mediator cosignaling pathway. Proceedings of the National Academy of Sciences 102:13218-13223.
387. Ware CF, Šedý JR. 2011. TNF Superfamily Networks: bidirectional and interference pathways of the herpesvirus entry mediator (TNFSF14). Curr Opin Immunol 23:627-631.
388. Murphy KM, Nelson CA, Šedý JR. 2006. Balancing co-stimulation and inhibition with BTLA and HVEM. Nature Reviews Immunology 6:671-681.
389. Picarda G, Benedict CA. 2018. Cytomegalovirus: shape-shifting the immune system. The Journal of Immunology 200:3881-3889.
390. Bitra A, Nemčovičová I, Picarda G, Doukov T, Wang J, Benedict CA, Zajonc DM. 2019. Structure of human cytomegalovirus UL144, an HVEM orthologue, bound to the B and T cell Lymphocyte Attenuator. J Biol Chem 294:10519-10529.
391. Ware CF. 2008. Targeting lymphocyte activation through the lymphotoxin and LIGHT pathways. Immunol Rev 223:186-201.
392. Ritter T, Brandt C, Prösch S, Vergopoulos A, Vogt K, Kolls J, Volk H-D. 2000. Stimulatory and inhibitory action of cytokines on the regulation of hCMV-IE promoter activity in human endothelial cells. Cytokine 12:1163-1170.
393. Chawanpaiboon S, Vogel JP, Moller A-B, Lumbiganon P, Petzold M, Hogan D, Landoulsi S, Jampathong N, Kongwattanakul K, Laopaiboon M. 2019. Global, regional, and national estimates of levels of preterm birth in 2014: a systematic review and modelling analysis. The Lancet Global Health 7:e37-e46.
394. Gidrewicz DA, Fenton TR. 2014. A systematic review and meta-analysis of the nutrient content of preterm and term breast milk. BMC pediatrics 14:216.
395. Agarwal S, Karmaus W, Davis S, Gangur V. 2011. Immune markers in breast milk and fetal and maternal body fluids: a systematic review of perinatal concentrations. Journal of Human Lactation 27:171-186.
396. Khan S, Hepworth AR, Prime DK, Lai CT, Trengove NJ, Hartmann PE. 2013. Variation in fat, lactose, and protein composition in breast milk over 24 hours: associations with infant feeding patterns. Journal of human lactation 29:81-89.
397. Bapistella S, Hamprecht K, Thomas W, Speer CP, Dietz K, Maschmann J, Poets CF, Goelz R. 2019. Short-term pasteurization of breast milk to prevent postnatal cytomegalovirus transmission in very preterm infants. Clin Infect Dis 69:438-444.

7 Supplement

Supplement table 1: Synopsis of BlooMil study cell subset frequencies
NK: natural killer cells, T_{EMRA}: TEMRA cells, $T_{naïve}$: naïve T cells, T_{EM}: effector memory T cells, T_{CM}: central memory T cells, BM: breast milk. Friedman test shows significances in the kinetics, while the linear mixed model points out different developments of the kinetics between HCMV-seropositive or-negative mothers.

Cell subsets	compartment	CMV	T1 [% mean ± SD]	T2 [% mean ± SD]	T3 [% mean ± SD]	T4 [% mean ± SD]	Friedman test [p-value]	linear mixed model
CD45⁺ Leukocytes	PBMC	IgG⁺	**86.6 ± 5.8**	**91.3 ± 3.3**	**90.9 ± 3.1**	**92.0 ± 3.7**	**0.001**	0.280
		IgG-	**78.0 ± 26.2**	**90.7 ± 3.3**	**92.3 ± 1.7**	**92.0 ± 4.0**	**0.004**	
	BMC	IgG⁺	8.0 ± 16.4	6.6 ± 7.4	9.50 ± 17.5	4.09 ± 5.0	0.208	0.537
		IgG-	3.7 ± 7.1	3.6 ± 5.4	7.7 ± 12.4	5.6 ± 7.9	0.197	
CD14⁺ Monocytes	PBMC	IgG⁺	18.6 ± 7.5	16.0 ± 3.9	18.1 ± 4.9	17.2 ± 4.9	0.196	0.437
		IgG-	18.8 ± 4.9	18.3 ± 3.7	18.7 ± 5.8	17.4 ± 5.1	0.293	
	BMC	IgG⁺	**27.0 ± 11.7**	**22.6 ± 12.7**	**12.3 ± 5.3**	**15.8 ± 11.0**	**0.004**	0.212
		IgG-	**25.1 ± 17.4**	**18.4 ± 12.4**	**16.6 ± 10.6**	**15.9 ± 8.8**	**0.045**	
CD14⁺, HLA-DR⁺ MDSC	PBMC	IgG⁺	*17.5 ± 7.1*	*14.9 ± 3.6*	*17.1 ± 4.5*	*16.3 ± 4.7*	*0.078*	0.341
		IgG-	17.7 ± 4.6	17.3 ± 3.5	17.7 ± 5.7	16.3 ± 4.8	0.430	
	BMC	IgG⁺	**3.1 ± 3.1**	**2.6 ± 3.5**	**1.1 ± 0.8**	**1.0 ± 0.8**	**0.009**	0.585
		IgG-	6.0 ± 9.6	2.6 ± 2.3	1.9 ± 1.3	1.9 ± 1.5	0.672	
CD3⁺ T cells	PBMC	IgG⁺	57.3 ± 9.7	60.3 ± 6.5	57.6 ± 7.9	59.7 ± 5.9	0.514	0.829
		IgG-	58.1 ± 5.4	59.5 ± 4.9	58.9 ± 7.9	59.6 ± 7.1	0.160	
	BMC	IgG⁺	**25.1 ± 14.4**	**29.7 ± 18.5**	**38.6 ± 19.7**	**43.7 ± 15.1**	**0.008**	**0.043**
		IgG-	25.6 ± 10.2	25.6 ± 11.5	24.6 ± 11.4	21.9 ± 13.3	0.218	
CD4⁺ T cells	PBMC	IgG⁺	**62.6 ± 7.5**	**62.0 ± 7.1**	**61.6 ± 7.8**	**60.6 ± 7.5**	**0.015**	0.901
		IgG-	64.3 ± 5.6	64.2 ± 5.6	63.5 ± 6.1	63.1 ± 6.2	0.564	
	BMC	IgG⁺	51.8 ± 9.3	49.9 ± 10.5	50.6 ± 12.3	49.4 ± 9.1	0.863	0.141
		IgG-	*60.3 ± 7.0*	*61.0 ± 11.9*	*63.3 ± 10.0*	*65.9 ± 6.5*	*0.077*	
CD4⁺ CD38⁺ T cells	PBMC	IgG⁺	**67.4 ± 10.1**	**66.2 ± 9.2**	**65.0 ± 10.1**	**63.8 ± 10.0**	**0.006**	0.288
		IgG-	67.4 ± 10.9	68.5 ± 11.3	67.9 ± 9.5	67.9 ± 9.8	0.840	
	BMC	IgG⁺	42.0 ± 12.1	47.0 ± 13.7	46.9 ± 11.7	45.0 ± 9.6	0.255	0.349
		IgG-	41.5 ± 16.0	41.3 ± 10.5	36.5 ± 6.9	34.7 ± 7.0	0.293	
CD4⁺ HLA-DR⁺ T cells	PBMC	IgG⁺	*2.3 ± 1.4*	*2.7 ± 1.4*	*3.0 ± 2.0*	*2.7 ± 1.3*	*0.057*	0.442
		IgG-	2.1 ± 1.2	2.0 ± 0.8	1.9 ± 0.5	1.6 ± 0.4	0.451	
	BMC	IgG⁺	**11.1 ± 4.4**	**14.9 ± 6.8**	**18.6 ± 7.2**	**19.6 ± 7.3**	**<0.001**	0.108
		IgG-	15.1 ± 10.4	15.1 ± 4.2	15.4 ± 5.7	14.8 ± 7.0	0.472	
CD4⁺ T_N	PBMC	IgG⁺	**56.5 ± 10.6**	**54.1 ± 9.9**	**53.3 ± 11.0**	**51.7 ± 10.5**	**0.008**	**0.025**
		IgG-	60.0 ± 12.2	62.7 ± 12.3	61.6 ± 10.0	61.5 ± 10.7	0.293	
	BMC	IgG⁺	**3.8 ± 2.0**	**4.1 ± 1.9**	**3.9 ± 3.0**	**2.6 ± 1.3**	**0.015**	0.349
		IgG-	4.0 ± 1.8	4.0 ± 1.8	3.6 ± 1.3	3.9 ± 2.0	0.540	
CD4⁺ T_{CM}	PBMC	IgG⁺	30.1 ± 7.2	30.9 ± 7.6	31.2 ± 7.5	31.2 ± 6.3	0.500	0.242
		IgG-	31.5 ± 11.7	29.6 ± 11.2	29.7 ± 8.8	30.1 ± 8.9	0.339	
	BMC	IgG⁺	**55.0 ± 7.0**	**54.4 ± 7.9**	**52.3 ± 9.6**	**46.8 ± 7.9**	**0.002**	0.295
		IgG-	51.0 ± 13.4	52.7 ± 9.6	51.9 ± 10.9	50.9 ± 10.2	0.896	
CD4⁺ T_{EM}	PBMC	IgG⁺	**10.5 ± 6.3**	**11.5 ± 5.4**	**12.0 ± 5.6**	**13.6 ± 7.1**	**<0.001**	*0.053*
		IgG-	**7.8 ± 1.7**	**6.9 ± 1.3**	**7.9 ± 1.9**	**7.7 ± 2.0**	**0.036**	

	BMC	IgG$^+$	**38.4 ± 6.4**	**39.1 ± 7.8**	**41.6 ± 8.6**	**47.9 ± 7.6**	**<0.001**	0.237
		IgG-	41.4 ± 13.1	40.6 ± 10.6	41.8 ± 10.7	42.3 ± 10.6	0.923	
CD4$^+$ T_{EMRA}	PBMC	IgG$^+$	3.0 ± 2.2	3.6 ± 3.0	3.4 ± 2.6	3.6 ± 2.6	0.295	0.421
		IgG-	0.7 ± 0.3	0.8 ± 0.3	0.8 ± 0.3	0.7 ± 0.3	0.218	
	BMC	IgG$^+$	2.7 ± 2.2	2.4 ± 1.5	2.2 ± 1.6	2.6 ± 2.5	0.295	0.668
		IgG-	3.6 ± 1.9	2.7 ± 2.1	2.7 ± 1.8	3.0 ± 2.4	0.253	
CD8$^+$ T cells	PBMC	IgG$^+$	*30.1 ± 6.7*	*30.7 ± 6.2*	*30.9 ± 6.9*	*31.5 ± 6.5*	*0.089*	0.854
		IgG-	29.2 ± 3.9	29.3 ± 4.1	29.6 ± 4.5	29.9 ± 4.6	0.668	
	BMC	IgG$^+$	33.7 ± 6.0	36.6 ± 8.9	36.5 ± 10.5	37.5 ± 6.9	0.184	**0.028**
		IgG-	27.1 ± 6.6	26.2 ± 7.1	24.9 ± 8.1	22.7 ± 6.4	0.356	
CD8$^+$ CD38$^+$ T cells	PBMC	IgG$^+$	**69.8 ± 10.7**	**67.7 ± 9.7**	**65.9 ± 10.1**	**64.1 ± 10.9**	**<0.001**	0.501
		IgG-	66.7 ± 12.5	67.3 ± 11.7	66.1 ± 11.5	64.5 ± 11.2	0.696	
	BMC	IgG$^+$	*56.8 ± 9.0*	*57.9 ± 11.6*	*63.0 ± 12.0*	*61.8 ± 10.6*	*0.083*	0.603
		IgG-	59.4 ± 12.8	59.5 ± 12.0	60.2 ± 11.1	58.2 ± 13.0	0.696	
CD8$^+$ HLA-DR$^+$ T cells	PBMC	IgG$^+$	7.1 ± 3.6	6.4 ± 2.8	6.2 ± 3.0	5.4 ± 2.8	0.089	0.378
		IgG-	2.5 ± 1.2	3.0 ± 1.3	3.4 ± 1.6	2.6 ± 1.5	0.615	
	BMC	IgG$^+$	**15.3 ± 8.1**	**18.3 ± 9.1**	**24.9 ± 12.5**	**25.1 ± 9.2**	**0.001**	0.327
		IgG-	9.8 ± 4.1	15.0 ± 6.4	16.8 ± 7.5	15.1 ± 9.0	0.494	
CD8$^+$ T_N	PBMC	IgG$^+$	**51.6 ± 11.7**	**48.9 ± 11.9**	**47.4 ± 12.4**	**45.2 ± 12.6**	**<0.001**	**0.043**
		IgG-	63.2 ± 10.7	66.3 ± 10.6	63.5 ± 9.2	62.7 ± 11.1	0.356	
	BMC	IgG$^+$	**15.8 ± 5.0**	**15.3 ± 5.9**	**13.1 ± 6.1**	**10.6 ± 4.3**	**0.001**	0.379
		IgG-	13.7 ± 6.4	12.5 ± 4.7	13.4 ± 5.6	11.7 ± 4.0	0.323	
CD8$^+$ T_{CM}	PBMC	IgG$^+$	5.4 ± 2.8	5.2 ± 2.8	5.1 ± 2.5	5.3 ± 2.1	0.392	0.858
		IgG-	4.9 ± 2.5	4.3 ± 2.0	4.3± 1.8	4.7 ± 1.8	0.266	
	BMC	IgG$^+$	11.6 ± 5.1	10.7 ± 3.7	11.3 ± 5.0	10.7 ± 4.5	0.678	0.740
		IgG-	12.1 ± 5.3	11.5 ± 5.4	13.8 ± 7.6	12.3 ± 5.0	0.589	
CD8$^+$ T_{EM}	PBMC	IgG$^+$	**10.3 ± 4.1**	**11.1 ± 5.0**	**11.8 ± 5.2**	**12.8 ± 5.4**	**<0.001**	0.106
		IgG-	10.0 ± 5.3	8.7 ± 4.1	9.7 ± 4.0	10.6 ± 5.0	0.104	
	BMC	IgG$^+$	**30.0 ± 8.3**	**30.0 ± 10.9**	**33.0 ± 9.6**	**35.8 ± 11.1**	**0.027**	0.448
		IgG-	**28.5 ± 10.0**	**32.3 ± 12.7**	**31.7 ± 10.9**	**34.9 ± 12.7**	**0.026**	
CD8$^+$ T_{EMRA}	PBMC	IgG$^+$	*32.7 ± 9.9*	*34.8 ± 10.1*	*35.7 ± 10.2*	*36.8 ± 11.2*	*0.061*	0.237
		IgG-	21.9 ± 6.4	20.7 ± 7.1	22.5 ± 6.5	22.1 ± 7.8	0.293	
	BMC	IgG$^+$	42.6 ± 10.8	44.1 ± 12.0	42.6 ± 11.0	42.9 ± 11.5	0.392	0.529
		IgG-	45.7 ± 8.9	43.7 ± 14.7	41.0 ± 13.6	41.2 ± 13.6	0.753	
CD56$^+$ NK cells	PBMC	IgG$^+$	8.9 ± 3.8	9.1 ± 3.8	9.3 ± 4.2	9.4 ± 4.1	0.957	0.698
		IgG-	10.8 ± 2.6	9.8 ± 2.0	9.9 ± 2.4	10.2 ± 3.2	0.615	
	BMC	IgG$^+$	**4.7 ± 3.2**	**3.5 ± 2.2**	**4.1 ± 2.0**	**5.0 ± 3.0**	**0.028**	0.292
		IgG-	6.3 ± 2.3	5.9 ± 3.5	6.2 ± 5.4	5.3 ± 3.5	0.229	
CD3$^+$ CD56$^+$ NKT-like cells	PBMC	IgG$^+$	5.3 ± 3.6	5.3 ± 3.5	5.0 ± 3.3	5.1 ± 3.2	0.248	0.420
		IgG-	4.6 ± 2.7	4.1 ± 3.2	4.3 ± 3.2	4.4 ± 3.2	0.292	
	BMC	IgG$^+$	**3.6 ± 2.3**	**3.8 ± 3.5**	**3.0 ± 2.0**	**2.8 ± 1.7**	**0.025**	0.911
		IgG-	5.1 ± 2.7	4.7 ± 3.4	3.9 ± 2.7	3.8 ± 2.3	0.218	

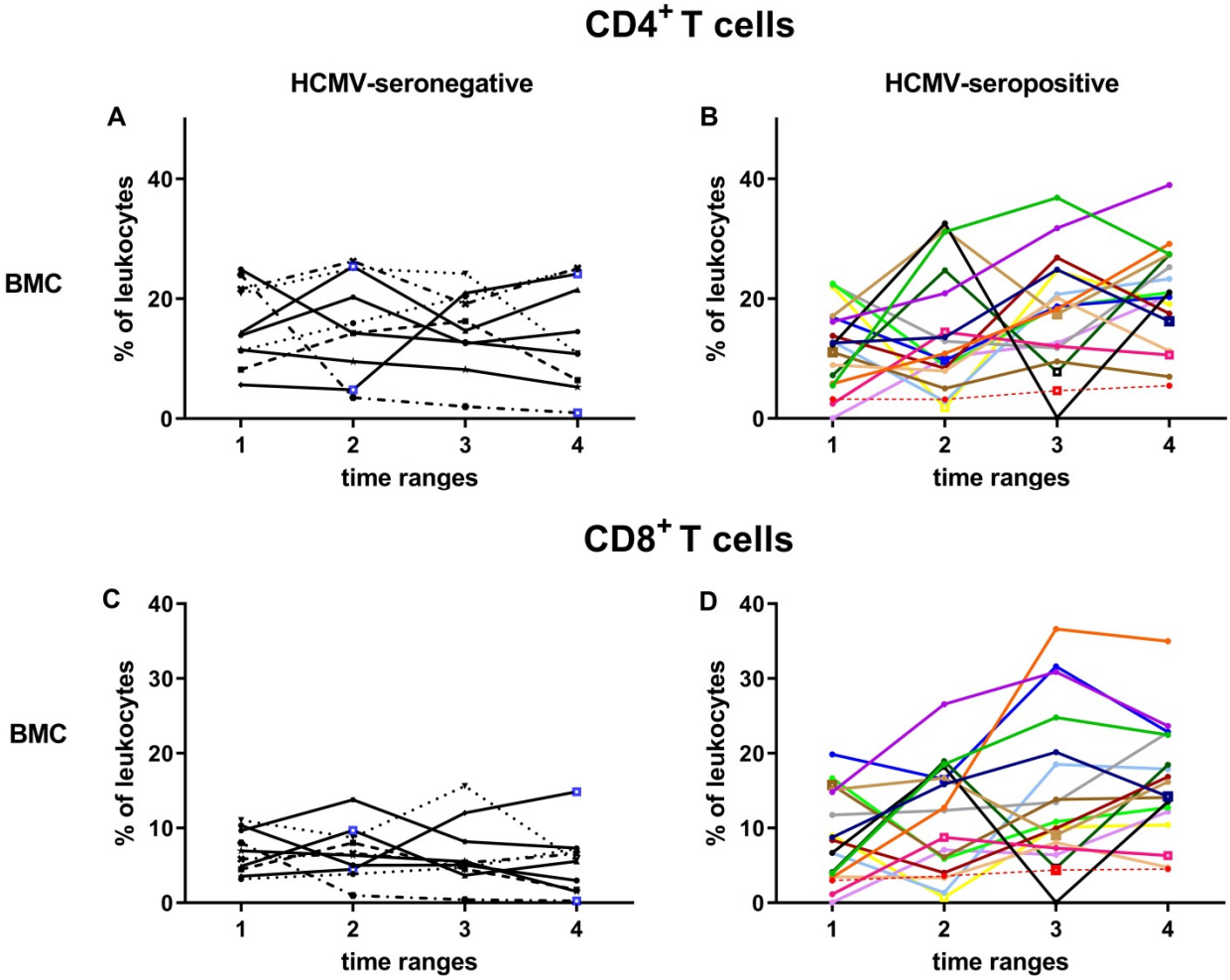

Supplement figure 1: CD4⁺ and CD8⁺ T cell kinetics in breast milk of BlooMil study mothers. *CD4⁺ T cell frequencies of leukocytes acquired by flow cytometry are shown of breast milk cells (BMC) in (A) HCMV-seronegative mothers and (B) seropositive mothers. CD8⁺ T cell frequencies of breast milk cells (BMC) are displayed of (C) HCMV-seronegative and (D) seropositive mothers. Mother 12 (red, dotted line) was excluded from statistical analysis due to HCMV-primary infection during pregnancy. The time ranges are T1 - 10 to 15, T2 - 25 to 30, T3 - 40 to 45 and T4 - 55 to 60 days p.p. Square data point symbols instead of round symbols indicate a time point, where breast milk cells showed a slightly red color in the cell pellet (presumably an indicator for mastitis).*

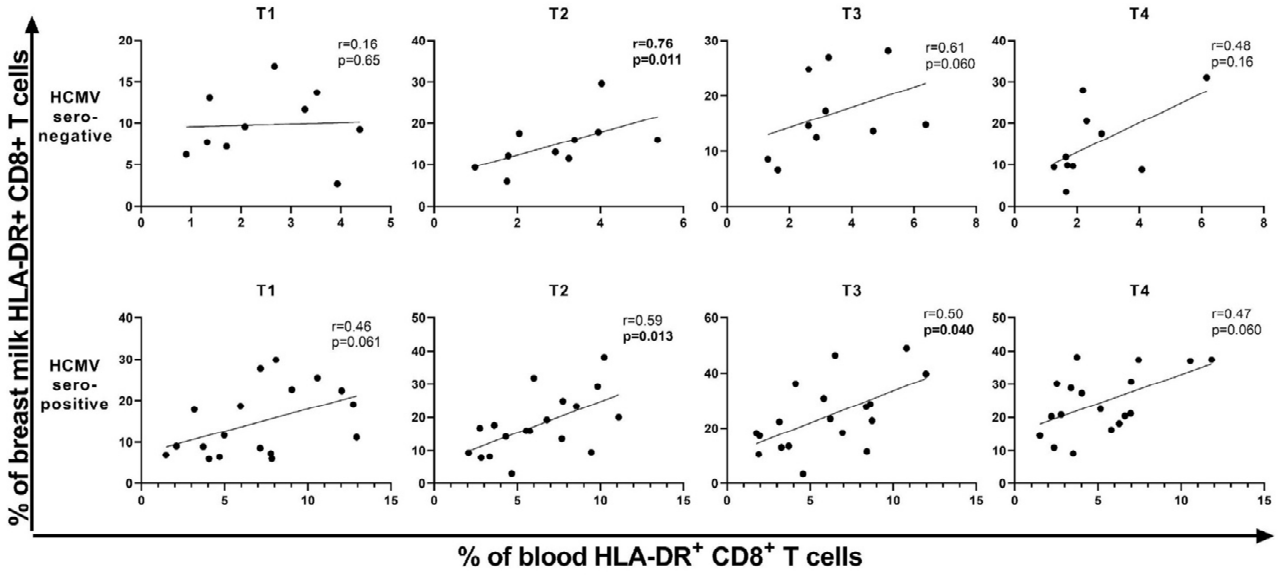

Supplement figure 2: Correlation of CD8⁺ HLA-DR⁺ T cells *Spearman's rank correlation was performed, and a non-linear regression used to display the line. Correlations of blood and breast milk CD8⁺ HLA-DR⁺ T cells of HCMV-seronegative and seropositive mothers at T1 – 10 to 15 days, T2 – 25 to 30, T3 – 40 to 45 and T4 – 55 to 60 days p.p.*

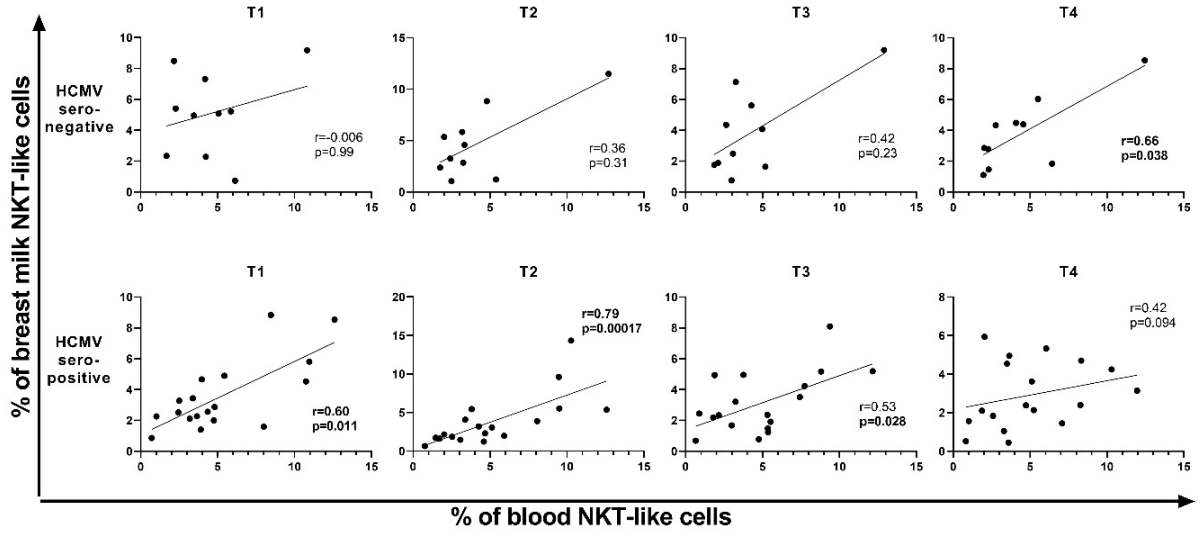

Supplement figure 3: NKT-like cell correlations *Spearman's rank correlation was performed, and a non-linear regression used to display the line. Correlations of blood and breast milk NKT-like cells of HCMV-seronegative and seropositive mothers at T1 – 10 to 15 days, T2 – 25 to 30, T3 – 40 to 45 and T4 – 55 to 60 days p.p.*

Supplement table 2: CD4⁺ T cell memory phenotype statistics

CD4⁺ T cells				
Naïve (CCR7⁺,CD45RA⁺)	PBMC HCMV pos	PBMC HCMV neg	BMC HCMV pos	BMC HCMV neg
Friedman test	**0.0083**	0.29	**0.015**	0.54
post-hoc test with Bonferroni correction	T1 to T2: 0.28 T1 to T3: 0.10 **T1 to T4: 0.0054** T2 to T3: 1.0	-	T1 to T2: 1.0 T1 to T3: 1.0 **T1 to T4: 0.032** T2 to T3: 1.0 **T2 to T4: 0.032**	-

	T2 to T4: 1.0 T3 to T4: 1.0		T3 to T4: 0.67	
Linear mixed model	**0.025**		0.35	
Mann-Whitney U with B. correction T1‘s T2‘s T3‘s T4‘s	 1.0 0.16 0.33 0.094		 1.0 1.0 1.0 0.51	
Wilcoxon with B. correction	PBMC HCMV pos	BMC HCMV pos	PBMC HCMV neg	BMC HCMV neg
T1‘s T2‘s T3‘s T4‘s	**0.0012** **0.0012** **0.0012** **0.0012**		**0.020** **0.020** **0.020** **0.020**	
Central memory (CCR7⁺, CD45RA-)	PBMC HCMV pos	PBMC HCMV neg	BMC HCMV pos	BMC HCMV neg
Friedman test	0.50	0.34	**0.0018**	0.90
post-hoc test with Bonferroni correction			T1 to T2: 1.0 T1 to T3: 0.86 **T1 to T4: 0.0020** T2 to T3: 1.0 **T2 to T4: 0.013** T3 to T4: 0.20	
Linear mixed model	0.24		0.30	
Mann-Whitney U with B. correction	all 1.0		all 1.0	
Wilcoxon with B. correction	PBMC HCMV pos	BMC HCMV pos	PBMC HCMV neg	BMC HCMV neg
T1‘s T2‘s T3‘s T4‘s	**0.0012** **0.0012** **0.0012** **0.0017**		**0.020** **0.020** **0.020** **0.020**	
Effector memory (CCR7-, CD45RA-)	PBMC HCMV pos	PBMC HCMV neg	BMC HCMV pos	BMC HCMV neg
Friedman test	**0.000048**	0.36	**0.00035**	0.92
post-hoc test with Bonferroni correction	T1 to T2: 0.20 **T1 to T3: 0.013** **T1 to T4: 0.00002** T2 to T3: 1.0 T2 to T4: 0.070 T3 to T4: 0.67	-	T1 to T2: 1.0 T1 to T3: 1.0 **T1 to T4: 0.0012** T2 to T3: 1.0 **T2 to T4: 0.0012** T3 to T4: 0.10	-
Linear mixed model	0.053		0.24	
Mann-Whitney U with B. correction T1‘s T2‘s T3‘s T4‘s	 1.0 **0.022** 0.16 **0.044**		 1.0 1.0 1.0 0.51	
Wilcoxon with B. correction	PBMC HCMV pos	BMC HCMV pos	PBMC HCMV neg	BMC HCMV neg
T1‘s T2‘s T3‘s T4‘s	**0.0012** **0.0012** **0.0012** **0.0012**		**0.020** **0.020** **0.020** **0.020**	

TEMRA (CCR7-, CD45RA$^+$)	PBMC HCMV pos	PBMC HCMV neg	BMC HCMV pos	BMC HCMV neg
Friedman test	0.30	0.22	0.30	0.25
post-hoc test with Bonferroni correction	-	-	-	-
Linear mixed model	0.42		0.67	
Mann-Whitney U with B. correction				
T1‘s	**0.0023**		0.68	
T2‘s	**0.00062**		1.0	
T3‘s	**0.0011**		1.0	
T4‘s	**0.00047**		1.0	
Wilcoxon with B. correction	PBMC HCMV pos	BMC HCMV pos	PBMC HCMV neg	BMC HCMV neg
T1‘s	1.0		**0.020**	
T2‘s	0.34		**0.028**	
T3‘s	0.30		**0.020**	
T4‘s	0.84		**0.020**	

Supplement table 3: CD8$^+$ T cell memory phenotype statistics

CD8$^+$ T cells				
Naïve (CCR7$^+$,CD45RA$^+$)	PBMC HCMV pos	PBMC HCMV neg	BMC HCMV pos	BMC HCMV neg
Friedman test	**0.00046**	0.24	**0.00082**	0.32
post-hoc test with Bonferroni correction	T1 to T2: 1.0 T1 to T3: 0.38 **T1 to T4: 0.0004** T2 to T3: 1.0 **T2 to T4: 0.009** T3 to T4: 0.20	-	T1 to T2: 1.0 T1 to T3: 0.86 **T1 to T4: 0.0012** T2 to T3: 1.0 **T2 to T4: 0.0054** T3 to T4: 0.14	-
Linear mixed model	**0.043**		0.38	
Mann-Whitney U with B. correction				
T1‘s	0.094		1.0	
T2‘s	**0.013**		1.0	
T3‘s	**0.015**		1.0	
T4‘s	**0.027**		1.0	
Wilcoxon with B. correction	PBMC HCMV pos	BMC HCMV pos	PBMC HCMV neg	BMC HCMV neg
T1‘s	**0.0012**		**0.020**	
T2‘s	**0.0012**		**0.020**	
T3‘s	**0.0012**		**0.020**	
T4‘s	**0.0012**		**0.020**	
Central memory (CCR7$^+$, CD45RA-)	PBMC HCMV pos	PBMC HCMV neg	BMC HCMV pos	BMC HCMV neg
Friedman test	0.39	0.27	0.27	0.59
post-hoc test with Bonferroni correction	-	-	-	-
Linear mixed model	0.86		0.74	
Wilcoxon with B. correction	PBMC HCMV pos	BMC HCMV pos	PBMC HCMV neg	BMC HCMV neg
T1‘s	**0.0012**		**0.020**	
T2‘s	**0.0024**		**0.020**	
T3‘s	**0.0024**		**0.020**	
T4‘s	**0.0040**		**0.020**	

Effector memory (CCR7-, CD45RA-)	PBMC HCMV pos	PBMC HCMV neg	BMC HCMV pos	BMC HCMV neg
Friedman test	**0.00024**	0.10	**0.027**	**0.026**
post-hoc test with Bonferroni correction	T1 to T2: 0.51 **T1 to T3: 0.032** **T1 to T4: 0.0001** T2 to T3: 1.0 T2 to T4: 0.070 T3 to T4: 0.86	-	T1 to T2: 1.0 T1 to T3: 1.0 **T1 to T4: 0.032** T2 to T3: 1.0 T2 to T4: 0.10 T3 to T4: 0.28	T1 to T2: 0.23 T1 to T3: 0.34 **T1 to T4: 0.019** T2 to T3: 1.0 T2 to T4: 1.0 T3 to T4: 1.0
Linear mixed model	0.11		0.45	
Wilcoxon with B. correction	PBMC HCMV pos	BMC HCMV pos	PBMC HCMV neg	BMC HCMV neg
T1‘s	**0.0012**		**0.020**	
T2‘s	**0.0012**		**0.020**	
T3‘s	**0.0012**		**0.020**	
T4‘s	**0.0012**		**0.020**	
TEMRA (CCR7-, CD45RA^{+})	PBMC HCMV pos	PBMC HCMV neg	BMC HCMV pos	BMC HCMV neg
Friedman test	0.061	0.29	0.39	0.75
post-hoc test with Bonferroni correction	-	-	-	-
Linear mixed model	0.24		0.53	
Mann-Whitney U with B. correction				
T1‘s	**0.037**		1.0	
T2‘s	**0.0023**		1.0	
T3‘s	**0.0029**		1.0	
T4‘s	**0.010**		1.0	
Wilcoxon with B. correction	PBMC HCMV pos	BMC HCMV pos	PBMC HCMV neg	BMC HCMV neg
T1‘s	0.098		**0.020**	
T2‘s	0.16		**0.020**	
T3‘s	0.20		**0.020**	
T4‘s	0.65		**0.020**	

8 Abbreviations

AD 169	HCMV laboratory strain
AC	Assembly complex
AEC	3-Amino-9-ethylcarbazole
ADCC	Antibody-dependent cell-mediated cytotoxicity
APC	Antigen presenting cells or Allophycocyanin
APC-H7	Allophycocyanin-H7
ARPE-19	Arterial retina pigment epithelial cells-19
A700	Alexa fluor 700
BM	Breast milk
BMC	Breast milk cells
BSA	Bovine serum albumin
BV711/510/421	Brilliant Violet 711 / 510 / 421
BW	Birth weight
CCR7	C-C chemokine receptor type 7
CD	Cluster of differentiation
CID	Cytomegalic inclusion disease
CM2	Fusion protein of UL57 and pUL44
CPE	Cytopathic effect
CO_2	Carbon dioxide
Colostrum	Breast milk expressed directly after birth to up to one week postpartum, high protein content
COI	Cut-off index
DMEM	Dulbecco's Modified Eagle Medium
DMF	N,N-Dimethylformamide
DMSO	Dimethylsulfoxide
DNA	Deoxyribonucleic acid
DNAemia	Detection of HCMV in blood/plasma (systemic infection)
DNAlactia	HCMV DNA was found in breast milk
dNTP	Deoxynucleotide triphosphate
ds	Double stranded
ECLIA	Electrochemiluminescence immunoassay
EDTA	Ethylenediaminetetraacetic acid
ELISA	Enzyme-linked immunosorbent assay
EMA	Ethidium monoazide bromide
ER	Endoplasmic reticulum

FACS	Fluorescence-activated cell sorting
FCS	Fetal calf serum
FMO	Fluorescence minus one
FSC	Forward scatter
FSC-A	Forward scatter- area
FSC-H	Forward scatter-height
FITC	Fluorescein isothiocyanate
g	Glycoprotein
GA	Gestational age
gB	Glycoprotein B
HBSS	Hanks balanced salt solution
HCMV	Human cytomegalovirus
HDAC	Histone deacetylase
HFF	Human foreskin fibroblasts
HHV5	Human herpesvirus 5
HIG	Hyperimmunoglobulin
HIV	Human immunodeficiency virus
HLA	Human leukocyte antigen
HP1	Heterochromatin protein 1
HRP	Horseradish peroxidase
IE	Immediate early protein
IEA	Immediate early antigen
IFN	Interferon
IgG	immunoglobulin G
IgM	Immunglobulin M
IL	Interleukin
Kbp	Kilo base pair
kD	Kilo Dalton
LB-broth	Luria Bertani broth
LCRed-640	LightCycler Red 640
LOD	Limit of detection
Mature milk	Breast milk expressed after 30 days postpartum
MHC	Major Histocompatibility Complex
MIEP	Major Immediate Early Promoter
M-MDSC	Monocytic myeloid derived suppressor cells
MW	Molecular weight
miRNA	Micro RNA

NaCl	Sodium chloride
NCAM	Neural cell adhesion molecule
ND10	Nuclear domain 10
NK cells	Natural killer cells
NT	Neutralization
NT-50	Dilution, where neutralization capacity is at 50%
nPCR	nested PCR
NPX	normalized protein eXpression
ORF	Open reading frame
p.a.	Pro analysi
PBMC	Peripheral blood mononuclear cells
PBS	Phosphate buffered saline
PCR	Polymerase chain reaction
PE	Phycoerythrin
PE-Cy7	Phycoerythrin-Cy7
PEI	Paul Ehrlich Institute
Pen/strep	Penicillin/streptomycin
PFEA	FACS staining buffer (PBS, FCS, EDTA, sodium azide)
PH	Phosphorylated
pIgR	Polymeric Immunoglobulin Receptor
pp	Phosphoprotein
p.p.	Postpartum
PUFA	Polyunsaturated fatty acid
qPCR	Quantitative real time PCR
RFLP	Restriction fragment length polymorphism
RNA	Ribonucleic acid
RPMI	Roswell Park Memorial Institute medium
RT	Room temperature
SC	Secretory component
SCT	Stem cell transplantation
SD	Standard deviation
SOT	Solid organ transplantation
SSC	Side scatter
SSC-A	Side scatter - area
SSC-H	Side scatter - height
TBE	Tris-borate EDTA
TBS	Tris buffered saline

T_{CM}	Central memory T cells ($CD45RA^-$, $CCR7^+$)
T_{EM}	Effector memory T cells ($CD45RA^-$, $CCR7^-$)
T_{EMRA}	TEMRA cells, finally differentiated T cells re-expressing CD45RA ($CD45RA^+$, $CCR7^-$)
TLR	Toll-like receptor
TM	Trade mark
T_N	naïve T cells ($CD45RA^+$, $CCR7^+$)
TNF	Tumor necrosis factor
Transient milk	Breast milk expressed between colostrum and mature milk: seven to 30 days postpartum
TTV	Torque Teno Virus
Unimodal	Course of viral load: low amount in the beginning, then an increase, followed by a decrease after a maximum
UTR	Untranslated region
Virolactia	Infectious virus was found in breast milk
WHO	World Health Organization

9 List of figures

10 List of tables

11 Acknowledgement

First, I would like to thank the Ministry of Science Baden-Württemberg for funding my project (Verbundprojekt CMV Immunkontrolle (Ulm, Freiburg, Tuebingen).
I would like to thank Prof. Dr. Thomas Iftner, as well as Prof. emeritus Dr. Gerhard Jahn for the opportunity of working at the Institute of Medical Virology and Epidemiology of Viral Diseases.
I am deeply appreciating Prof. Dr. Dr. Klaus Hamprecht for supervising my work and giving me the opportunity to participate in this interdisciplinary project as well as the opportunity to expand my horizon at conferences.
I would also like to thank Prof. Dr. Rammensee for being my secondary advisor. A special thank you is for Dr. Kilian Wistuba-Hamprecht, whose advice and support regarding the immunological aspects was so important to my work.
I would also like to thank Dr. Rangmar Goelz for all his support with the BlooMil study in the Neonatology Department. I am very grateful for all the assistance, help and advices, as well as companionship from Karin Kollender, Wioleta Kapis, Edeltraud Faigle, Irina Krotova, Veronique Baudy, Susanne Rack, Andrea Baumeister, Thorsten Kussman and last but not at all least Dr. Henning Zelba. I also want to appreciate Tabea Rabe for helping and supporting me during the study. I am very grateful for Imma Fischer, who gave me statistical advice. I deeply appreciate the effort of Norman Davis, who did some English corrections of my work.
My deepest appreciation goes to all the participating mothers in my study. Thanks for joining the study, enduring sometimes longer waiting times than expected, attending the appointments and donating milk and blood, while being in a situation, which can’t be easy.
Furthermore, I would like to mention Jonas Bochem, Trinh Weitbrecht and Anna Keib for their friendship, moral support and lively discussions. I would like to give a special thanks to Janine Spreuer for moral support during the study and Matthias Schampera for proofreading my thesis.
A warm felt thank you is for my family. My parents, my brothers and my husband Jonas Lazar, who encouraged and stood by me throughout the whole time.

12 Contributions

Tabea Rabe performed about 8% of all breast milk separation procedures. To be able to conduct the phenotypical analysis of BMCs and PBMCs and simultaneously observe the virological data, support of the diagnostic team of the institute was essential. About half of all qPCRs (CMV-Argene kit) and nested PCRs, as well as almost all microculture assays and ECLIA tests were performed by the diagnostic team (Edeltraud Faigle, Karin Kollender, Susanne Rack, Wioleta Kapis, Andrea Baumeister and Veronique Baudy) (Figure 14 (microculture), Figure 16 (ECLIA), Figure 17 (microculture) and Figure 31 (some qPCRs)). The cytokine analysis was performed by Olink in Uppsala, Sweden, as well as the statistical analysis (Figure 58 to Figure 61).